ISSN 2686-9454

Ministry of Science and Higher Education of the Russian Federation
Far Eastern Federal University

The 9TH ANNUAL STUDENT SCIENTIFIC CONFERENCE IN ENGLISH

Vladivostok

25 – 31 May 2022

CONFERENCE PROCEEDINGS

Scientific electronic publication

Vladivostok
Far Eastern Federal University
2022

UDC 082
LBC 94.3
T44

The 9th annual student scientific conference in English, Vladivostok, 25–31 May 2022 [Electronic resource]: conference proceedings / Chief editor V.Y.Ermachenko. – Electr. dat. – Vladivostok: Far Eastern Federal University, 2022. Uniform Resource Locator: https://www.dvfu.ru/institute_of_high_technologies_and_advanced_materials/Conferences/. – Title screen.

ISSN 2686-9454

The collected volume contains proceedings of the contest of scientific reports in English and the results of scientific studies made by students, master's degree students and postgraduate students of the School of Natural Sciences, FEFU 25 – 31 May 2022.

UDC 082
LBC 94.3

Text electronic edition
Minimum System Requirements:
Минимальные системные требования:
Web browser Internet Explorer 6.0 or higher,
Opera version 7.0 or higher,
Google Chrome version 3.0 or higher

a computer with Internet access

Posted on the website of 29.07.2021

Volume 8.6 MB

Far Eastern Federal University
690922, Vladivostok, Russky Island, 10 Ajax Bay,

THE 9th ANNUAL STUDENT SCIENTIFIC CONFERENCE IN ENGLISH
Vladivostok, 25–31 May 2022

CONTENTS

Section I
BIOLOGY AND ECOLOGY

Borovkova A. D [1]

MONITORING OF ORGANOCHLORINE PESTICIDES (DDT AND HCH) IN SOFT TISSUE OF BIVALVES FROM THE POSYET BAY AND THE PETER THE GREAT BAY (THE SEA OF JAPAN)

[1] Far Eastern Federal University, Institute of the World Ocean
[2] Far Eastern Federal University, Oriental Institute School of Regional and International Studies, FEFU
Scientific adviser – Tsygankov V. Yu [1]
Scientific consultant–G. L. Ardeeva [2]

Persistent organic pollutants (POPs) are a class of the most hazardous organic compounds that include organochlorine pesticides (OCPs), such as HCCH, DDT, etc. COPs are highly toxic and bioaccumulative, and decompose extremely slowly in the environment. Due to atmospheric transport, COPs are deposited far away from the source of pollution and accumulate in aquatic and terrestrial ecosystems. Most of these substances have a negative impact on living organisms and human health [**Ошибка! Источник ссылки не найден.**].

Currently, since coastal waters of the Sea of Japan contamination issue by persistent organic pollutants are not enough studied our research is relevant.

The aim of this work is to study the temporal trends in the accumulation of OCPs in bivalve mollusks of the Peter the Great Bay on the basis of comparison of our data and the results of earlier studies.

Lipids were extracted from soft tissue homogenates using a mixture of n-hexane and acetone, followed by destruction of the fat components with concentrated sulfuric acid [**Ошибка! Источник ссылки не найден.**]. The obtained POPs extract was separated into non-polar (for PCB) and polar (for OCP) solvents on a chromatographic column with Florisil®. Among the OCPs in the samples studied the following were determined: α-, β- and γ-HCCH, 4,4'- DDT, 2,4'-DDT, 4,4'-DDD, 2,4'-DDD, 4,4'- DDE and 2,4'-DDE.

Earlier studies [**Ошибка! Источник ссылки не найден.**] of OCPs content in bivalves from Peter the Great Bay conducted in 2002 showed the presence of all HCH isomers in the soft tissues of *Crenomytilus grayanus* and *Mizuhopecten yessoensis* with a predominance of β-form. The presence of DDT and its metabolites was recorded only in *C. grayanus,* the main metabolite being DDD. The results are presented in Table 1.

Table 1

OCP content in bivalves collected in Posyet Bay, the Sea of Japan (June-July 2002) [**Ошибка! Источник ссылки не найден.**]

Species	Organ	C, ng/g, wet weight					
		HCH isomers			DDT metabolites		
		α	β	γ	DDT	DDD	DDE
Crenomytilus grayanus	Soft tissues	17	108	45	2	350	94
Mizuhopecten yessoensis		18	360	17	–	–	–

In samples of *C. grayanus* and *Modiolus modiolus* collected in 2017, all isomers of HCH were also detected, among which the β-form prevailed, indicating a long-term input of contaminants. DDT and its metabolites were dominated by DDE, which demonstrates the decomposition of the parent compound. The results are presented in table 2.

Table 2

OCP content in bivalves collected in different parts of the Peter the Great Bay, the Sea of Japan (summer 2017)

Species	Organ	C, ng/g, wet weight					
		HCH isomers			DDT metabolites		
		α	β	γ	DDT	DDD	DDE
Crenomytilus grayanus	Soft tissues	0,31	4,674	0,358	–	0,11	11,219
Modiolus modiolus		0,417	0,272	0,741	–	0,074	30,658

Thus, the results demonstrate a decrease in concentrations of organochlorine pesticides in the soft tissues of mollusks over 15 years. A growing number of countries may have reduced concentrations of OCPs by not using pesticides for medical or agricultural purposes in accordance with the Stockholm Convention. At the same time, the presence of low concentrations of forms indicating of recent input of contaminants may be associated with transboundary transport by water and air masses from areas where OCPs continue to be used to treat crops against pests and to control malaria vector.

References

1. Tsygankov, V. Yu. Sample Preparation Method for the Determination of Organochlorine Pesticides in Aquatic Organisms by Gas Chromatography/ V.Yu. Tsygankov, M.D. Boyarova. // Achievements in the Life Sciences. – 2015. – V. 9. – P. 65–68.

2. Boyarova, M. D. Current Levels of Organochlorine Pesticides in Aquatic Organisms from Peter the Great Bay (Japanese Sea) and Lake Khanka: abstract, dissertation of candidate of biological science/ Boyarova M. D. – Vladivostok: Far East Federal University, 2008. – 24 p.

3. Donets, M. M. Current levels of pollutants in commercial objects of the Far Eastern seas of Russia/ Donets M. M., Tsygankov V. Yu. // Bulletin of the Far Eastern Branch of the Russian Academy of Sciences. – 2019. – № 4. – P. 90-103.

4. Tsygankov, V. Yu. Persistent organic pollutants (POPs) in the Far East region: seas, organisms, people: monograph/ Tsygankov V. Yu., Donets M. M., Khristoforova N. K., et al. – Vladivostok: Far East Federal University, 2020. – 344 p.

Andreev M.E.[1,2], Vainutis K.S.[1], Voronova A.N.[1], Pankratov D.V.[1], Shchelkanov M.Yu.[1,3,4]

MORPHOLOGICAL DESCRIPTION OF NEMATODES OF THE GENUS *DICTYOCAULUS* (TRICHOSTRONGYLOIDEA: DICTYOCAULIDAE) FROM FAR EASTERN RED DEER (*CERVUS ELAPHUS XANTHOPYGUS* (H. MILNE-EDWARDS, 1867))

[1]G.P. Somov Institute of Epidemiology and Microbiology, Russian Federal Service for Surveillance on Consumer Rights Protection and Human Wellbeing

[2] Far Eastern Federal University, Institute of the World Ocean

[3]Federal Scientific Centre of the East Asia Terrestrial Biodiversity, FEB RAS

[4]Institute of Life Sciences and Biomedicine, Far Eastern Federal University

[5]Far Eastern Federal University, Oriental Institute School of Regional and International Studies, FEFU

Scientific adviser – Voronova A.N.[1]

Scientific consultant–G. L. Ardeeva[5]

Parasitic diseases caused by numerous helminths are of great importance in the dynamics of wildlife. Adults of the genus *Dictyocaulus*, which parasitize in the bronchi of domestic and wild ruminants, can be especially

dangerous. These nematodes cause parasitic bronchitis – dictyoculosis. The disease is characterized by cough, nasal discharge, emphysema, and pneumonia [2]. Dictyocaulosis is a potential threat to biodiversity as well as to the development of the game industry in Russia [3].

Until the beginning of the 21st century, most species of *Dictyocaulus*, due to their morphological identity, were commonly identified by the host in which the parasite was found. For example, for a long time scientists considered *D. eckerti* to be the only representative of dictyocaulids parasitizing in Deer (Cervidae). However, with the development of genetic technologies, two new species affecting Cervidae were discovered: *D. capreolus*, a parasite of roe deer and moose [1], and *D. cervi*, a parasite of red deer [5]. The aim of the study is to give a morphological description of nematodes of the genus *Dictyoculus* from the lungs of the Far Eastern red deer (*Cervus elaphus xanthopygus* (H. Milne-Edwards) of Primorsky Krai.

Twelve individuals of parasitic nematodes: 5 females and 7 males were found in the lungs of *C. elaphus xanthopygus*, which was hunted near the village Sinegorye in the Kavalerovsky district of Primorsky Krai. Of these, 8 individuals (2 males and 2 females) were preserved in 96% ethanol for genetic analysis and 4 were preserved in 70% ethanol to prepare permanent zoological preparations. Nematodes from 70% ethanol were placed in a 1:7 solution of glycerol and water, then placed on a slide and fixed with glycerol-gelatin [4]. The preparations were analyzed under a ZEISS Primo Star light microscope (Carl Zeiss, Germany). Total histological preparations were measured in ZEISS AxioVision 4.8.1 software (Carl Zeiss, Germany) at the Department of Cell Biology and Genetics, Far Eastern Federal University. General morphology: Filamentous nematodes of whitish color, with tapering body at the ends. The cuticle is transversely striated. The mouth opening is terminal and surrounded by four lips. The cephalic vesicle is present. The buccal capsule is 15.270-19.633 μm wide and 14.676-16.756 μm long. The buccal capsule wall is 6.673-13.990 μm wide and 19.619-30.417 μm long. The esophagus is cylindrical in shape, extending to the posterior end.

Male: Body length is 36.65-49.5 mm, oesophagus is 0.88-0.9 mm long. Nerve ring and excretory pore are removed 0.30-0.41 mm and 0.46-0.60 mm from the anterior end, respectively Copulatory bursa is 190.058-302 μm long. Spicules are porous, massive, brown in color, 243.01-263.6 μm in length and 30.795-36.187 μm in width. Gubernaculum is lighter than the spicules, oval in shape, 54.691-60.109 μm long and 10.634-13.467 μm wide. The structure of bursa: dorsal rays are distinct, split at apex each; externodorsal rays are independent, thickened at apex, shorter than two adjacent rays; medio- and postero-lateral rays are merged, completely fused, long, bent at the end.

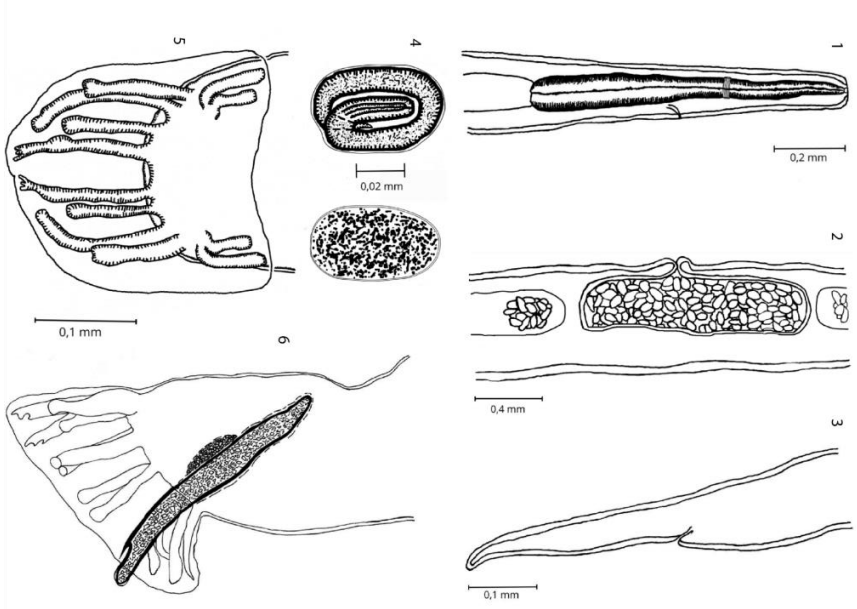

Figure 1 – *Dictyocaulus* n. sp. from the Far Eastern red deer
1 – anterior end; 2 – vulva area; 3 – posterior end of the female; 4 – immature and mature embryonated eggs; 5 - male bursa; 6 – posterior end of the male

Female: body length is 39.9-45.4 mm, esophagus is 0.84-0.98 mm long. The nerve ring and excretory pore were removed 0.33-0.38 mm and 0.50-057 mm from the anterior end, respectively. The vulva is in the first half of the body at a distance of 17.6-19.47 mm from the anterior end. Eggs are oval in shape, measuring 51.77-58.16 μm long and 33.42-38.26 μm wide.

Studied nematodes have a morphological structure typical for the genus (Fig. 1). In addition, the presence of three lobes on dorsal rays and length of spicules unite our species with other dictyocauluses from Cervids. According to morphometry, the worms are unique, since they do not correspond to any of the known *Dictyocaulus*. The maximum length of males is similar to *D. capreolus* and *D. cervi* but exceeds the length of males of *D. eckerti* (49.35 > 47 mm). The minimum length of the female esophagus is the same only for *D. eckerty*, compared with other dictyocauli from the cervids, it is less (0.84 < 0.88 and 0.86 for *D. capreolus* and *D. cervi*, respectively). The maximum distance from the anterior end to the nerve ring in males is greater than in *D. capreolus* (0.41 > 0.4 mm). And the maximum distance from the anterior end to the excretory pore is greater than that of *D. cervi* (0.6 > 0.54 mm) [3].

It is surprising, but such insignificant morphometric differences from other representatives of the genus *Dictyocaulus* are sufficient to describe the new species. For example, the recently described *D. capreolus* differed morphometrically from *D. eckerti* only in the thickness of the buccal capsule [1]. Nevertheless, molecular genetic analysis is necessary for a definitive conclusion. Thus, a comparison of the sequences obtained using the genetic markers 18S rRNA and cox1 showed a strict isolation of the studied nematodes from other species of the genus.

To sum up, the presented morphological description together with previously obtained genetic data allow us to describe a new species *Dictyocaulus* from the Far Eastern red deer in Primorsky Krai.

References

1. Gibbons L.M. *Dictyocaulus capreolus* n. sp. (Nematoda: Trichostrongyloidea) from roe deer, *Capreolus capreolus* and moose, *Alces alces* in Sweden / L.M. Gibbons, J. Hoglund // Journal of Helminthology – 2002. – T. 76 – P.119-124.

2. Henker L.C. Dictyocaulosis in dairy cows in Brazil: an epidemiological, clinical-pathological and therapeutic approach / L.C. Henker, C.I. Schwertz, N.J. Lucca, M.M. Piva, P. Giacomin, A. Gris, L. A. Rhoden, L.J. Norbury, A.S. da Silva, R.A. da Rosa, R.E. Mendes // Acta parasitological – 2017. – T. 62 – № 1 – P.129-132.

3. Pyziel A.M. Interrelationships of *Dictyocaulus* spp. in Wild Ruminants with Morphological Description of *Dictyocaulus cervi* n. sp. (Nematoda: Trichostrongyloidea) from Red Deer, *Cervus elaphus* / A.M. Pyziel, Z. Laskowski, A.W. Demiaszkiewicz, J. Hogland // Journal of Parasitology – 2017. – T. 103 – № 5 – P.506-118.

4. Roskin G.I. Mikroskopicheskaya tekhnika / G.I. Roskin, L.B. Levinson – M.: «Sovetskaya nauka», 1957. – 469.

5. Skryabin K.I. Osnovy nematodologii. Tom IV / K.I. Skryabin, N.P. Shihobalova, R.S. SHul'c. – M.: IZDATEL'STVO AKADEMII NAUK SSSR, 1954. – 323.

Buinovskaya N.S.[1,2], Likhatskaya G.N.[2], Kovalchuk S.N.[2], Balabanova L.A.[2]

PREDICTION OF NEW LIGAND-BINDING PROPERTIES OF A GALACTOS-SPECIFIC LECTIN BY IN SILICO MUTAGENESIS

[1]Department of Chemistry and Materials IHTAM FEFU
[2]G.B. Elyakov Pacific Institute of Bioorganic Chemistry FEB RAS
[3]Institute of Oriental Studies - School of Regional and International Studies, FEFU
Scientific adviser – L.A. Balabanova[2]
Scientific consultant – I.N. Lazareva [3]

Lectins are the general name of glycoproteins, as well as proteins of non-immune origin, capable of selectively and reversibly binding to carbohydrates [1, 3]. Such carbohydrate-protein interactions form the basis of many physiological processes in the body. The most interesting of them relate to the emergence and development of malignant tumors, adhesion of individual cells and microorganisms to tissues, participation in a nonspecific immune response to various pathogens, intercellular contacts through chemoreceptor "recognition" of each other by cells [1, 3].

Lectins are able to recognize minor changes in the carbohydrate profile of the cell surfaces of cancerous tumors, and therefore deserve special attention among the variety of modern antitumor arsenal.

It is known that the cell surface is a rather complex structure consisting of a double layer of phospholipids, various proteins, glycoproteins, and glycolipids (Fig. 1). The last two classes of compounds contain heterooligosaccharides, which consist of different monosaccharide units, such as galactose, glucose, fucose, mannose, sialic acid, and several others. Numerous studies conducted since the middle of the 20th century have established that changes in these structures invariably accompany the processes of malignant growth of tumors. In particular, there are several characteristic pathways for cell surface reglycosylation during cell transformation:

- there is an increase in the number of branched oligosaccharide chains;
- the expression of embryonic carbohydrate antigens starts;
- increases the degree of fucosylation and the content of sialic acid in the terminal position [4].

This is the first weakness of the tumor cell: it allows carbohydrate-binding proteins to “discover” itself. And all these changes can be tracked with the help of lectins.

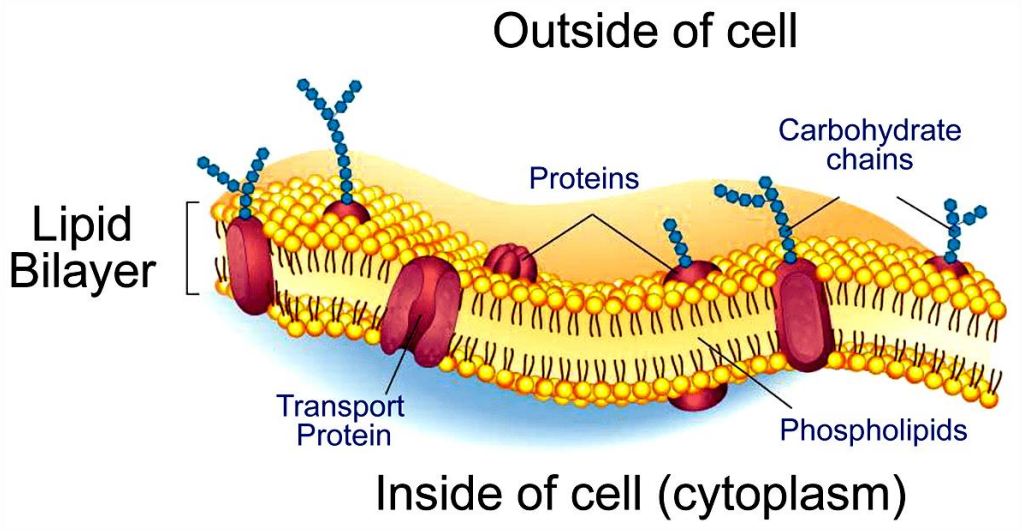

Figure 1. The structure of the cell membrane.

Based on the ability of the galactose-specific lectin CGL from the marine mollusk *Crenomytilus grayanus* to bind to many tumor markers, a solid-phase lectin-enzymatic method for the analysis of biological samples was

proposed. [1]. The recombinant bifunctional lectin CmAP/CGL with highly active alkaline phosphatase from the marine bacterium Cobetia amphilecti KMM 296 makes it possible, without additional steps, to detect bound lectin-ligand complexes in samples containing structures with galactose residues, such as cancer embryonic antigen (CEA), acid beta-glycoprotein, and others. (CA19-9, CA125, CA72-4, alpha-fetoprotein (AFP) and prostate-specific antigen (PSA)) [1]. However, many of the listed tumor markers can also be found in samples from healthy people.

To enable the differentiation of transformed and healthy cells, in silico mutagenesis of the CGL lectin and molecular docking of its mutants in complex with various carbohydrate residues from the PDA crystal structure database (https://g.co/kgs/Ug5sVS) were carried out using the MOE 2018.01 program [2]. characteristic of the carbohydrate profile of tumors.

Thus, using the methods of structural bioinformatics, we obtained several spatial structures of the CGL lectin with a predicted change in specificity from a galactose residue to Neu5G sialic acid residues, which is absent in glycoproteins of healthy human cells (Fig. 2). The substitution of amino acid residues at positions H37, H85, and H129 for an alanine residue at three binding sites, respectively, led to a change in the conformation of the carbohydrate-binding sites in the H37A, H85A, and H129A mutants, which causes the breaking of the hydrogen bonds of these residues with galactose and the appearance of a high affinity of the binding sites for sialic acids (Fig. 2). The loss of galactose specificity of CGL has been shown experimentally. Mutants H37A, H85A, and H129A bind much weaker to mucin compared to wild-type lectin. [3].

The ability of mutant CGL to form complexes with sialic acid in samples will increase the specificity for the carbohydrate profile of tumor markers of cancer cells when using diagnostic test systems based on recombinant CGL lectin with a highly active marine bacterium alkaline phosphatase.

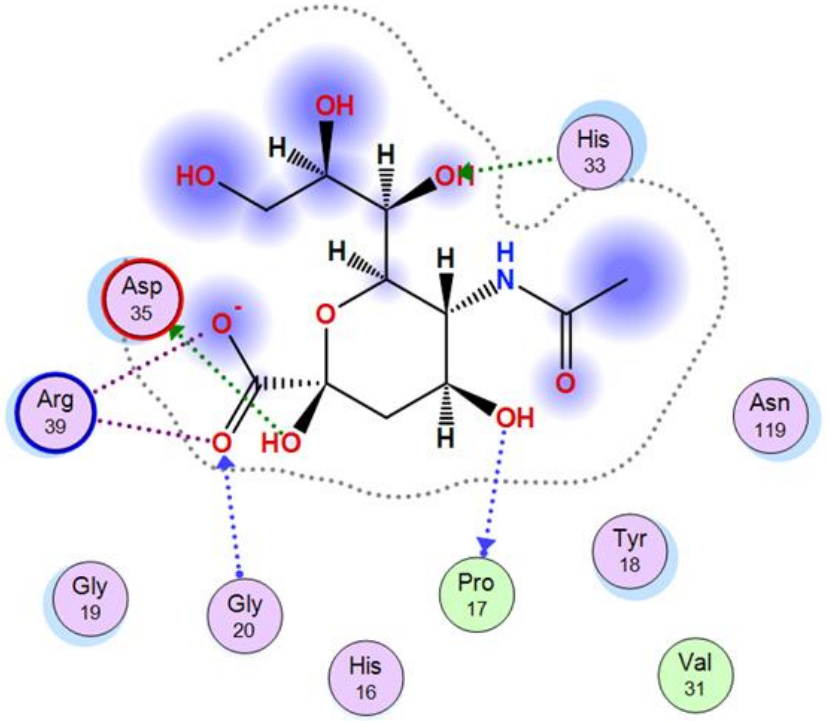

Figure 2. Mutant lectin-sialic acid complex.

References

1. Chikalovets I. V., Molchanova V. I., Chernikov O. V., Luk′yanov P. A. Domain organization of lectin from the mussel Crenomytilus grayanus // Chemistry of Natural Compounds. – 2014. – Vol. 50, N 4. – P. 706–709.

– Bibliogr.: 13 ref. WoS, Scopus;

2. Kovalchuk S. N., Buinovskaya N. S., Likhatskaya G. N., Rasskazov V. A., Son O. M., Tekutyeva L. A., Balabanova L. A. Mutagenesis studies and structure-function relationships for GalNAc/Gal-specific lectin from the sea mussel Crenomytilus grayanus // Marine Drugs. – 2018. – Vol. 16, N 12. – P. 471[1–10]. – Bibliogr.: 24 ref. doi:10.3390/md16120471 WoS, Scopus.

3. Kovalchuk S. N., Golotin V. A., Balabanova L. A., Buinovskaya N. S., Likhatskaya G. N., Rasskazov V. A. Carbohydrate-binding motifs in a novel type lectin from the sea mussel Crenomytilus grayanus: homology modeling study and site-specific mutagenesis // Fish & Shellfish Immunology. – 2015. – Vol. 47, N 1. – P. 565–571. – Bibliogr.: 25 ref. WoS, Scopus;

4. Oliver M T Pearce and Heinz Läubli. Sialic acids in cancer biology and immunity // Glycobiology, 2016, vol. 26, no. 2, 111–128. doi:10.1093/glycob/cwv097;

Grebenkin P.V.[1], Sabutski Y.E.[2], Likhatskaya G.N.[2]

BINDING OF 1,4-NAPHTHOQUINONE DERIVATIVES TO THE MAIN BLOOD TRANSPORT PROTEIN

[1] Far Eastern Federal University, Institute of the World Ocean, FEFU
[2] G.B. Elyakov Pacific Institute of Bioorganic Chemistry, FEB RAS
[3] Far Eastern Federal University, Oriental Institute School of Regional and International Studies, FEFU
Scientific adviser – Likhatskaya G.N.[2]
Scientific consultant–G. L. Ardeeva [3]

Derivatives of 1,4-naphthoquinononones are pharmacologically active, they are characterized by cytotoxic, antibacterial, antifungal, antiviral, antioxidant and cardioprotective properties [2,3,5]. However, 1.4-naphthoquinones are poorly soluble in water, and therefore require special means of their transfer to the target cells. The main blood transport protein is human serum albumin (HSA). Its normal concentration ranges from 35 to 50 g/l. The molecular weight of the protein is 66.5 kDa [4]. The HSA structure contains three homologous α-helical domains: I (residues 1-195), II (196-383) and III (384-585). These domains include ten antiparallel helices and are divided into two subdomains – A of six helices and B of four [1,4]. HSA regulates redox potential, colloidal osmotic plasma pressure between blood and tissues; It acts as a carrier of endogenous and exogenous low molecular weight compounds, protects them from the destructive environmental impacts, reducing toxicity and increasing their half-life [4]. HSA also improves the solubility of hydrophobic compounds in plasma, which may facilitate the transfer of 1,4-naphthoquinone derivatives to their targets.

In this work, potential binding sites of 1,4-naphthoquinone derivatives, compounds U-573 and U-443 obtained at the Pacific Institute of Bioorganic Chemistry, with human serum albumin are evaluated using *in silico* methods The spatial structures of 1,4-naphthoquinone molecules were obtained using the Discovery Studio and MOE (Molecular Operating Environment) programs. Stabilization of the structures was performed using the potential of Amber99 forces. The crystal structure of albumin was obtained from the PDB database (PDB ID 1AO6). Potential ligand binding sites were identified using the Site Finder module of the MOE program. A warfarin binding site located in the IIA domain of albumin was chosen for U-573. Binding site was determined based on 2BXD model analysis (albumin + warfarin). For U-443, a site located between the I and III domains of HSA was chosen because of the large size of the molecule under study. For U-573 free binding energy ΔE (kcal/mol) calculated with MM/GBVI parameters range from -13 to -20, affinity (pKi) ranges from 9.3 to 10.5, and efficiency is greater than 0.5. The number of ligand contacts with the site is 3 or 4. For U-443, ΔE values range from -18 to -25, affinity (pKi) ranges from 6.3 to 9.5, and efficiency is not more than 0.22. The number of ligand contacts with the site is from 1

to 3. For warfarin ΔE = -27.8, affinity (pKi) = 8.5, efficiency = 0.4. The number of ligand contacts with site is 4. Thus, compounds U-573 and U-443 have the potential to bind to albumin. Using the GRAMM (Global Range Molecular Matching) program, two more potential ligand binding sites were identified for each of the molecules. One of the sites located in domain I overlaps for both substances. Future experiments on the binding of U-443 and U-573 to human albumin are planned to determine the binding parameters by fluorescence spectroscopy.

References

1. Ali, M.S. Experimental and Computational Investigation on the Interaction of Anticancer Drug Gemcitabine with Human Plasma Protein: Effect of Copresence of Ibuprofen on the Binding / M.S. Ali, H.A. Al-Lohedan // Molecules. – 2021. - Vol. 27(5). - № 1635. – P. 1-20. DOI: https://doi.org/10.3390/molecules27051635
2. Aminin, D.L. 1,4-Naphthoquinones: Some Biological Properties and Application / D.L. Aminin, S.G. Polonik // Chemical and Pharmaceutical Bulletin. – 2020. – Vol. 68 (1). – P. 46-57. DOI: https://doi.org/10.1248/cpb.c19-0091
3. Iunikhina, O.V. Comparative In Vitro Study of Antiherpetic Activity of Echinochrome A and Product of Its Oxidation Dehydroechinochrome / O. V. Iunikhina, N. V. Krylova, N. P. Mishchenko, E. A. Vasileva, S. A. Fedoreyev, M. Yu. Shchelkanov // Bulletin of Experimental Biology and Medicine. – 2021. – Vol. 171. – P. 464–467. DOI: https://doi.org/10.1007/s10517-021-05251-y
4. Rabbani, G. Structure, enzymatic activities, glycation and therapeutic potential of human serum albumin: A natural cargo / G. Rabbani, S. N. Ahn // International Journal of Biological Macromolecules. – 2019. – Vol. 123. – P. 979-990. DOI: https://doi.org/10.1016/j.ijbiomac.2018.11.053
5. Yoon, C. S. The protective effects of echinochrome A structural analogs against oxidative stress and doxorubicin in AC16 cardiomyocytes / C. S. Yoon, K. H. Kim, N. P. Mishchenko, E. A. Vasileva, S. A. Fedoreyev, O. P. Shestak, N. N. Balaneva, V. L. Novikov, V. A. Stonik, J. Han // Molecular & Cellular Toxicology. – 2019. – Vol. 15. – P. 407–414. DOI: https://doi.org/10.1007/s13273-019-0044-6

Mezentseva S.A.[1]

PCR DIAGNOSTICS OF MYCOPLASMAS IN PACIFIC OYSTERS FROM COASTAL WATERS OF VLADIVOSTOK

[1]Far Eastern Federal University, Institute of the World Ocean
[2] Far Eastern Federal University, Oriental Institute School of Regional and International Studies, FEFU
Scientific adviser –E. A. Bogatyrenko[1]
Scientific consultant–G. L. Ardeeva[2]

Mycoplasmas are opportunistic microorganisms that are part of the normal microbiota of many oyster species [1]. According to literature, the prevalence of mycoplasmas in oysters ranges from 65% to 95% [2]. Although mycoplasmas can occur in fairly large numbers in the intestines of many aquatic animals, their functions in the body remain unknown [3]. Outbreaks of infectious diseases of oysters caused by mycoplasmas are known [4]. This may be due to the weakening of the immunity of animals against the background of deteriorating conditions of their habitat.

The aim of the work is to perform PCR diagnostics of internal organs of Pacific oyster Crassostrea gigas samples from Vladivostok coastal waters to detect mycoplasmas in them.

The water areas of Vladivostok with varying degrees of anthropogenic load were selected as study areas: Eastern Bosphorus Strait, Vtoraya Rechka Bay, Novik Bay, Ajax Bay, and Stark Strait. Animal specimens were sampled at a depth of 1.5–2 m. Under sterile conditions, the tissues of the gastrointestinal tract, gonads and gills

were extracted and frozen for further study. Total bacterial DNA was isolated from tissue samples using a commercial NK sorbent Base kit (Littech, Russia). A pair of primers was used for identification by PCR analysis: Myco1 GTTGCGCTCGTTGCGGGAC; Myco2-GTTGCGCTCGTTGCAGGAC [5]. PCR was performed in 25 µl of a reaction mixture containing BioMaster HS-qPCR (2x) (Biolabmix, Russia) using forward and reverse primers, sterile water, and DNA matrix. PCR was performed according to a program: pre-denaturation at 95°C (30 min) followed by 35 cycles of denaturation at 95°C (30 s), annealing at 56°C (30 s), elongation at 72°C (30 s), with a final elongation at 72°C for 10 min [5]. All PCR products were visualized by horizontal electrophoresis in 1.5% agarose gel on Tris-borate buffer containing ethidium bromide (Fig. 1).

PCR-diagnostics of internal organs of the Pacific oyster Crassostrea gigas from coastal waters of Vladivostok showed that 18 of 60 samples obtained contained members of the family Mycoplasmataceae. These samples were obtained from animals from the Eastern Bosphorus Strait, Vtoraya Rechka Bay, Novik Bay and Ajax Bay. Mycoplasmas were found to be part of the microbiota of 45% of the mollusk specimens studied. Mycoplasmas were found in the gastrointestinal tract of Pacific oysters (39% of all positive samples), in the gills (33%) and in the gonads (28%).

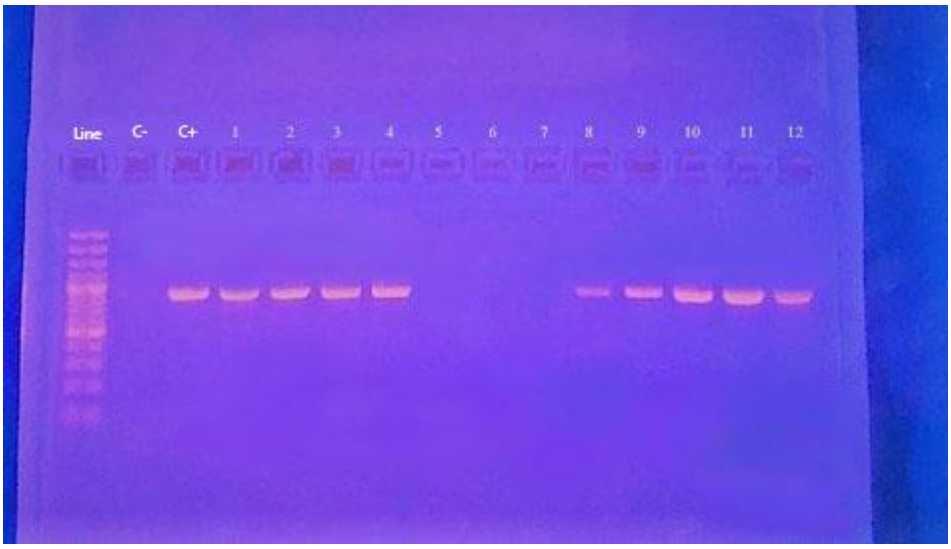

Fig.1 - Gel electrophoresis with results of mycoplasma detection in of Pacific oyster internal organ samples

References

1. Horodesky, A. Metagenomic analysis of the bacterial microbiota associated with cultured oysters (Crassostrea sp.) in estuarine environments / A. Horodesky, G. G. Castilho-Westphal, G. D. Pont, H. Faoro, E. Balsanelli, M. Z. Tadra-Sfeir, N. Cozer, M.R. Pie, A. Ostrensky // An Acad Bras Cienc. – 2020. – P. 1-15.

2. Biessy, L. Seasonal and Spatial Variations in Bacterial Communities From Tetrodotoxin-Bearing and Non-tetrodotoxin-Bearing / L. Biessy, J. K. Pearman, K. F. Smith, I. Hawes, S. A. Wood // Clams. Front Microbiol. – 2020. − 33 pp.

3. Bano, N. Dominance of Mycoplasma in the guts of the long-jawed mudsucker, Gillichthys mirabilis, from five California salt marshes. Environ. / N. Bano, A. Smith, W. Bennett, L. Vasquez, J. T. Hollibaugh // Microbiol. 9. − 2007. – P. 2636–2641. doi: 10.1111/j.1462-2920.2007.01381.x

4. Wegner, K. M. Disturbance induced decoupling between host genetics and composition of the associated microbiome. / K. M. Wegner, N. Volkenborn, H. Peter, A. Eiler // BMC Microbiol 13, 252. −2013. [Electronic source] – URL: https://doi.org/10.1186/1471-2180-13-252

5. Elshin, N. D. Studying the possibility of using the qPCR method to control the absence of mycoplasma contamination in cell cultures / N. D. Elshin, A.V. Petrov // St. Petersburg: Biopreparations. Prevention, diagnosis, treatment. – 2017. – P. 173-179.

Metreveli. V.E.[1], Mironova E.K.[1], Boyarova M.D.[1], Tsygankov V.Yu.[1]

PERSISTENT ORGANIC POLLUTANTS IN THE GREENLAND HALIBUT *REINHADTRIUS HIPPOGLOSSOIDES MATSUURAE* FROM THE NORTHWEST BERING SEA

[1] Far Eastern Federal University, Institute of the World Ocean, FEFU
[2] Far Eastern Federal University, Oriental Institute School of Regional and International Studies, FEFU
Scientific adviser – V.Yu. Tsygankov [1]
Scientific consultant–G. L. Ardeeva [2]

Among the seas of the Far Eastern fishery basin one of the most important is the Bering Sea with its high productivity and abundance of commercial species of hydrobionts [4]. However, despite its significant commercial significance, at present no monitoring studies at the state level are implemented in this water area, and the regulatory and legal framework of the Russian Federation lacks background concentrations of toxicants that are widespread in the environment [2]. At the same time, there are data on the determination of persistent organic pollutants (POPs) in such valuable fishery species as Pacific salmon (Oncorhynchus), flatfish (Pleuronectidae), and marine mammals of the seas of the Russian Far East [1,2,3,6,7,8]. The presence of concentrations of such pollutants in fishing objects makes this alarming. In this regard, the monitoring of pollutant content is a necessary process to help understand the level of danger of POPs pollution in the environment.

The Greenland halibut (*Reinhardtius hippoglossoides matsuurae*), the most numerous of the four halibut species inhabiting the Far Eastern seas, occupies a special place among important targets of commercial fishing in the Bering Sea. Its meat, being both fatty and tender, is highly valued for its taste qualities and is in high demand among consumers [10].

Thus, the aim of this work is to analyze organochlorine pesticides (OCP) and polychlorinated biphenyls (PCB) in organs of the Greenland halibut caught in the northwestern Bering Sea.

The Greenland halibut were sampled in the northwestern Bering Sea in the fall of 2020. After transportation to the laboratory, the samples were thawed and prepared according to the standard methods for the identification of organochlorine pesticides (OCPs) HCCH isomers (α-, β-, γ-, and -HCCH) and DDT, including its metabolites (o,p'-DDT, p,p'-DDT, o,p'-DDDD, p,p'-DDE, o,p'-DDE) and polychlorinated biphenyl (PCB) congeners (28, 52, 101, 118, 138, 153 and 180). The main determination of the mass content of the compounds under study in the biomaterial was performed on a Shimadzu GC MS-QP 2010 Ultra gas chromatograph mass spectrometer. Sample preparation was performed according to the procedure given in [7].

Mean concentrations of ∑HCH and ∑DDT in muscle tissue were 0.005±0,007 and 0,003±0,003, in liver – 0.002±0,001 and 0,008±0,005, in male gonads – 0.006±0,004 and 0,007±0,002, in eggs– 0.005±0,002 mg/kg wet weight, respectively.

HCH isomers were detected in almost all samples. The most frequent form is γ-HCH, which may indicate a possible ongoing input of this compound to the ecosystem. Of the DDT metabolites, the DDE group dominated indicating that the original DDT entered the environment a long time ago and was subsequently degraded.

The mean ∑PCB concentrations in muscle, liver, roe, and gonads of males were 0,002±0,002, 0,006±0,005, 0,0005±0.0005, and 0,0003±0,0002 mg/kg wet weight, respectively. In the sexual products of males, exclusively low-chlorinated PCB congeners (28 and 52) were found, while muscles, liver and roe of the studied individuals had a more diverse composition, the main part of which was represented by highly chlorinated PCB congeners (101, 118, 153, 138 and 180). The obtained results indicate the intake of a significant amount of PCBs at the time of lipid accumulation by the hydrobiont during the formation of eggs, as a fattier organ compared to the sexual products of males.

The obtained concentrations in the organs of the Greenland halibut were compared with their maximum

permissible concentrations (MPCs) for fish and non-fish objects of fishing [5] (Table 1).

Table 1

Comparison of average POPs concentrations in organs of the Greenland halibut with MPCs for fish and non-fish fisheries, mg/kg wet weight.

Organ	Xenobiotic					
	∑HCH[1]	MPC	∑DDT[2]	MPC	∑PCB[3]	MPC
Muscles	0,005±0,007	0,2	0,003±0,003	0,2	0,002±0,002	2,0
Liver	0,002±0,001	1,0	0,008±0,005	3,0	0,006±0,005	5,0
Roe	0,005±0,002	0,2	–	0,2	0,0005±0,0005	2,0
Male gonads	0,006±0,004	0,2	0,007±0,002	0,2	0,0003±0,0002	2,0

[1]HCH (α-, β-, γ-)
[2]DDT (*o,p'*-DDT, *p,p'*-DDT, *o,p'*-DDD, *p,p'*-DDD, *o,p'*-DDE, *p,p'*-DDE)
[3]PCB marker congeners: 28, 52, 101, 138, 153 and 180

According to the results, no organ exceeded the maximum permissible concentrations, indicating the safe use of the Greenland halibut as a food item. However, an assessment of acceptable consumption based on POPs content is necessary to confirm safe consumption of this species.

Thus, OCPs and PCBs were detected in all organs of the Greenland halibut. Since the Bering Sea is a zone quite distant from the active agricultural activity and industrial production, the presence of organochlorine pesticide compounds in the analyzed samples is a manifestation of the global background of xenobiotics that has formed on the planet at the present time. When comparing POP concentrations in organs with MPCs, no exceedances were found. Consequently, one of the most important tasks is to expand research on deep-sea commercial or potentially commercially exploitable fish species to assess the safety of their consumption, as well as to monitor the condition of the ecosystem as a whole.

This study was supported by the Russian Science Foundation (agreement no. 18-14-00120).

References

1. Flounders as indicators of environmental contamination by persistent organic pollutants and health risk / M.M. Donets, V.Yu. Tsygankov, M.D. Boyarova [et al.] // Marine Pollution Bulletin. — 2021. — Iss. 164. — P. 1-8.

2. Korshenko, A.N. The quality of sea waters in terms of hydrochemical indicators // Yearbook 2017. — Moscow: Nauka, 2018. — 220 p.

3. Lukyanova, O.N. Organochlorine pesticides and polychlorinated biphenyls in the Bering flounder (*Hippoglossoides robustus*) from the Sea of Okhotsk / O.N. Lukyanova, V.Yu. Tsygankov, M.D. Boyarova // Marine Pollution Bulletin. — 2018. — Iss. 137. — P. 152-156.

4. Shuntov, V.P. Biology of the Russian Far Eastern Seas: in 3 volumes / V.P. Shuntov. – Vladivostok: TINRO-Center, 2016. – Vol. 2. – 604 p.

5. TR CU 021/2011. Technical Regulations of the Customs Union “On Food Safety”. — 2011. — 212 p.

6. Tsygankov, V.Yu. Bioaccumulation of persistent organochlorine pesticides (OCPs) by gray whale and Pacific walrus from the western part of the Bering Sea / V.Yu. Tsygankov, M.D. Boyarova, O.N. Lukyanova // Marine Pollution Bulletin. — 2015. — Vol. 99, № 1-2. — P. 235-239.

7. Tsygankov, V.Yu. Bioindicators of organochlorine pesticides in the Sea of Okhotsk and the Western Bering Sea / V.Yu. Tsygankov, M.D. Boyarova, O.N. Lukyanova, N.K. Khristoforova // Archives of Environmental Contamination and Toxicology. — 2017. — Iss. 73. — P. 176-184.

8. Tsygankov, V.Yu. Organochlorine pesticides in marine ecosystems of the Far Eastern Seas of Russia (2000-2017) / V.Yu. Tsygankov // Water Research. — 2019. — Iss. 161. — P. 43-53.

9. Tsygankov, V.Yu. Sample preparation method for the determination of organochlorine pesticides in

aquatic organisms by gas chromatography / V.Yu. Tsygankov, M.D. Boyarova // Achievements in the Life Sciences 9. – 2015. — P. 65-68.

10. Tuponogov, V.N. Atlas of commercial fish cpecies of the Far Eastern seas of Russia / V.N. Tuponogov, V.A. Snytko — Vladivostok: TINRO-Center, 2014. — 206 p.

Ovsiannikova D. M.[1]

THERMOSTABLE PEPTIDS ARE PROTEASE INHIBITORS OF THE KUNITZ TYPE SELECTED FROM THE SEA ANEMON *HETERACTIS CRISPA*

[1] Far Eastern Federal University, World Ocean Institute (School), FEFU
[2] G. B. Elyakov Pacific Institute of Bioorganic Chemistry, FEB RAS
[3] Far Eastern Federal University, Oriental Institute School of Regional and International Studies, FEFU
Scientific supervisor – N. M. Sanina[1]
Scientific supervisor – A. N. Kvetkina [2]
Scientific consultant–G. L. Ardeeva[3]

The search for new biologically active compounds as potential components for the creation of pharmacological drugs, the study of their structural and functional relationships and mechanism of action is a fascinating task of biochemistry and biotechnology. In this context, the peptides of the Kunitz/BPTI family are of great research interest due to their wide representation among both venomous terrestrial and marine animals and their ability to interact with various targets (serine proteases, ion channels) involved in various physiological processes [1; 2]. Their polypeptide chain contains 60-80 aa which is stabilized by three conserved intradomain disulfide bonds (CysI–CysVI, CysII–CysIV, CysIII–CysV) accompanied by the formation of two loops responsible for protease inhibition. The amino acid residues of the main protease-binding loop, in particular the residues of the reactive site (positions P1-P1’), form the majority of contacts with the active centre of the protease and contribute to the association energy of the protein-enzyme complex [3].

Sea anemones are a rich source of Kunitz-peptides, which are encoded by multigene families and form a large variety of peptide isoforms in the content of venom secretion. Such multigene families were found in *Stichodactyla haddoni* [4], *Anemonia viridis* [5], *Heteractis magnifica* and *Heteractis crispa* [6]. The main function of most known Kunitz-type peptides is protease inhibition, some Kunitz peptides from sea anemone exhibit analgesic [7; 8], anti-inflammatory [9] and neuroprotective [10] activities.

One of the important characteristics of Kunitz-peptides is a high stability of the domain structure due to the presence of three disulfide bonds. This feature allows them to retain protease inhibitory activity over a wide range of temperatures and pH values.

The aim of this work was to obtain recombinant peptides, HCIQ2c1 and HCIQ4c7, belonging to combinatorial library of sea anemone *H. crispa* and to study their thermostability.

Heterologic expression in bacterial systems is a widespread method of producing recombinant peptides. *Escherichia coli* BL21 (DE3) cells were transformed with recombinant plasmids pET32b/HCIQ2c1 and pET32b/HCIQ4c7. Heterological expression was performed in Luria-Bertani medium with 0.5 mM and 0.2 mM isopropyl-β-D-1-thiogalactopyranoside for HCIQ2c1 and HCIQ4c7, respectively, at 37 °C for 3 hours. Fusion proteins consisting of target peptides, thioredoxin, a poly-histidine tag, and a methionine residue were isolated by metal-affinity chromatography and cleaved with CNBr for the methionine residue. The target peptides were then purified by RP-HPLC. The final yields of HCIQ2c1 and HCIQ4c7 were 10 and 13 mg/L cell culture, respectively. The molecular weights of HCIQ2c1 and HCIQ4c7 determined by MALDI TOF MS were 6330 and 6404 Da, consistent with the predicted molecular weights.

The temperature effect on the spacial structure and biological activity of peptides was analyzed by both CD spectroscopy and protease inhibition analysis. The CD spectra of HCIQ2c1 and HCIQ4c7 solutions showed no significant changes after heating to 90 °C and 80 °C, respectively. Further heating of the solutions to 100 °C resulted in a reduction of α-helixes in both peptides. To confirm the thermostability of HCIQ2c1 and HCIQ4c7, their ability to inhibit trypsin after heating in the temperature range from 25 to 100 ° C for 30 minutes was studied. It was shown that HCIQ2c1 completely inhibited trypsin over the entire temperature range, whereas the activity of HCIQ4c7 decreased by 7% after heating the solution to 100 °C. Thus, we obtained recombinant HCIQ2c1 and HCIQ4c7 peptides and showed that they are highly thermostable, retaining their conformation and biological activity up to 90–100 °C.

This work was funded by RFBR and SC RA, project number 20-54-05006.

References:

1. Scott, C. J. Biologic protease inhibitors as novel therapeutic agents / C. J. Scott, C. C. Taggart // Biochimie. - 2010. - Vol. 92. - P.1681-1688.
2. Reich E., Rifldn D.B., Shaw E. Proteases and control. N. Y. Cold Spring Harbour Laboratory, 1975. 1021 p.
3. Krowarsch, D. Canonical protein inhibitors of serine proteases / D. Krowarsch, T. Cierpicki, F. Jelen, J. Otlewski // CMLS. - 2003. - V. 60. - P. 2427–2444.
4. Madio, B. Sea anemone toxins: a structural overview / B. Madio, G. King F., E. A. B. Undheim // Mar Drugs. - 2019. - Vol. 17. - № 6. - P. 1-26.
5. Kozlov, S. A. New polypeptide components from the Heteractis crispa sea anemone with analgesic activity / S. A. Kozlov, I. A. Andreev, A. N. Murashev, D. I. Skobtsov, I. A. D'iachenko, E. V. Grishin // Bioorg Khim. - 2009. - Vol. 35. - № 6. - P. 789-798.
6. Isaeva, M.P. A new multigene superfamily of Kunitz-type protease inhibitors from sea anemone Heteractis crispa / M. P. Isaeva, V. E. Chausova, E. A. Zelepuga, K. V. Guzev, V. M. Tabakmakher, M. M. Monastyrnaya, E. P. Kozlovskaya // Peptides. - 2012. - Vol. 34. - P. 88–97.
7. Andreev, Y. A. Polypeptide modulators of TRPV1 produce analgesia without hyperthermian / Y. A. Andreev, S. A. Kozlov, Y. V. Korolkova, I. A. Dyachenko, D. A. Bondarenko, D. I. Skobtsov, A. N. Murashev, P. D. Kotova, O. A. Rogachevskaja, N. V. Kabanova, S. S. Kolesnikov, E. V. Grishin // Mar. Drugs. - 2013. - Vol. 11. - P. 5100-5115.
8. Tabakmakher, V. M. Analgesic effect of novel Kunitz-type polypeptides of the sea anemone Heteractis crispa / V. M. Tabakmakher, O. V. Sintsova, O. N. Krivoshapko, E. A. Zelepuga, M. M. Monastyrnaya, E. P. Kozlovskaya // Dokl Biochem Biophys. – 2015. - № 461. – P. 80-83.
9. Sintsova, O. V. Anti-Inflammatory Activity of the Polypeptide of the Sea Anemone, Heteractis crispa / O. V. Sintsova, M. M. Monastyrnaya, E. A. Pislyagin, E. S. Menchinskaya, E. V. Leychenko, D. L. Aminin, E. P. Kozlovskaya // Bioorg Khim. - 2015. – Vol. 41. - № 6. – P. 657-663.
10. Kvetkina, A. A new multigene HCIQ subfamily from the sea anemone Heteractis crispa encodes Kunitz-peptides exhibiting neuroprotective activity against 6-hydroxydopamine / A. Kvetkina, E. Leychenko, V. Chausova, E. Zelepuga, N. Chernysheva, K. Guzev, E. Pislyagin, E. Yurchenko, E. Menchinskaya, D. Aminin, L. Kaluzhskiy, A. Ivanov, S. Peigneur, J. Tytgat, E. Kozlovskaya, M. Isaeva // Sci Rep. – 2020. - Vol. 10. – N 1. – P. 4205.

Pivovarov V. E[1]., Ardeeva G.L.[2]

THE MAIN RESULTS OF STUDYING THE NATURE OF ORGANIC POLLUTION IN VOSTOK BAY (SEA OF JAPAN) BY OXYGEN INDICATORS

[1]Far Eastern Federal University, World Ocean Institute, FEFU
[2] Far Eastern Federal University, Oriental Institute School of Regional and International Studies, FEFU
Scientific adviser – N.K. Khristoforova[1]
Scientific consultant–O.K.Titova[2]

Vostok Bay is a small bay of the second order, located in the eastern part of the Peter the Great Bay. Located at some distance from industrial enterprises, Vostok Bay did not experience a serious anthropogenic load, since its shores are poorly developed by industry and agriculture. The bay is a nursery for many invertebrates, the larvae of which are carried by currents through the waters of Peter the Great Bay. Since the late 1990s - early 2000s, the environmental situation in Vostok Bay began to change especially noticeably deteriorating in its upper part under the influence of the growing recreational pressure.

The assessment of the state of dissolved oxygen distribution in the waters of Vostok Bay was carried out in October 2020 and May 2021 based on the hydrochemical parameters of BOD obtained by the standard Winkler method and sounding results. This made it possible to get an idea of the bay pollution with easily oxidized organic matter as well as to draw conclusions about the pollution of the water area with hard-to-oxidize substances.

The results obtained during the analysis of water samples for the content of dissolved oxygen and its biochemical consumption in the waters of Vostok Bay in the fall of 2020 are presented in Table 1.

Table 1

Average concentrations of biochemical consumption of dissolved oxygen in the waters of Vostok Bay, October 2020, (mean ± standard deviation, n=3).

Station	Dissolved oxygen, mg/l	BOD1, mg/l	BOD5, mg/l	BOD10, mg/l	BOD20, mg/l	Temperature, °C	Salinity, ‰
Cape Peshchurov	8,22	0,10 ± 0,01	0,67	1,78 ± 0,06	2,31 ± 0,03	15	33
Gaydamak Bay	6,72	0,11 ± 0,01	0,9	1,04 ± 0,01	1,37 ± 0,02	15,1	32,8
Cape Elizarov	8,25	0,06 ± 0,03	0,5	1,74 ± 0,15	2,21 ± 0,01	15,1	33
Near the village Volchanets	8,44	0,07 ± 0,02	0,33	1,45 ± 0,04	2,17 ± 0,01	14,5	32,6
Mouth of the Volchanka River	8,18	0,07 ± 0,03	0,71	1,85 ± 0,01	2,61 ± 0,03	14,5	32,3

It follows from the data in Table 1 that the concentration of dissolved oxygen distributed over the water area of Vostok Bay in autumn fluctuates around 8 mg/l which indicates low pollution of the waters of the bay. The exception is the data obtained at the entrance to Gaydamak Bay (6.72 mg/l), which is lower than the average values for the bay and is clearly out of the general pattern of the distribution of dissolved oxygen concentrations in the Vostok Bay water area (Figure 1). The BOD values obtained during the work for the Gaydamak Bay station turned

out to be low which indicates water pollution with a small amount of easily oxidizable organic matter and a large intake of hard-to-oxidize organic substances. It is most likely that the reason for this in the water area of the station in Gaydamak Bay is the influx of polluted waters: the Dobroflot fish cannery is located in this bay, as well as a small ship repair base.

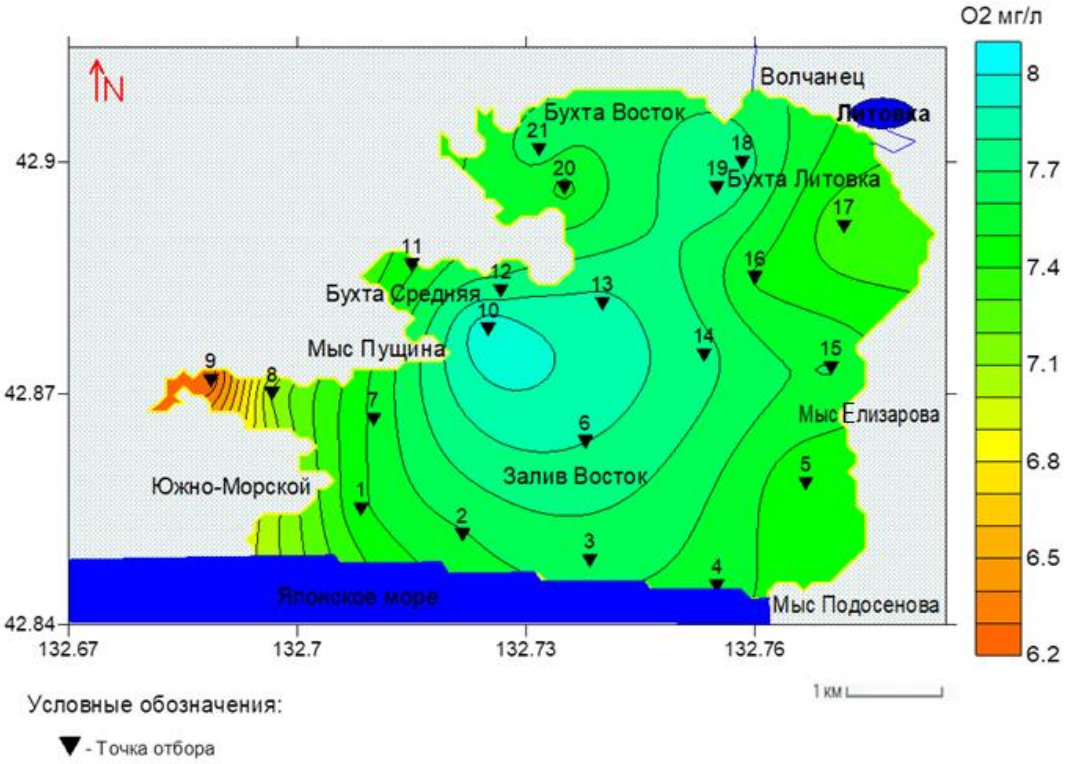

Figure 1. Dissolved oxygen concentrations in Vostok Bay in autumn 2020 (according to the ASTD102-Rinko probe)

High concentrations of dissolved oxygen obtained during the analysis of water samples in Vostok Bay are normal for the fall season when temperatures are already decreasing thereby increasing the solubility of oxygen in water and reducing the activity of microalgae preventing them from blooming. It also rained with strong wind just before sampling. As a result of such weather events, the water was naturally enriched with oxygen. This is confirmed by the BOD indicators the values of which are low, which characterizes the low water pollution in the areas of sampling stations. The results obtained during the analysis of water samples for the content of dissolved oxygen and its biochemical consumption in the Vostok Bay water area in 2021 are presented in Table 2.

Table 2

Average concentrations of biochemical consumption of dissolved oxygen in the waters of Vostok Bay, May 2021, (mean ± standard deviation, n=2).

Station	Dissolved oxygen, mg/l	BOD1, mg/l	BOD5, mg/l	BOD10, mg/l	BOD20, mg/l	Temperature, °C	Salinity, ‰
Cape Peshchurov	9,66	0,51 ± 0,04	1,07 ± 0,28	2,26 ± 0,04	2,51 ± 0,08	11,4	27,0
Gaydamak Bay	9,77	0,88 ± 0,07	2,34 ± 0,03	3,16 ± 0,11	3,37 ± 0,08	12,6	28,1
Cape Elizarov	10,15	0,82 ± 0,01	2,01 ± 0,33	2,54 ± 0,01	2,85 ± 0,01	12,2	31,2

Near the village Volchanets	9,96	0,57 ± 0,01	1,50 ± 0,01	2,09 ± 0,07	2,57 ± 0,05	13,2	28,9
Mouth of the Volchanka River	9,96	0,44 ± 0,06	1,38 ± 0,27	2,25 ± 0,02	2,62 ± 0,03	13,9	27,8

According to the data in Table 2, the dissolved oxygen concentrations distributed over the Vostok Bay water area during the spring period fluctuates around 10 mg/l, which indicates low pollution of the bay waters. Increased oxygen concentrations in the spring compared to the fall period can be caused by lower water temperatures According to the BOD parameters, the station in Gaydamak Bay is again singled out, this time having the highest values (0.88; 2.34; 3.16; 3.37 mg/l) among all stations indicating an increased input of easily oxidized organic matter. During the movement to the sampling point, suspended solids with a distinct "fishy" odor were observed in the waters near the entrance to this bay.

Thus, the analysis of the spatial distribution of the biological consumption of dissolved oxygen in the Vostok Bay allows us to identify areas experiencing the greatest pollution. Gaydamak Bay turned out to be such an area, the water area of which is subject to industrial runoff. Observations in the top of the bay near recreational areas usually revealed anthropogenic pressure, especially evident near the Volchanets settlement and at the mouth of the Volchanka River, in 2020 showed that the estimated anthropogenic pressure on the coastal water area decreased dramatically due to restrictions on movement within Primorsky Krai caused by the covid pandemic.

References

1. Ogorodnikova AA, Ecological and economic assessment of the impact of coastal sources of pollution on the natural environment and bioresources of Peter the Great Bay. Vladivostok: TINRO Center. 2001. 193 p.
2. N.K. Khristoforova, T.V. Boychenko, A.D. Kobzar. Hydrochemical and microbiological assessment of the current state of the Vostok Bay waters. Vestnik FEB RAS. 2020. No. 2
3. Khristoforova N.K., Zhuravel E.V., Mironova Yu.A. Recreational impact on Vostok Bay (Sea of Japan) // Biology of the sea. 2002. V. 28, No. 4. P. 300–303
4. Khristoforova N.K. Gulf of Peter the Great: natural conditions and biodiversity // Modern ecological state of the Gulf of Peter the Great of the Sea of Japan: monograph / executive editor N.K. Khristoforova. Vladivostok Publishing House of the Far Eastern Federal Institute, 2012. P. 12-26.

Chukhlomina E.N.[1,2], Vasyutkina E.A.[2], Yugay Y.A.[1], Mazeika A.N.[2], Shkryl Y.N.[2]

FUNCTIONAL PROPERTIES OF THE *ROLB/C* GENE FROM NATURALLY TRANSGENIC PLANT SWEET POTATO *IPOMOEA BATATAS*

[1] Far Eastern Federal University, Institute of the World Ocean,
[2] Federal Scientific Center of the East Asia Terrestrial Biodiversity
[3]Far Eastern Federal University, Oriental Institute School of Regional and International Studies, FEFU
Scientific adviser - Yugay Y. A. [1]
Scientific adviser - Mazeika A. N. [2]
Scientific consultant–G. L. Ardeeva[3]

Lateral or horizontal gene transfer (HGT) is the movement of genetic material between reproductively isolated species, common among prokaryotes, where it occurs mainly through phages and plasmids [1]. One of the best known examples of HPG in plants is the transfer of a DNA fragment (T-DNA) in megaplasmids from

Agrobacterium spp. into the genome of dicotyledonous plants, resulting in the appearance of neoplasms in the form of crown galls or "hairy" roots. Regeneration or generative reproduction of these transformed tissues could occasionally give rise to naturally transgenic plants, containing fragments of so called cellular T-DNA (cT-DNA) [2]. Currently, about 7% of plants, such as tea, hops, peanuts, cranberries, walnuts, bananas, sweet potatoes, and others traditionally used in food, beverages, and medicine, are considered to be naturally transgenic [3]. Thus, the naturally transgenic sweet potato *Ipomoea batatas* contains two cT-DNA sites (IbT-DNA1 and IbT-DNA2) with genes homologous to *Agrobacterium spp.*, both related to oncogenes of the plast family and not [4]. In particular, the *rolB/C* gene from *I. batatas* cT-DNA2 was found to have some similarity to the two well-known oncogenes *rolB* and *rolC* from *A. rhizogenes*. We believe that a comprehensive study of the molecular and functional properties of cT-DNA genes can contribute to a better understanding of the fundamental principles of the HGT and, to some extent, mitigatethe the existing consumer distrust of transgenic food plants. At present, there is no information about the properties of *rolB/C* gene in the literature, so this topic seems to be a very important and relevant task.

In the first stage of our work, we studied the effect of various external stimuli on the expression level of *rolB/C* gene in *I. batatas* leaves (Fig. 1). There was a 9-fold increase in *rolB/*C expression when exposed to high temperature (47℃) and an 11-fold increase in expression when exposed to low temperature (4℃), and a weak 1.4-fold increase in expression when exposed to ultraviolet radiation. Exposure to hormones such as indolylacetic acid (IAA), kinetin, and abscisic acid (ABA), and salinity caused a 5-10-fold decrease in *rolB/C* gene expression. Salicylic acid (SA), methyl jasmonate (MeJA), osmotic stress (mannitol), and oxidative stress (paraquat) had no significant effect on *rolB/C* gene expression.

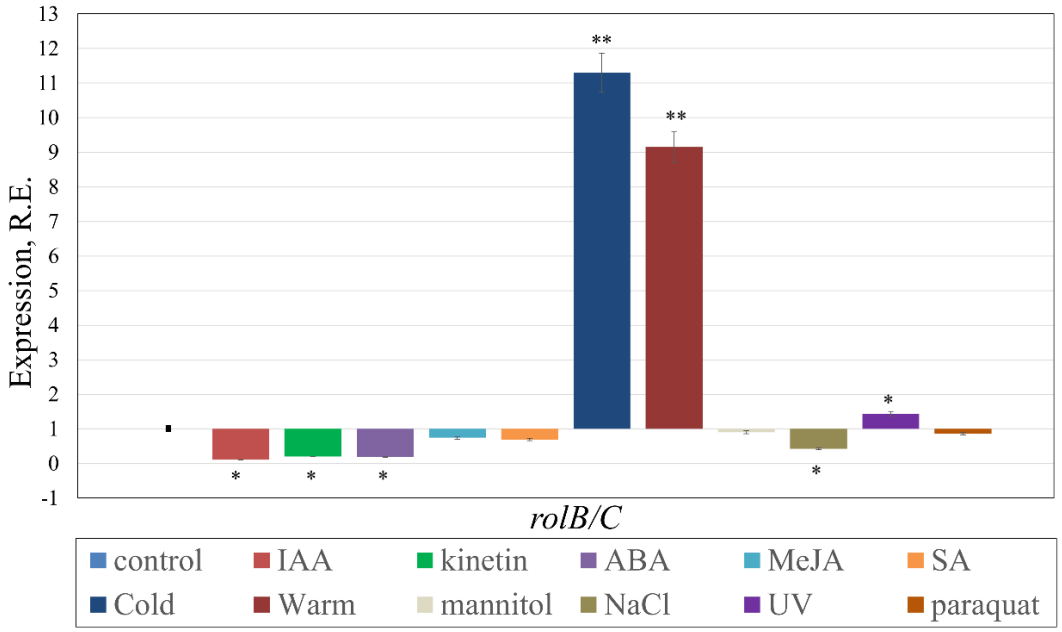

Figure 1 – The expression of *rolB/C* gene under different stimuli

As a model system to study the effects of *rolB/C* gene in a heterologous object, we obtained two independent transgenic lines of *Arabidopsis thaliana* plants (AtBC1 and AtBC2) and investigated their morphological and physiological features. Compared to the non-transformed Columbia-0 (Col-0) plant, AtBC1 and AtBC2 lines showed various phenotypic changes: apical dominance effect, changes in plant height, internodes and petioles length, number of lateral roots, and significantly wider leaf plates. In addition, the effect of early flowering was noted - the number of true rosette leaves at the start of flowering of plants in the control group was 14, while in *rolB/C*-the number of leaves was 10.

To determine the functional properties of the *rolB/C* gene, the content of major plant hormones and the accumulation of phytoalexins were examined by analytical liquid chromatography with mass spectrometry. We

found that the content of IAA and SA increased in the AtBC1 and AtBC2 lines by 4.5 and 1.5 times, respectively, compared with the control, while the concentration of ABA remained at the same level. Overexpression of the *rolB/C* gene also caused significant changes in the content of secondary metabolites (Table 1). In particular, the content of flavonoid glycosides in transgenic plants increased 1.6 -1.8- fold, while the level of accumulation of glycosinolates, both indole and aliphatic, decreased 1.6-fold. One of the interesting effects we found was the induction of the synthesis of camalexin, a metabolite with antibacterial properties. The content of this compound in AtBC1 and AtBC2 lines increased 21-fold compared to the control. The transgene effect in all described cases was more pronounced in the AtBC2 line, which correlates with the level of *rolB/C* expression in transgenic plants.

Table – Content of secondary metabolites in control (Col-0) and transgenic (AtBC1 and AtBC2) plants of *A. thaliana*

Metabolite group	Col-0, μM/g	AtBC1, μM/g	AtBC2, μM/g
Flavonoid glycosides	2,74±0,19	4,40±0,30	5,02±0,35
Indole glycosinolates	0,62±0,03	0,48±0,02	0,39±0,02
Aliphatic glycosinolates	0,76±0,02	0,61±0,02	0,48±0,01
Camalexin	0	0,03±0,01	0,21±0,01

In this work, we first isolated and studied some functional features of the plast *rolB/C* gene from the naturally transgenic plant *I. batatas*. It was found that the expression of this gene in the plant is induced by temperature stress. On the other hand, the *rolB/C* gene itself activates the accumulation of valuable secondary metabolites with high potential biotechnological applications. Based on the data obtained, we can also assume that the *rolB/C* gene is involved in modulation of plant hormonal status pathways. Understanding how these circumstances affect the plant will help to understand the functional characteristics of RolB/C in sweet potatoes.

Financial support was provided by the Russian Science Foundation, Grant no. 22-24-00082 (Y.N. Shkryl).

References

1. Matveeva, Tatiana & Sokornova, Sonie., 2017. Biological traits of naturally transgenic plants and their evolutional roles. Russian Journal of Plant Physiology. 64. 635-648

2. Matveeva TV, Otten L. Widespread occurrence of natural genetic transformation of plants by Agrobacterium. Plant Mol Biol. 2019 Nov;101(4–5):415-437.

3. Kyndt T, Quispe D, Zhai H, Jarret R, Ghislain M, Liu Q, Gheysen G, Kreuze JF. The genome of cultivated sweet potato contains Agrobacterium T-DNAs with expressed genes: An example of a naturally transgenic food crop. Proc Natl Acad Sci U S A. 2015 May 5;112(18)

Yusupova E.P [1], Ardeeva G. L.[2]

COMPARATIVE ANALYSIS OF THE PSYCHOPHYSIOLOGICAL RESPONSE TO STRESS IN ANIMALS AND HUMANS

[1] Far Eastern Federal University, World Ocean Institute (School), FEFU
[2] Far Eastern Federal University, Oriental Institute School of Regional and International Studies, FEFU
Scientific consultant–O.K.Titova[2]

The life of any person and animal is impossible without stress. And stress is part of our daily experience. Since the nervous and endocrine systems are the main regulatory systems of the body, changes in their function are accompanied by changes in almost all other organs and organ systems.

By its biological nature, stress is an adaptive response that occurs under the influence of unusual,

extraordinary or extreme influences on the body, contributing to the body's adaptation to new conditions. However, a sufficiently strong and prolonged exposure of the body to a stressor can cause a breakdown of compensatory reactions and homeostasis disruption.

The effect of stress is realized through the receptors of the peripheral nervous system, emotional stress can be induced through the visual, auditory and other analyzers. Receptor stimulation causes activation of the autonomic nervous system, mainly its sympathetic section, and intensification of formation of a number of releasing factors in the hypothalamus. The hypothalamus, in turn, stimulates the secretion of ACTH, TSH, STH by the anterior pituitary lobe. By eaching the adrenal cortex, ACTH stimulates the secretion of glucocorticoids (cortisol or corticosterone). Under the influence of sympathetic stimuli, catecholamine (epinephrine, norepinephrine, dopamine) is released from the adrenal medulla. In parallel with the leading mechanisms of stress, there is an increased production of somatotropic hormone, increased formation of thyroxine and triiodothyronine. There is also an activation of the "stress-limiting systems".

Humans and animals have similar physiological and mental responses to stress.

Table 1

Similar signs of stress in animals and humans

Animals	Humans
Fidgeting, nervousness, tremor	
Greedy swallowing of food, tendency to chew/swallow inedible objects	Eating disorder
Compulsive movements	Signs of obsessive-compulsive disorder
Unmotivated aggressive behavior	Irascibility, aggression

References

1. Vinogradov V.V. Hormones, adaptation and systemic reactions of the body. - M.: 1989. - 222 p.
2. V.F. Lysov [and others] Physiology and ethology of animals.; ed. IN AND. Maksimov. - M.: KolosS, 2012. - 605 p.
3. Smolin, S.G. Physiology of man and animals [Electronic resource] / S.G. Smolin; Krasnoyar. state agrarian un-t. – Krasnoyarsk, 2011.

Popkova D.V.[1,2], Sintsova O.V.[2], Palikov V.A.[3], Dyachenko I.A.[3,4]

DETERMINATION OF THE EFFECTIVENESS OF PEPTIDE α-AMYLASE INHIBITORS FOR THE REDUCTION OF POSTRANDIAL HYPERGLYCEMIA IN TYPE 1 DIABETES MELLITUS

[1] Department of Chemistry and Materials IHTAM FEFU
[2] G.B. Elyakov Pacific Institute of Bioorganic Chemistry FEB RAS
[3] Shemyakin - Ovchinnikov Institute of Bioorganic Chemistry RAS
[4] 'Pushchino' "Nursery of laboratory animals" FIBC RAS
[5] Institute of Oriental Studies - School of Regional and International Studies, FEFU
Scientific adviser – O. V. Sintsova [1]
Scientific consultant – I. N. Lazareva [5]

Maintaining a stable postprandial (after eating) blood glucose level in diabetes mellitus is the most important task for ensuring the normal functioning of the body. One of the ways to avoid hyperglycemia is the inhibition of pancreatic α-amylase, which hydrolyzes the main food polysaccharide, starch, which significantly reduces the entry

of glucose into the blood from the gastrointestinal tract. Pharmaceutical preparations miglitol (Glyset™), voglibose (Voglib™) and acarbose (Precose™ or Glucobay™) reduce the activity of α-glucosidases, however, due to the low inhibitory activity, the use of high concentrations of the active substance is required, which leads to side effects from the gastrointestinal tract, nervous system, and liver [1]. It has been shown that the peptides magnificamide and magnificamide-II isolated from the sea anemone *Heteractis magnifica* have a high inhibitory activity against salivary and pancreatic α-amylases, and therefore can be used as a therapeutic agent for controlling glucose levels in type 1 and type 2 diabetes, as well as in obesity [2]. Based on this, the aim of the work is to obtain recombinant α-amylase inhibitors, magnificamide and magnificamide II, and determine their effectiveness in a model of induced type 2 diabetes mellitus.

The use of recombinant DNA technology makes it possible to obtain biologically active substances of a protein nature using bacterial or yeast systems without the laborious process of isolating native molecules. Recombinant magnificamide was obtained in *Escherichia coli* cells of the SHuffle® strain, which allows expressing proteins with a high content of disulfide bonds [3]. As a result of the isolation of the target peptide by a combination of metal affinity chromatography, refolding [4], treatment with enterokinase, and final purification by RP-HPLC, 6 mg per 1 liter of cell culture was obtained. Magnificamide-II was obtained according to a similar scheme with a yield of 8 mg/l of cell culture.

To determine the biological activity of the obtained recombinants *in vivo*, a model of metabolic syndrome of the type 1 diabetes mellitus caused by streptozocin was developed and put into mice. Male ICR mice were divided into groups, after which type 1 diabetes was induced by intraperitoneal injection. On day 14, after the development of hyperglycemia, a starch tolerance test was performed at a dose of 3 g/kg of body weight. The test peptides at concentrations of 0.1, 0.01, 0.005 and 0.0025 mg/kg were orally administered to mice 30 or 45 minutes before starch. Inhibition efficacy was measured relative to the action of the antidiabetic drug acarbose (Glucobay™) at a dose of 3 mg/kg. The measurements were performed on an empty stomach before the introduction of starch and then after 30, 60, 90 and 120 minutes after. As a result, it was shown that the magnificamide at doses of 0.1 and 0.005 mg/kg and magnificamide-II at doses of 0.01 and 0.005 mg/kg have the most effective inhibitory effect compared to acarbose and allow maintaining lower blood glucose concentrations.

This work was supported by the Russian Science Foundation grant no. 21-74-20147.

References

1. Tarling, C.; Woods, K.; Zhang, R.; Brastianos, H.; Brayer, G.; Andersen, R.; Withers, S. The Search for Novel Human Pancreatic α-Amylase Inhibitors: High-Throughput Screening of Terrestrial and Marine Natural Product Extracts. ChemBioChem. 2008, V. 9. P. 433–438, doi: 10.1002/cbic.200700470.

2. Sintsova, O.; Gladkikh, I.; Kalinovskii, A.; Zelepuga, E.; Monastyrnaya, M.; Kim, N.; Shevchenko, L.; Peigneur, S.; Tytgat, J.; Kozlovskaya, E.; Leychenko, E. Magnificamide, a β-Defensin-Like Peptide from the Mucus of the Sea Anemone Heteractis magnifica, Is a Strong Inhibitor of Mammalian α-Amylases. Mar. Drugs. 2019, V. 17, P. 1–15, doi:10.3390/md17100542.

3. Lobstein, J.; Emrich, C. A.; Jeans, C.; Faulkner, M.; Riggs, P.; Berkmen, M. SHuffle, a novel Escherichia coli protein expression strain capable of correctly folding disulfide bonded proteins in its cytoplasm. Microbial Cell Factories. 2012, V. 11. doi:10.1186/1475-2859-11-56.

4. Logashina, Y.; Korolkova, Y.; Maleeva, E.; Osmakov, D.; Kozlov, S.; Andreev, Y. Refolding of disulfide containing peptides in fusion with thioredoxin. Mendeleev Communications. 2020, V. 30. P. 214–216. doi: 10.1016/j.mencom.2020.03.028.

Section II
CHEMISTRY AND CHEMICAL TECHNOLOGY

Rastorguev V.L.[1], Samus M.A.[1], Gribova V.V.[1], Kolycheva V.B.[2]

THE APPLICATION POSSIBILITY OF POLYCOBALTPHENYLSILOXANE FOR THE METHYL ORANGE DESTRUCTION

[1]Far Eastern Federal University, Institute of High Technologies and Advanced Materials
[3]Far Eastern Federal University, Oriental Institute School of Regional and International Studies
Scientific adviser - V.V. Gribova[1]
Scientific consultant - V.B. Kolycheva[2]

An actual problem is the treatment of wastewater from various substances of organic nature since the low effectiveness of treatment applying standard biological methods. Nowadays the most relevant methods involve the use of such promising oxidative processes as the generation of hydroxyl radicals. According to [1], the most efficient processes are the oxidation of organic compounds with hydrogen peroxide in the presence of metal ions of variable valence (Fe^{2+}, Cu^{2+}, Mn^{2+}, Co^{2+}); such catalysts should operate in different pH ranges and metal ions should be firmly fixed on the surface of the support. Polymetalloorganosiloxanes containing transition metal atoms are promising materials [2]. Amorphous silicon dioxide (characterized by a high specific surface area, chemical resistance and lack of toxicity) is widely used as a carrier.

Samples of amorphous silicon dioxide were obtained by hydrolysis of raw materials with 1M sodium hydroxide solution, followed by precipitation of silica with hydrochloric acid solution. Polycobaltphenylsiloxane (PCoPS) was obtained by the exchange decomposition method in the DMSO-toluene system according to the following scheme:

$$(PhSiO1{,}5)n + nNaOH = (PhSi(O)ONa)n$$

$$2(PhSi(O)ONa)n + nCoCl2 = \{(PhSiO1{,}5)2CoO\}n + 2nNaCl$$

The resulting dark gray polymer was in an amorphous state at room temperature. According to gel permeation chromatography (GPC), the molar mass of the substance was more than 5000 not containing low molecular weight fractions. The polymer was characterized by physicochemical methods of analysis: elemental analysis, IR, XRF.

Composites were obtained by applying polycobaltphenylsiloxane on silicon dioxide under various conditions. To obtain PCoPS/SiO_2-1 and PCoPS/SiO_2-2 composites, the resulting polymer was dissolved in toluene (mass concentration of polymer to silicon dioxide 1:1); silicon dioxide was placed in the polymer solution and stirred for 48 hours at room temperature. Then, the solvent was removed from the PCoPS/SiO_2-1 composite by evaporation, and upon preparation of the PCoPS/SiO_2-2 composite, the system was separated by filtration into soluble and insoluble. The PCoPS/SiO_2-3 composite was obtained by treating silicon dioxide with a boiling mixture of solvents toluene-butanol (2:1) with separation of water into a Dean-Stark trap.

All obtained composites were tested for catalytic activity in the destruction of methyl orange in the presence of hydrogen peroxide and UV irradiation.

References

1. V.V. Emzhina, S.N. Mirzoeva, N.A. Ivantsov. Advances in chemistry and chem. technology. XXVIII, 5, 22-25 (2014).

2. O.D. Arefieva, M.A. Samus, A.I. Pisartseva, S.G. Krasitskaya, M.V. Vasilyeva, N.V. Maslova. Photo-Fenton degradation of methyl orange using heterogeneous catalysts based on polyphenylferrosiloxane. Chemical

safety. 4, 117-130 (2020).

Bedareva A.K.[1]

PRODUCTION OF LEAD-FREE CERAMICS BCZT BY HYDROTHERMAL SYNTHESIS

[1]Tomsk Polytechnic University, Engineering School of Nuclear Technologies, TPU
Scientific adviser – R.A. Surmenev [1]

In our study, hydrothermal synthesis of $Ba_{0,85}Ca_{0,15}Ti_{0,9}Zr_{0,1}O_3$ was carried out in order to synthesize lead-free ceramics. Due to excellent properties such as high d_{33} and k_p, lead zirconate titanates (PZT) have been commercially used as piezoelectric materials in many fields for more than half a century. However, recently considerable attention has been paid to the development of lead-free piezoceramics due to some environmental problems [1]. For a long period of time, the $Ba_xCa_{1-x}Ti_yZr_{1y}O_3$ system attracted considerable attention, as a leading candidate, and was considered to be a promising lead-free piezoceramics. The study demonstrates that lead-free piezoceramics combined with a biodegradable piezopolymer can lead to the creation of bioflexible piezoelectric nanogenerators with outstanding characteristics and particularly useful in autonomous medical devices.

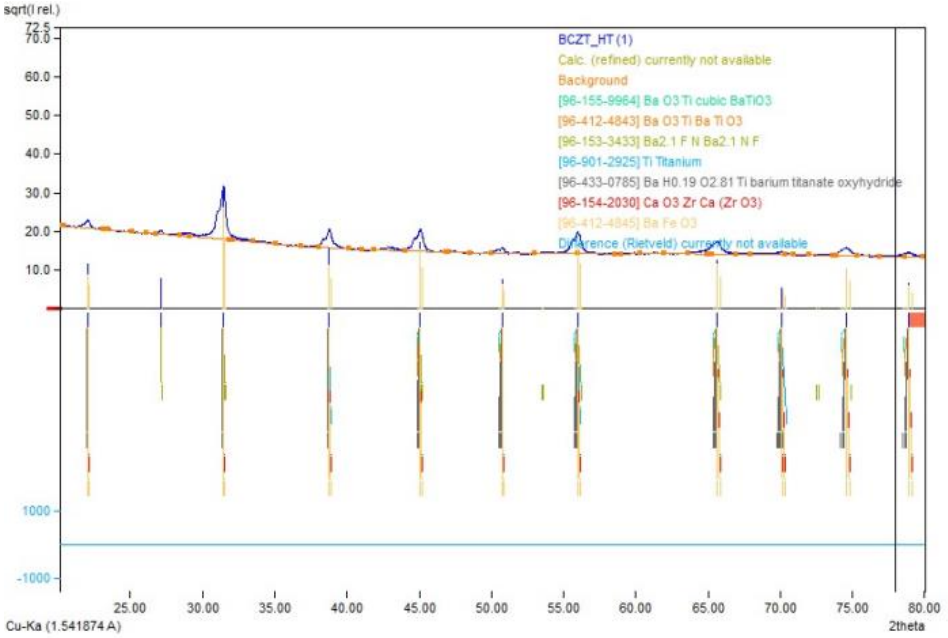

Fig. 1. The results of X-ray diffraction analysis

$Ba_{0.9}Ca_{0.1}Ti_{0.9}Zr_{0.1}O_3$ ceramics with Nd^{3+} doping were prepared by a hydrothermal method. The $BaCl_2{\cdot}2H_2O$ (SCRC), $CaCl_2$, $TiCl_4$, $ZrOCl_2{\cdot}8H_2O$ and $Nd(NO_3)_3$ were used as raw materials. $BaCl_2{\cdot}2H_2O$, $CaCl_2$, $ZrOCl_2{\cdot}8H_2O$ and $Nd(NO_3)_3$ were first dissolved in distilled water separately and then were mixed. The $TiCl_4$ was added into the mixtures dropwise to obtain the precursors. Finally, the NaOH was added to regulate the pH>14. The three precursors were put into the heating-autoclave; then, the distilled water was added until the total volume reached ~80% of the autoclave. The hydrothermal reactions were carried out at 180 °C for 10 h and finally the three powders were mixed and dried. After that, the powder was pressed into pellets of 12 mm diameter, and the pellets were sintered at 1280 °C for 10 min under microwaves. The crystal structure was examined by using an X-ray diffraction system with Cu Ka radiation [2].

References

1. Leontsev S.O. Progress in engineering high strain lead free piezoelectric ceramics/ S.O. Leontsev, R.E. Eitel. — M.: Sci Technol Adv Mater, 2010. — 13 p.

2. Takenaka T. Current status and prospects of lead-free piezoelectric ceramics/ T. Takenaka, H. Nagata.

– J.: Eur Ceram Soc, 2005. – 2693-2700 p.

Khisamova M.N.[1], Stepanov E. S.[2], Krasitskaya S.G. [1], Kolycheva V.B. [3]

STUDY OF THE MIXING PROCESS OF CEMENT COMPOSITIONS MODIFIED WITH ORGANOSILICON COMPOUNDS BY THERMOGRAVIMETRY

[1]Department of Materials Chemistry, Institute of High Technologies and Advanced Materials, FEFU
[2] Depatment of Nuclear technologies, Institute of High Technologies and Advanced Material, FEFU
[3]Academic Dep. of English Language, Oriental Institute School of Regional and International Studies, FEFU
[1]Scientific adviser – S.G. Krasitskaya
[3]Scientific consultant – V.B. Kolycheva

Obtaining a new generation of concrete with special properties is impossible without the use of additives to modify the properties of concrete mixtures. The introduction of additives is one of the most technological, flexible, affordable and versatile ways to improve all the properties of concrete mixtures and concretes and give them new properties, as well as reducing labor costs, cement consumption, saving heat and electricity, improving technology, increasing the productivity of enterprises of building industry. To improve the properties of concrete, various modifiers are used, and organosilicon compounds occupy a special place.

Organosilicon compounds are widely used in construction for plasticizing concrete mixtures, imparting hydrophobic properties to structures and materials, to increase the corrosion resistance and frost resistance of concrete and reinforced concrete structures, especially in aggressive environments such as sea water. Various polyorganosiloxanes are commonly used for such purposes: liquids, alkyl silicones of alkali metals, resins, as well as compositions based on them and elastomers (sealants). Such materials not only increase the service life of building structures, but also reduce operating costs. Therefore, they are of great national economic importance.

It is well known, that the formation of calcium hydroxide during hydration of cement compositions reduces the mechanical strength and frost resistance of cement stone. Therefore, the process of cement hydration for 28 days and the effect on it of silicone-organic modifiers reducing the formation of calcium hydroxide and thereby improving the performance characteristics were investigated. The content of adsorption water and water formed during the decomposition of calcium hydroxide was determined by TGA method.

The modification was carried out by mechanochemical activation according to the method described in the literature [1]. Low-molecular-weight heat-resistant synthetic rubber (LSR) and polyphenylsiloxane (PPS) were used as modifiers. Cement compositions were grouted for 28 days. During this time, the cement stones were examined by thermogravimetry after 3 days, 7 days, and 28 days after curing. The results of thermogravimetric analysis are presented in Table 1.

Table 1

Results of thermogravimetric analysis of modified cements

			LSR		PPS	
			Water yield content at temperature ±100, %	Water yield content at decomposition $Ca(OH)_2$, %	Water yield content at temperature ±100, %	Water yield content at decomposition $Ca(OH)_2$, %

Based on the data in Table 1. we can conclude that the percentage of dehydration of cements with the PFS modifier increased during aging of cement samples, but less than that of SKTN.

The cement composition without the modifier was also set to compare how well the modifier binds water in the cement composition. The data are shown in Table 2.

Table 2

Results of thermogravimetric analysis of cement without modifier

Number	Water yield content, %	Output temperature, °C	Water yield content at decomposition $Ca(OH)_2$, %	Output temperature, °C
1	10.1	102	1.9	460
2	11.1	102	2.2	457
3	12.1	100	2.7	463

Comparing the results given in Tables 1 and 2, we can conclude that during aging of cement samples with modifiers compared to pure cement, the formation of calcium hydroxide in the modified samples either decreases or remains virtually unchanged.

References

1. Tokar, E.A. Synthesis of polycalciumphenylsiloxane and study of the possibility of its introduction as a modifier of cement compositions / E.A. Tokar. - Vladivostok: FEFU, 2017. - 60 p.

Vashchenko M.V.[1]

SYNTHESIS OF FUNCTIONAL DERIVATIVES OF 2,3,4,5,6,7-HEXAHYDROBENZOFURAN BY THREE-COMPONENT CONDENSATION

[1]Far Eastern Federal University, Institute of High Technologies and Advanced Materials
[2] Far Eastern Federal University, Oriental Institute School of Regional and International Studies
Scientific adviser – A.N. Andin[1]
Scientific consultant - V.B. Kolycheva[2]

In recent times a significant number of studies have been devoted to functional derivatives of furan, 2,3-dihydrofuran, as well as to their fused and spiro analogous. This is due to the availability of initial reagents and the possibility of obtaining products with useful properties, in particular, with potential biological activity. Thus, the literature gives information on the antibacterial [1] and hypocholesterolemic [2] activity of compounds containing the spirodihydrofuran fragment. Derivatives obtained from aldehydes and cyclic 1,3-diketones may have fungicidal [3] and insecticidal [4] activity. Also, the tetrahydrobenzofuran system is part of a number of natural compounds, for example, evodone, calaminthone.

We have studied the three-component condensation of 2-bromodimedone, aromatic aldehydes and

malononitrile. The reaction was carried out in ethanol-pyridine solution in the presence of catalytic amounts of piperidine using the in one pot methodology. The mixture was kept at 75-80 ° C for 2 hours, as a result, functional derivatives of 2,3,4,5,6,7-hexahydrobenzofuran **1** were isolated with yields of 63- 97%.

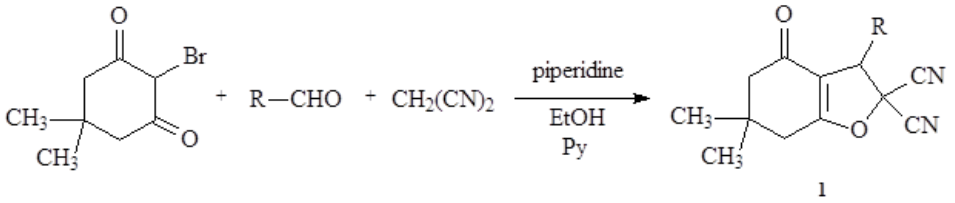

1

R = Ph, 4-$CH_3OC_6H_4$, 4-FC_6H_4 , 2,4-$Cl_2C_6H_3$

The structure of the obtained compounds has been proved by NMR and IR spectroscopy.

References

1. Antibacterial properties of 3H-spiro[1-benzofuran-2,1'-cyclohexane] derivatives from Heliotropium filifolium / A. Urzúa, J. Echeverría, M.C. Rezende, M. Wilkens // Molecules. - 2008. - Vol. 13. - P. 2385-2393.

2. Synthesis and pharmacological evaluation of a clofibrate-related tricyclic spirolactone, 5-chloro-4',5'-dihydrospiro[benzofuran-2(3H),3'(2'H)-furan]-2'-one / D.T. Witiak, R.C. Cavestri, H.A. Newman, J.R. Baldwin, C.L. Sober, D.R. Feller // J. Med. Chem. - 1978. - Vol. 21. - P. 1198-1202.

3. Dimedone derivative of dialdehydes / R.G. Tabor // Patent US № 3904693, 1975.

4. Thiazolyl-substituted carbocylic 1,3-diones as pesticidal agents / R. Fischer, A. Ullmann, A. Trautwein, M.W. Drewes, C. Erdelen, A. Lubos-Erdelen, P. Dahmen, D. Feucht, R. Pontzen, K.H. Kuck, U. Wachendorff-Neumann // Patent US № 0135630, 2007.

D.A. Nikolaeva [1], O.D. Arefieva [1,2,4], M.S. Vasilyeva [3,4], P.S. Minakova [5]

MODIFICATION OF Bi_2O_3/Bi_2SiO_5 OXIDE HETEROSTRUCTURE BY GOLD NANOPARTICLES

[1]Department of Petroleum Technology and Petrochemistry, Polytechnic Institute, FEFU
[2]Department of Nuclear Technology, Institute of Science-Intensive Technologies and Advanced Materials, FEFU
[3] Dep. of Chemistry and Materials, Institute of Science-Intensive Technologies and Advanced Materials, FEFU
[4]Institute of chemistry, Far East Branch, Russian Academy of Sciences
[5]Academic Department of English Language, FEFU, PhD in Education, Associate Professor
Scientific adviser – O.D. Arefieva [1,2,4]

Heterogeneous photocatalysis has become one of the promising methods of water treatment over the past two decades due to the effective non-selective decomposition of organic pollutants with the formation of non-toxic products. Therefore, the creation of new effective photocatalysts is one of the most promising directions in modern materials chemistry. Bi_2O_3/Bi_2SiO_5 heterostructured photocatalysts are of interest due to their simple methods of production, non-toxicity and thermal stability [1]. But despite several advantages, they show low sensitivity to visible light. Therefore, the purpose of this work was to study the photocatalytic activity of gold-modified Bi_2O_3/Bi_2SiO_5 heterostructured photocatalysts.

In this work, a photocatalytically active Bi_2O_3/Bi_2SiO_5 oxide heterostructure was obtained. Biogenic silica from rice husk (RH) of the "Valley" variety was used as a source of silicon oxide. The biogenic silica sample was obtained by hydrolysis of RH with 1 M sodium hydroxide solution followed by precipitation of silica with concentrated hydrochloric acid solution to pH 5-6 [2]. The photocatalyst was obtained by a simple mechanical stirring method without the use of any solvents [3].

An oxide Bi_2O_3/Bi_2SiO_5 heterostructure modified with gold nanoparticles by the impregnation method was

synthesized [4]. Biogenic silica from RH, also modified by gold nanoparticles by the impregnation method, was used as a control sample.

The elemental analysis of the photocatalyst samples was performed using energy dispersive X-ray fluorescence analysis on an EDX 800 HS spectrometer (Shimadzu, Japan).

The photocatalytic properties of the obtained samples were evaluated using the degradation reaction of Methyl Orange (pH 6.8) under UV, xenon, and sunlight irradiation. The concentration of Methyl Orange (MO) was 10 mg/L. SiO_2, SiO_2-Au, 4-Bi-Si and 4-Bi-Si-Au samples were used as photocatalysts. The catalyst loading was determined at the rate of 1 g of catalyst per 1 L of MO solution.

Studies of the elemental composition of unmodified and modified photocatalysts showed that after calcination of 4-Bi-Si and 4-Bi-Si-Au samples the silica content slightly increased. This is due to the decomposition of $Bi(NO_3)_3$, which leads to a decrease in sample mass. The gold content after modification in the control sample and in the photocatalyst is the same and amounts to 0.14 %.

The results of photocatalytic tests showed that the gold-modified Bi_2O_3/Bi_2SiO_5 heterostructures exhibit higher photocatalytic activity in the degradation reaction of Methyl Orange, under solar and xenon light irradiation. Under UV irradiation, the modified samples show almost the same activity as the unmodified samples, which is 77%. Gold modification affects the activity of the samples when irradiated with sunlight and xenon light. Their photocatalytic activity increases in sunlight from 10% to 32%, in xenon light from 0% to 23%.

In the same work, the duration of sunlight irradiation after UV, sunlight and xenon exposure on the degree of dye degradation using 4-Bi-Si-Au catalyst was studied. With increasing time of solar exposure after UV irradiation, the degree of MO degradation increases from 77 % to 96 %, after solar - from 32 % to 63 %, after xenon - from 23 % to 71 %.

Thus, a photocatalytically active heterostructural Bi_2O_3/Bi_2SiO_5 photocatalyst modified with gold by the impregnation method was obtained in this work. According to the energy dispersive X-ray fluorescence analysis it was found that the synthesized samples contain gold compounds. It was shown that the gold-modified Bi_2O_3/Bi_2SiO_5 heterostructure exhibits rather high photocatalytic activity in the oxidation reaction of Methyl Orange under irradiation with UV, solar and xenon light.

References

1. Ionic liquid-assisted preparation of thin Bi_2SiO_5 nanosheets for effective photocatalytic degradation of RhB / L. Dou, Y. Xiang, J. Zhong [et. al.]. – DOI 10.1016/j.matlet.2019.127117 // Materials Letters. – 2020. – Vol. 261. – P. 1-4.

2. Properties of Amorphous Silica Produced from Rice and Oat Processing Waste / L. A. Zemnukhova, A. G. Egorov, G. A. Fedorishcheva [et. al.]. // Inorganic Materials. – 2006. – Vol. 42. № 1. – P. 27-32.

3. A high-performance Bi_2O_3/Bi_2SiO_5 p-n heterojunction photocatalyst induced by phase transition of Bi_2O_3 / H. Lu, Q. Hao, T. Chen [et. al.]. – DOI 10.1016/j.apcatb.2018.05.069 // Applied Catalysis B: Environmental. – 2018. – Vol. 237, № 5. – P. 59–67.

4. Preparation of supported gold nanoparticles by a modified incipient wetness impregnation method / L. Delannoy, N. E. Hassan, A. Musi, [et. al.]. – DOI 10.1021/jp062130l // Journal of Physical Chemistry B. – 2006. – Vol. 110, N 45. – P. 22471-22478.

Galimova D.A. [1], Kovekhova A.V. [1,2,3], Arefieva O.D. [1, 2, 3], Minakova P.S. [4]

OBTAINING BIOSORBENTS FROM SUNFLOWER STEMS

[1]Department of Petroleum Technology and Petrochemistry, Polytechnic Institute, FEFU
[2]Dep. of Chemistry and Materials, Institute of Science-Intensive Technologies and Advanced Materials, FEFU
[3]Institute of Chemistry, Far Eastern Branch, Russian Academy of Sciences
Scientific Adviser – PhD in Chemical Science, Associate Professor A.V. Kovekhova [1,2,3,]
[4] Academic Department of English Language, FEFU, PhD in Education, Associate Professor P.S. Minakova

The use of agricultural waste is of great interest especially from the point of view of creating resource-saving technological processes,. Nowadays numerous researches are aimed at the search for the replacement of traditional sorbents by the materials obtained from secondary raw materials, in particular agricultural wastes. Sorbents derived from renewable plant raw materials are an organic part of the ecosystem and meet the international environmental requirements to the greatest extent.

The annual sunflower, which is grown practically all over the world, can be one of them. Its production waste in the form of stems is a cheap and available raw material for lignocarbon sorbents.

Purpose of work: obtaining and research of biosorbents from sunflower stems.

Samples of sunflower stems (Heliánthus ánnuus) collected in the Khasan district of Primorsky Krai were used as an object of the study. The stems were dried to air-dry and ground to a particle size of 1-5 mm.

Experimental studies of the dried and crushed separate component of sunflower stalks – outer shell - were conducted in this work.

A sample of crushed outer part of sunflower stems was placed in a heat-resistant beaker, distilled water, a solution of hydrochloric acid (0.1 mol/L), phosphoric acid (0.1 mol/L), sulfuric acid (0.1 mol/L) or sodium hydroxide (0.1 mol/L) in the ratio S:L = 1:20 were added. Hydrolysis was carried out under heating to 90 °C for 1 h under stirring. Solid residue was filtered through filter paper "blue tape", washed with distilled water to neutral reaction of the medium and dried at 85 °C to constant weight. Characteristics of the composition of raw materials were determined according to [1]. The study of the chemical composition of wastewater formed in the process of biosorbents production was carried out by the main hydrochemical indicators. Color and turbidity were determined [2, 3]; chemical oxygen demand (COD) [4, 5]. These indicators were determined before the wastewater treatment process.

The research results showed that the outer part of the sunflower stalk contains: pentosans – 17 %, lignin – 29 %, cellulose – 51 %, pectin – 3 %, easily and hardly hydrolyzed polysaccharides – 13 and 31 %. The yield of substances soluble in cold water was 11.5 %, in hot water – 15.8 %.

The yield of biosorbent samples after their treatment with various extractants showed, the lowest yield is characterized by a sample treated with sodium hydroxide – 73 %, because in this case alkaline lignin and polysaccharides of alkaline extraction are extracted into the solution. The yield of samples after acid treatments are within the same limits and amounts to 76-79 %. Modification of sunflower stems with acids promotes the extraction of mainly acid extraction polysaccharides from biomass. The highest sample yield was 84 % after aqueous hydrolysis.

Table 1 shows the composition of wastewater generated in the production of biosorbents before treatment. Wastewater formed after acid, alkaline and water treatment is characterized by high values of color, turbidity, chemical oxygen demand (COD) and content of phenolic compounds.

Table 1

Wastewater quality indicators before treatment

Extractant	Indicators			
	Turbidity, mg/l	Color, deg.	COD, mgO/l	Phenolic acid equivalent, mg/l
H_2O	360	4500	13000	14.21
NaOH, 0.1 M	390	7000	24000	27.78
HCl, 0.1 M	140	1900	7900	18.60
H_2SO_4, 0.1 M	130	1200	4100	14.73
H_3PO_4, 0.1 M	85	900	8400	11.75

The study of sunflower outer part treatment wastewater showed that the wastewater is a mixture of organic compounds which mainly consists of polysaccharides, phenolic compounds and low molecular weight lignin.

References

1. Obolenskaya A. V. Laboratory work on the chemistry of wood and cellulose : textbook for universities / A. V. Obolenskaya, Z. P. Elnitskaya, A. A. Leonovich ; Moscow : Ecology, 1991. – 320 p. – ISBN 5 7120-0264-7.

2. GOST 31868-2012. Methods of determination of chromaticity / Protektor Limited Liability Company together with Closed Joint Stock Company "Water Research and Control Center". – Moscow : Standardinform, 2014. – 8 p.

3. GOST P 57164-2016. Methods of odor, taste and turbidity determination / developed by the Technical Committee on Standardization TC 343 "Water Quality" and CJSC "Center for Water Research and Control". – Moscow : Standardinform, 2019. – 18 p.

4. PU 21-2008. Practical recommendations for measurements of bichromate oxidation (chemical oxygen demand) on the fluid analyzer "Fluorat-02-2M" and "Fluorat-02-3M" : version 3 / developed by 21 LLC "Lumex-marketing". – Saint-Petersburg : Lumex-marketing, 2012. – [2], 8 p.

5. PND F 14.1:2:4.190-2003. Quantitative chemical analysis of waters. Methods of measurement of bichromatic acidity (chemical oxygen demand) in natural, potable and waste water samples by the photometric method using a Fluorat-02 liquid analyzer : 2012 edition / developed by Lumex-Marketing Ltd. – St. Petersburg, 2012. – [2], 24 p.

Petin. V.S.[1], Arefieva O.D.[1], Kovekhova A.V. [1], Kolycheva V.B. [2]

OBTAINING POTASSIUM ALUMINOSILICATES FROM RICE PRODUCTION WASTES

[1]Department of Petroleum and Gas Technologies and Petrochemistry, PI FEFU
[2]Academic Dep. of English Language, Oriental Institute School of Regional and International Studies, FEFU
Scientific advisers - O.D. Arefieva[1], A.V. Kovekhova[1]
Scientific consultant – V.B. Kolycheva[2]

Aluminosilicates constituting a vast group of silicates are formed from silicon dioxide (silica) and oxides of other elements. Aluminosilicates stand out among other classes of inorganic compounds and are of interest primarily due to the variety of functional properties depending on the structure and chemical composition [1].

Rice ranks second after wheat in terms of crop area in the world agriculture. For every ton of grain produced, at least 1.35 tons of rice straw remains in the fields. At various stages of rice processing solid wastes are generated, of which rice husk is 20 %. Based on the volume of rice production, the amount of rice straw and husk is obvious to be extremely large throughout the world [2-4].

Rice straw is unique compared with straw of other grains in little lignin and a lot of silica, as well as the presence of a fatty layer on the outer and inner surface of the straw, which has hydrophobic properties and has a

protective function. The content of mineral components in rice straw reaches 10-20 %, of which silica accounts for 80-95 % [2, 3].

Rice husk (RH) is a large-tonnage byproduct of rice production. The main components of RH are cellulose, lignin, and mineral ash, consisting of 92-97 % silica. This waste disposal represents an important technical task [2, 4].

The purpose of our work was to give a comparative characteristic of samples of potassium aluminosilicates from straw and rice hulls by physical and chemical characteristics.

Potassium aluminosilicate obtained from rice straw (different varieties, Far East breeding) and rice husk (variety "Cascade", Far East breeding) was used as the object of the study.

To obtain samples of potassium aluminosilicates, rice straw (husks) was taken and placed in a heat-resistant beaker of 2 L, pre-prepared KOH solution (64 g per 250 ml of water) was added, then 1 L of water was added and hydrolyzed. Hydrolysis was performed by heating to 90 ºC using an EKT Hei-Con apparatus (Heidolph, Germany) for 1 h under stirring. The hydrolysate was collected in a conical flask and a saturated solution of 7.5 g $Al_2(SO_4)_3 \cdot 18H_2O$ was added under stirring. Then the pH value was corrected to 7 using a solution of HCl (concentrated) and a pH meter. After that, the solution was incubated under slow boiling for 2 hours. The precipitated potassium aluminosilicate was washed by decantation with distilled water until colorless wash water was obtained and dried in the desiccator at 105ºC.

As a result, samples of potassium aluminosilicate from straw and rice hulls were obtained, whichwere powdery materials of light gray and beige color. The yield of the target product was 7.4 g for the straw and 10.7 g for the husk.

The samples were then examined for the following physico-chemical characteristics: mass fraction of water-soluble substances, pH of the aqueous extract, pH of the suspensions over time, and bulk density.

When the samples were boiled for 2 hours, water-soluble substances were better removed from the sample obtained from rice husk - 17.4 %, in contrast to the sample obtained from rice straw - 11.9 %.

The pH values of the aqueous extract of the samples obtained from rice hulls and rice straw ranged from 8.1 to 8.4. The alkaline effect of the interaction with water of the rice husk sample was slightly higher than that of the rice straw sample.

The determination results of the bulk density values of the studied samples were 376.7 kg/m^3 and 466.7 kg/m^3, respectively. determination of the bulk density value of the studied samples

Thus, the samples of potassium aluminosilicates obtained from straw (different varieties, Far East breeding) and rice husks (variety "Cascade", Far East breeding) were analyzed in the work. A comparative characteristic of the samples according to physico-chemical indices was given.

References

1. Regulation of sorption processes in natural nanoporous aluminosilicates. 2. Determination of the ratio between active sites / L. I. Belchinskaya, N. A. Khodosova, L. A. Novikova [et al.] // Physicochemistry of surface and protection of materials. - 2016. - T. 52, № 4. - P. 363-370.

2. Renewable sources of chemical raw materials: integrated waste processing of rice and buckwheat / V. I. Sergienko, L. A. Zemnukhova, A. G. Egorov [et al.] // Russian Chemical Journal. - 2005. - № 86. - P. 116-124.

3. Sustainable production of pure silica from rice husk waste in Kazakhstan / S. Azat, A. V. Korobeinyk, K. Moustakas, V. J. Inglezakis. – DOI 10.1016/j.jclepro.2019.01.142 // Journal of Cleaner Production. – 2019. – Vol. 217. – P. 352–359.

4. Quispe, I. Life Cycle Assessment of rice husk as an energy source. A Peruvian case study / I. Quispe, R. Navia, R. Kahhat. – DOI 10.1016/j.jclepro.2018.10.312 // Journal of Cleaner Production. – 2019. – Vol. 209. – P. 1235–1244.

Nomerovsky A.D.[1,2], Gnedenkov A.S.[1], Tsvetnikov A.K.[1], Sinebryukhov S.L.[1], Gnedenkov S.V.[1]

FORMATION AND INVESTIGATION OF PROTECTIVE COATINGS ON STEEL BY THE COLD SPRAY METHOD

[1]Institute of Chemistry FEB RAS
[2]Department of Chemistry and Materials, FEFU
[3]Academic Dep. of English Language, Oriental Institute School of Regional and International Studies, FEFU
[1]Scientific adviser –A.S. Gnedenkov
[3]Scientific consultant – V.B. Kolycheva

Steel structures are actively used in the manufacture of various products, including: railway tracks and trains, reinforced concrete structures (bridges, structures of structures, power lines, airfield slabs, etc.), water and heat supply pipes. Steel products are widely used in aggressive environments (acid gases, temperature extremes, UV radiation, static and dynamic loads)[1]. In this regard, the process of corrosion of steel structures is inevitable.

In order to protect steel from corrosion, a method of cold gas-dynamic spraying was proposed [2]. Cold gas-dynamic spraying (cold spraying, CS) is used to apply thick coatings or any components of arbitrary shape to the surface to be treated.[3]. CS method is a solid state processing method in which micron-sized particles are accelerated (at supersonic speed) towards the substrate at relatively low temperatures (up to 600 K) [4].

In this work, various types of coatings formed using the CS method were obtained on samples of steel St3 (S): copper-zinc coatings (SC) (thickness of the order of 50-70 μm); SC coatings followed by surface heat treatment up to 500°C (SC-500); SC-500 coatings friction coated with ultrafine polytetrafluoroethylene (UPTFE) (SC-500-FF); SC-500-FF coatings followed by heat treatment at 350°C (SC-500-FF-350). The electrochemical and morphological properties of steel samples were investigated, both without a protective layer and with a coating.

As a result of processing the samples by the CS method, the formed coating has good continuity and a low concentration of pores, which is confirmed by the analysis of the image of a transverse section obtained from a scanning electron microscope (SEM) (Figure 1). The obtained potentiodynamic curves (Figure 2) indicate an increase in the protective properties of the sample as a result of coating formation (corrosion current density for sample S is 14.2 μA/cm^2, for SC - 11.5 μA/cm^2 and for SC-500 - 3.7 μA/cm^2). The change in the corrosion potential of the samples is a consequence of the change in the potential of the determining reaction as a result of the formation of a protective coating (from -0.43 V for S to -0.94 V for SC and to -0.24 V for SC-500).

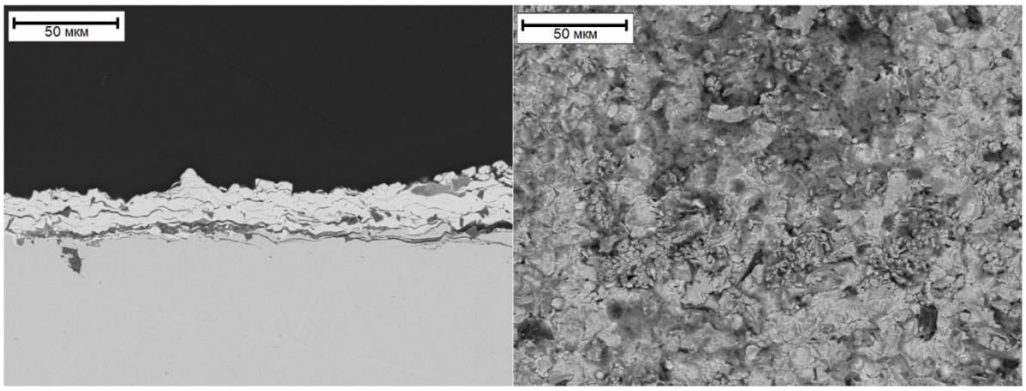

Figure 1 - SEM image of the cross section (left) and surface (right) of the SC sample

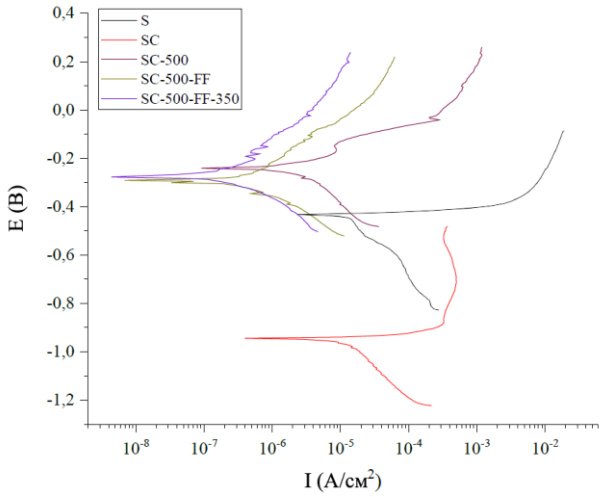

Figure 2 - Potentiodynamic curves obtained for a series of samples

The effect of UPTFE on the electrochemical properties of the coating was established, namely, the reduction in the corrosion current density to 0.8 μA/cm^2 for SC-500-FF and 0.5 μA/cm^2 for SC-500-FF-350. This is due to the uniform deposition of UPTFE on the sample surface and the creation of an additional barrier layer that protects the material from aggressive environmental influences. Annealing at 350°C of the sample coated with UPTFE did not significantly change the electrochemical properties of the sample.

This work was supported by the Russian Science Foundation grant no. 21-73-10148.

References

1. Adasooriya, N. D. Environment-assisted corrosion damage of steel bridges: A conceptual framework for structural integrity / N. D. Adasooriya, T. Hemmingsen, D. Pavlou. – DOI 10.1515/corrrev-2019-0066 // Corrosion Reviews - De Gruyter. – 2020. – Vol. 38, N 1. – P. 49-65.

2. Bonding mechanism in cold gas spraying / H. Assadi, F. Gärtner, T. Stoltenhoff, H. Kreye. – DOI 10.1016/S1359-6454(03)00274-X // Acta Materialia. – 2003. – Vol. 51, N 15. – P. 4379-4394.

3. An investigation into microstructure, tribological and mechanical properties of cold sprayed Inconel 625 coatings / Wu K., Sun W., Wei-Yee Tan A. [et al.]. – DOI 10.1016/j.surfcoat.2021.127660 // Surface and Coatings Technology. – 2021. – Vol. 424. – N 127660.

4. Current Research Status on Cold Sprayed Amorphous Alloy Coatings: A Review / Wang Q., Peng Han P., Yin S. [et al.]. – DOI 10.3390/coatings11020206 // Coatings. – 2021. – Vol. 11, N 2. – N 206.

Stafeeva M.A.[1], Frolov K.R.[1, 2]

ASSESSMENT OF THE CONSEQUENCES OF POSSIBLE ACCIDENTS AT RADIATION HAZARDOUS FACILITIES IN PRIMORSKY KRAI FOR PUBLIC HEALTH

[1] Department of Nuclear technologies, Institute of High Technologies and Advanced Material, FEFU
[2] Department of Oil, Gas and Petrochemical Industry, Polytechnic Institute, FEFU
[1, 2] Scientific adviser – K.R. Frolov

Introduction. The south of Primorsky Krai is the most saturated with radiation-hazardous objects part of the Russian Far East. Therefore, it is important to assess airborne transfer of radionuclides negative impact on the environment and human health. Radionuclides can get into the environment because of radiation accidents during disposal of nuclear reactors of the Navy facilities, during the management of spent nuclear fuel (SNF), and from radioactive waste (RW). Purpose of this work is to evaluate the consequences of radiation accidents at the Primorsky

Krai radiation-hazardous objects for the population health. Objectives: 1) to characterize radiation hazardous facilities of Primorsky Krai; 2) to calculate the spread of radionuclides in the air as a result of radiation accidents at these objects using Nostradamus software; 3) to assess the consequences of radiation accidents for public health.

Experiment. Radionuclide spreading was calculated for two radiation-hazardous facilities in Primorsky Krai: Far Eastern Plant Zvezda (DVZ Zvezda) in city of Bolshoi Kamen, and Far Eastern Center DalRAO (DVC DalRAO) in city of Fokino. The scenario considered for both facilities was a beyond design basis accident at nuclear reactor dismantlement facilities, namely a spontaneous chain reaction (SCR) during SNF unloading from a nuclear submarine. The simulations were performed in the Nostradamus software and based on the analysis of long-term weather observations in Bolshoi Kamen and Fokino in 2015-2020 [1, 2].

For each case of an accident, models of radioactive substances transfer were generated in the Nostradamus software. The parameter "Source of release" was formed based on literature data [2], where radionuclide activities in point sources simulating a smoke column at the height of 10 m are: ^{90}Sr (4.50-10^{12} Bq), ^{99}Tc (9.30-10^{8} Bq), ^{129}I (2.30- 10^{7} Bq), ^{134}Cs (2.50-10^{11} Bq). Forecasting and assessment of the consequences of radiation accidents included calculation and consideration of total dose (for 2 and 10 days) for the population exposed as a result of the accident, and comparison of the obtained values with the requirements of document SanPiN 2.6.1.2523-09 (NRB-99/2009).

Results and discussion. Figure 1 shows the spread of radioactive contamination for the hypothetical accident at the DVZ Zvezda in Bolshoi Kamen in winter time. The figure shows that the spread of contamination is directed to the south-west to Ussuriisk Bay, and then moves into the open sea. The total effective dose for 10 days in a radius of 50 meters will be 380 mSv, the maximum value is observed in a radius of 16 km and will be $1.7 \cdot 10^{4}$ mSv.

Exposure of the population as a result of the radioactive cloud spread will occur in the following settlements: Bolshoy Kamen (the maximum value of total effective dose for adults is 110 mSv in 9 minutes after the accident); Petrovka settlement ($3 \cdot 10^{-10}$ mSv, 16.5). According to SanPiN 2.6.1.2523-09 (NRB-99/2009) [4], these values imply that urgent interventions will not be required, as the whole body dose load does not exceed 1000 mSv during 2 days.

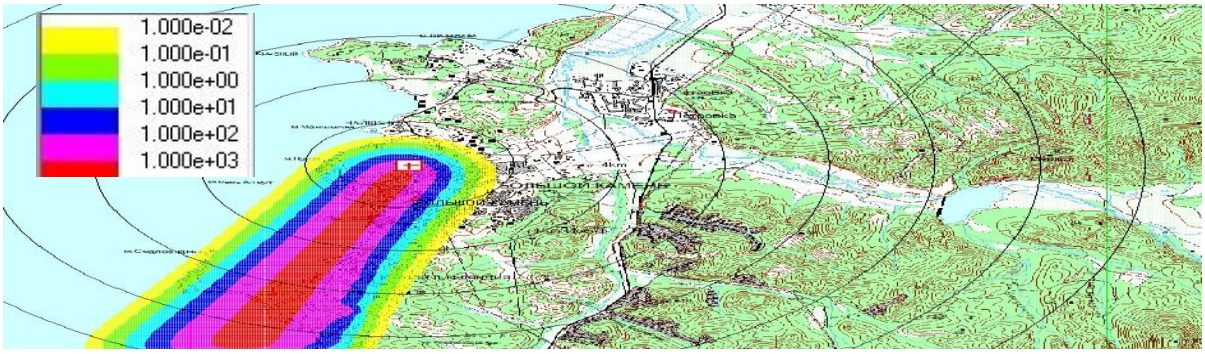

Figure 1 - Total effective dose over 10 days, DVZ Zvezda accident, mSv

Figure 2 shows the spread of radioactive contamination for DVC DalRAO facility in Razboinik bay, Fokino during the winter period.

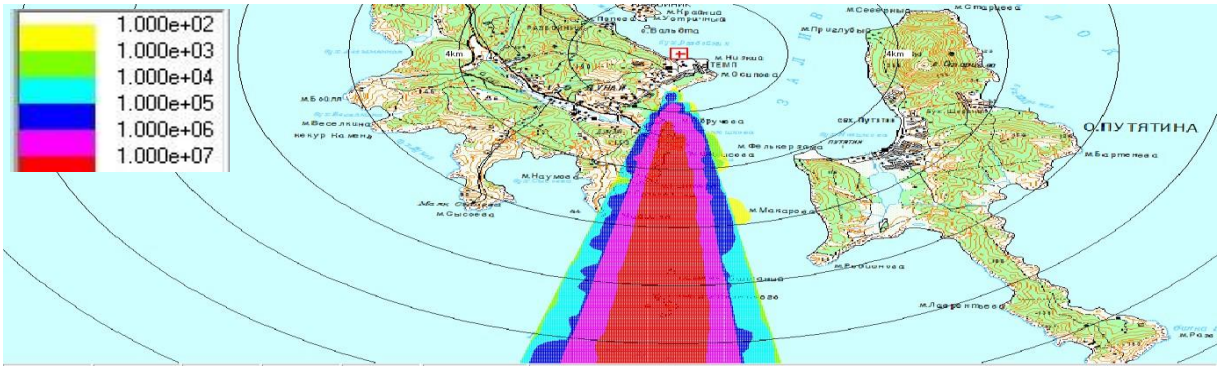

Figure 2 - Total effective dose over 10 days, DVC DalRAO accident, mSv

The spread of contamination is directed to the south, towards the uninhabited Askold island and to the open sea. The total effective dose for 10 days in the radius of 1.1 km will be 29.8 mSv, and the maximum value is observed in the radius of 10.5 km and will be $7.7\text{-}10^7$ mSv. Thus, the irradiation of the population as a result of the radioactive cloud spread in the nearest settlements will not occur. The plant's employees will be exposed to radiation.

Conclusions.

In case of an accident at DVZ Zvezda during the winter period, the maximum values of total effective dose in the town of Bolshoi Kamen reach 110 mSv, and in Petrovka – 800 mSv. According to the requirements of NRB-99/2009, no urgent interventions are required.

During the accident at the DVC DalRAO, the spread of contamination during winter period is directed to the northeast. It reaches maximum values around elevated terrain – unpopulated hills. There will be no irradiation of the population in the settlements closest to the facility.

In accordance with the requirements of NRB-99/2009, for all cases of accidents considered, urgent interventions are not required.

References

1. Gismeteo.Diary: Fokino weather diary : [website]. – GISMETEO.RU, 2021. – URL: https://www.gismeteo.ru/diary/12715/2015/1/ (Access date: 18.10.2021).

2. Gismeteo. Diary: The weather diary in Bolshoi Kamen : [website]. – GISMETEO.RU, 2021. – URL: https://www.gismeteo.ru/diary/12714/2020/1/ (Access date: 18.10.2021).

3. Radioecological Consequences of Operation and Disposal of Nuclear Fleet Facilities in the Far East Region / S. V. Antipov, V. D. Akhunov, V. P. Bilashenko [et al]. – Moscow: IBRAE RAS, 2010. – 388 c. – ISBN 978-5-9907220-3-3.

4. SP 2.6.1.2523-09. Norms of radiation safety (NRB-99/2009) : sanitary rules and regulations : official edition : approved and put into effect by the Decree of the Chief State Sanitary Doctor of the Russian Federation of 07.07.2009 № 47 : date of entry 14.08.2009 / developed by the Federal Budgetary Scientific Institution "Research Institute of Radiation Hygiene". [et al] – Moscow : Federal Center for Hygiene and Epidemiology Rospotrebnadzora, 2009. – 100 p.

Artemova M.I.[1], Artemov P.M.[1], Frolov, K.R.[1, 2]

MINING-CHEMICAL AND MINING PLANTS WASTEWATER TREATMENT USING ARTIFICIAL GEOCHEMICAL BARRIERS

[1] Department of Oil, Gas and Petrochemical Industry, Polytechnic Institute, FEFU
[2] Depatment of Nuclear technologies, Institute of High Technologies and Advanced Material, FEFU
[3]Academic Dep. of English Language, Oriental Institute School of Regional and International Studies, FEFU
[1, 2] Scientific adviser – K.R. Frolov
[3]Scientific consultant – V.B. Kolycheva

Introduction. The problem of anthropogenic pollution of natural waters caused by industrial activities is particularly important in the field of environmental protection and conservation. Artificial geochemical barriers can be one of its solutions. Their use for the treatment of technogenic water is a cost-effective method of eliminating the negative consequences of the mining activities [2]. The purpose of this work was to investigate the possibility of using different materials as sorbents for creating artificial geochemical barriers.

Materials and methods. The experiment consisted of purifying water samples with a known concentration of a pollutant using the geochemical barrier method (tube method). Each 3.5 cm diameter glass tube was filled with

24 cm^3 of sorbent: the upper or lower Primorsky Krai typical soils horizon, and the taurite sorbent. A 120 mL blank sample or model solution was passed five times successively through the tubes. Distilled water was used as a blank sample, and 0.2 mg/L copper (II) sulphate solution was used as a model solution. In each case a parallel of three columns was considered. The copper content in the filtrate was determined according to the method of GOST 4388-72 "Methods for determining the mass concentration of copper" [1].

Results and discussions. Figure 1 shows a graph with the dependence of the average concentration of copper (II) ions on the volume of the filtrate in the filtrate of the model solution and the blank sample, passed through the columns filled with taurite sorbent.

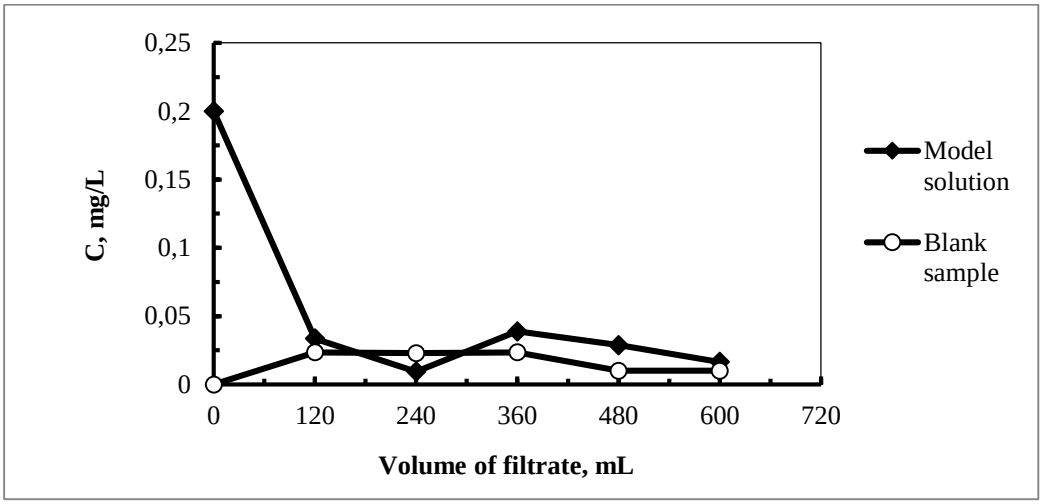

Figure 1 – Dependence of copper (II) ion concentration on filtrate volume

In the case of the model solution, the sharp decrease in the concentration of copper (II) ions in the first filtrate sample (120 mL) is due to the binding of copper ions to taurite by adsorption processes. The alkaline nature of the taurite and the slightly acidic environment (pH = 5.7) of the copper (II) sulphate model solution contribute to the decrease in concentration. In subsequent filtrate samples (240, 360, 480 and 600 mL) no sharp change in copper (II) ion concentration was observed, and the concentration was between 0.016 and 0.038 mg/L. In the case of the blank sample, the graph shows taurite to contain some copper in its composition, so its concentration in the filtrate decreases as the distilled water passes through the sorbent: from 0.023 to 0.006 mg/L.

Figure 2 shows a graph with the dependence of the hydrogen index averaged values on the volume of the filtrate for the model solution and the blank sample for taurite sorbent columns.

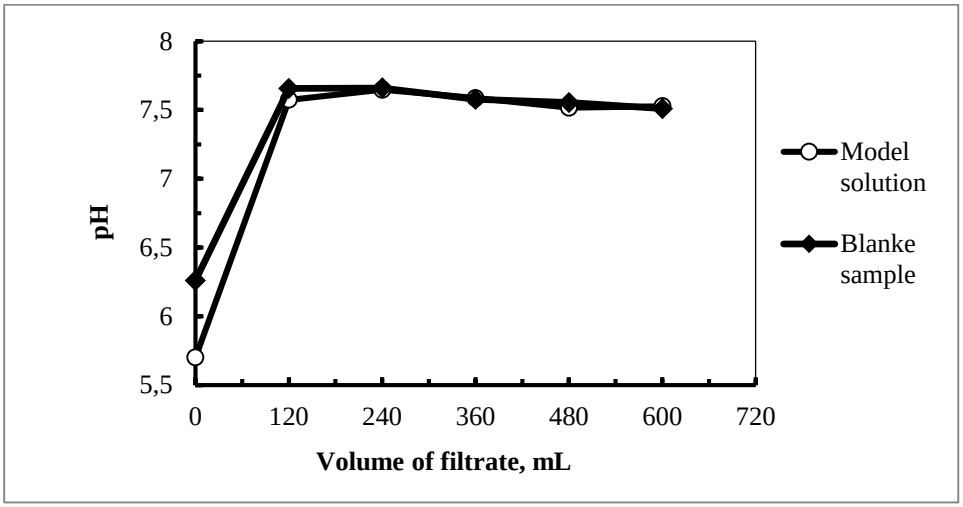

Figure 2 – Dependence of pH values on filtrate volume

The pH value of the model solution is 5.5, indicating the tendency of copper (II) sulphate to hydrolysis by cation. Due to the carbonate nature of the taurite, the pH value in the filtrate rises to 7.6 due to neutralisation of the protons. The further constancy of pH value up to 7,5 is connected with filling of pores of the sorbent with ions of

copper (II) which is proved by the character of dependence in figure 1. The pH value in the filtrate of the blank sample has a near-neutral character (7,5) caused by insolubility of carbonates and weak dissociation of ions which can influence the pH value.

Similarly, experiments for the blank sample and model solution were carried out for artificial geochemical barriers of the Primorsky Krai upper and lower soil horizons. According to the GOST 4388-72 methodology of copper (II) ions content analysis [2], after adding the necessary reagents the solution should have a yellow color. The intensity of the color corresponds to the content of copper (II) ions. Nevertheless, spontaneous acquisition of yellow color by the filtrates of the blank sample and the model solution was observed. This distorts the analytical signal in advance and introduces an unspecified proportion of the error in the determination of the contaminant content.

Conclusion. As a result of purification of the model solution with taurite sorbent by the column method, a decrease in the concentration of copper (II) ions in the filtrate from 0.2 to 0.02 mg/L is observed. This indicates the possibility of its application as a material for creating artificial geochemical barriers. It was not possible to establish the possibility of purification of the model solution by the upper and lower horizons of typical soils of Primorsky Krai by the method of GOST 4388-72.

References

1. GOST 4388-72. Drinking water. Methods for determination of copper mass concentration. – Moscow : Standartinform, 2010. – 10 p. – (Interstate Standard).

2. Gruschakova, N. V. Environmental condition of industrial zones of liquidated coal mining enterprises in Primorsky Krai: thesis of chemical sciences candidate / N. V. Gruschakova – Vladivostok: 2018. – 187 p.

Balatskiy D. V.[1,2], Budnikova Yu. B.[1,2], Vasilyeva M. S.[1,2]

MÖSSBAUER STUDY OF THE THERMAL BEHAVIOR OF Feo_x-TiO_2 LAYERS FORMED BY PLASMA-ELECTROLYTIC TREATMENT OF TITANIUM

[1] Department of Chemistry and Materials, Institute of High Technologies and Advanced Materials, FEFU
[2] Institute of Chemistry, Far Eastern Branch of Russian Academy of Sciences
[3]Oriental Institute School of Regional and International Studies, FEFU
[1,2]Scientific adviser – M.S. Vasilyeva
[3]Scientific consultant – V. B. Kolycheva

One of the promising methods of surface engineering of valve metals and their alloys is the technology of plasma electrolytic (microarc) oxidation (PEO), which allows obtaining surface oxide layers with a unique set of properties on objects of almost any geometric shape [1]. The properties of the resulting oxide coatings depend to a greater extent on the ordering, the nearest environment of the atoms located not only in the surface layer, but also in the bulk of the coating [2]. In this work, the thermal behavior of iron-containing oxide coatings formed on titanium by the PEO method was studied by Mössbauer spectroscopy. Oxide layers on titanium were formed in a galvanostatic mode at a current density of 0.1 A/cm^2 for 10 min in an aqueous electrolyte containing 0.05 M Na_3PO_4 + 0.05 M EDTA + 0.05 M $Fe_2C_2O_4$. After PEO treatment, the coated sample was washed with water and dried in air at 70 °C. The coatings were carefully removed from the titanium base and pulverized to obtain Mössbauer spectra. The resulting powder was annealed in air at temperatures of 100-900 °C for 1 hour.

Mössbauer spectra of iron-containing oxide powders were obtained at room temperature in transmission geometry on a Wissel spectrometer (Germany). The ^{57}Co isotope in a rhodium matrix (RITVERZ JSC, Russia) was used as a source of γ-radiation. The velocity scale was calibrated using the spectrum of sodium nitroprusside with

further conversion to metallic iron (α-Fe).

Figure 1 shows the Mössbauer spectra of iron-containing oxide powders annealed at different temperatures.

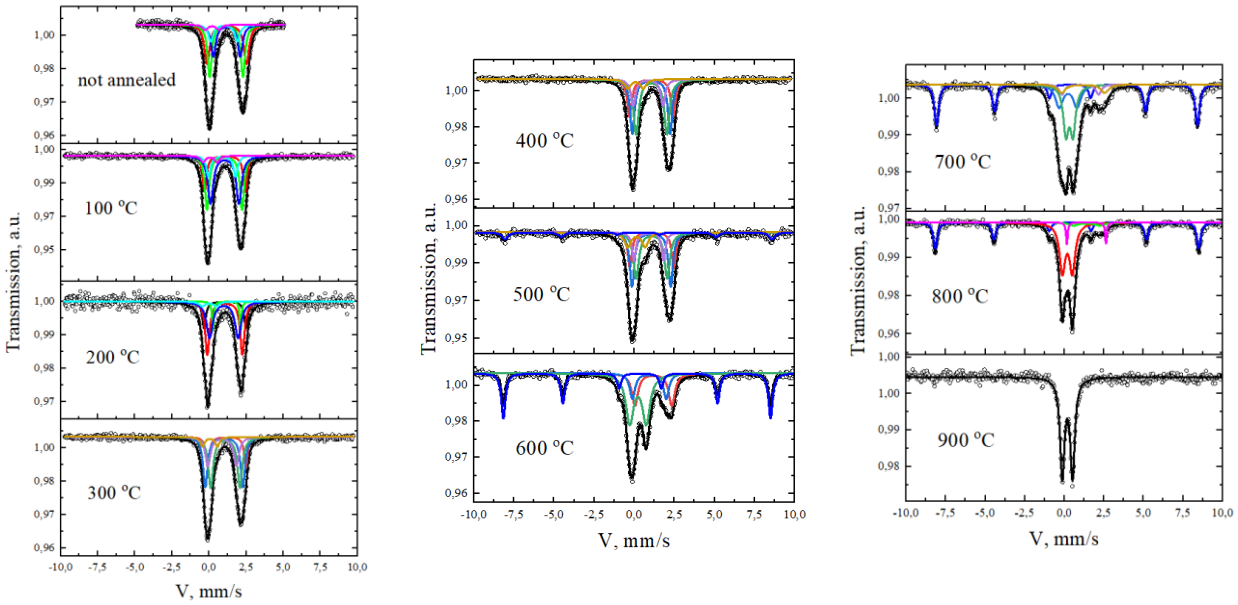

Figure 1 - Mössbauer spectra of iron-containing oxide powders depending on the heat treatment temperature

When comparing the processing parameters of the spectra of the original samples and those annealed at temperatures of 100-400 °C, no obvious changes were found. These spectra were processed using a model containing five paramagnetic doublets, four of which corresponded to Fe(II) and one to Fe(III). With an increase in the annealing temperature from 100 to 400 °C, the proportion of Fe(III) increased slightly. Thus, we can conclude that the resulting coatings are thermally stable in this temperature range.

The spectrum obtained after annealing at a temperature of 500 °C demonstrates the appearance of an additional sextet component, the processing parameters of which correspond to the α-Fe_2O_3 phase [3]. In this case, the proportion of Fe (III) in the powder increases to 22.3%. This fact indicates that the temperature of 500 °C is the temperature after which the powder begins to oxidize leading to the formation of the α-Fe_2O_3 phase.

Further annealing in the temperature range of 600-900 °C leads to continued oxidation of the powder. The spectrum obtained after heat treatment at 900 °C shows the absence of the α-Fe_2O_3 phase, the absence of Fe (II) and the presence of only Fe (III) in the powder under study.

Figure 2 shows the dependence of the content of Fe (II) and Fe (III) in iron-containing oxide powder depending on the heat treatment temperature.

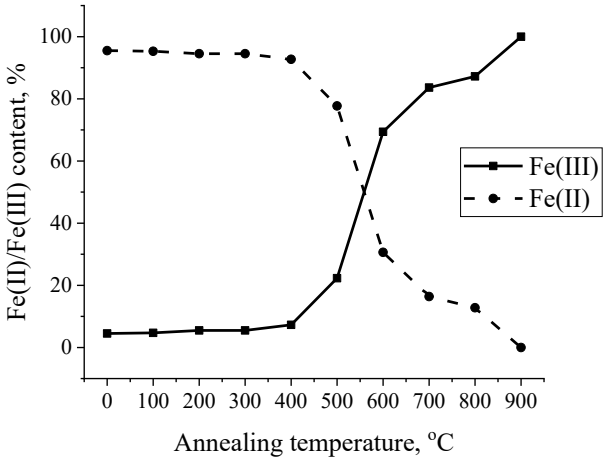

Figure 2 - The content of Fe(II) and Fe(III) in iron-containing oxide powder depending on the heat treatment temperature

Thus, using the method of Mössbauer spectroscopy, it was found the main phase changes in iron-containing

PEO coatings to occur after their annealing at temperatures of 500°C and above.

The work was carried out within the framework of the State Order of the Institute of Chemistry of FEB RAS, projects Nos. 0205-2021-0003 (fabrication of PEO coating) and 0205-2021-0002 (Mössbauer spectroscopy investigations).

References

1. Recent progress in surface modification of metals coated by plasma electrolytic oxidation: Principle, structure, and performance / M. Kaseem, S. Fatimah, N. Nashrah, Y. Gun Ko // Progress in Materials Science. – 2021. – Vol. 117 – P. 100735.

2. Magnetic properties of plasma electrolytic iron-containing oxide coatings on aluminum / V.S. Rudnev, A.Yu. Ustinov, I.V. Lukiyanchuk, P.V. Kharitonskii et.al. // Doklady Physical Chemistry. – 2009. – Vol. 428. – P. 189-192.

3. Фабричный, П. Б. Мессбауэровская спектроскопия и ее применение для химической диагностики неорганических материалов: конспект лекций для студентов старших курсов и аспирантов Химического факультета МГУ им. М. В. Ломоносова. / П. Б. Фабричный, К. В. Похолок – М. : ЗАО "Принт-Ателье", 2009. – 142 с.

Bezhan A.D. [1]

THE STUDY OF CHLORAMPHENICOL PH SOLUTION EFFECT ON THE MAXIMUM ABSORPTION IN THE UV SPECTRUM

[1]FEFU, Institute of High Technologies and Advanced Materials, Department of Chemistry and Materials
[2]FEFU, Oriental Institute School of Regional and International Studies, Academic Dep. of English Language
Scientific adviser - L.I. Sokolova[1]
Scientific consultant - V.B. Kolycheva[2]

Antibiotic chloramphenicol (Levomycetin) is widely used as an effective anti-infective agent. Its residual amounts are found in food, wastewater and other objects [1]. The content of chloramphenicol in food is regulated by the relevant regulatory documents [2]. Various analytical methods are used to control its content in food: enzyme immunoassay, high-performance liquid chromatography [3]. However, these methods are not always available and appropriate. This problem can be solved by attracting a relatively inexpensive and available method of spectrophotometric analysis. Although the sensitivity of this method is often lower than that of immunoassay and chromatography, it can be improved by selecting optimal analytical conditions, including isolation, concentration of the analyte, and conditions for its direct photometric analysis.

Using UV-spectrometry it is necessary to take into account the pH of the analyzed solutions as a factor influencing the intensity and position of the maximum absorption of the antibiotic.

The purpose of our work was to study the effect of pH of chloramphenicol solution on the absorption maximum in the UV spectrum.

We studied a 3% alcohol solution of chloramphenicol diluted with ethanol to a concentration of 0.012 mg/L, and photometrically analyzed with a UV-spectrometer "UV-mini 1240" by Shimadzu at a wavelength range of 200-400 nm, the thickness of the quartz cuvette being 1 cm.

The position of the absorption maximum of chloramphenicol depends on the pH value of the solution, namely, the absorption maximum in the UV spectra shifts to the longer wavelength (batochromic shift) part of the spectrum. The pH value of the solution was changed by adding NaOH and HCl solutions. Table 1 shows the change in the wavelength of the absorption maximum of the chloramphenicol solution and its optical density from the pH of the solution.

Table 1

Values of the absorption maximum wavelength and optical density of chloramphenicol solution at different pH values of the solution.

Solution pH	Wavelength, λ, nm	Optical density, A
1.4	277	0.207
2.1	274	0.306
3.1	273	0.441
3.7	273	0.399
4.3	273	0.382
5.2	273	0.372
5.6	273	0.233
6.7	274	0.387
7.9	275	0.388
8.7	275	0.409
9.7	274	0.450
11.9	274	0.510

As can be seen from the table, the maximum concentration of chloramphenicol is observed in the most alkaline environment.

Thus, we can assume that the changes in the absorption maxima were due to the change in the structure of chloramphenicol. Apparently, when the pH of the solution was increased, the formation of the sodium salt occurred; acidification of the levomycetin solution with hydrochloric acid reduced the nitro group in the chloramphenicol molecule to the amino group. The increase in pH led to a slightly batochromic shift in the chloramphenicol molecule, which was likely to indicate minor structural changes in the chloramphenicol molecule.

As a result of the study, it was found that in an acidic environment (pH=1.4) the structure of chloramphenicol started to break down, while in a strongly alkaline environment (pH=11.9) the substance in question was stable; this may be due to the presence of a large number of hydroxyl groups. Therefore, it is most expedient to carry out analytical determination of chloramphenicol in the area of alkaline values of hydrogen ion exponent from 8.7 to 11.9, which leads to increase of determination sensitivity (increase of optical density).

References

1. Sokolova L.I. Determination of antibiotics (levomycetin and tetracycline) in food products with different matrices / L.I. Sokolova, K.O. Belyustova, Yu.O. Privar, NP Shapkin and [others] // Technique and technology of food production. - 2015. - T.38. - № 3. - C. 146- 152.

2. Unified sanitary-epidemiological and hygienic requirements for products (goods) subject to sanitary and epidemiological supervision (control) / developed on the basis of the legislation of member states, as well as using international documents in the field of food safety. - Moscow : Publishers of standards, 2010. - 2347 c.

3. Beltyukova S.V. Methods of determination of antibiotics in food products / S.V. Beltyukova, E.O. Liventsova // Methods and objects of chemical analysis. - 2013. - №1. - C. 4-5.

Galkina, D.V.[1]

POLYCARBONATE AS A MATERIAL FOR MOLDING NONWOVEN FIBER MATERIALS

[1]Far Eastern Federal University, Polytechnic Institute, FEFU
[2]Far Eastern Federal University, Oriental Institute School of Regional and International Studies, FEFU
Scientific adviser – L.A. Lim[1]
Scientific consultant – N.S. Fedchenko[2]

Polycarbonate (PC) is one of the outstanding engineering polymers with excellent properties: chemical and

mechanical resistance, light weight, transparency, stiffness, heat resistance. Products made of this polymer have a wide range of applications: medical devices, electronic equipment, etc. [1].

Today, a lot of attention is paid to the ways of creating micro- and nanofibers because of their properties that distinguish them from conventional fibers. Micro- and nanofibers have an increased specific surface area, high porosity, lower density and excellent mechanical properties due to their interconnected structure [2, 3]. Currently, there are no works on polycarbonate microfibers molding by centrifugal molding, most likely due to the complexity of dissolution and brittleness of the resulting material.

The purpose of the work is to mold fibrous material from two different grades of polycarbonate by centrifugal molding and to compare them.

The molecular weight of polycarbonate samples was determined by hydrodynamic viscometry. Viscosity was determined using a glass capillary viscometer "VTL2-0,34" at 25 °C according to the methodology [4]. Then through the Mark-Kuhn-Hauvinck equation (formula 1) the molecular weight of two polycarbonate grades was determined (table 1).

$$[\eta] = KM^{\alpha} \quad (1)$$

where, $[\eta]$ – the characteristic viscosity of the polymer solution;
K, α – constants characterizing the polymer-solvent system at temperature 25 °C;
M – molecular weight of polymer.

Table 1

Molecular weight of two grades of polycarbonate

PC grade	$K \cdot 10^4$	α	$[\eta]$	M
1	27,70	0,50	0,53	37146
2			0,57	42466

Polycarbonate solutions with different concentrations were prepared (table 2).

Table 2

Characteristics of polycarbonate and fiber solutions

Sample №	Solution concentration, g/ml	Mass of polymer in 30 ml of solvent, g	Fiber yield, g/%	d±Δ, мкм
Grade №1				
1	0,37	11,12	9,68/87	21,64±3,14
2	0,34	10,24	9,55/94	15,71±2,15
3	0,30	9,12	8,43/92	8,32±0,96
4	0,28	8,41	4,46/53	8,29±0,71
Grade №2				
1	0,19	5,70	~0	–
2	0,2	6,00	2,61/45	5,24±0,28
3	0,21	6,30	4,66/74	6,44±0,44
4	0,22	6,60	4,20/63	7,21±0,58

The prepared solutions were used in the process of no-flat centrifugal spinning on a laboratory unit (figure 1), resulting in a fiber material with radial fiber distribution.

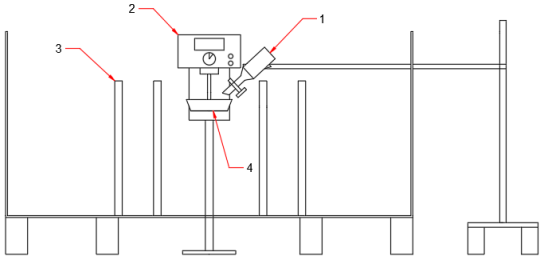

1 - funnel with polymer solution; 2 - mover; 3 – collectors; 4 – forming nozzle
Fig. 1. Centrifugal molding unit

The obtained samples of fibrous material (figure 2) were examined on an Olympus SZX16 optical microscope using Stream Basic software. The sampling points are marked in figure 3. For each sample, at least one hundred measurements were made at eight points.

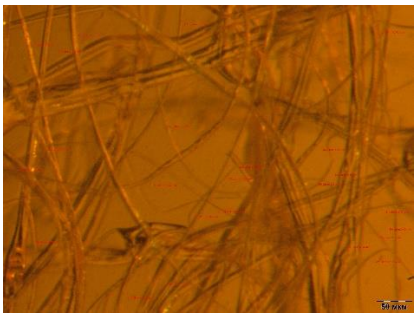

Fig.2. Microphotograph of fibers

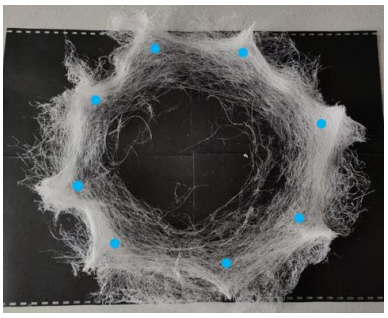

Fig.3. Sampling scheme

Statistical processing of the experimental data was carried out with standard means of Microsoft Excel (table 1). Histograms of the dependence of fiber diameter on the relative frequency of their occurrence were plotted according to the data obtained (figures 4, 5).

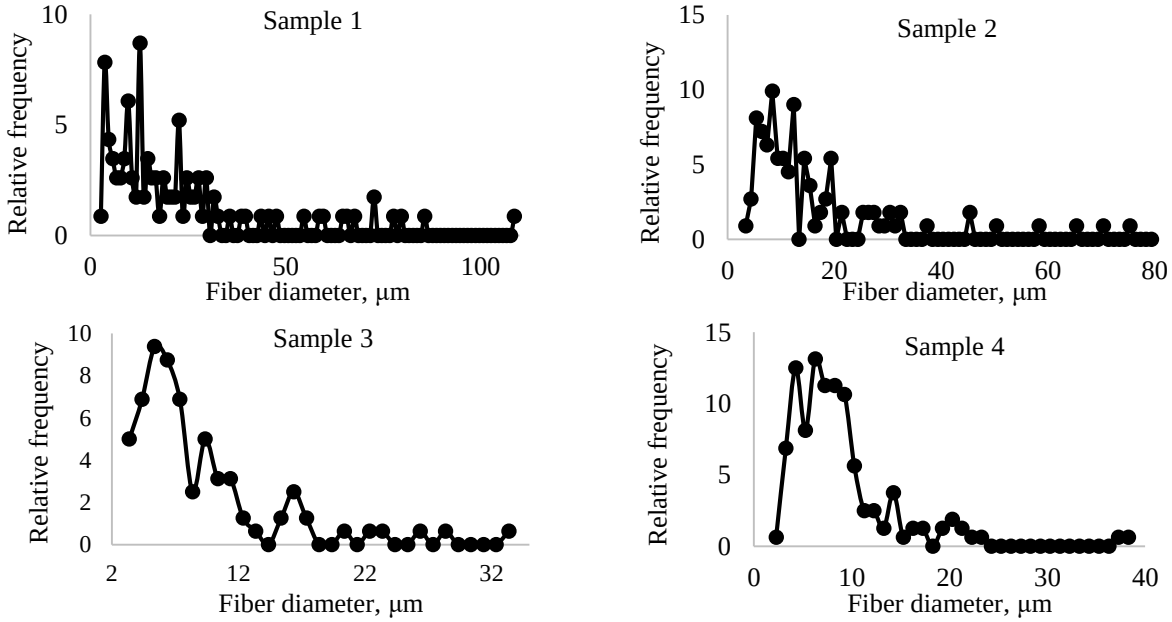

Fig.4. Distribution curves of fibers diameters of PC grade 1

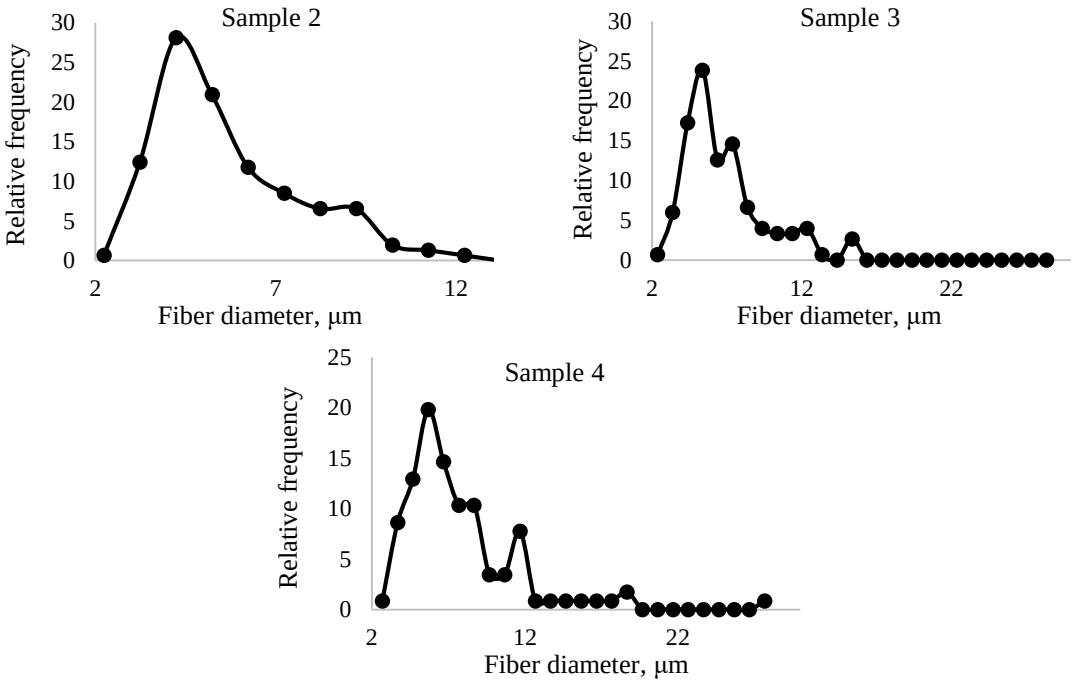

Fig.5. Distribution curves of fibers diameters of PC grade 2

On the basis of the data, we can conclude that for further work it is necessary to use polycarbonate grade 2, due to the higher molecular weight, polycarbonate solutions at concentrations of 0.21 and 0.22 g/ml have the necessary viscosity for molding a thin fiber material, therefore, the consumption of raw materials will be reduced by ~ 40%, and the thickness of the fiber will be reduced by three times. The statistical analysis showed that the grade № 2 is characterized by a homogeneous distribution of diameters. Grade №1 at concentrations of 0.37 and 0.34 g/ml is characterized by a heterogeneous diameter distribution and a pronounced multimodal distribution. This is due to the fact that with increasing concentration, in addition to thin fibers, sticky thick fibers are formed, as at high concentrations the solvent evaporates more slowly.

References

1. A new approach for the shaping up of very fine and beadless UV light absorbing polycarbonate fibers by electrospinning / T. Baby, T. Jose, G. Gegjo [et al.] – DOI 10.1016/j.polymertesting.2019.106103 // Polymer Testing. – 2019, Vol. 80. – P. 1-10.

2. Applications of electrospun nanofibers / J. Fang, H. Niu, T. Lin, X. G. Wang – DOI 10.1007/s11434-008-0319-0 // Science Bulletin. – 2008. – Vol. 53, N. 15. – P. 2265-2286.

3. Self-assembling nanofibers inhibit glial scar formation and promote axon elongation after spinal cord injury / V.M. Tysseling-Mattiace, V. Sahni, K. Niece [et al.] – DOI 10.1523/JNEUROSCI.0143-08.2008 // The Journal of Neuroscience. – 2008. – Vol. 28, N. 14. – P. 3814-3823.

4. Semchikov, Yu. D. High-molecular compounds / Yu. D. Semchikov. – Moscow : Publishing Center "Academia", 2003. – P. 368. – ISBN 5-7695-1324-1.

D.V. Gritcuk [1], E.K. Papynov [1], Kolycheva V.B.[2]

SYNTHESIS OF MINERAL-LIKE $SrWO_4$ CERAMICS WITH THE SHEELITE STRUCTURE AND A RADIOISOTOPE PRODUCT BASED ON IT

[1]Far Eastern Federal University, Institute of High Technologies and Advanced Materials
[2]Far Eastern Federal University, Oriental Institute School of Regional and International Studies, Academic Department of English Language
Scientific adviser — E.K. Papynov [1]
Scientific consultant – Kolycheva V.B.[2]

An efficient method of hydrothermal synthesis of nanocrystalline $SrWO_4$ powder with the scheelite structure and the spark plasma sintering (SPS) of ceramics based on it was presented. The composition, morphology, and structure of samples under various synthesis temperature conditions were studied by EDX, SEM (figure 1), and XRD (figure 2).

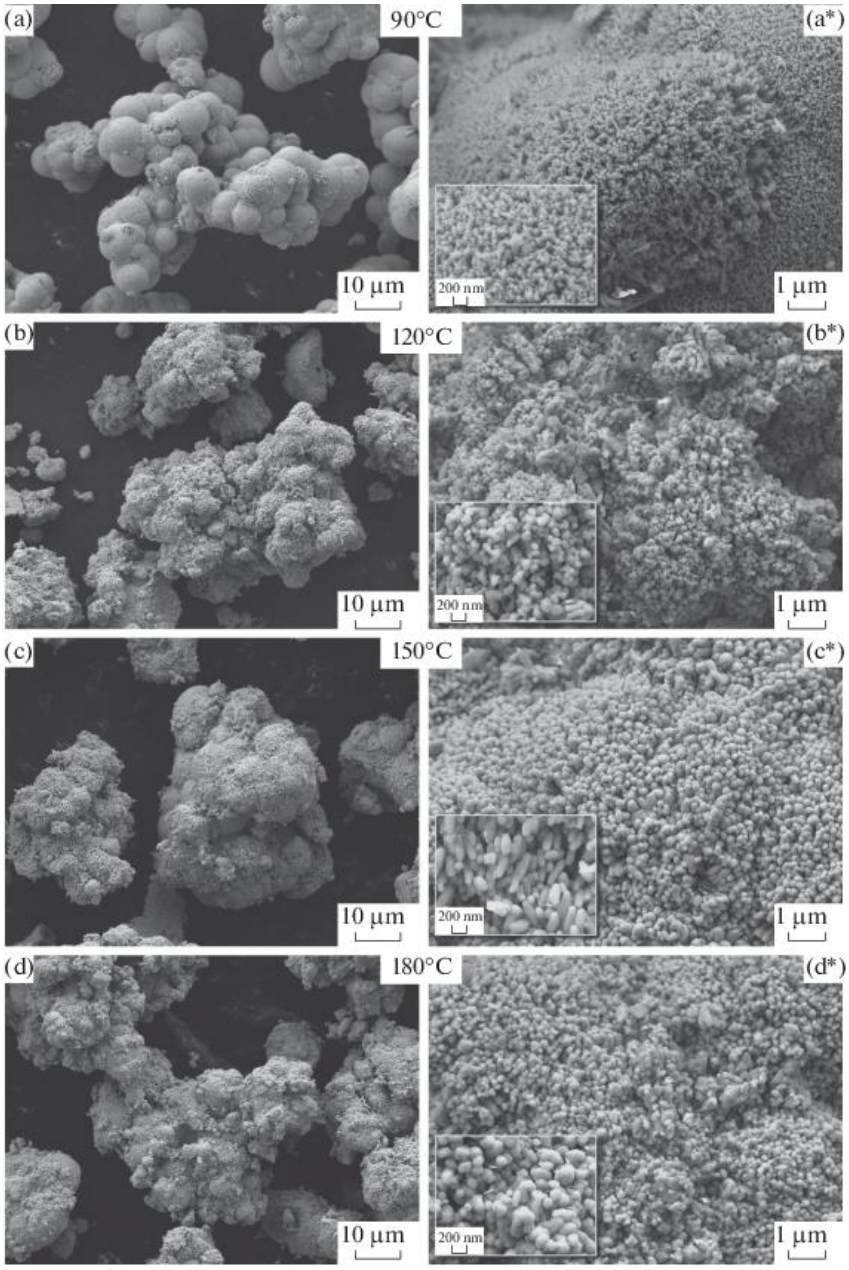

Fig. 1. Scanning electron microscopy.

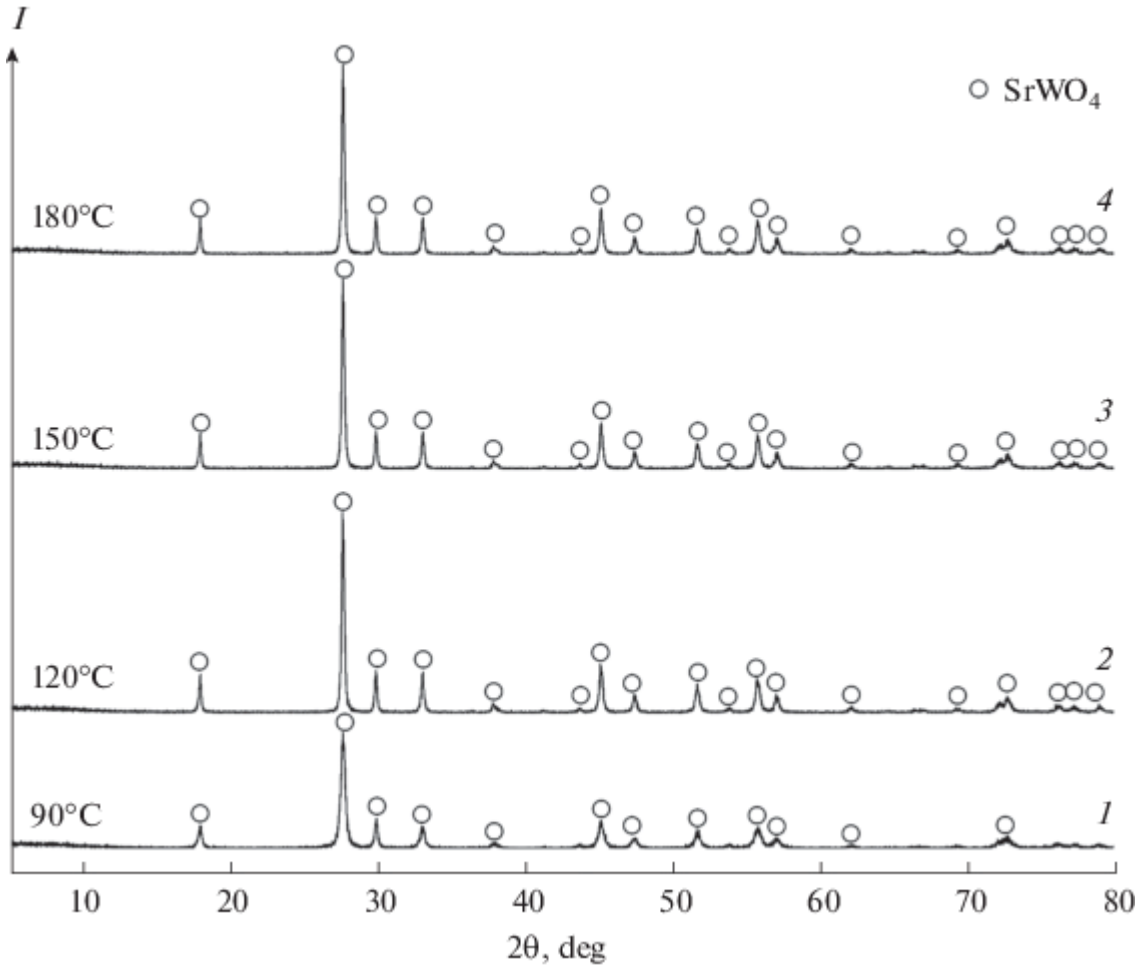

Fig. 2. X-ray powder diffraction analysis.

In the temperature range (90–180°C) chosen for investigation, the phase composition of samples was found to remain unchanged with the exception of the lowest-temperature sample (figure 1, curve 1) having lower intensities of diffraction maxima and the smallest crystallite size compared to other samples. This conclusion was supported by the crystallite sizes calculated by the Williamson–Hall method for the studied tungstates, which were 30.6, 61.5, 67.9, and 181.2 nm for the samples obtained at 90, 120, 150, and 180°C, respectively. The efficiency of the ultrafast (several minutes long) sintering of the nanocrystalline $SrWO_4$ powder was described by the dynamics of its consolidation as a function of the SPS time and temperature. The temperature of formation was determined for a single-phase $SrWO_4$ ceramic with a high relative density and a low strontium leaching rate (GOST R 50926–96) required as matrices for the reliable immobilization of the high-energy strontium-90 radionuclide.

For the first time, a method for obtaining a composite material from ceramics of the $SrWO_4$ composition and high-alloy steel by the spark plasma sintering (SPS) was implemented as a test product for an open source of ionizing radiation. The method consisted in the diffusion sintering of materials within a single step at 1000°C for 5 min with the mandatory use of a sintering additive in the form of a metals mixture.

References

1. Liao J. et al. Hydrothermal synthesis and photoluminescence of SrWO4:Tb3+ novel green phosphor // Mater. Res. Bull. 2009. Vol. 44, № 9.

2. Olevsky E.A., Dudina D. V. Field-assisted sintering: Science and applications // Field-Assisted Sintering: Science and Applications. 2018.

3. Ungár T. Strain broadening caused by dislocations // Mater. Sci. Forum. 1998. Vol. 278–281, № PART 1.

Dudnik A.A.[1], Maslova N.A.[1], Samus M. A.[1], S. G. Krasitskaya[1], V.B. Kolycheva[2]

SORPTION ACTIVITY OF MODIFIED ALUMOSILICATES OF PAlPS AND PFePS

[1]FEFU, Institute of High Technologies and Advanced Materials, Department of Chemistry and Materials
[2]FEFU, Oriental Institute School of Regional and International Studies, Academic Dep. of English Language
Scientific adviser – S. G. Krasitskaya[1]
Scientific consultant – V.B. Kolycheva[2]

Currently, great attention is paid to the development of new more effective methods of wastewater treatment. Sorption using synthetic and natural aluminosilicates is one of the promising methods, sorbents being modified to improve the adsorption properties. Zeolite and vermiculite are proposed as sorbents for wastewater treatment. Zeolite is a frame aluminosilicate, the crystal structure of which is formed by tetrahedra $[AlO_4]^{5-}$ and $[SiO_4]^{4-}$ connected by common vertices into a three-dimensional frame penetrated by cavities and channels. The framework is a system in which mobile cations and water molecules are located. Vermiculite being a mineral of the mica group formed from iron or magnesium silicates has a high moisture-retaining capacity including oxides of silicon, magnesium, iron, aluminum, and some other elements. To improve the already existing properties of aluminosilicates, they are modified.

The aim of the work was to study the effect of the modifiers of PAlPS and PFePS in an acidic medium on the sorption activity of zeolites and vermiculites in relation to methylene blue and methylene orange.

The objects of the study were sorbents based on vermiculite of Koksharsky field (Primorsky Krai) and zeolite of the Chuguevsky deposit, which were subjected to PAlPS and PFePS modifications and treated with hydrochloric acid. The experiment was carried out by step-by-step production of 9 samples (Table 1):

Table 1

Samples of modified sorbents

№	Modified sorbent
1	Base zeolite
2	Base vermiculite
3	Vermiculite modified with hydrochloric acid (12% HCl solution)
4	Zeolite modified with PAlPS
5	Zeolite, modified with PFeFC
6	Vermiculite, modified with PAlPS
7	Vermiculite, modified with PFePS
8	Vermiculite modified with hydrochloric acid (12% HCl solution) and PAlPS
9	Vermiculite modified with hydrochloric acid (12% HCl solution) and PFePS

The sorption activity of the obtained sorbents for methylene blue and orange was determined according to GOST 4453-74. A comparison of the sorption activity of the samples by methylene blue and orange is shown in Table 2.

Table 2

Results of sorption activity of samples with respect to dyes

№	Sorption activity with respect to dyes, mg/g	
	Methyl Orange	Methylene Blue
1	11.290	5.260
2	5.640	4.690
3	16.320	7.910
4	2.970	1.240
5	0.001	0.001

6	21.260	0.001
7	3.620	0.001
8	4.030	0.001
9	22.490	0.09

For zeolites the table shows that there is a decrease in sorption activity for methylene blue and orange after treatment with PAlPS and PFePS; this effect was caused by the overlap of the sorbent pores and the imposition of a structure with less affinity to dyes. The opposite pattern is observed for vermiculites washed with a 12% HCl solution in the samples; there is an increase in sorption activity for both dyes. With PAlPS applied to vermiculite, the sorption activity of the sample decreased in methylene blue and increased in methylene orange. The combination of acid treatment of vermiculite and application of PAlPS on its surface led to a slight increase in sorption activity for methylene orange, while no changes were observed for methyl blue. The treatment of vermiculite with PFePS led to a decrease in sorption activity for dyes, but with preliminary acid treatment, the activity to methylene orange increased slightly.

All modified samples showed low sorption activity to methylene blue and methyl orange. However, the samples of vermiculite modified with hydrochloric acid, vermiculite modified with PAlPS, vermiculite modified with PFePS and hydrochloric acid exceed 2.9; 3.8; 3.9 times, respectively, the sorption activity of the initial vermiculite to methyl orange. A sample of vermiculite modified with hydrochloric acid exceeded 1.7 times the sorption activity of the original vermiculite to methylene blue.

References

1. GOST 4453-74. Active brightening charcoal powdered wood. Technical condition: interstate standard / developed by V. F. Olontsev, S. L. Glushankov, Yu. A. Romanov, G. N. Speshilov – Moscow : Standartinform, 1976. – 32 p.

Zhuravlev I. A.[1]

MODIFICATION OF POLYDIMETHYLSILOXANE POLYMERS WITH TERMINAL VINYL GROUPS

[1]FEFU, Institute of High Technologies and Advanced Materials, Department of Chemistry and Materials
[2]FEFU, Oriental Institute School of Regional and International Studies, Academic Dep. of English Language
Scientific supervisors – M. V. Tutov[1]
Scientific consultant – Kolycheva V.B. [2]

The use of siloxane elastomers in additive technologies is of great interest for such areas as industry and medicine. Now this is a difficult and costly process at the industry level. In this work SKTN-A was modified for further use in 3D printing technology.

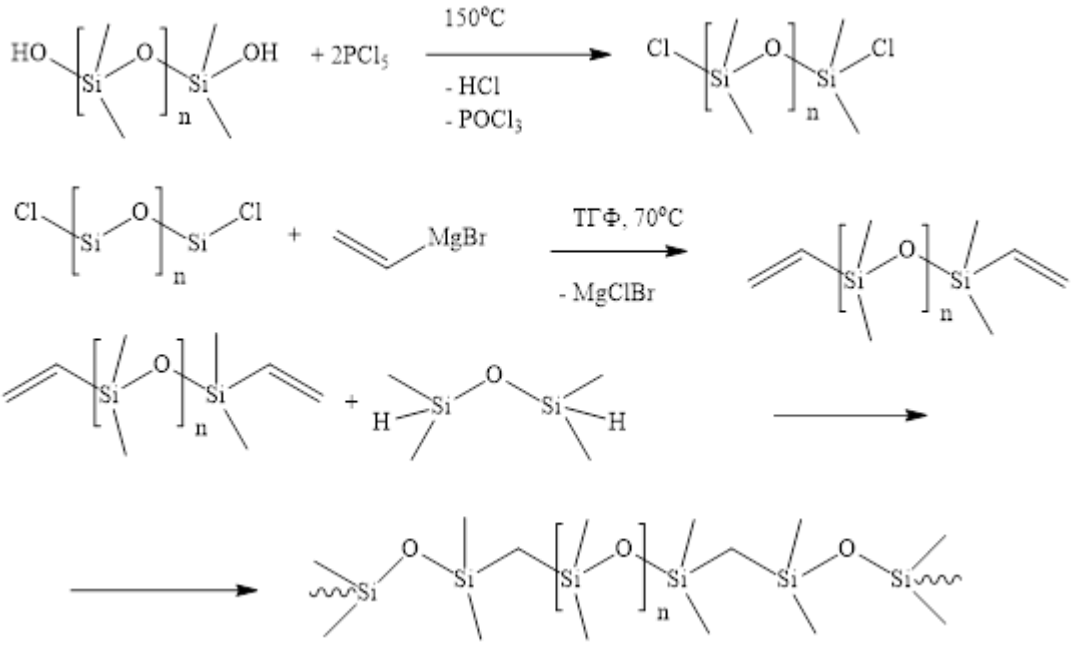

Figure 1 – Scheme of modification of SKTN-A

Modification of the polydimethylsiloxane polymer produced by Russian enterprises under the trademark SKTN-A was carried out in three stages (Figure 1). The first stage was the chlorination of the terminal OH groups of the polymer with PCl_5 in stoichiometric amounts without a solvent at a temperature of 150 °C. Then, vinyl groups were introduced into the compound through active Si-Cl bonds by reaction with vinylmagnesium bromide in tetrahydrofuran. The third step was to increase the viscosity of the polymer to the value required for further use of the polymer in 3D printing. A polymer with a viscosity in the range of 70,000–90,000 cSt has been experimentally established to meet the indicated requirements.

To obtain a polymer with a given viscosity, it was cross-linked at the vinyl groups with tetramethyldisiloxane in the presence of Karsted's catalyst by the hydrosilylation reaction. The synthesis of Karsted's catalyst was carried out according to a modified procedure [1] (Figure 2).

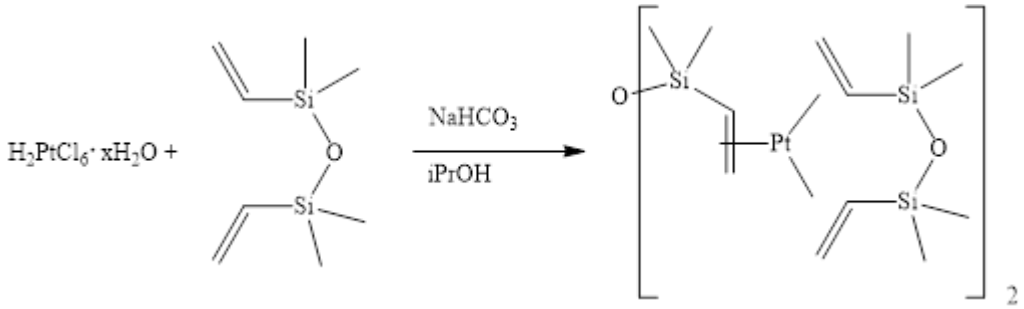

Figure 2 – Scheme of synthesis of Carstedt’s catalyst

A polymer with a given viscosity was found to be obtained at a ratio of the crosslinking agent and the original polymer of 2.9:1.

Under the conditions of 3D printing, the material must be able to cure and maintain a given shape for a long time. For curing siloxane polymers, a UV crosslinking was proposed using dendrimeric crosslinkers with SH groups for thiol-ene reaction with the polymer and octyl groups for better dissolution of the dendrimer in polydimethylsiloxane.

Octavinylsilsesquioxane (OVS) was obtained by hydrolytic polycondensation. The synthesis of OVS derivatives containing octyl and vinyl groups was carried out under UV in THF by placing OVS and octanethiol in a molar ratio of 1:4 and 1:2 into the reaction mixture without using a photoinitiator. The reaction was assumed to proceed according to the scheme shown in Figure 3.

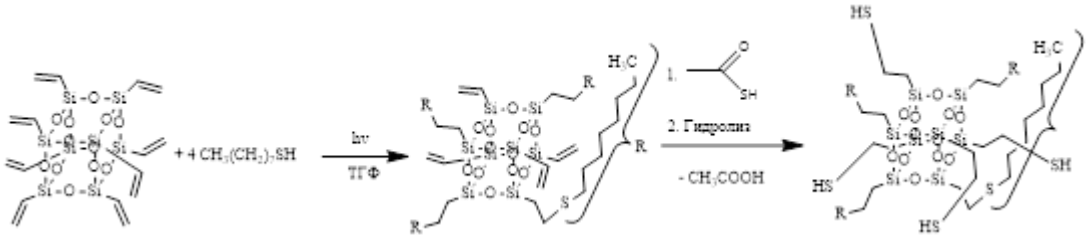

Figure 3 – Scheme of synthesis of curing agent

The resulting OVS octyl derivatives are precursors for the subsequent synthesis of crosslinking agents with many terminal SH groups for UV curing of vinyl-terminated polydimethylsiloxane.

To sum up, vinyl-terminated polydimethylsiloxane with a given viscosity based on SKTN-A was obtained, and octyl derivatives of OBC were obtained for further synthesis of cross-linking agents.

References

1. Cornelissen L. Copper-Catalyzed Cross-Coupling of Vinylsiloxanes with Bromoalkynes: Synthesis of Enynes / L. Cornelissen, M. Lefrancq, O. Riant // Organic Letters. – 2014. – Vol. 16, N 11. – P. 3024–3027.

Ivanova A. E.[1], Azon S. A.[1], Shichalin O. O.[1], Papinov E. K .[1], Kolodeznikov E. C .[1]

DEVISING OF METHODS FOR THE SYNTHESIS AND RESEARCH OF STRONTIUM CERATES USABLE AS COMPONENTS OF FUEL SYSTEMS

[1]Far Eastern Federal University, Institute of Science-Intensive Technologies and Advanced Materials
Scientific adviser – O. O. Shichalin[1]

High-temperature proton-conducting materials are a unique class of oxide materials capable of proton conductivity in reducing atmospheres. In addition to the fact that such systems are of considerable fundamental interest, their practical application is also undeniable since proton conductivity in them can reach high values. This opens the possibility of using ceramics based on such systems for fabrication of solid electrolytes for a wide range of medium- and high-temperature solid-oxide electrochemical devices. Recent advances in the field of solid-oxide proton conducting materials are related to the synthesis of materials with perovskite structure, such as $BaCeO_3$, $BaZrO_3$, $BaCeO_3$–$BaZrO_3$, $SrCeO_3$, and $LaScO_3$ [1].

Materials based on $SrCeO_3$ are of practical interest because of their potential application in fuel cells, hydrogen sensors, H_2-D_2 gas storages, etc. These materials are usually produced by solid-phase synthesis at high (over 1200 ºC) temperatures for a long time (up to 14 hours) [2]. Therefore, there is a need to reduce the synthesis time of these materials.

The materials were synthesized according to the following scheme: stoichiometric amounts of $SrCO_3$ and CeO_2 powders were mixed in a high-energy planetary mill (Tencan, XQM-0.4 A), the mass of grinding bodies was 0,33 of the mass of powders, the speed of rotation was 550 s, grinding time 1 h. The obtained powders were pressed in an isostatic press (SJYP-12TS) at a compaction pressure of 200 MPa. The obtained tablets, 10 mm in diameter, were annealed in a high-temperature muffle furnace (SafTherm, STM-8-17) at 1500 ºC with different holding times (1, 2, 3, 4, 5, 6 hours).

During annealing, the decomposition reaction of $SrCO_3$ proceeded to form SrO. SrO, in turn, reacted with CeO_2, to produce $SrCeO_3$.

$$SrCO_3 \rightarrow SrO + CO_2 \quad (1)$$

$$SrO + CeO_2 \rightarrow SrCeO_3 \quad (2)$$

In order to compare the characteristics of the obtained ceramics, the ceramics of $SrCeO_3$ composition was also obtained according to the method, which presented in the literature data [3].

The received samples were investigated by the method of the X-ray phase analysis. Quantitative measurement of mass fractions of phases in ceramic samples was carried out by Rietveld refinement method in "Profex" software. Diffractograms of the samples are shown in Figure 1. Phase ratios in the samples are presented in Table.

According to the results of the X-ray phase analysis, all the samples are characterized by the content of two phases: $SrCeO_3$ и CeO_2, and the phase ratios in the samples obtained by the developed method remained constant, which allows us to conclude about the optimal annealing time of 1 h. In the sample obtained by the method (2) the CeO_2 content was comparatively higher. Probably, simultaneously with the reaction of $SrCeO_3$ formation, there is a process of SrO evaporation, and as the annealing temperature increases, the speed of processes grows irregularly: the reaction speed grows faster.

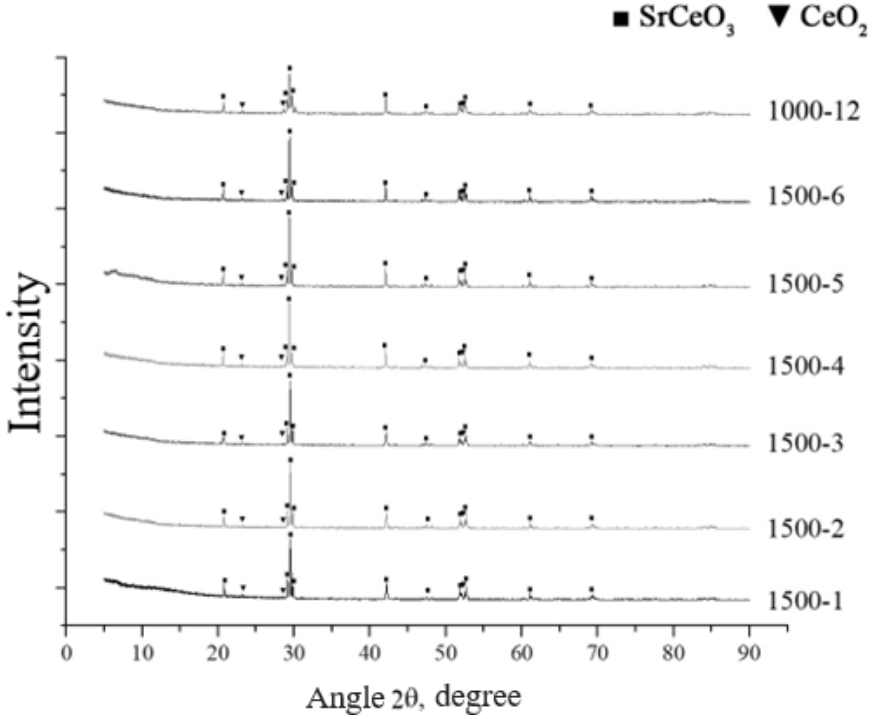

Figure 1: Diffractograms of the obtained ceramics.

Table

Mass ratios of phases in the obtained samples

Name of the sample	Mass ratio of $SrCeO_3$, wt. %	Mass ratio of CeO_2, wt. %
$SrCeO_3$ 1500-1	99.9	0.01
$SrCeO_3$ 1500-2	98.6	1.4
$SrCeO_3$ 1500-3	98.8	1.2
$SrCeO_3$ 1500-4	98.6	1.4
$SrCeO_3$ 1500-5	98.5	1.5
$SrCeO_3$ 1500-6	98.7	1.3
$SrCeO_3$ 1000-14	95.1	4.9

This work was performed within the framework of the state assignment of the Ministry of Science and Higher Education of the Russian Federation № 00657-2020-0006.

Reference

1. Recent activity in the development of proton-conducting oxides for high-temperature applications / N. Kochetova, I. Animitsa, D. Medvedev, A. Demin [et al.]. – DOI 10.1039/c6ra13347a // RSC Advances. – 2016 – V. 77, N 6. –P. 73222–73268.

2. Review of experimental and modelling developments for ceria-based solid oxide fuel cells free from internal short circuits / Y. Ling, X. Wang, Z. Ma, K. Wei [et al.]. – DOI 10.1007/s10853-019-03876-z // Journal of Materials Science. – 2019. – V. 55. – P. 1–23.

3. SrCeO3 as a novel thermal barrier coating candidate for high-temperature applications / J. Yuan, J Sun, J. Wang, H. Zhang [et al.]. – DOI 10.1016/j.jallcom.2018.01.021 // Journal of Alloys and Compounds. – 2018. – V. 740. – P. 519–528.

Kashepa V.V.[1,2], Imshinetskiy I.M.[2], Nadaraia[2] K.V., Mashtalyar[2] D.V., Sinebryukhov[2] S.L., Gnedenkov[2] S.V.

INFLUENCE OF HALLOYSITE NANOTUBES INCORPORATION ON THE PROPERTIES OF PEO LAYERS FORMED ON MA8 ALLOY

[1]Far Eastern Federal University, Polytechnic Institute, Department of Oil, Gas and Petrochemical Industry
[2]Far Eastern Branch Russian Academy of Sciences, Institute of Chemistry
[3]Far Eastern Federal University, Oriental Institute School of Regional and International Studies
Scientific adviser – I. M. Imshinetskiy[2]
Scientific consultant – V.B. Kolycheva[3]

Magnesium alloys are lightweight and durable construction materials that found application in many engineering areas. However, despite the high damping capacity and low density, the use of magnesium alloys is limited by their low corrosion resistance. One of the most promising methods of protective surface modification for light alloys is a process of plasma electrolytic oxidation (PEO). PEO coatings combine corrosion resistance improvement along with functional properties development. PEO has become widely investigated by scientific community due to a broad range of adjustable process parameters and the ability to control the properties of coatings. The ceramic-like coatings formed by the PEO method can be improved by nanoparticles incorporation. The PEO-coatings with various nano-scaled additives demonstrate improved anti-corrosive properties [1], hardness [2] and even photocatalytic activity [3]. Halloysite nanotubes is naturally formed nanoparticles that can be incorporated into the PEO coatings and used as an entrapment system [4] for loading, storage, and controlled release of active molecules such as drugs, corrosion inhibitors, proteins, etc.

In our research, the formation of the protective multifunctional coatings by the PEO method with the halloysite nanotubes incorporation on the MA8 alloy was investigated. The electrochemical and mechanical properties of the obtained PEO layers were studied.

Plates made of MA8 magnesium alloy (Mn 1.30; Ce 0.15; Mg bal. (wt.%)) were used as a substrate. The size of specimens was 20 mm × 15 mm × 2 mm. The solution, containing sodium fluoride (5 g/l) and sodium silicate (20 g/l), was chosen as a base electrolyte. In this work, we used halloysite nanotubes (CAS № 1332-58-7; Sigma Aldrich, USA) with a length of 1-3 μm, an outer diameter of 50-70 nm, and a lumen diameter of 15-30 nm. Nanoparticles were dispersed in the base electrolyte in concentrations of 0, 10, 20, 30, and 40 g/l (Table). The process of coatings formation was carried out using a plasma electrolytic oxidation unit. Coatings morphology was studied with optical laser profilometry and scanning electron microscopy (SEM). The elemental composition was determined by energy dispersive X-ray spectroscopy (EDS). Electrochemical properties of the coatings were investigated by potentiodynamic polarization. The study of the mechanical properties of the coatings was carried out with microhardness and scratch testing.

Table

Composition of the used electrolytes

Samples	The concertation of the electrolyte components, g/l			
	$Na_2SiO_3 \cdot 5H_2O$	NaF	$NaC_{12}H_{25}SO_4$	Halloysite nanotubes
H0	20	5	0	0
H10			0.25	10
H20				20
H30				30
H40				40

Since halloysite is an aluminosilicate with ability to dehydrate under the plasma discharge temperatures into corresponding oxides, it is supposed to change PEO coating properties deeply. Halloysite nanotubes are expected to improve the chemical stability and mechanical properties of the coatings. Moreover, an increase of specific surface area due to nanoparticles agglomerates' presence is expected.

It has been established that PEO-coatings formed on the MA8 magnesium alloy in electrolytes containing halloysite nanotubes have improved electrochemical characteristics in comparison with the surface layers obtained without the use of the nanoparticles. Based on the obtained results it has been concluded that the coatings formed in the electrolyte with the nanoparticles concentration of 20 g/l have the highest protective properties in the corrosive medium. At the same time, the highest adhesion to the substrate was demonstrated by the H30 samples coatings. The incorporation of nanoparticles led to the increase in the microhardness of the surface layers by 1.5 times. The highest magnitudes of microhardness were observed for the H20 and H30 samples. Formed coatings are perspective for biomedical applications due to their biocompatibility and corrosion resistance.

Research was carried out within the framework of the Grant of the Russian Science Foundation, project № 22-23-00937.

References

1. Active protection of Mg alloy by composite PEO coating loaded with corrosion inhibitors / Y. Chen, X. Lu, S.V. Lamaka [et al.]. – DOI 10.1016/j.apsusc.2019.144462 // Applied Surface Science. – 2020. – V. 504, Art. 144462. – 30 p.

2. Hard wearproof PEO-coatings formed on Mg alloy using TiN nanoparticles / D.V. Mashtalyar, S.L. Sinebryukhov, I.M. Imshinetskiy [et al.]. – DOI 10.1016/j.apsusc.2019.144062 // Applied Surface Science. – 2019. – V. 503, Art. 144062. – 36 p.

3. Structural, photoluminescent and photocatalytic properties of TiO_2:Eu^{3+} coatings formed by plasma electrolytic oxidation / S. Stojadinovic, N. Radic, B. Grbic [et al.]. – DOI 10.1016/j.apsusc.2016.02.131 // Applied Surface Science. – 2016. – V. 370. – P. 218-228.

4. Halloysite Clay Nanotubes for Controlled Release of Protective Agents. / Yu. M. Lvov, D. G. Shchukin, H. Möhwald, Helmuth, R.R. Price. – DOI 10.1021/nn800259q // ACS Nano. – 2008. V. 2, Art. 5. – P. 814 – 820.

Kozhemiakina E.K.[1]

A NEW CATALYST FOR POLYMERIZATION OF METHYL METHACRYLATE – 2,2- DIFLUORO-4-(P-DIMETHYLAMINOSTRYL)-6-PHENYL-1,3,2-DIOXABORINE

[1] FEFU, Institute of High Technologies and Advanced Materials, Department of Chemistry and Materials
[2]Institute of Chemistry FEB RAS
[3]FEFU, Oriental Institute School of Regional and International Studies, Academic Dep. of English Language
Scientific supervisors – I. V. Svistunova[1], E. V. Fedorenko[2]
Scientific consultant – Kolycheva V.B. [3]

Boron difluoride β-diketonates are characterized by bright luminescence both in the crystalline state and in solutions [1], which makes it possible to use them as organic light emitting diodes, smart inks for marking securities, as well as solar concentrators. These substances in high concentrations are able to form excimers in solutions and polymer matrices, increasing significantly the photostability of dye compounds obtained from this class of compounds. One of these dyes is 2,2-difluoro-4-(p-dimethylaminostyryl)-6-phenyl-1,3,2-dioxaborine (Fig. 1).

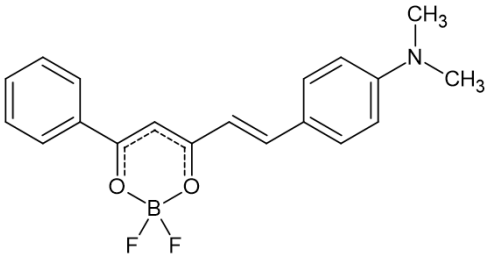

Fig. 1 2,2-difluoro-4-(p-dimethylaminostyryl)-6-phenyl-1,3,2-dioxaborine

Copolymers 1 and 2 were obtained by polymerization of the above dye and methyl methacrylate (MMA) in the absence of an initiator at temperatures of 85 and 90°C. Copolymers 3–6 were prepared by polymerization of these compounds with the addition of an initiator, benzoyl peroxide. The amount of polymethine dye taken was different: for copolymers 1-4, its amount was 1 mg, and for copolymers 5 and 6, respectively, 2 and 7 mg. The content of benzoylacetonate (BAc) groups was higher in the products synthesized in the absence of an initiator than in analogous polymers obtained in its presence. An increase in the amount of polymethine dye also led to an increase in the percentage of BAc groups. The copolymers were purified from methyl methacrylate residues by reprecipitation with heptane from chloroform and the initial dye by converting it into a water-soluble salt.

In the course of the work the polymethine dye was found to have catalytic properties and to be a polymerization initiator comparable in activity to benzoyl peroxide. In the presence of a dye, the molecular weight of the polymer increased by 3-5 times.

Polymer solutions had three emission centers in the ground state: non-aggregated BF_2-benzoylacetonate fragments, J-aggregates, and charge-transfer complexes with N,N-dimethylaniline fragments. When the system was excited by light exciting monomeric luminescence, intense luminescence of excimers and exciplexes was also recorded in the spectrum confirmed by the data of time-resolved luminescence spectroscopy.

The light-guiding properties of composites based on copolymer films and quartz glass were found (Fig. 2). The character of luminescence at the ends of quartz glass depended on the degree of aggregation of BF_2-benzoylacetonate fragments in the copolymer composition.

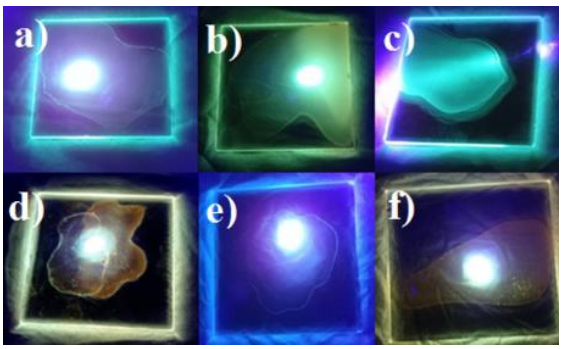

Fig. 2 Luminescence of copolymers 1-6 on quartz glass; a-f - copolymer 1-6 illuminated by a laser with a wavelength of 405 nm

References

1. Luminescence of a Polymer Composite Doped with Boron Chelates. Mechanism of Luminescence Sensitization / A. A. Khrebtov, E. V. Fedorenko, L. A. Lim, V. A. Reutov // Optics and Spectroscopy. – 2018. – Vol. 124, №. 1. – P. 68-71.

Kulagina K. S.[1]

ISOLATION AND IDENTIFICATION OF TRITERPENOIDS FROM THE INFLORESCENCES OF *ATRACTYLODES OVATA* (THUNB.) DC.

[1]Far Eastern Federal University, Institute of High Technologies and Advanced Materials
[2]Far Eastern Federal University, Oriental Institute School of Regional and International Studies
Scientific adviser – A.V. Myagchilov [1]
Scientific consultant – V. B. Kolycheva[2]

The increasing interest in pharmaceutical products of natural origin stimulates the search for plants rich in biologically active compounds.

The territory of the Russian Far East is distinguished by a unique and peculiar flora having a high potential for the use of its representatives in pharmacology, but the actual use of its species composition is slight, due to relatively low state of exploration. One of such insufficiently studied plants growing in the Russian Far East is *Atractylodes ovata* (Thunb.) DC.

The plant is not included in the State Pharmacopoeia of the Russian Federation and is not officially used in medicine; however, it is widely used in Chinese medicine for the treatment of chronic gastritis, peptic ulcer, stomach cancer, liver diseases, and chronic nephritis [1]. This plant has anti-inflammatory, diuretic, anticoagulant, vasodilating properties. The medicinal properties of *Atractylodes ovata* (Thunb.) DC. are due to the presence of coumarins, alkaloids, flavonoids and sesquiterpenoids in its composition, so this plant can be considered as a promising source of biologically active compounds [2–5].

The aim of this work was to study the composition of triterpenoids in the inflorescences of *Atractylodes ovata* (Thunb.) DC.

Triterpenoids were isolated and identified for the first time from the inflorescences of *Atractylodes ovata* (Thunb.) DC. by extraction and preparative column chromatography: lupeol **1**, taraxasterol **2**, α-amyrin **3**, β-amyrin **4**, 3-O-acetyllupeol **5**, 3-O-acetyl- α-amyrin **6**, 3-O-acetyl-β-amyrin **7**, 3-O-acetyltaraxasterol **8**. The isolated compounds were identified by NMR spectroscopy and mass spectrometry with electron ionization.

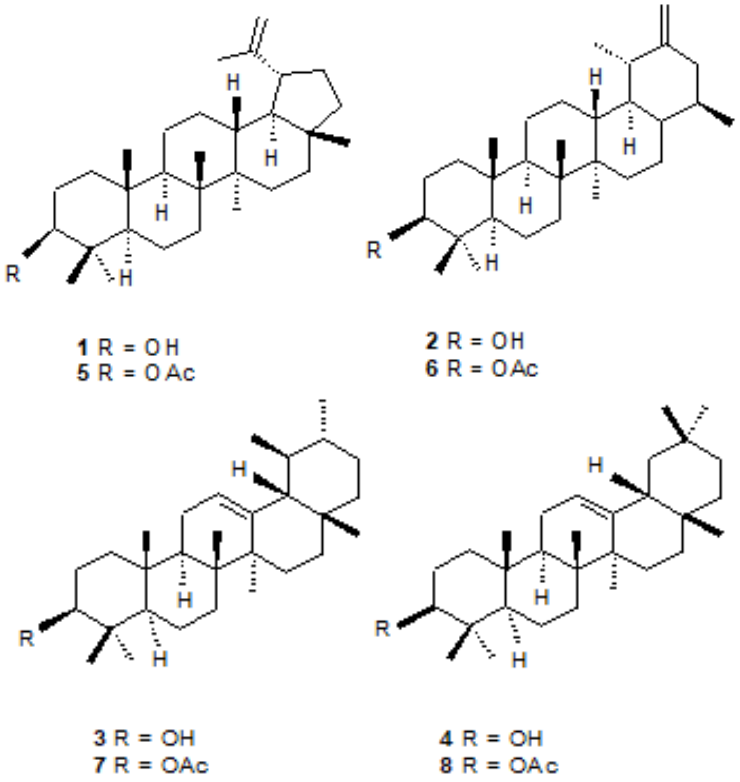

References

1. Fruentov N. K. Medicinal plants of the Far East / N. K. Fruentov. - Khabarovsk: Khabarovsk Book Publishing House, 1987. - 368 p. - p. 31

2. Chemical constituents of Atractylodes chinensis (DC.) Koidz. / H. Meng, G. Li, R. Dai, Y. Ma, K. Zhang, C. Zhang, X. Li, J. Wang. – DOI: 10.1016/j.bse.2010.12.023 // Biochemical Systematics and Ecology. – 2010. – Vol.38, № 6. – p. 1220-1223

3. Anti-Oxidative Abilities of Essential Oils from Atractylodes ovata Rhizome. Evidence-Based Complementary and Alternative Medicine / K. T. Wang, L. G. Chen, D. S. Chou, W. L. Liang, C. C. Wang. – DOI: 10.1093/ecam/neq006 // Evidence-based Complementary and Alternative Medicine. – 2011. – Vol. 2011, Art. 204892. – URL: https://www.hindawi.com/journals/ecam/2011/204892/

4. Glycosides of Atractylodes ovata. / J. Kitajima, A. Kamoshita, T. Ishikawa, A. Takano, T. Fukuda, S. Isoda, Y. Ida. – DOI: 10.1248/cpb.51.1106 // Chemical and Pharmaceutical Bulletin. – 2003. – Vol. 51, № 9. – p. 1106 - 1108

5. Teplyakova D. V. Phenolic compounds of Atractylodes ovata THUNB. DC./ Graduate qualification work. - 2021. - p.47

Meleshko A. A.[1], Khalchenko I. G.[1], Shapkin N. P. [1] Kolycheva V.B.[2]

SYNTHESIS AND RESEARCH OF A COMPOSITE BASED ON THE SKELETON OF A SEA URCHIN AND CALCIUM CARBONATE

[1]Far Eastern Federal University, Institute of High Technologies and Advanced Materials
[2] Far Eastern Federal University, Oriental Institute School of Regional and International Studies
Scientific supervisor –I. G. Khalchenko[1]
Scientific consultant – Kolycheva V.B.[2]

One of the ways to obtain materials with pores of a given size and shape is template synthesis. The synthesis

of protein molecules (nucleic acids serve as templates for the synthesis of protein molecules) is one of the most striking examples of template or template synthesis. In addition, matrix synthesis is used to produce new complex compounds and polymer-polymer composites. Using polymetallorganosioxanes (PMOS) as filler is advantageous for template synthesis, since an important property of PMOS being resistance to the process of thermal oxidation. The possibility to use the mechanochemical activation method for the synthesis of polymetallorganosiloxanes was shown in [1, 2]. The undoubted advantages of which are: the absence of solvents, a reduction in the synthesis time, versatility, a higher yield of the product compared to synthesis in solution, convenience and simplicity of hardware design.

The aim of the study was to obtain a structurally ordered composite by mechanochemical activation based on the skeleton of a sea urchin as a template and polycalciumethylsilsesquioxane (PCES) as filler and to study its properties.

By the method of mechanochemical activation, polycalciumethylsilsesquioxane PCES was obtained based on the skeleton of a sea urchin (synthesis 1) and calcium carbonate (synthesis 2). The reaction proceeded according to the equation: $(C_2H_5SiO_{1,5})_n + nCaCO_3 \rightarrow [(C_2H_5SiO_{1,5})CAO]_n + nCO_2$. Then, the sea urchin skeleton was treated with polymers obtained by two methods (syntheses 1 and 2), calcined at a temperature of 500-600 °C and treated with 4% hydrochloric acid to remove the template; composites 1 and 2 were obtained, respectively. (Figure 1 shows the SEM (scanning electron microscope) data for composites 1 and 2 at different scales.)

After the skeleton having been treated with hydrochloric acid, calcite dissolved and a three-dimensional structure polymer was obtained with its internal structure being inverted relative to the original structure of the hedgehog skeleton. The images also show that a polymer based on calcium carbonate (Figure 1d) during template synthesis does not cover the channels of the template with a thin layer, but clogs them, while a polymer based on the skeleton of a sea urchin covers the inner walls of the channels with a thin layer (Figure 1a).

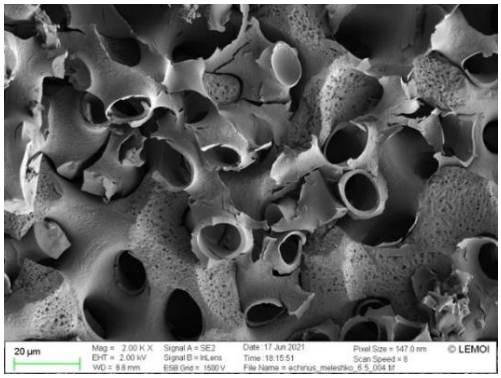

a)

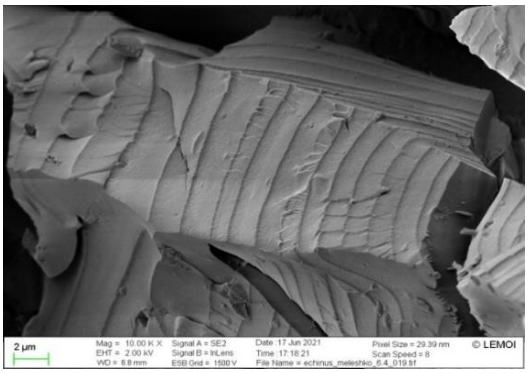

b)

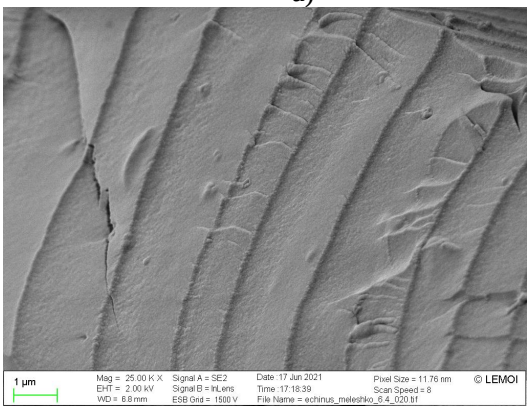

c)

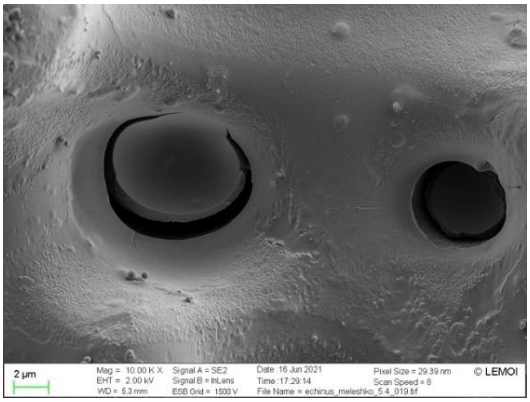

d)

Figure 1 – a, b) composite 1; c, d) composite 2 in a scanning electron microscope

Table

Data of elemental analysis by the EDX method at 2 points

Connection	Ca (%)	Si (%)	C (%)
Composite 1	0.46	28.45	8.20
Composite 1	11.30	12.96	16.33
Composite 2	30.32	0.28	14.38
Composite 2	22.59	3.27	17.05

The SEM images (Figure 1) show composites to have a layered structure, and it is confirmed by the data of the EDX elemental analysis (Table) that a layer in which calcium atoms predominate (the skeleton of a sea urchin) alternates with a layer dominated by silicon atoms (the introduced polymer).

Thus, in the course of template synthesis, in which the skeleton of a gray sea urchin was used as a structuring template, and polycalcium ethylsilsesquioxane as filler, a material with a layered structure inverted relative to the original one was obtained.

References

1. Shapkin N. P., Synthesis of polyalumo- and polygaliphenylsiloxanes under conditions of mechanochemical activation/ N. P. Shapkin, V. V. Libanov // Butlerov communications. – 2015. – No. 3. – pp. 18-21.

2. Kapustina A. A., Synthesis of polyelementoorganosiloxanes under conditions of mechanochemical activation/ Kapustina A. A., Shapkin N. P., Libanov V. V.// Organosilicon compounds. Synthesis, properties, application: abstracts of the 13th Andrianov Conference, June 28 – July 1, 2015, Moscow. – 73 p.

Pelageev D.N.[1,3]

SYNTHESIS OF NATURAL QUINOID COMPOUNDS AND THEIR ANALOGUES BASED ON AZIDO DERIVATIVES OF NAPHTHAZARIN

[1]Far Eastern Federal University, Institute of High Technologies and Advanced Materials
[2] Far Eastern Federal University, Oriental Institute School of Regional and International Studies
[3]G.B. Elyakov Pacific Institute of Bioorganic Chemistry, FEB RAS, PIBOC FEB RAS
Scientific adviser – V.Ph. Anufriev [3]
Scientific consultant - I.N. Lazareva[2]

Natural polyhydroxylated naphthazarins (5,8-dihydroxy-1,4-naphthoquinones) are a group of compounds found in echinoderms and lichens [1]. Due to the wide range of biological activity, the development of efficient routes for the synthesis of their most promising derivatives remains urgent. To date, several methods for the synthesis of these compounds have been described. The most common of them are based on the reaction of halogen atoms substitution in available chlorinated naphthazarins with various nucleophiles, followed by modification of the resulting products [2–4]. In turn, organic azides are very reactive synthetically useful reagents that can be used for the preparative synthesis of a wide range of compounds, including various nitrogen-containing heterocycles such as carbazoles, furoxans, azepines, triazoles, aziridines, etc. At the same time, the chemistry of azido derivatives of naphthazarin has not been extensively studied [5].

We propose a simple preparative synthesis of spinazarins (2,3-dihydroxynaphthazarins) **3a-i** via the corresponding 2,3-diazido derivatives **2a-i**, which can be obtained from chlorinated derivatives naphthazarin **1a-i** by reaction with sodium azide in methanol or dimethyl sulfoxide.

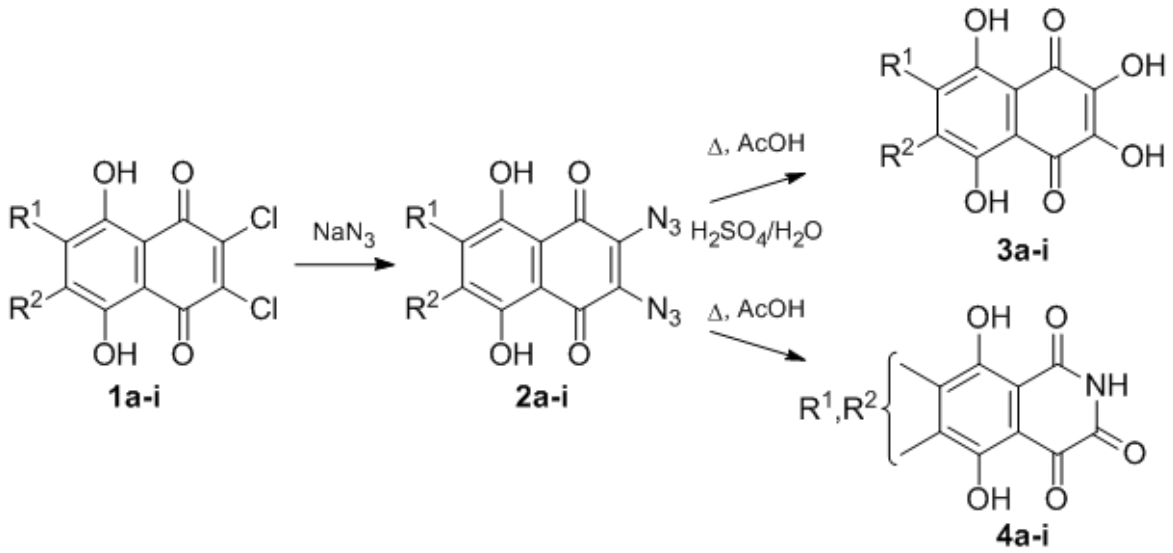

1,2,3,4 R^1,R^2: H,H (**a**); Me,Me (**b**); OMe,OMe (**c**); H,Me (**d**); H, Et (**e**); H,OH (**f**); H, OBu(**g**); OH,Me (**h**); OH,Et(**i**)

Fig.1. Synthesis and conversion of 2,3-diazidonapthazarins **2**

We have found that heating of 2,3-diazidonapthazarins 2a-i in acetic acid leads to the formation of the corresponding 5,8-dihydroxyisoquinoline-1,3,4(2H)-trione derivatives **4a-i** (Fig 1), analogs of mimosamycin alkaloid previously isolated from the sponge *Haliclona cribricutis* [6] (Fig 2). Previously, it was found that compounds 4a-i are formed by the interaction of spinazarins **3a-i** with an aqueous solution of ammonia [7]. However, the described conversion **1a i→2a-i** is more efficient.

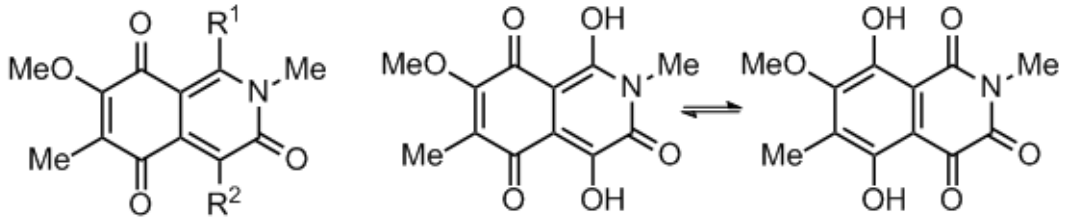

R^1,R^2: H,H mimosamycin (*Streptomyces lavendulae*); H,OH 4-hydroxymimosamycin; (marine sponges of genera Reniera, Petrosia, Xestospongia, and Haliclona)

1,4-dihydroxymimosamycin

Fig.2. Structures of mimosamycin and related alkaloids

Under the same conditions, 2-azidonapthazarines **5a-c** give 1*H*-naphtho[2,3-*b*]azirine-2,7(1aH,7aH)-dione derivatives **6a-c** (Fig. 3). The addition of water and a strong acid (sulphuric or methanesulfonic acid) to the reaction mixtures leads to the formal substitution of the azido group with the hydroxy group and the formation of the corresponding (poly)hydroxy derivatives **3a-i** (Fig. 1) and **7a-c** (Fig. 3). For some spinazarins (**3e**, **3f**), this method is more efficient than the known ones.

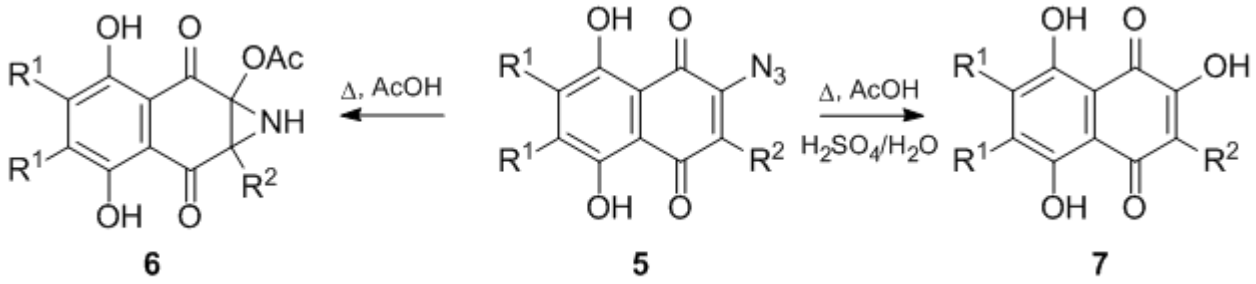

5,6,7 R^1,R^2: H,H (**a**); Me,Me (**b**); H, Me (**c**)

Fig.3. Conversion of 2-azidonaphthazarins **5**

References

1. Thomson, R.H. Naturally occurring quinones. – London: Chapman & Hall, 1997. – 742 p.

2. Anufriev, V.Ph. Fluoride salts-alcohols-alumina as reagents for nucleophilic substitution of chlorine atoms for alkoxy groups in 2,3-dichlorosubstituted juglones, naphthazarines, and quinizarines / V. Ph.Anufriev, V. L.Novikov// Tetrahedron Lett. – 1995. – P. 2515-2518.

3. Polonik, N. S DMSO-mediated transformation of 3-amino-2-hydroxynaphthazarins to natural 2,3-dihydroxynaphthazarins and related compounds / N. S.Polonik, S. G.Polonik // Tetrahedron Lett. – 2016. – P. 3303-3306.

4. Sabutskii, Yu. E. The Acid-Catalyzed 2-O-Alkylation of Substituted 2-Hydroxy-1,4-naphthoquinones by Alcohols: Versatile Preparative Synthesis of Spinochrome D and Its 6-Alkoxy Derivatives / Yu. E. Sabutskii , V. A. Denisenko , S. G. Polonik// Synthesis – 2018. – P. 3738-3748.

5. Pokhilo, N. D. Synthesis of Echinamines A and B, the First Aminated Hydroxynaphthazarins Produced by the Sea Urchin Scaphechinus mirabilis and Its Analogues / N. D. Pokhilo, M. I. Shuvalova, M. V. Lebedko, G. I. Sopelnyak, A. Ya. Yakubovskaya, N. P. Mischenko, S. A. Fedoreyev, V. Ph. Anufriev // J. Nat. Prod. – 2006. – P. 1125-1129.

6. Parameswaran, P.S. Renieramycins H and I, two novel alkaloids from the sponge Haliclona cribricutis Dendy / P. S. Parameswaran, C. G. Naik, S. Y. Kamat // Ind. J. Chem.– 1998. – P. 1258-1263.

7. Borisova, K. L. Conversion of 2,3-dihydroxynaphthazarins to isoquinoline-1,3,4(2H)-trione derivatives / K. L. Borisova, G. I. Mel′man, V. A. Denisenko, V. P. Glazunov, and V. F. Anufriev // Russ. Chem. Bull., Int. Ed.– 2012. – P. 616—622.

Ramm N.A.[1], Dyshlovoy S.A.[2]

THE CYTOTOXICITY OF 7-*TERT*-BUTYLFASCAPLYSIN STUDY

[1]Far Eastern Federal University, Institute of High Technologies and Advanced Materials
[2]Institute of Marine Biology named after A. V. Zhirmunsky FEB RAS
[3]Far Eastern Federal University, Oriental Institute School of Regional and International Studies
Scientific adviser – M. E. Zhidkov[1]
Scientific consultant - V.B. Kolycheva[3]

Fascaplysin being a biologically active compound has the chemical structure containing a β-carboline fragment. This alkaloid exhibits various pharmacological activities, such as antitumor, antibacterial, antiplasmodial, antiangiogenic, antimalarial, and it is also an inhibitor of cyclin-dependent kinase-4. However, fascaplysin has a high toxicity not allowing its use as a drug. Its toxicity is believed to be due to the flat structure of the molecule, which causes intercalation in DNA.

Synthesis of 7-*tert*-butylfascaplysin was carried out to suppress this mechanism, (Figure 1). In this case, a decrease in toxicity with respect to non-tumor cells was expected i.e., an increase in selectivity [1].

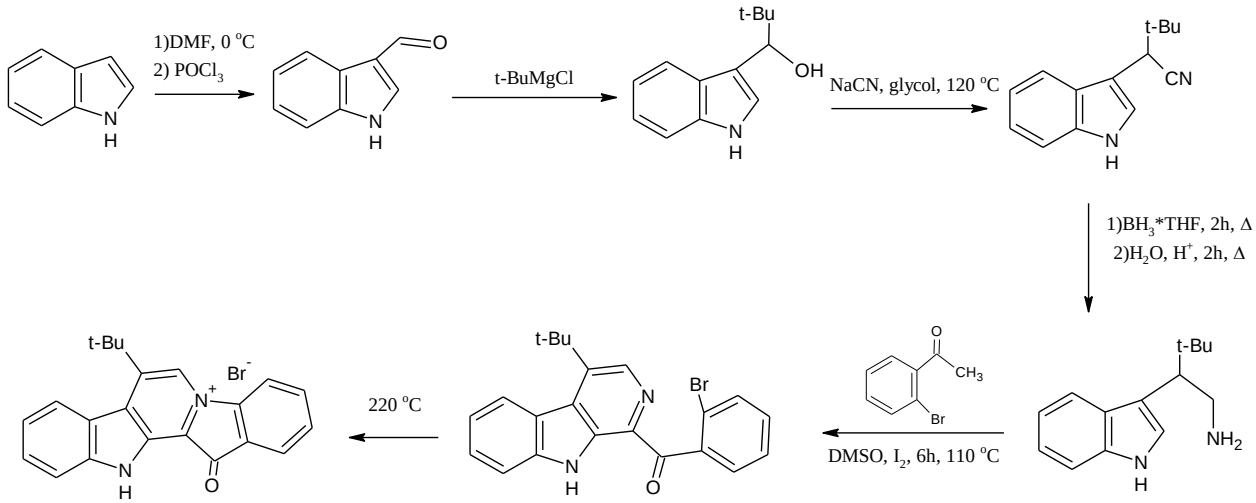

Figure 1 - Scheme for the synthesis of 7-*tert*-butylfascaplysin

Biological activity tests were performed for 6-*tert*-butylfascaplysin and 7-*tert*-butylfascaplysin against several prostate cancer cell lines (PC-3, 22Rv1, DU145, LNCaP, VCaP), which showed that non-planar derivatives of fascaplysin did not differ in selectivity from fascaplysin, while the cytotoxicity of 6-tert-butylfascaplysin decreased, and that of 7-*tert*-butylfascaplysin increased [2].

The obtained results set the task of revealing the mechanisms of 7-*tert*-butylfascaplysin action. To do this, the activity of 140 major kinases was measured under the action of the obtained substance using the functional kinomics analysis developed by Pam Technology. A general aspect of the biological action of the compound was the effect on the activity of some serine/threonine kinases (CDKL1, TBK1, CK1a1 (CSNK1A1), CDK5, RHOK (Grk1), NLK, MLKL, GCN2 (DKFZP434P061), COT (MAP3K8), caMLCK (MLCK)) having various aspects of biological action, including control of the cell cycle, signal transmission inside the cell, the development of necrosis, and others (Figure 2). The conservative structure of these kinases apparently determined the wide spectrum of activity of the compound and its high toxicity to both tumor and non-tumor cells.

Figure 2 - The effect of 7-*tert*-butylfascaplysin on 10 kinases with the most significant changes in activity

References

1. Ramm N.A., Synthesis of 7-*tert*-butylfascaplyzine: final qualification work: defended 05.07.2021 / N.A. Ramm - Vladivostok, 2021. - p. 33-40

2. Kantemirov A.V., Synthesis and activity of 6 and 7-*tert*-butylfascaplysin / A.V. Kantemirov, N.A. Ramm, E.V. Kantemirova, M.E. Zhidkov //Chemistry and Chemical Education: VIII International Symposium, October 4-6, 2021 - Vladivostok: Far Eastern Federal University, 2021. - p. 22-23

Rybalka A.A.[1], Budnikova Yu.B.[1,3], Lukiyanchuk I.V.[2], Vasilyeva M.S.[1,2,3], Kolycheva V.B.[4]

SYNTHESIS AND STUDY OF TIO_2-WO_3-$ZNWO_4$ FILM HETEROSTRUCTURES ON TITANIUM

[1] FEFU, Institute of High Technologies and Advanced Materials, Department of Nuclear Technology
[2] Institute of Chemistry FEB RAS
[3] FEFU, Institute of High Technologies and Advanced Materials, Department of Chemistry and Materials
[4] FEFU, Oriental Institute School of Regional and International Studies, Academic Dep. of English Language
Scientific adviser – M.S. Vasilyeva [1]
Scientific consultant – V.B. Kolycheva[4]

$ZnWO_4$ and WO_3 are important inorganic compounds extensively studied as heterogeneous photocatalysts for the degradation of organic pollutants [1]. The use of film composites based on oxygen compounds of tungsten is of particular interest, since it does not require the cost of separating the photocatalyst from the treated solution at the end of the technological cycle. Plasma-electrolytic oxidation (PEO) of metals with simultaneous or subsequent modification of the surface by active components can be used to obtain complex oxide film composites [2, 3].

This paper presents the results of a study of the composition, surface morphology, optical and photocatalytic properties of Zn-, W-containing films on titanium obtained by a combination of PEO, impregnation and annealing methods. W-containing oxide coatings on titanium were formed by the PEO method in galvanostatic mode at a current density 0.1 A/cm^2 for 10 min in aqueous electrolyte containing Na_2WO_4 and $Na_2B_4O_7$. Further, the PEO layers were kept for 1 hour in an alcohol solution containing zinc acetate, and then they were dried in air and annealed in a muffle furnace at temperatures of 500 and 700^{o}C for 1 hour. Depending on the modification conditions and the annealing temperature, the formed PEO layers received the designations Ti/W, Ti/W/Zn-500 and Ti/W/Zn-700.

The phase composition of the modified samples depends on the annealing temperature (Table 1). Both modified samples contain titanium dioxide in anatase and rutile modification. Ti/W/Zn-500 and Ti/W/Zn-700 composites additionally include zinc and tungsten oxide compounds. According to the Ti/W energy-dispersive analysis, the samples contain C, O, Ti and 0.1 at.% W. Carbon is detected in the modified PEO coatings, 0.2 at.% Zn appears, and the concentration of tungsten increases (Table 1).

Table 1

Phase and Elemental Composition of the Composites

Sample	Phase	Elemental composition, (at.%)					
		C	O	Na	Ti	Zn	W
Ti/W	(анатаз)	13.1	73.1	9.5	9.5	–	0.1
Ti/W/Zn-500	(анатаз, рутил), ZnO	20.5	74.5	–	4.5	0.2	0.3
Ti/W/Zn-700	(анатаз, рутил), WO_3, $ZnWO_4$,	17.1	74.7	2.6	4.9	0.4	0.3

Figure 1 shows the SEM images of the surface of the obtained PEO coatings. The morphology of PEO coatings largely depends on the annealing temperature. All coatings are heterogeneous, there are micron-sized pores on the surface. The surface of the initial coatings is smooth. After annealing of the samples at 500 and 700^{0}C, crystal formation is observed.

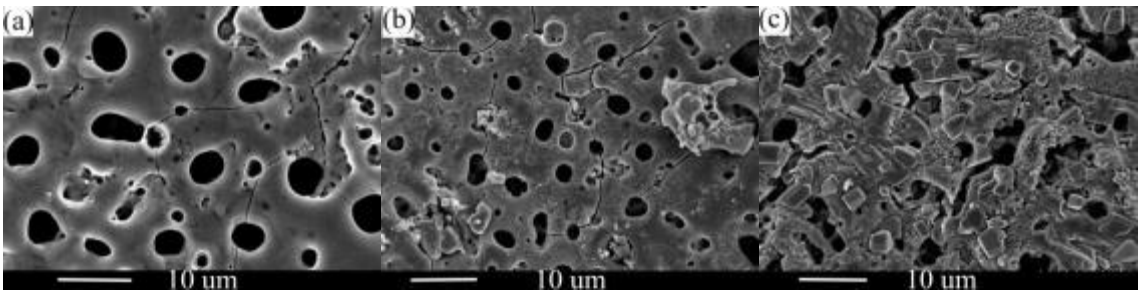

Figure 1 – SEM images of the sample surface: (a) – Ti/W, (b) – Ti/W/Zn-500, (c) – Ti/W/Zn-700

Photocatalytic studies have shown that the formed composites are active in the degradation reaction of indigo carmine (IC) only under UV light irradiation. Obviously, this is due to the fact that all samples are characterized by high values of the forbidden band width (Table 2).

Table 2

Direct (n=1/2) and Indirect (n=2) Band Gaps E_g and Photocatalytic Activity of the Composites

Sample	E_g, (eV)		IC degradation degree, (%)	
	n=1/2	n=2	Visible light	UV light
Ti/W	3.23	3.05	1	10
Ti/W/Zn-500	3.24	3.1	5	51
Ti/W/Zn-700	3.26	3.03	3	22

Thus, in this work, a combination of PEO, impregnation and annealing methods formed oxide layers on titanium containing zinc tungstate and/or tungsten oxide, promising for use as photocatalysts for degradation of organic pollutants under UV irradiation.

References

1. S. Mostafa Hosseinpour-Mashkani. Precipitation Synthesis, Characterization, Morphological Control, and Photocatalyst Application of $ZnWO_4$ Nanoparticles / S.M. Hosseinpour-Mashkani, M. Maddahfar, A. Sobhani-Nasab // Journal of Electronic Materials – 2016. – Vol. 45, No. 7. – P. 3612–3620

2. Suminov, I.V., Belkin P.N., Epelfeld A.V. et al. Plasma-electrolytic modification of the surface of metals and alloys: in 2 volumes Vol. II / under the general ed. by I. V. Suminov. Moscow: Technosphere, 2011. 512 p.

3. Rudnev V.S. Temperature-controlled growth of micro- and nanocrystals on the surface of NiO+CuO/TiO_2/Ti composites / V.S. Rudnev, I.V. Lukiyanchuk, M.S. Vasilyeva, T.A. Kaidalova // Vacuum – 2019. – Vol. 167. – P. 397–406.

Saidakova K.V.[1], Eremeeva A.A.[2]

INFLUENCE OF THE MOLECULAR WEIGHT OF THE POLYMER ON THE STRUCTURE OF THE MEMBRANE, MADE BY PHASE INVERSION METHOD

[1]Far Easter Federal University, Polytechnic institute
[2]Far Easter Federal University, Institute of Science Technology and Advanced Materials
3Far Eastern Federal University, Oriental Institute School of Regional and International Studies
Scientific adviser – L.A. Lim[1]
Scientific consultant – V. B. Kolycheva[3]

Nowadays membrane processes are the most versatile way to purify and desalinate water. A promising direction in the field of membrane technologies is the development of polymeric membrane materials with high

performance, mechanical strength and low cost.

The most popular method for producing polymer membranes is the method of wet molding from a solution by phase inversion including the steps of polymer dissolution, solution degassing, film casting on a substrate, membrane deposition in a nonsolvent, washing and drying of the obtained membranes [1].

In the production of high-tech membranes, a balance must be achieved between the cost of the resulting material and its characteristics for this reason polyvinyl chloride is increasingly used in modern research as a membrane matrix. PVC is an excellent material due to a low-cost, high-volume production, physical and mechanical properties, high resistance to most chemicals and the ease of dissolution in many organic solvents: dimethylacetamide, tetrahydrofuran (THF), dimethylformamide (DMF), dimethyl sulfoxide, N-methyl-2 - pyrrolidone, dichloromethane (DCM) [2].

Obtaining membranes from solutions of PVC in dimethylformamide with different molecular weights, the concentrations of the polymer solution are used in the range of 8-15 wt. % for pure solvent and up to 20 wt. % mixtures of solvents with DMF (table).

Table

Correspondence of the concentration and molecular weight of the polymer in PVC membranes

Molecular weight of PVC, g/mol	Solvent	The concentration of PVC in the casting solution, wt. %	Source
55000	DMF	9–11	[3]
65000-85000	DMF	8–12	[4]
48400	DMF	8	[5]
91000	DMF + THF	10	[6]
-	DMF + DCM	20	[7]

The authors of [4] found the porosity of membranes to increase with a decrease in the PVC molecular weight. Membranes made from lower molecular weight PVC are characterized by a higher void volume and a more open-celled structure. This fact can be explained by the greater mobility of PVC particles in the casting solution.

In our study solutions of PVC-C-7058-MTS (Mm = 90470 g/mol) were prepared with concentrations of 7, 9 and 10 wt. %. When manufacturing a series of membranes by phase inversion, the impossibility was found out to obtain a homogeneous casting solution with a high polymer concentration, and, consequently, a monolithic membrane: already at concentrations above 7 wt. % solution was a jelly and could not be evenly distributed on the substrate at low tide (figure 1). Insufficient dissolution of PVC (9 wt. %) was confirmed by SEM photographs (figure 2), showing the presence of clear globules in the structure of the obtained membranes.

Figure 1 - View of a sample with a PVC concentration of 9 wt. %

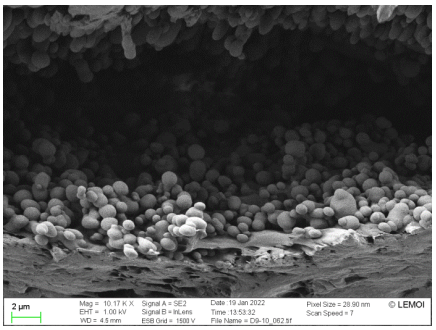

Figure 2 – SEM-image of a sample with a PVC concentration of 9 wt. %

These values of the maximum possible concentration are associated not only with the molecular weight of the polymer, but also with the relatively high difference in the solubility parameters of PVC and DMF. From this point of view, in order to obtain more concentrated PVC casting solutions with a molecular weight of 90470 g/mol, it is possible to use mixtures of DMF with solvents with a high affinity for polyvinyl chloride.

Thus, for grades of PVC with a high molecular weight, there are limitations associated with the concentration of the polymer and the viscosity of the casting solution for the production of membranes by the phase inversion method.

References

1. Дубяга, В. П. Полимерные мембраны / В. П. Дубяга, Л. П. Перепечкин, Е. Е. Каталевский. – Москва : Химия, 1981. – 232 с.

2. Mei, S. Preparation of porous PVC membrane via a phase inversion method from PVC/DMAc/water/additives / S. Mei, C. Xiao, X. Hu – DOI 10.1002/app.33219 // Journal of applied polymer science. – 2011. – Vol. 120, N 1. – P. 557-562.

3. Ramesh, P. B. Preparation, structure, and transport properties of ultrafiltration membranes of poly(vinyl chloride) and poly(vinyl pyrrolidone) blends / P. B. Ramesh, V. G. Gaikar – DOI 10.1002/1097-4628 // Journal of applied polymer science. – 2000. – Vol. 77, Is. 12. – P. 2606-2620.

4. Bodzek, M. The influence of molecular mass of poly (vinyl chloride) on the structure and transport characteristics of ultrafiltration membranes / M. Bodzek, K. Konieczny // Journal Of membrane science. – 1991. – Vol. 61. – P. 131-156.

5. Polyvinylhcloride membrane for a glucose sensor / S. Hirose, M. Hayashi, N. Tamura et al. – DOI 10.1016/0304-5102(79)80031-0 // Journal of molecular catalysis. – 1979. – Vol. 6, Is. 4. – P. 251-260.

6. Maghsoud, Z. Preparation of polyvinylchloride membranes from solvent mixture by immersion precipitation / Z. Maghsoud, M. Famili, S. Madaeni – DOI 10.1002/APP.40206 // Journal of applied polymer science. – 2013. Vol. 131, Is. 8. – P. 1-8.

7. Utilization of waste polyvinyl chloride (PVC) for ultrafiltration membrane fabrication and its characterization / M. Aji, S. Narendren, M. Purkait, V. Katiyar – DOI 10.1016/J.JECE.2019.103650 // Journal of environmental chemical engineering. – 2020. – Vol. 8, Is. 2. – P. 1-8.

A.A. Spesivaya[1], M.R. Kaigorodova[1], L.I. Sokolova[1],V.B. Kolycheva[2]

DETERMINATION OF SORPTION CAPACITY OF DESOLAC AND SPILL-SORB SORBENTS

[1]FEFU, Institute of High Technologies and Advanced Materials, Department of Chemistry and Materials
[2]FEFU, Oriental Institute School of Regional and International Studies, Academic Dep. of English Language
Scientific adviser – L.I. Sokolova[1]
Scientific consultant – V.B. Kolycheva[2]

Modern civilization cannot do without the use of oil and petroleum products; however, their extraction, storage, transportation and processing often become a source of environmental pollution. In recent years, oil spills have become more frequent during transportation by sea. Crude oil and heavy petroleum products (fuel oil, diesel, lubricating oils) entering the water settle on the bottom and mix with silt forming stable conglomerates that negatively affect flora and fauna. That is why there is a need to clean seawater, sediments and coastal zones from petroleum products. For this purpose, various sorbents are created that have a natural ability to biodegrade absorbed hydrocarbons.

Together with the Fire and Rescue Academy we conducted determination of petroleum products at model landfills in order to find out the efficiency of sorbents. The aim of the work was to study the dynamics of petroleum products distribution between two phases (seawater and bottom soil) using desolac and spill-sorb sorbents.

Sorbent from the water surface and oil-contaminated soils with sorbent and without sorbent were taken for the study. The mass content of petroleum products was determined by gravimetry. The content of petroleum

products in the soil sample changed from 29768.64±8930.59 mg/kg to 8861.42±2658.43 mg/kg and in the sand sample from 5531.67±1659.50 mg/kg to 331.32±99.40 mg/kg, indicating the process of absorption of hydrocarbons. The mass fraction of petroleum products in the sorbents was noticed to increase significantly in analyzed sorbent from the water surface. For sorbent taken from the surface of water contaminated with diesel, the values increased from 56196.57±16858.97 mg/kg to 13548.56±40628.57 mg/kg; for water contaminated with fuel oil the values increased from 314245.75±94273.73 mg/kg to 475288.97±142586.69 mg/kg. This can be explained by the fact that the sorbent has absorbed a sufficiently large amount of hydrocarbons.

The content of petroleum products in contaminated samples significantly decreased with the addition of the sorbent indicating the high sorption capacity of dezolak and spill-sorb.

References

1. Drugov Yu.S. Environmental analyses in oil and petroleum product spills/ Drugov Y.S., Rodin A.A.– S.-Pb., 2000 – 250 p.

2. Method of measuring the mass fraction of petroleum products in samples of soils, soils, sediments, silts, sewage sludge, production and consumption waste by gravimetric method. MON F 16.1:2:2.2:2.3:3.64-10./ Moscow, 2010 – 18p.

Sumarokova D.V. [1], Chernyaev A.P. [1], Kolycheva V.B. [2]

CHROMATOGRAPHIC ANALYSIS OF THE CURRENT CONTENT OF POLYAROMATIC HYDROCARBONS IN THE COMPONENTS OF MARINE ECOSYSTEMS OF WESTERN KAMCHATKA

[1] FEFU, Institute of High Technologies and Advanced Materials Department of Chemistry and Materials
[2] FEFU, Oriental Institute School of Regional and International Studies, Academic Dep. of English Language
Scientific supervisor - A.P. Chernyaev [1]
Scientific consultant – Kolycheva V.B. [2]

There are large emissions of harmful substances into the environment as a result of the active development of industrial production, energy enterprises, the chemical and oil refining industries, and transport. Polyaromatic hydrocarbons are important anthropogenic pollutants [1, 2, 3]. The objective of the work was to assess the current content of polyaromatic hydrocarbons in the components of marine ecosystems of Western Kamchatka.

In this regard, the following tasks were set and solved:

1) to investigate the spectrophotometric properties of priority PAHs;

2) to propose a gradient elution program with a gradient change in the conditions of absorption and emission of individual PAHs under conditions of HPLC with fluorescent detection;

3) to determine the content of PAHs in bottom sediments and hydrobionts using the proposed methodology.

The following results were obtained from the analysis.

As a result of the analysis of bottom sediments samples (sea urchins *Strongylocentrotus: polyacanthus*, Gray mussels *Crenomytilus grayanus*, mussels *Bolocera multicornis* and sea anemones *Actinia equine*) by reverse phase high-performance liquid chromatography using a fluorescent detector the highest concentration of PAHs among hydrobionts was found in a sample of a sea urchin of station 2 0.065 mg/kg.

The sea urchin samples from stations 1 and 3 contained 0.046 mg/kg. PAH concentrations in samples of algae, sea anemones, fingerling mussels and Gray mussels were 0.030; 0.043; 0.049; 0.055 mg/kg, respectively.

The lowest concentration of PAHs was found in the sample of the bottom sediments of station 2 0.011 mg/kg. The maximum toxicity of PAHs was detected in the bottom sediments of station 1, where the index

was 0.0058.

In all samples the index was in the range of 0.0014-0.0058. The permissible levels of benz(a)pyrene in marine invertebrates and algae were not exceeded at any station. Thus, the conclusion was made about the low degree of PAHs impact on the components of ecosystems of Western Kamchatka.

1. In this study the fluorimetric properties of 17 priority PAHs were studied. According to the data obtained, the characteristic wavelengths of absorption and emission of the components were revealed.

2. A program of gradient elution under conditions of HPLC allowing reducing the analysis time to 45 minutes was proposed.

3. The content of PAHs in bottom sediments and hydrobionts of western Kamchatka was determined. The PAH content in bottom sediments was in the range (0.011-0.045 mg/kg), in hydrobionts - (0.03-0.065 mg/kg).

4. The equivalent toxicity index was calculated. The existing PAH contents was shown not to cause a significant negative effect on the ecosystem components of the studied water area.

References

1. Education and accumulation of PAHs [Electronic resource] - URL: http://www.ecostam.ru/eaecos-36-1.html

2. Polycyclic aromatic hydrocarbon [Electronic resource] - URL: https://ru.xcv.wiki/wiki/Polycyclic_aromatic_hydrocarbon

3. Polycyclic aromatic compounds. Polynuclear aromatic hydrocarbons [Electronic resource] - URL: https://tugulympu.ru/policiklicheskie-aromaticheskie-soedineniya-poliyadernye-aromaticheskie/

Tokareva T.V.[1], Selin P.E.[1], Dmitrienko I.V.[2]

ACTIVATION OF REFRACTORY GOLD-CONTAINING ORES BY PULSED ELECTRIC DISCHARGE AND ELECTRON BEAM

[1]National Research Tomsk Polytechnic University, School of Nuclear Science & Engineering, TPU,
[2]LLC «Promgeotecnology»
Scientific adviser – Dmitrienko V.P.[1]

At present, due to the depletion of the raw material base, many companies increasingly use refractory ores [1]. The purpose of this work is to determine the effect of the impact of pulsed electrical discharges and a pulsed electron beam on the gold leaching degree in gold-bearing ore materials and to substantiate the practical use of these methods. 4 samples of technogenic wastes from various deposits with refractory sulfide ores containing pyrite, arsenopyrite and carbonaceous substances are provided for the research.

Neutron activation analysis (NAA), inductively coupled plasma mass spectrometry, optical microscopy, IR spectroscopy, coal petrographic analysis were used in the work.

Taking into account the organic and mineral components of ore materials, two ore activation methods were used: based on an electric discharge, which provides interphase defragmentation of the processed material, and an electron beam, which provides the organic compounds destruction.

All initial samples of technogenic wastes and concentrate from deposit B submitted by the customer were subjected to neutron activation analysis. The number of measurements on one sample was 3. The mass of encrypted samples submitted for neutron activation analysis, taken after quartering: A – 2.0 g, B – 2.0 g, V – 2.02 g, D - 2.04 g. The results are shown in *Table 1*, which shows the average values of the content of metals in the samples.

Table 1

Results of the sample analysis by NAA method

№	Deposit	Defined element			
		Au, g/t	Ag, g/t	As, g/t	Fe, %
1	A	0,014	<0,7	10,17	41,09
2	B	83,41	<0,7	89494	27,03
3	C	27,99	<0,7	30654	23,60
4	D	1,149	6,70	426,1	40,31

The high content of arsenic and iron confirms the presence of pyrite and arsenopyrite in samples B and C. Sample A of the initial concentrate from deposit B was analyzed on a mass spectrometer, containing the following amounts of elements: Au – 65.5 g/t (sample 1); Ag – 2.73 g/t, Fe – 164206 g/t, As – 26604 g/t.

We revealed a good convergence of the analysis for gold, carried out at the Plasma Chemical Analytical Center (65.5 g/t), and declared by the customer (63 g/t). The contents of other metals differ significantly from the results obtained by the NAA method, as well as for gold (83.41 g/t).

Coal petrographic analysis was carried out for samples from deposits B and C. Most of the organic matter is sapropelite matter, humus matter is represented by individual grains. In general, organic matter in sample B is 21%, in sample C — 18%; 79 and 82% of mineral impurities respectively. The microtexture of the sapropelite main mass is represented by “cindery” massive aggregates in the form of large grains. The content of organic matter at the level of 18-21% and the presence of hydrocarbon and cyclic compounds indicate an increased content of organic carbon. Radiation treatment makes it possible to effectively destroy these organic compounds and conduct leaching with a high gold extraction degree.

The initial samples were activated by the methods of electric discharge pulsed processing (EDPD) and exposure to an electron beam on a pulsed electron accelerator with the sample placed in a dielectric (EU-1) and conductive (EU-2) boats. The activated samples were transferred to the leaching stage.

Leaching parameters: ThiO – 30 g/l, $FeCl_3 \cdot 6H_2O$ – 4.0 g/l, H_2SO_4 – 5 g/l, S:L = 1:3, leaching time – 16 hours.

Process solutions were subjected to analysis on an ELAN ICP mass spectrometer model DRC-e no. W 1520501 after leaching of the initial and activated by two methods samples. The results are shown in *Table 2*.

Table 2

The analysis of process solutions of deposit B without activation and with activation by an electron beam (EB) and electric discharge treatment (EDT)

№	Gold content in process solution, mg/l						
Sample 1	Initial-B 0,0094	EB-1B	EB-2B	EDT-B	K_{EB-1B}	K_{EB-2B}	K_{EDT-B}
		0,019	0,042	0,034	2,02	4,46	3,61
Sample 2	Initial-C 0,032	0,037	0,043	0,049	1,16	1,34	1,53

The value of coefficients K was calculated by formula .

$$K = \frac{C_{in}}{C_{sp}},$$

C_{in}, C_{sp} are the gold content in the leaching solution of the initial sample and in the leaching solution of the activated sample respectively.

The results of the experiments show a significant impulse activation effect on the leaching degree of gold-bearing ores of double refractory (pyrites, arsenopyrites and carbonaceous substances). The increase in the gold content in the productive solution reaches from 2 to 4.4 times for sample B, and from 1.16 to 1.5 times for sample C. However the obtained results must be treated as estimates, and it is necessary to conduct systematic research on the development of technology activation of refractory ores in this way.

References

1. V.P. Dmitrienko, I.V. Dmitrienko, Y.M. Makaseev, M.E. Sidorov. Thiourea leaching of gold from gravitational concentrate. // Gold and tecnology -2013-№.-P.82-4

2. S. Yudin [et al.] Electrical discharge drilling of granite with positive and negative polarity of voltage pulses // International Journal of Rock Mechanics and Mining Sciences. — 2019. — Vol. 123. — [104058, 7 p.].

Khudyakova E.A.[1], Arefieva O.D.[1,2,3], Minakova P.S.[4]

COMPOSITION OF WASTEWATER FROM THE GALVANIC «VARYAG PLANT» SHOP

[1]Department of Oil and Gas Technology and Petrochemistry, FEFU

[2] Department of Nuclear Technology INTIPM FEFU

[3] Institute of Chemistry FEB RAS

[4]Academic Dep. of English Language, FEFU, PhD in Education, Associate Professor P.S. Minakova

Scientific adviser - O.D. Arefieva[1,2,3]

Untreated wastewater leads to the pollution of water bodies, land, atmosphere, biosphere. And the fact that water consumption over time only increases – the issue of wastewater treatment is a matter of existence for humans [1]. Now most enterprises have systems of local treatment of industrial water, allowing to treatment wastewater to the established limit concentrations of pollutants for discharge into sewage systems. Creation of local treatment facilities requires compliance with a certain sequence of works. First of all, it is the preparation of competent technical specifications based on reliable baseline data not only on the amount and composition of effluents, but also the nature of the production itself (mode of operation, irregularity of water disposal, etc.) [2]. Depending on the type of pollutants contained in the effluent, the type of local treatment facilities or a set of treatment methods is selected [3]. Therefore, the purpose of the present work is to study the chemical composition of industrial wastewater of the galvanic shop of Public Joint Stock Company «Varyag Plant».

The object of the study was industrial wastewater from the galvanic shop of «Varyag Plant» of two types: chromium (№ 1-cw), acid-alkali (№ 2 a-aw). The samples were taken in November, 2021.

Every technological process of galvanic metal coatings consists of a number of separate operations: preparatory work, main process, finishing operations [4, 5]. After each operation the product is washed in cold running water, and after processing in alkaline solutions - sequentially in hot and cold water. At the final stage of processing the product is consistently washed in cold and hot water and dried. Thus, galvanic production is inextricably linked with the discharge of waste washing water [5].

In the studied water samples were determined by chemical indicators of water quality: total hardness, the content of calcium ions, total alkalinity, chlorides, sulfates, pH, the content of nickel, cobalt, chromium (VI), copper (cuprum), iron (total) (ferrum), aluminum, salt content.

The results of the study showed that some of the values of pollutants in the wastewater of the galvanic shop of «Varyag Plant», selected before entering the local treatment facilities (samples 1-cw and 2-a-aw), exceed the regulatory values, municipal water (maximum permissible concentrations) [6].

Acid-alkaline water (№ 2 – a-aw) has high salt content, alkalinity and chloride content compared to chromium water, but the obtained indicators do not exceed the established norms of maximum permissible concentrations. In chrome water, the content of metals (nickel, chromium, aluminum, and iron) was exceeded by - 13; 9; 2 and 3 times, respectively.

It was found that the chromium water of the galvanic shop «Varyag Plant» does not meet the standards for municipal water in terms of chromium (VI), aluminum, iron and nickel, so it is necessary to treat it at local treatment facilities. The quality indicators of acid-alkali water do not exceed maximum permissible concentrations [6].

References

1. Modern wastewater treatment plants - Article // Official website of NPO Agrostroyservis LLC: [website]. – 2021. – URL: https://acs-nnov.ru/sovremennye-lokalnye-ochistnye-sooruzheniya.html.
2. Garzanov, A.L. Waiting for changes / A.L. Garzanov, A.A. Klyachko. A. // Dairy Industry. – 2014. – № 8. – P. 42-43.
3. Local sewage treatment plants - Article // Official website of the company "Megaline" LLC: [website]. – 2020. – URL: https://www.megaln.ru/news/lokalnie-ochistnie-sooruzheniya-los/.
4. Treiman, M.G. Modern electroplating and its ecologization / M.G. Treiman // Actual problems of humanities and natural sciences. – 2009. - № 9. – P. 15 – 17.
5. Galvanic production: environmental problems and modern ways to solve them. - Article // VII International student scientific conference - Student scientific forum: [website]. – 2015. – URL: https://scienceforum.ru/2015/article/2015012729.
6. On approval of sanitary rules and regulations SanPiN 1.2.3685-21 "Hygienic standards and requirements to ensure safety and (or) harmlessness to humans of the factors of habitat" of January 28, 2021 № 2 // Electronic fund of legal and regulatory and technical documents. [website]. - 2021. - URL: https://docs.cntd.ru/document/573500115.

Cheshkin A.E. [1] Minakova P.C.

BALEISKY GOLD-BEARING AREA TECHNOGENIC WATER` TREATMENT TECHNOLOGIES

[1] Department of Oil, Gas and Petrochemical Industry, Polytechnic Institute, FEFU
[2] Department of Nuclear technologies, Institute of High Technologies and Advanced Material, FEFU
[3]Academic Dep. of English Language, Oriental Institute School of Regional and International Studies, FEFU
[1, 2] Scientific adviser – K.R. Frolov
[3]Scientific consultant – Minakova P.C.

Introduction. Zabaikalsky Krai is one of the centers of gold mining: more than 7 % of all-Russian gold reserves are concentrated here in complex ores and placers [1]. One of the long-standing gold mining areas in Eastern Transbaikalia is the Baleisky gold-bearing region [2]. In the process of gold extraction and development of ore bodies there was an active negative impact on natural geosystems. But even after the liquidation of the enterprises, the mine continues to have a negative impact on the soil, vegetation and the surface layer of the atmosphere, as well as aquifers and surface water bodies. The purpose of the work is to show the negative impact of the Baleisky gold-bearing area on the environment, and to characterize its technogenic water treatment technologies.

General characteristics and negative impact. The Baleyzoloto Combine operated from 1929 to 1993, three gold deposits were mined in the Baleysko-Taseevskoye (Baley) ore field [3]. Technogenic transformations of natural landscapes influence the inflow of heavy metals into surface waters. In addition to dredge dumps, they are represented by three ore pits, two tailings pits of gold concentration plants (GCPs), dumps of overburden and host rocks, excavation pits of gold sands, and sludge pits [2]. The Baleisky Mining and Processing Plant (MPP), in comparison with other plants in the Trans-Baikal Territory, has a large amount of technogenic raw materials from tailings ponds (34.27 million tons) and dumps of overburden rocks and poor ores (81.87 million tons). In 1929 a running amalgamation factory was put into operation, which included mercury in the technological process of processing ores and sands [4]. This technology was used until negative effects on the safety and livelihood of service personnel were identified. According to [5], the ore was further enriched by flotation followed by cyanidation of the concentrates. Over the entire period of time, GCP-1 and GCP-2 produced 365 tons of ore gold, and the reserves have not been depleted.

The authors [6] conducted water sampling from the flooded open pits of the Baleisky and Taseevsky deposits. Values of pH and metal concentrations repeatedly exceed the maximum permissible concentrations (MPC's) for fishery water bodies (times): by Sr – 5.43 times, Al – 10825, Mn – 12300, Fe – 4520, Cr – 41, As – 87, Cu – 33500, Zn – 5090, Pb – 6.7, Cd – 220, Ni – 6400, Co – 1160.

Technogenic water` treatment technologies. Methods of technogenic water treatment can be divided into mechanical, chemical, physical-chemical, and biological [7]. Next, let us consider technologies (methods) of technogenic water treatment, which are applicable to technogenic water of the object in question.

The essence of reagent methods is to convert water-soluble substances into insoluble ones by adding various reagents with their subsequent separation from water in the form of precipitation. Calcium and sodium hydroxides, sodium sulfide, and various wastes such as ferrochrome slag are used as reagents [8]. The advantage of this method is that it covers many pollutants. The disadvantages include a significant consumption of reagents, increased salt content of treated water, insufficient efficiency when it is necessary to clean up to MPC of fishery water bodies, the formation of fine-dispersed poorly settling sludge [9].

The ion exchange method is a process of interaction between a solution and a solid, an ion exchanger, which can exchange the ions contained in it for the ions present in the solution [10]. Ion exchange is a promising but expensive method of extraction of high cost resins modified by the introduction of functional groups, low capacity of ion exchangers and the need for frequent regeneration [9].

The essence of the extraction method is to add to water an extractant that is not soluble in the liquid but dissolves the substance to be extracted. Application of extraction from the economic point of view is expedient in case of significant concentrations of extractable components or their high marketable value, as well as in case of treatment of highly toxic wastewater when other methods are not acceptable [11].

The sorption method allows one substance to be extracted with another substance, solid or liquid by absorption. The advantages of this method are the ability to absorb substances from multicomponent mixtures and a high degree of purification. However, sorption of heavy metals from wastewater is most effective at low concentrations of pollutants, so the use of sorption by this material at the stage of mine water pretreatment is expedient [8].

Conclusion. During the study of the Baleisky gold-bearing area, it was found that the operating pits at the site of the deposits were flooded with aggressive acidic waters with a high concentration of heavy metals. Among traditional purification methods, the reagent method is the most suitable, as it covers a larger number of pollutants. However, it does not allow achieving treatment efficiency up to the levels of maximum permissible concentrations of harmful substances for fishery water bodies. Therefore, it is necessary to use combined methods, new methods, and technical solutions.

References

1. Shevchenko, Y.S. Gold mining industry of Zabaikalsky Krai: status and near-term development prospects / Y.S. Shevchenko, O.I. Rybakova, A.A. Sarvanov // Mountain Information and Analytical Bulletin (scientific and technical journal). – 2010. – № 4 – P. 51-54.

2. Zamana, L.V. Mercury in surface waters of Balei-Taseevsky gold mining unit / L.V. Zamana // Notes of Zabaikalsky Branch of Russian Geographical Society. – 2012. – № 131. – P. 83-86.

3. Yurgenson G.A. Leaking gold-bearing tailings of Baleyzoloto combine: the problem of recycling / G.A. Yurgenson, L.V. Shumilova, A.N. Khatkova. – DOI 10.21209/2227 // Bulletin of ZabGU. – 2021. – Vol. 27, № 4. – P. 45-54.

4. Mezentseva, I.V. Baley: "Golden" History of Trans-Baikal Gold Mining Flagship and Present Realities / I.V. Mezentseva // Border Region in Historical Development: Partnership and Cooperation : Proceedings of the International Scientific-Practical Conference on the 80th Anniversary of the Victory of the Soviet and Mongolian Forces on the Khalkhin-Gol River, Chita, September 18, 2019. – Chita : Zabaikalye State University, 2019 – P. 211-214.

5. Baleiskoe ore field (geology, mineralogy, genesis issues) / Central Research Geological Exploration Institute of Non-Ferrous and Precious Metals of the USSR Ministry of Geology; edited by I.A. Korotchenko. – Moscow, 1984. – 271 p.

6. Zamana, L.V. Ecological and hydrogeochemical characteristics of water bodies of gold mining Baleisko-Taseevskoe ore field (Eastern Transbaikalia) / L.V. Zamana, M.T. Usmanov // Proceedings of the Siberian Branch of the Section of Earth Sciences of RAS. – 2009. – Vol. 1, № 34. – P. 106-111.

7. Voronov, Y.V. Water disposal and wastewater treatment / Y.V. Voronov, S.V. Yakovlev. – Moscow: Association of Building Universities Publishing House, 2006. – 704 p. – ISBN 5-93093-119-4.

8. Stripling L.O. Fundamentals of wastewater treatment and solid waste processing: a training manual / L.O. Stripling, F.P. Turenko. – Omsk: OmSTU Press, 2005. – 193 p.

9. Orekhova N.N. Scientific rationale and development of technology for integrated processing and recycling of anthropogenic copper-zinc water of mining enterprises : specialty 25.00.36 – "Geoecology (mining and processing industry)". D. thesis / N.N. Orekhova – Magnitogorsk, 2014. – 353 p.

10. Maung L.M., Shitova V.O., Kagramanov G.G. Wastewater treatment from heavy metals by ion exchange / L.M. Maung, V.O., Kagramanov G.G. // Advances in Chemistry and Chemical Technology. – 2016. – Vol. 9, № 2. – P. 109-110.

11. Korneeva, T.V. Geochemical characteristics of the mechanism of interaction between neutral man-made flow and natural waters of Salair ore field / / T.V. Korneeva // Chemistry for sustainable development. T.V. Korneeva // Chemistry for sustainable development. – 2010. – Vol. 18, № 2. – P. 197-208.

Shilov A. N.[1,2], Panasenko A. E.[2], Tkachenko I. A.[2]

MAGNETOACTIVE COMPOSITE SORBENT $CoFe_2O_4$-SiO_2: MAGNETIC, SORPTION AND DESORPTION PROPERTIES

[1]Far Eastern Federal University, Polytechnical Institute
[2]Institute of Chemistry FEB RAS
[3]Far Eastern Federal University, Oriental Institute School of Regional and International Studies
Scientific adviser – A. E. Panasenko[2]
Scientific consultant – V. B. Kolycheva[3]

Introduction. Composites based on cobalt ferrite are of great interest due to the possibility of creating magnetically sensitive sorbents. This determines the prospects for their use for medical purposes for the transportation of medicines, as well as for solving problems associated with pollution of water objects and purification of gases from pollutants.

Silicon dioxide owing to the developed surface shows a high sorption capacity in combination with chemical inertness and non-toxicity. An additional advantage of using silica is the solution to the problem of disposal of rice production waste - husks and straw containing up to 21% SiO_2. Hundreds of millions of tons of rice husks are formed annually, which can be used as a cheap renewable raw material for obtaining high-purity silica [1].

The study of the various substances desorption from the surface of sorbents is of significant interest, including those containing $CoFe_2O_4$ [2], under the action of microwave radiation, which at the moment is economically more profitable and faster, and is already actively used around the world in various fields from drying bulk materials to accelerating the process of regeneration of catalysts and desorption of drugs from the surface of sorbents [3,4]. The purpose of this work was to obtain composites with $CoFe_2O_4$-SiO_2 structure, to study their magnetic and sorption properties, as well as to analyze their desorption properties using microwave radiation.

Materials and methods. Composite materials $CoFe_2O_4$-SiO_2 were synthesized according to the procedure

described in [5] by hydrolytic deposition of a SiO_2 layer on the surface of $CoFe_2O_4$ colloidal particles. The composition of the samples and the sorption capacity in relation to copper (II) ions are shown in Table 1.

Table 1

The composition of the obtained samples

Sample	Synthesis method	Fe_2O_3, %	$CoFe_2O_4$, %	SiO_2, %	H_2O, %	A, mg/g
1	$CoFe_2O_4$+SiO_2 (pH=8-9)	-	51.9	12.4	9.8	7.8
2	$CoFe_2O_4$+SiO_2 (pH=12-14)	22.5	23.4	21.3	15.9	23.4

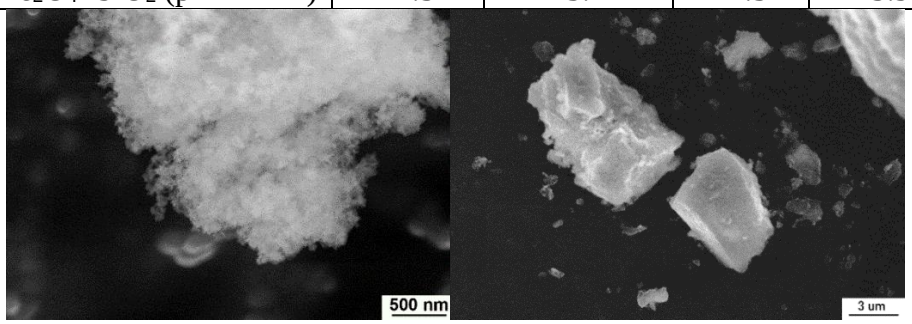

Figure 1 - Micrographs of the composite material $CoFe_2O_4$-SiO_2

Results and discussion. On the X-ray diffraction patterns (Fig. 2), the position of the reflections corresponds to cobalt ferrite $CoFe_2O_4$. Particles obtained at a higher pH value are more crystallized, which is manifested in increased intensity of reflections. The IR absorption spectra (Fig. 2) show absorption bands corresponding to the stretching and bending vibrations of the O-H bonds of adsorbed and bound water (3439-3327 cm^{-1}, 1633-1622 cm^{-1}). The presence of absorption bands at 1086, 1082, and 457 cm^{-1} is characteristic of stretching and bending vibrations of O–Si–O bonds.

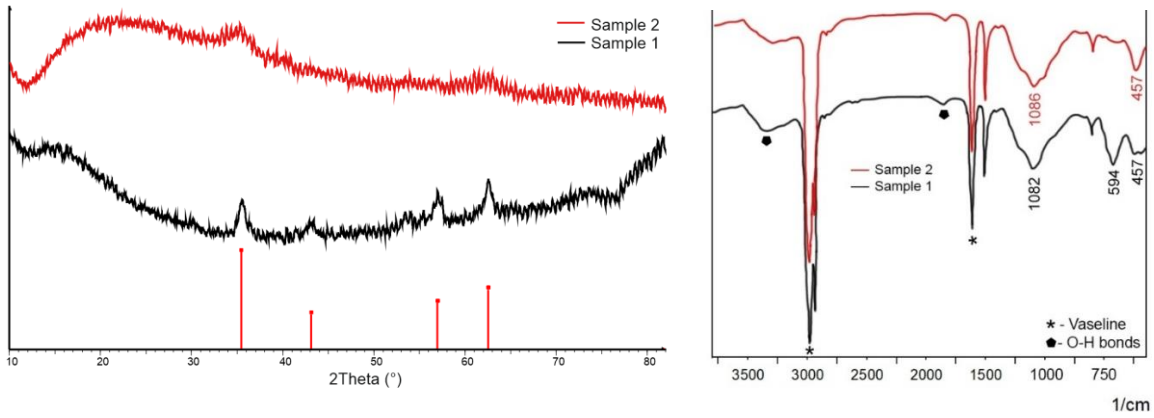

Figure 2 - X-ray patterns and IR spectra of the obtained samples

A distinctive feature of the IR spectrum of sample 1 is the presence of an absorption band in the region of 594 cm^{-1}, which indicates the stretching vibration of the Me–O bond in $CoFe_2O_4$, being consistent with the results of elemental and phase analysis. Comparing this band with the absorption band of pure cobalt ferrite, its weakening appears probably due to the modification of SiO_2 [6].

Table 2

Magnetic characteristics of samples

Sample	Ms, emu/g		Hc, Oe	
	250 K(1)/300 K(2)	2 K	250 K(1)/300 K(2)	2 K
1	43.2	56.7	−249	−6568
			+247	+6470
2	3.7	18.3	−13	−2642
			+14	+1281

The field dependences of the samples are shown in Figure 3. Based on the shape of the curves obtained at 300 and 250 K, as well as the values of the coercive force, it can be concluded that sample 1 is magnetically hard, and sample 2 is magnetically soft (Table 2). The lower saturation magnetization of sample 2 in comparison with sample 1 is associated with a lower content of cobalt ferrite (Table 1). In the sample 2, the displacement of hysteresis loop to the region of negative fields is recorded. The value of displacement is 681 Oe. This displacement can indicate an interaction of the antiferromagnet-ferromagnet type. This type of interaction can confirm the presence of a metal oxide phase, namely Fe_2O_3, which, according to elemental analysis data presented in sample 2 (Table 1). This oxide is known to have antiferromagnetic properties.

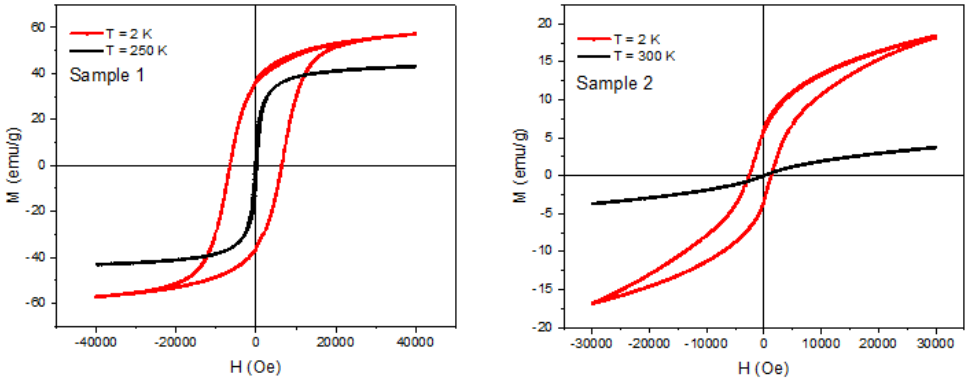

Figure 3 - Field dependences of the magnetization for the obtained samples

Silicon dioxide being known as a good sorbent, the copper (II) ions desorption from the resulting composite material under the action of electromagnetic radiation was studied. A microwave magnetron with a radiation power of 111 W (mode 1) and 392 W (mode 2) was used as an EMR source; heating was carried out in a heat-insulated capsule. The absorption coefficient calculated according to [7] for a container with 10 ml of water was 0.5, for a container with 10 ml of a suspension of 0.1 g of the composite material in water was 0.56. The energy consumption for extracting the sorbed substance for modes 1 and 2 was 13374 J and 3729 J/mcg, respectively. The kinetic desorption curve (Fig. 4) shows the extraction of the substance to increase 3.2 times in mode 1 and 3.9 times in mode 2.

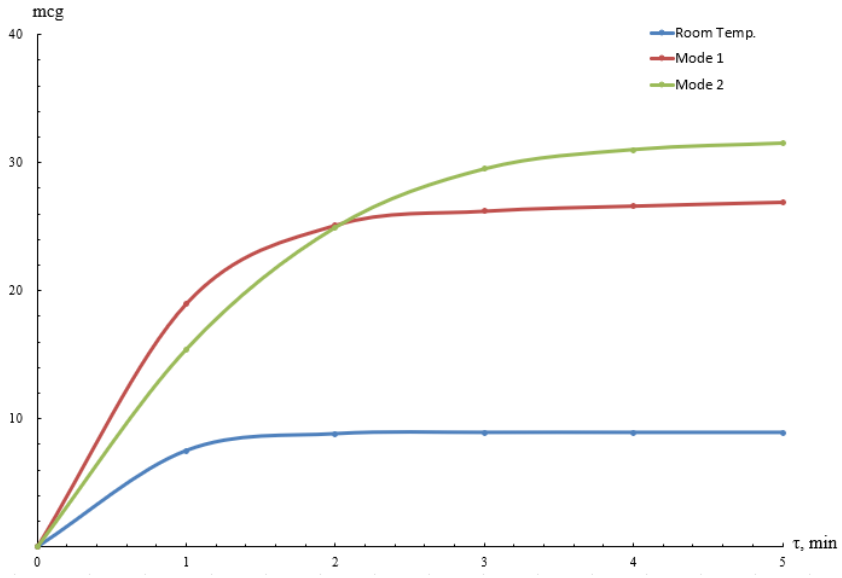

Figure 4 - Curves of EMI-induced desorption of Cu^{2+} for sample 2

References

1. Ngia, N. H. Complex processing of rice production with simultaneous production of silicon dioxide, lignin and cellulose / N. H. Ngia, L. A. Zenitova, L. K. Zien. – DOI 10.24411/1728-323X-209-12005 // Ecology. – 2019. – P. 5-11.

2. Tkachenko, I. A. Magnetoactive Composite Sorbents CoFe2O4–SiO2 / I. A. Tkachenko, A. E. Panasenko, M. M. Odinokov. – DOI 10.1134/S0036023620080173 // Russian Journal of Inorganic Chemistry. – 2020. – Vol. 65, N. 8. – P. 1142-1149.

3. Semenishcheva, E. L. Regeneration of granulated active carbon saturated with butanol vapor by microwave radiation / E. L. Semenishcheva, K. G. Starostin, V. N. Klushin // Young Scientist. – 2014. – Vol. 65, N 6. – P. 235-239.

4. Araichimani, P. Amorphous silica nanoparticles derived from biowaste via microwave combustion for drug delivery / P. Araichimani, G. S. Kumar, K. M. Prabu [et al.]. – DOI 10.1111/ijac.13693 // Int. Journal of Applied Ceramic Technology. – 2020. – Vol. 18. – P. 583-589.

5. Iler, R. Chemistry of silica / R. Iler. – Moscow: Mir, 1982. – 416 p.

6. Rahimi, Z. Hydrothermal synthesis of magnetic CoFe2O4 nanoparticles and CoFe2O4/MWCNTs nanocomposites for U and Pb removal from aqueous solutions. / Z. Rahimi, H. Sarafraz, Gh. Alahyarizadeh, A. S. Shirani. – DOI 10.1007/s10967-018-5894-1 // Journal of Radioanalytical and Nuclear Chemistry. – 2018. – Vol. 317. – P. 431-442.

7. Egorov, S. V. Absorption of microwave radiation in metal-ceramic powder materials / S. V. Egorov, A. G. Eremeev, I. V. Plotnikov [et al.] // Izvestiya vuzov. Radiophysics. – 2010. – Vol. 53, N 5-6. – P. 393-402.

Section III
EARTH SCIENCE

Ezhkova D.S.[1]

TOPONYMY OF PAVEL VLADIMIROVICH WITTENBURG

[1]Far Eastern Federal University, Institute of the World Ocean, FEFU
[2] Far Eastern Federal University, Oriental Institute, School of Regional and International Studies, FEFU
Scientific adviser – A.M. Sazykin [1]
Scientific consultant – I.N. Lazareva[2]

The toponymy of Vladivostok began to take shape in the second half of the 19th century. In 1858, there started a trend of replacing Chinese, Manchu and single English names by the Russian ones. At first, the names of the sea coasts appeared, then, in the course of economic development of the Muravyov-Amursky Peninsula, the toponymy of the land began to form. This gradual toponymic process was disrupted in 1912 by Pavel Vladimirovich Wittenburg, There was a need for a detailed description of the geological structure of Vladivostok city, so he needed to give names to a lot of nameless physical and geographical objects (mountains, bays, capes). Most of them were plotted on the map he published (Fig. 1). Pavel Vladimirovich Wittenburg (1884-1968) is a Russian and Soviet scientist, geologist and geographer. He explored in detail the entire Muravyov-Amursky Peninsula and Russky Island, collected a huge number of geological samples (1400 paleontological and 1200 petrographic exhibits). The map he created and the geological description are relevant to this day. For his work, the young scientist was awarded with Feodor Fedorovich Busse Prize. Subsequently, he participated in geological research mainly in the north of the country and in the Arctic. He continued to work in his specialty, even while in the GULAG on a fabricated case [3].

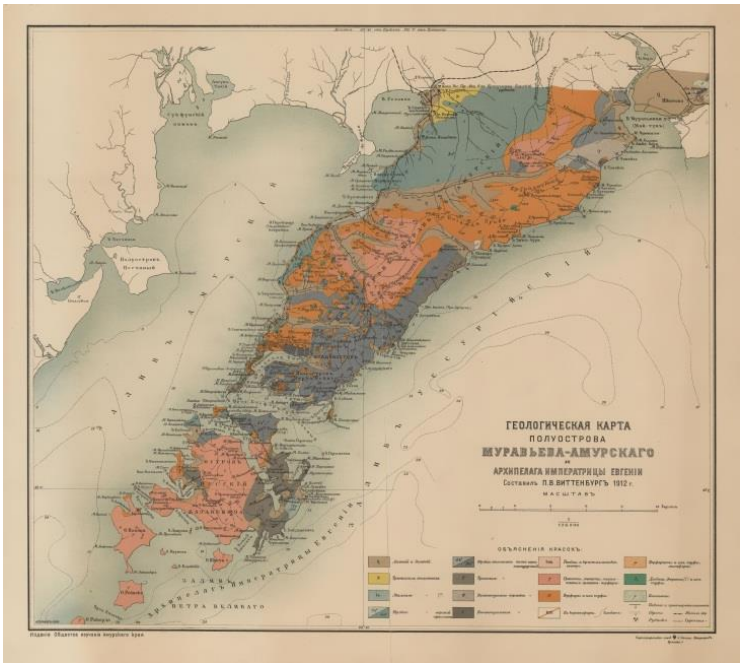

Figure 1 - Map of P.V. Wittenburg "Geological map of the Muravyov-Amursky Peninsula and the archipelago of Empress Eugenia (1912). [2]

To identify toponyms assigned by Pavel Vladimirovich Wittenburg, his map and maps of Vladivostok and the geological description [2] were published before 1912 The maritime toponymy of Wittenburg was studied in detail by Alexander Ivanovich Gruzdev [1]. Actually, no one had previously studied land place names.

Having studied the new toponymy, one can see that Pavel Vladimirovich Wittenburg rarely used "descriptive" toponyms indicating the natural features of the area (Peschanaya Bay, Red Cape). Most of the names are given after the names of famous people who contributed to the study of the Primorsky Territory and the

development of Vladivostok as a Russian outpost in the Pacific Ocean, less often after famous Russians who have never been to the Far East. Toponyms are given in honor of participants in hydrographic work in Peter the Great Bay, scientists, sailors, local historians, military engineers - builders of the fortress, civil and military commanders, Russian poets, etc. The structure of new anthropotoponyms is shown in the diagram (Fig. 2).

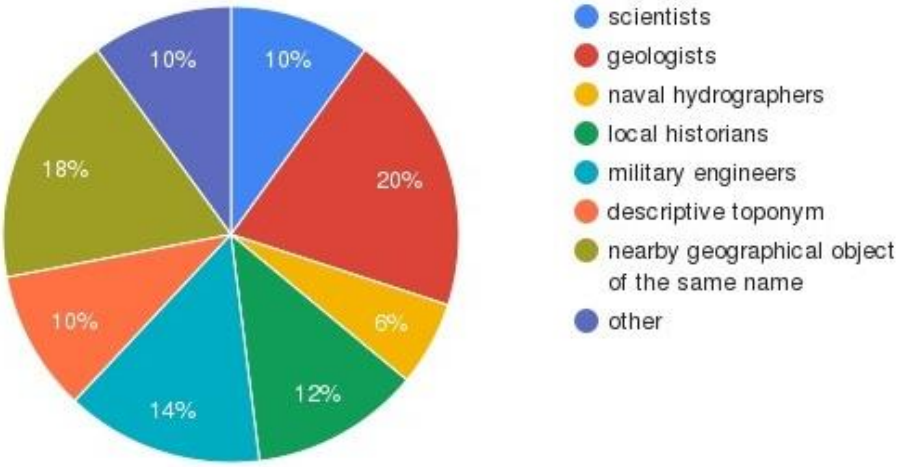

Figure 2 - Classification of anthropotoponyms mapped by Pavel Vladimirovich Wittenburg. [2].

The result of this study is a list of toponyms originated in 1912 thanks to Pavel Vladimirovich Wittenburg. A classification of toponyms and anthropotoponyms has been compiled. It includes the names given in honor of people who contributed to the history of Vladivostok city and the development of the Muravyov-Amur Peninsula.

References:

1. Gruzdev A.I. Coastline: name on the map. - Vladivostok, Dalnauka, 2016. - 278 pages.
2. Scientific results of the geological expedition of the Society for the Study of the Amur Territory in 1912 under the command of P. V. Wittenburg Part 1. [Electronic resource]. – URL:https://elib.dvfu.ru/vital/access/manager/Repository/vtls:000877931?query=Scientific+results+of+geological+expedition+Society+studies+of+Amur+territory+in+1912+year+under+commandship+P.+W.+Wittenburg&queryType=vitalDismax
3. Wittenburg E.P. Pavel Wittenburg: geologist, polar explorer, prisoner of the Gulag: (daughter's memories) / St. Petersburg. Institute of History of the Russian Academy of Sciences. - St. Petersburg. : Nestor-history, 2003. - 432.

Gusarova V. V.,[1] Pakhomova V.,[2] Zalishchak B.[2]

VERMICULITE DEPOSIT IN THE KONDER MASSIF (AYANO-MAISKY DISTRICT OF KHABAROVSKY KRAI)

[1]Far Eastern Federal University, Institute of High Technologies, and Advanced Materials, FEFU
[2]Far Eastern Geological Institute, Far East Branch, Russian Academy of Sciences
[3]Far Eastern Federal University, Oriental Institute-School of Regional and International Studies, FEFU
Scientific adviser - V.A. Pakhomova[2]
Scientific consultant– O.K. Titova[3]

The Konder deposit is known as one of the largest deposits of platinum. The massif was studied in detail in 1985-1991 by Konderskaya party of the Far Eastern Geological Administration and employees of the Far Eastern

Geological Institute of the Far Eastern Branch of the Russian Academy of Sciences. In the process of long-term studies of the area of the Konder massif, it was established that deposits of platinoids, gold, rare earths, vermiculite, etc. are combined here (Zalishchak B.L., 1998). This is a unique object, where geochemically contrasting groups of chemical elements are manifested, as well as complex post-ore processes. This report focuses on the vermiculite deposit, which has not been given due attention so far.

At the same time, vermiculite is an important and rather rare mineral, the practical use of which is associated with the properties of the mineral to delaminate when heated with an increase in volume by 6–20 times, with its low thermal conductivity, with the possibility of repeated use. Vermiculite can absorb liquids 5 times more than its own weight. The most well-known areas of its application are construction, agro- and steel industry.

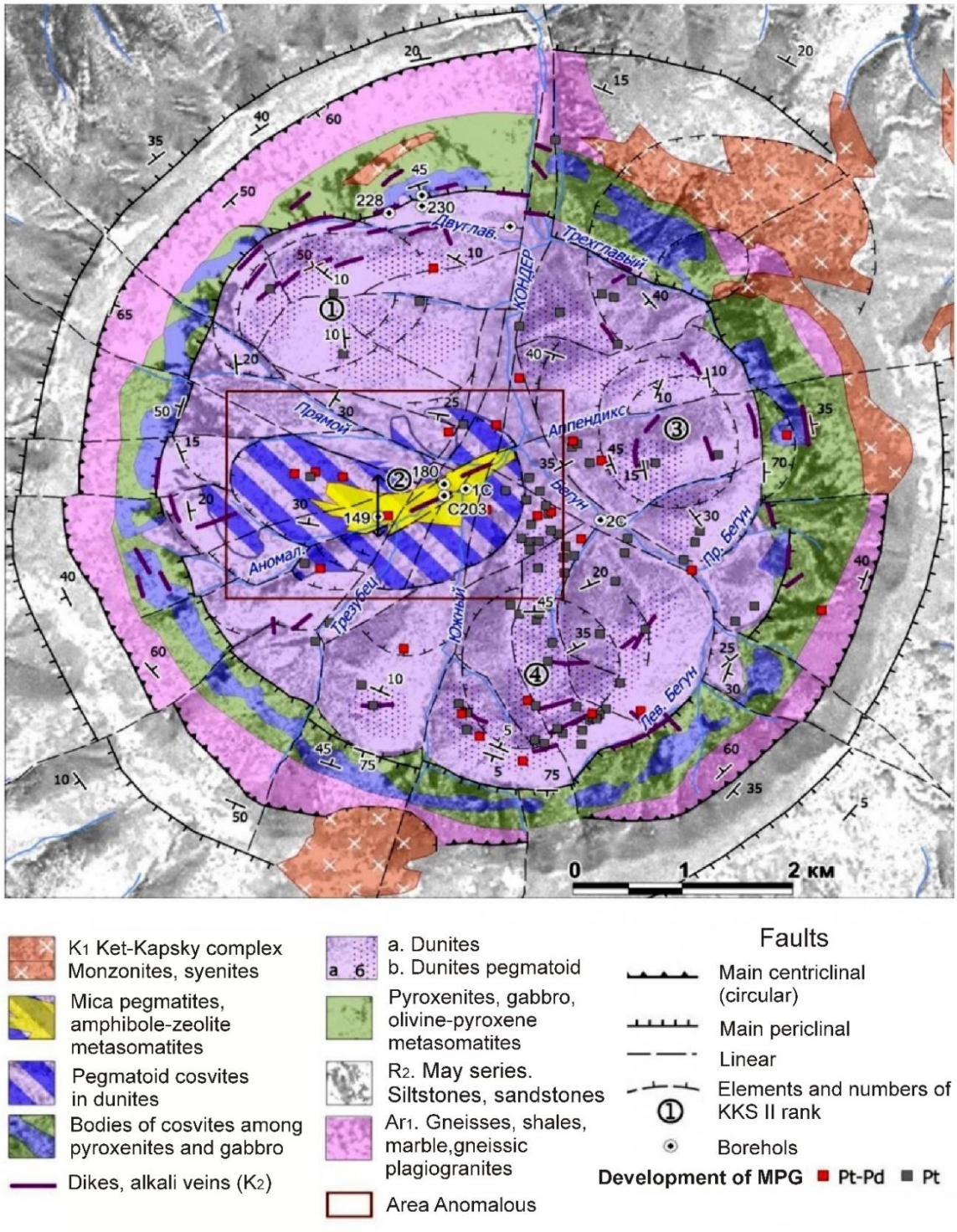

Fig.1. Geological structure of the Konder deposit. Map compiled according to the artel of miners “Amur”.

The Konder massif in the modern relief is a ring ridge, having the shape of an almost regular circle in plane, the diameter of the outer base of the ridge is 15 km, the diameter along the tops of the ridge is 8 km, the diameter of the inner basin is 6 km, the absolute height of the peaks of the Konder ridge above sea level is 1387-1200 m. Over the entire area of the inner cauldrons, composed of dunites, linear weathering crusts are developed, which consist of rock fragments, mineral grains and various manifestations of serpentine and clay minerals, as well as vermiculite, developed after phlogopite veins in dunites. These serpentine-montmorillonite-vermiculite rocks in the weathering crust compose bodies in natural areas of the relief, mainly in the cores of the inner parts of the basin, their thickness is 10-20 m, the depth of vermiculite is first tens of meters.

The place of origin of vermiculite is localized in phlogopite-pyroxene rocks in the western and central parts of the basin with a diameter in the plane of 3-2 km in the basin with a cross section of 3 - 2 km in the basin of the middle and lower course of the brook Anomalny (area “Anomalny”, fig.1). This area is surrounded by dunite spurs with weakly dissected typical relief. Here, an areal weathering crust with a vertical thickness of up to 100 m is developed, in which bedrocks are decomposed to the state of gruss, sand and clay. The bedrocks are represented by intertwining numerous zonal phlogopite-bearing veins in dunites, which make up to 60% of the total rock volume of the vermiculite deposit, forming a stockwork with a vertical thickness of at least 300 m. At the periphery of the stockwork, the number of veins of phlogopite-bearing rocks decreases to 20%, and beyond it in dunites is 2-5%. The structure (structure and texture) of phlogopite-bearing rocks is massive, mostly from coarse-grained to giant-grained. The size of the grains and crystals that make up their minerals is on average 5-10 mm, reaching 100-200 mm in diameter. Phlogopite plates have predominant dimensions of 10-100 - 3-30 mm. Mineral composition of rocks: pyroxene (diopside-augite) 20–50%, titanomagnetite 5–40%, apatite up to 10%, phlogopite 10–70%, veins with the presence of phlogopite 40–60% predominate, in some places there are admixtures of amphiboles (tremolite-actinolite), sphene, feldspars, zeolites, chrysocolla and some other minerals.

The predicted resources (reserves) of vermiculite, including hydrophlogopite, in the area of the Konder massif can be estimated at about 150-200 million tons, that exceeds the reserves of all jointly used deposits in Russia by 1.5 - 2 times. So, for example, the total pre-exploitation reserves of vermiculite at the eastern developed deposit of vermiculite Kovdor are over 45 million tons, phlogopite - over 10 million tons.

References

1. Andreev G.V. Konder massif of ultrabasic and alkaline rocks. Novosibirsk, Nauka, 1987. – 76 p.
2. Criteria for predictive assessment of territories for solid minerals. Ed. D.V. Rundqvist. L., Nedra, 1986. – pp. 544 – 563.
3. Gurovich V.G., Zemlyanukhin V.N., Emelianenko E.P. and other Geology, petrology and ore content of the Konder massif. M., Nauka, 1994. – 176 p.
4. Lvova I.A. Deposits of vermiculite in the USSR. L. Nedra. – 1974, 231 p.
5. Marakushev A.A., Emelyanenko E.P., Nekrasov I.Ya., Maslovsky A.N., Zalishchak B.L. Formation of the concentric-zonal structure of the Konder alkaline-ultrabasic massif. Doklady AN SSSR, 1990, volume 311, no. 1. – pp. 167-170.
6. Nekrasov I.Ya., Lennikov A.M., Oktyabrsky R.A., Zalishchak B.L., Sapin V.I. Petrology and platinum content of ring alkali-ultrabasic complexes. M., Nauka, 1994. – 381 p.
7. Nevsky V.A., Frolov A.A. Structures of ore deposits of ring type. M., Nauka, 1985. –247 p.
8. Orlova M.P. Geological structure and genesis of the Konder ultramafic massif (Khabarovsk Territory). Pacific Geology, 1991, No. 1. – pp. 80-88.
9. Perlite and vermiculite (geology, exploration technique and technology). M., Geoltekhizdat, 1962, 124 p. part 2. Vermiculiteю – p.80-123.
10. Zalishchak B.L. Koksharovsky massif of ultrabasic and alkaline rocks (Southern Primorye). M., Nauka, 1969. – 116 p.

11. Zalishchak B.L., Khomich V.G., Zarubin B.A. et al. Problems of metallogeny in the southeastern part of the Siberian platform. In book. "Patterns of distribution of minerals XV (Metallogeny of Siberia)". M., Nauka, 1988, 270 pp. – pp. 67-73.

Dzyuba E. D.[1]

CHANGES IN THE TEMPERATURE REGIME ON THE KAMCHATKA PENINSULA

[1]Far Eastern Federal University, Institute of the World Ocean, FEFU
[2]Far Eastern Federal University, Oriental Institute-School of Regional and International Studies, FEFU
Scientific adviser – L. N. Vasilevskaya [1]
Scientific consultant – O. K. Titova[2]

The uniqueness of Kamchatka implies a careful attitude to its natural resource potential and, the main task is to carefully study the climate change as a major factor affecting, among others, the biota of Kamchatka waters. All this determines the relevance of the topic of this work.

The purpose of the work was to study the temperature regime and its changes on the Kamchatka Peninsula. To achieve this goal, the following tasks were solved: the formation of the base for air temperature; assessment of structural features of temperature time series; the study of regime characteristics.

Source data. To study the spatio-temporal changes in air temperature, the materials of observations of 14 meteorological stations of the Kamchatka UGMS (Fig.1) for 1966–2019 were used. [http://www.meteo.ru]

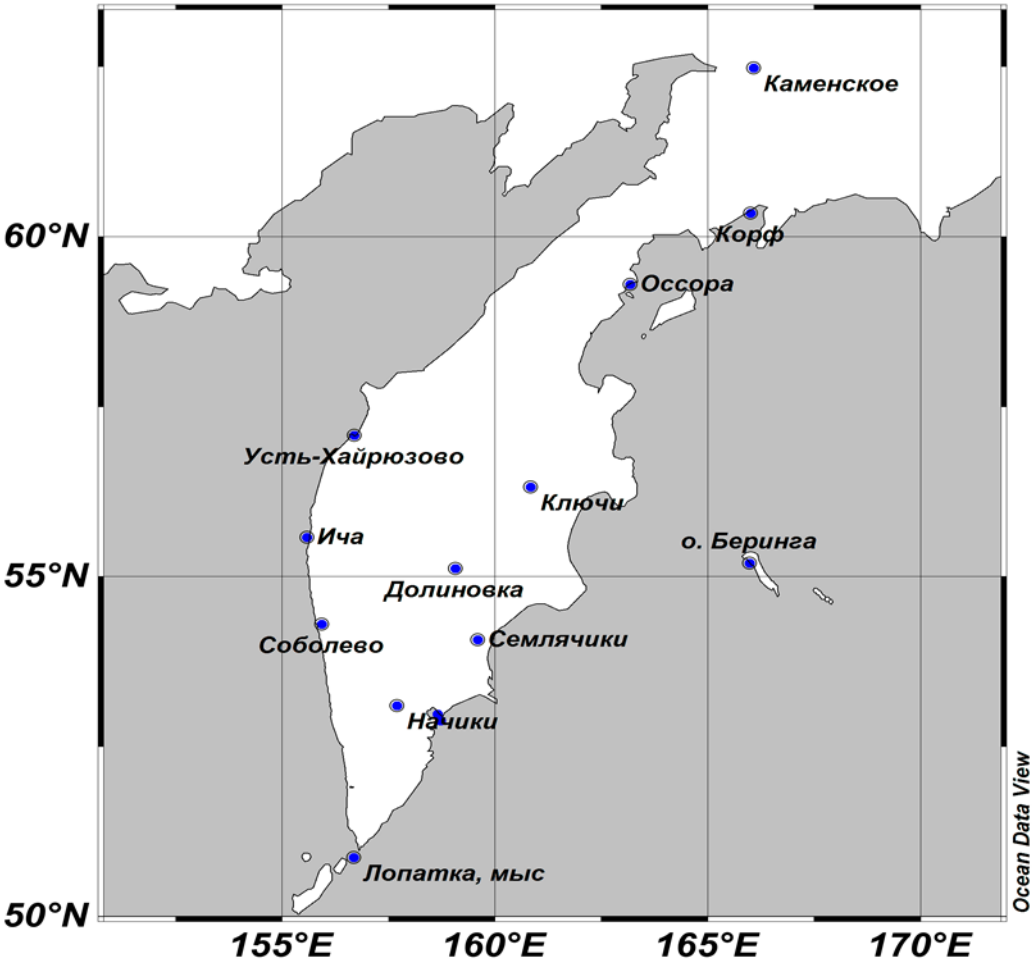

Figure 1 Map-scheme of location of meteorological stations

Annual air temperatures are rising in all areas of the Kamchatka Peninsula. This is evidenced by the

coefficients of linear trends built for a multi-year course at 14 weather stations. R2 exceeds the threshold = 0.07. The rate of the annual temperature increase is 0.2 - 0.5 °/10 years. The warmest is by 2.5 degrees in the south-western coast of the peninsula and in the mountainous region. The least is in the southeast and on Bering Island by about 1 degree Celsius. Consider the features of changes in seasonal temperatures and assess their influence on the change in annual temperature.

The most significant feature of the long-term dynamics of the spring thermal regime in Kamchatka is the presence of a warming trend in it, which can be traced at all the stations under study. The results of calculations of linear trend slope coefficients (CLLT) are given in Table 1. The largest stable increase in air temperature at the 95% significance level, observed on the west and east coasts, and in the mountainous regions of Kamchatka KNLT varies from 0.2 to 0.9 ° C /10. In March, at the Bolsheretsk station, the average temperature for the month over the past 53 years increased by 4 degrees, and in Sobolevo - by 5 degrees, on the east coast at the Ossora station in March and in May the temperature became higher by 3 degrees on average, in April - by 2.5 degrees; in the mountainous region, it warmed up the most in March at the stations Klyuchi (by 3 (C), Esso and Nachiki (by 4 (C) (Fig. 2).

Analysis of the long-term course of summer temperatures revealed the presence of warming, which can be traced at all the stations under study, and the greatest stable increase in air temperature is observed in the mountainous regions of Kamchatka: KNLT varies from 0.2 to 0.5 ° C / 10 years. In July, Klyuchi and Esso stations had the most significant growth rates in all the summer months. On the east, west and south coasts, the linear trend of summer temperatures at all stations is positive and significant (Fig. 2). In the area of the Dolinovka station (the valley of the Kamchatka River), there is a steady increase in summer temperature, most observed in mid and late summer: KNLT in July and August is 0.4 ° C / 10 years; at Cape Lopatka station – 0.2°C/10 years.

Table

Slope coefficients of linear trends in Kamchatka (1966–2019)

Station	Central months of the seasons				Year
	April	July	October	January	
Ossora	0,6	0,3	0,3	-0,2	0,3
Ust-Khayryuzovo	0,5	0,3	0,2	0,6	0,4
Cluchi	0,4	0,5	0,2	0,1	0,4
Esso	0,4	0,5	0,3	0,4	0,4
Icha	0,3	0,2	0,2	0,2	0,3
Dolinovka	0,3	0,4	0,1	0,4	0,4
Bering Island	0,2	0,3	0,2	0,1	0,2
Sobolevo	0,4	0,3	0,2	0,8	0,5
Semyachik	0,2	0,3	0,2	0,2	0,2
Nachiki	0,4	0,3	0,2	0,5	0,5
Sosnovka	0,3	0,3	0,2	0,2	0,3
Petropavlovsk	0,2	0,3	0,2	0,2	0,3
Bolsheretsk	0,4	0,3	0,2	0,6	0,5
Cape Lopatka	0,2	0,2	0,2	0,4	0,3

In autumn, as well as in spring and summer, the air temperature rises. At all stations, linear trends are statistically significant, the largest stable increase in air temperature is observed on the southwestern coast, in the northeast and in the mountainous regions of Kamchatka: KNLT in September and October varies from 0.2 to 0.3° / 10 years, and in November from 0.6 to 0.8°C/10 years. The most significant growth rates of autumn temperature are observed in November at Nachiki station (mountainous region) and on the east coast (Ossora station). Over the past 53 years, the average November temperature has risen by 4 degrees. At Cape Lopatka, this increase was about 2°C.

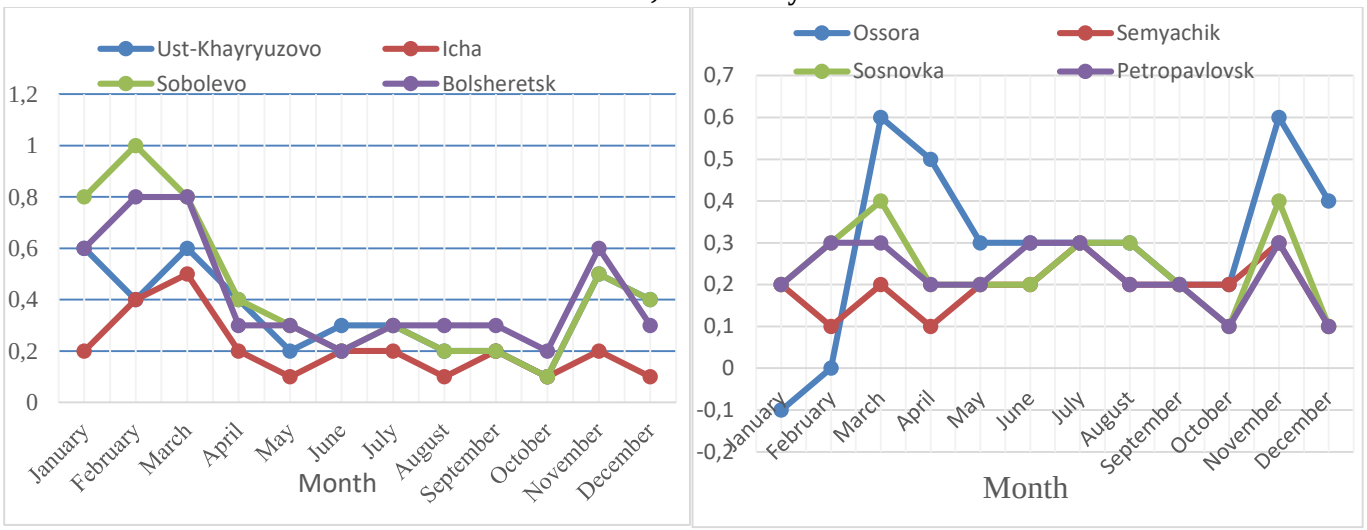

Figure 2 - Slope coefficients of linear trends of average monthly air temperature during the year on the western (left) and eastern (right) coasts of Kamchatka

In winter, the largest stable increase in air temperature is observed on the southwestern coast, and in the mountainous regions of Kamchatka: KNLT varies from 0.4 to 0.5 °C/10 years in December; in January - from 0.4 to 0.8°C/10 years and in February from 0.6 to 1.0°C/10 years. It should be noted that in the mountainous region at Nachiki station, unlike the other two stations, the temperature in December and January rises weakly, or does not rise at all. It should also be noted that, in contrast to other seasons, negative trends appeared at some stations in winter, and warming at some stations is unstable (coefficient of determination is less than 0.07). The only negative trend appeared in January at Ossora station, it amounted to 1 degree. The temperature trend is also positive in the extreme south (Cape Lopatka). But relative to other areas, the temperature increase is not so significant, it is only 0.1 °C / 10 years in December and 0.4 °C / 10 years - in January and February.

Thus, a stable increase in annual air temperatures on the Kamchatka Peninsula is due to the same stable increase in all calendar seasons. However, warming on the west coast occurs at a faster rate compared to the east coast in January-March. On both coasts, it is currently that the rate of temperature increase is the highest. In April-October, the rates decrease on both coasts, and in November they increase again.

References

1. Brooks K., Karuzers N. Application of statistical methods in meteorology / K. Brooks. - L.: Gidrometeoizdat, 1963. – 382 p.

2. Kondratyuk V.I. Climate of Kamchatka / V.I. Kondratyuk. - M.: Gidrometeoizdat, 1974. – 204 p.

3. Shkaberda O.A. Assessment of changes in air temperature in Kamchatka over the past 60 years / O.A. Shkaberda, L.N. Vasilevskaya // Bulletin of the Far Eastern Branch of the Russian Academy of Sciences - 2013 - No. 3. – pp. 69–77.

4. Shkaberda O.A. Long-term variability of the temperature and humidity regime on the Kamchatka Peninsula / O.A. Shkaberda, L.N. Vasilevskaya // News of TINRO, 2014 - T.178. – pp.217.

Vysotskiy S.V.,[3] Velivetskaya T. A.,[3] Ignatiev A. V.,[3] Kuleshevich L. V., Slabunov[4]A. I.,[4] Kosukhin K.P.[1]

MULTI-ISOTOPE ($\delta^{33}S$, $\delta^{34}S$, $\delta^{36}S$) COMPOSITION OF SULFUR IN SEDIMENTRY SULFIDES: IMPLICATIONS FOR DETERMINING THE SULFURE SOURCE AND BIOGEOCHEMICAL PROCESSES IN THE FORMATION OF MESOARCHEAN MASSIVE SULFIDE ORES

[1]Far Eastern Federal University, Institute of High Technologies, and Advanced Materials, FEFU
[2] Far Eastern Federal University, Oriental Institute-School of Regional and International Studies, FEFU
[3] Far Eastern Geological Institute, FEGI
[4]Institute of Geology, Karelian Research Centre
Scientific adviser – S.V. Vysotskiy[1], A. V. Aseeva[3]
Scientific consultant – O.K. Titova[2], S.V. Vysotskiy[1]

Introduction. Volcanogenic massive sulfide deposits consist of sulfide minerals. It is believed that they are genetically related to underwater volcanic activity and are formed during the deposition of ore minerals from a mixture of cold seawater and ascending hot metal-enriched hydrothermal solutions. During the formation of sedimentary sulfides, sulfur can be derived from different reservoirs represented by magmatic fluids, basement rocks, atmosphere, or sea water. The research of sulfur isotopic composition ($^{34}S/^{33}S/^{32}S$) in sedimentary sulfides is a method which allows us to identify atmospheric, hydrospheric and biological processes in the Archean sulfur cycle. In this paper we will demonstrate, on the example of the Mesoarchean VMS Leksa deposit (Karelia, Russia), how the analysis of the multi-isotope sulfur composition of sulfides allows to determine sulfur sources and the impact of atmosphere and bacterial activity on mineralization.

Geology. The VMS Leksa deposit (fig. 1) is in the southeastern part of the Kamennoeozoro structure, it occurs in the strata of quartz-albite-sericite and carbon bearing schists (Kuleshevich, 1992).

The mineralization is characterized by being stratiform, and it is associated with island-arc sedimentary-volcanogenic facies, the volcanic rock age of which (U-Pb zircon TIMS) is 2875 ± 2 Ma and 2876 ± 5 Ma (Puchtel et al., 1999).

Materials and methods. The samples for isotope study were taken from the core of drillholes (see fig. 2). Sulfur isotope analyses have been performed at the Laboratory of Stable Isotopes of the Analytical Centre of FEGI FEB RAS using a local laser method (Ignatiev et al., 2018). Sulfur isotope ratios have been measured with masses of 127 (32SF5+), 128 (33SF5+), 129 (34SF5+) in triple-beam mode using MAT-253.

Mineralogy. Sulfides are mainly represented by pyrite that form different morphological forms. Pyrrhotite, chalcopyrite, sphalerite, galena are less common.

Pyrite I. Globular, “kidney-shaped” pyrite forms semi-massive, layered aggregates consisting of grains of 0.2 mm in size (Fig 2C), and finely dispersed inclusions in quartz crystals (Fig 2A-B) are also noted. It is also found in acicular forms in accretions with a silicate mineral, forming dendritic textures (Fig 2F).

Pyrite II. Massive pyrite. It contains fine silicate inclusions, fills the space between pyrite I, replacing silicate minerals (Fig.2A-E). Subparallel quartz crystals contained in it form a "layered" texture.

Pyrite III. Euhedral pyrite forms idiomorphic cubic grains of pyrite with a size of ~0.05-0.2 mm in free spaces (Fig.2C).

Results. A total of 55 sulfur isotope analyses of $\delta^{33}S$ and $\delta^{34}S$ in 181 sulfide minerals of the Leksa deposit have been conducted (fig.3). The difference between the measured $\delta^{33}S$ values and expected values, calculated based on $\delta^{34}S$, is shown as $\Delta^{33}S$.

Samples of the studied sulfides are characterized by a wide range of $\delta^{34}S$ variations from

–10.2‰ to +27.5‰, and by the presence of $\Delta^{33}S$ isotopic anomaly, values of which vary from –0.30‰ to +2.64‰.

$\Delta^{33}S$ isotopic anomalies indicate that sulfur of the Leksa deposit sulfides registered a mark of atmospheric photochemical processes that resulted in MIF-S.

Values of $\delta^{34}S$ and $\delta^{33}S$, falling on the MIF-S trend of $\Delta^{33}S/\delta^{34}S \approx 1$, confirm the participation of sulfur, which underwent a cycle of sulfur transformation in this atmosphere.

Conclusions.

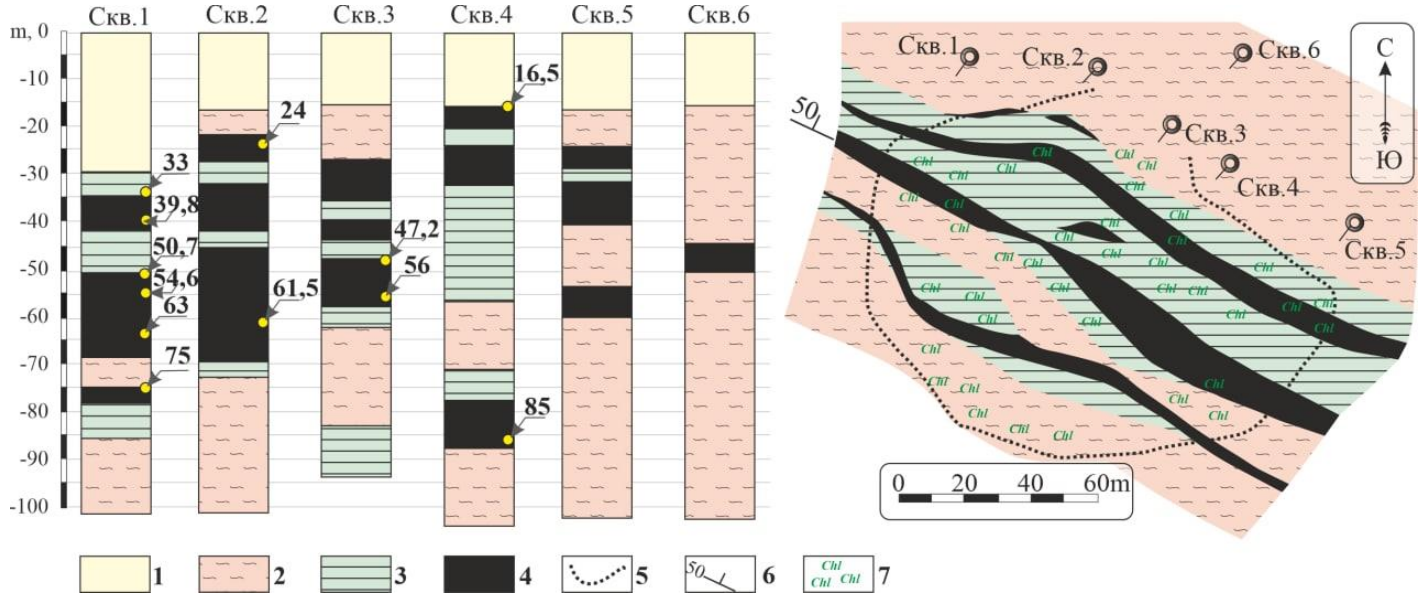

Fig.1. geological structure of Leksa deposit.

1 – quaternary deposit, 2 - sericite - albite- carbonate-quartz schists. 3 – carbon-bearing schists, 4 – massive sulfide ores, 5 – area of silicification, chlorite blaster and fuchsite are present 6 – drillholes, 7 – occurrence parameters

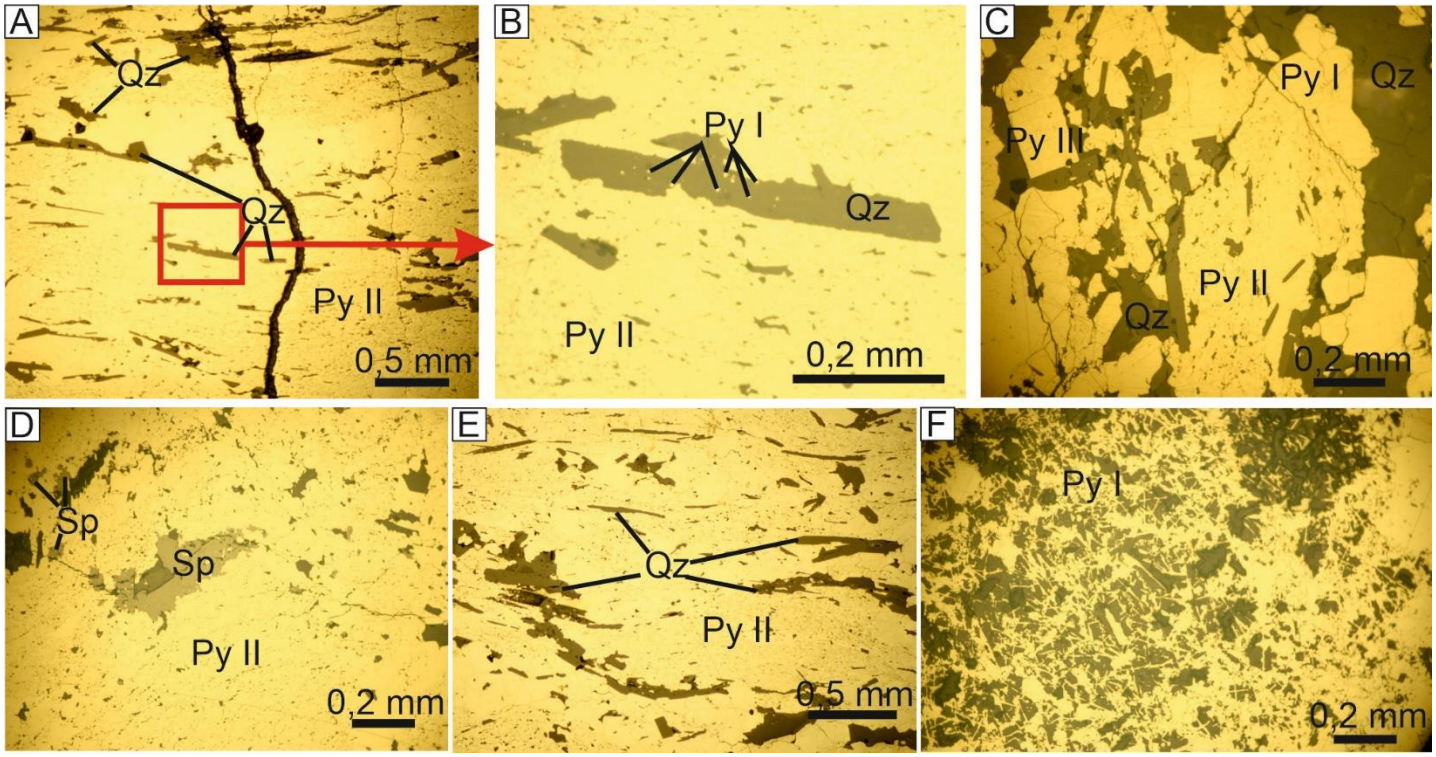

Fig. 2. Different types of pyrite.

A,B – fine inclusions of pyrite in quartz. C – aggregate of “kidney-shaped” pyrite, massive pyrite and idiomorphic pyrite. D – sphalerite inclusions in massive pyrite. E – subparallel texture is formed by quartz grains. F – acicular pyrite

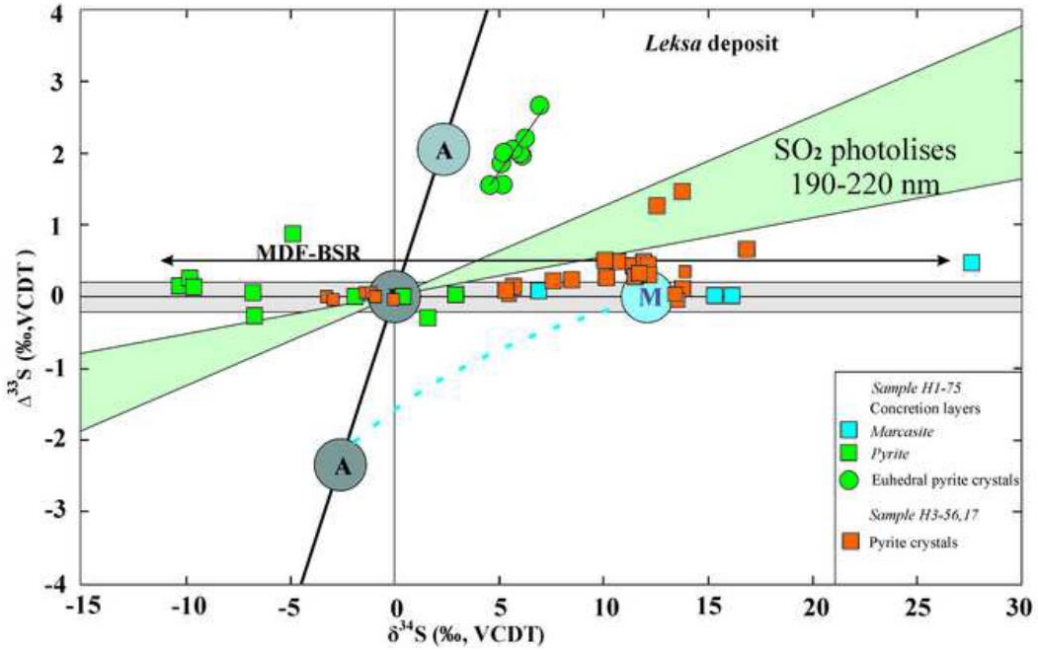

Fig. 3. Analysis results

References

1. Ignatiev A.V, Velivetskaya T.A. Budnitskiy S.Y., Yakovenko V.V., Vysotskiy S.V., Levitskii V.I. Precision analysis of multisulfur isotopes in sulfides by femtosecond laser ablation GC-IRMS at high spatial resolution, FEGI, 2018.

2. Kuleshevich L.V. Metamorphism and ore content of the Archean greenstone belts of the southeastern margin of the Baltic Shield. Petrozavodsk: Karelian Research Centre, 1992.

3. Puchtel I. S., Hofmann A. W., Amelin Yu. V. et al. Combined mantle plume-island arc model for the formation of the 2.9 Ga Sumozero-Kenozero greenstone belt, SE Baltic Shield: Isotope and trace element constraints // Geochimica et Cosmochimica acta. 1999. Vol. 63, N 21. – pp. 3579–3595.

Malitckii S. I.,[1] Glushko A.A.[1], Titova O.K.[2]

GEOGRAPHICAL ASPECTS OF ECONOMIC AND SOCIAL DEVELOPMENT OF THE LEAST DEVELOPED COUNTRIES OF ASIA AND THE PACIFIC RIM

[1]Far Eastern Federal University, Institute of the World Ocean, FEFU
[2]Far Eastern Federal University, Oriental Institute-School of Regional and International Studies, FEFU
Scientific adviser – A. A. Glushko[1]
Scientific consultant – O.K. Titova[2]

Currently, there are more than 200 countries in the world. They are usually divided into two large groups – developed and developing countries. The last group of countries occupies most of the globe, 80% of the world's population is concentrated in them. There is a great diversity among developing countries in terms of the level and features of socio-economic development. A special group is formed by the so-called least developed countries (LDCs). There are 47 such countries in the world; most of them are in Africa (34). There are 13 least developed countries in Asia and in the Pacific Rim area. They are characterized by common socio-economic problems: low incomes of the population, poverty, poor development of the education and health care system, lack of social protection systems, etc. At the same time, each country is individual. They differ in the peculiarities of economic development and population. The main reasons for the lag in the development for LDCs are unfavorable geographical location (for example, island - Kiribati, highland – Nepal, Bhutan),

political instability and wars (Afghanistan, Yemen), and their colonial past.

To analyze the spatial differences in the socio-economic development of the LDCs of Asia and the Pacific Rim, the next criteria were selected: GDP, GDP per capita, GDP growth rate, HDI, life expectancy, infant mortality. All the LDCs of the studied region are characterized by small-size economies. In total, their GDP in the world economy is about 1% [1]. At the same time, significant differences in the GDP indicator calculated per capita were revealed. So, in Afghanistan, it amounted to 2000 USD, while in Bhutan - 10900 USD, that is, in Bhutan, the values of GDP per capita are 5 times higher than in Afghanistan (Table).

Among LDCs of Asia and Pacific Rim, Bangladesh (3.5%), Myanmar (3%), Laos (0.5%) had positive GDP growth in 2020 (although it decreased compared to the previous period due to the Covid-19 pandemic). For most states, there is a reduction in the economy. The state where the decline in GDP has been observed for a long period is Yemen. The reason is the civil war, which has been going on since 2014. This led the country to the world's largest humanitarian disaster [2]. The HDI varies from 0.470 in Yemen to 0.657 in the Solomon Islands (Table). This is significantly lower than in developed countries – at least 0.900. In fact, the HDI is a complex indicator; its value indicates the level and quality of life of the population, considering the income of the population, the development of education and healthcare. For example, in developed countries the average life expectancy is more than 80 years, while in the studied LDCs the maximum indicator is 76.5 years (Solomon Islands), the minimum is marked for Afghanistan - 53 years. That is, on average, people in LDCs live from 4 to 30 years less than in developed countries. Also, for LDCs, there is a relatively low level of literacy among the adult population. If in developed countries almost 100 % of the population is literate, then for LDCs this indicator does not exceed 90% (Myanmar), and, for example, in Afghanistan it is 37 % [1].

An important characteristic of the quality of life of the population is mortality, including infant mortality (mortality of children under the age of 1 year). There are significant differences in this indicator between the countries. So, for Vanuatu, it is 14.7%, in Afghanistan – 106.8%, that is, in the latter case, every 10th child who was born alive does not live up to a year. The reasons are the low level of health care development in general, especially in rural areas. In other LDCs, the situation is somewhat better, but, compared with developed countries, infant mortality is very high here, for comparison, the UK - 7%, Japan – 5% [1].

As a result of the study, the spatial differentiation of the socio-economic development of the LDCs of Asia and the Pacific basin was revealed. With a generally unfavorable situation, Bhutan, Laos, and the Solomon Islands can be considered relatively successful countries being the first candidates to exit the world list of LDCs. The worst socio-economic situation is observed in Afghanistan and Yemen. According to all the criteria considered, these countries are in the rearguard. The reasons that hinder the development of these states are similar – military and political instability.

Table

Some indicators of social and economic development of countries [1]

№	Country	GDP, billion USD	GDP per capita, USD/person.	HDI	Duration of life, years	Literacy, %	Infant mortality, ‰
1	Afghanistan	77	2000	0.511	53	37	106,8
2	Bangladesh	793,5	4 800	0.632	74	75	31
3	Bhutan	8,4	10 900	0.654	71	67	36
4	Cambodia	70	4 200	0.594	66	80	45,6
5	Yemen	73,6	2 500	0.470	67	70	47,5
6	Kiribati	0,27	2 300	0.630	67	н/д	33,7
7	Lao PDR	56,7	7 800	0.613	66	85	49,5
8	Nepal	73	3 800	0.602	72	68	25,7
9	Vanuatu	0,85	2 800	0.609	75	87	14,7
10	Solomon Islands	1,71	2 500	0.657	76	н/д	20,5
11	Timor-Leste	4,19	3 200	0.606	69	68	34,5
12	Tuvalu	0,05	4 400	0.583	68	н/д	29,7
13	Myanmar	247	4 500	0.583	65	89	33,7

References

1. The World Factbook // Central Intelligence Agency [Electronic resource] – URL: https://www.cia.gov/the-world-factbook/

2. Waiting to declare famine «will be too late for Yemenis on brink of starvation // United Nations [Electronic resource] – URL: https://news.un.org/en/story/2020/07/1068101

3. Where we work // The World Bank [Electronic resource] – URL: https://www.worldbank.org/en/where-we-work

---

Kiyanitsin V. V.[1], Chermashentsev A. Yu.[1], Shirokova A.V.[1], Titova O.K.[2]

ANALYSIS OF CORRELATIONS BETWEEN SURVEY RESULTS AND INFRASTRUCTURE ON THE GAMOV PENINSULA

[1]Far Eastern Federal University, Institute of the World Ocean, FEFU
[2]Far Eastern Federal University, Oriental Institute-School of Regional and International Studies, FEFU
Scientific adviser – A. V. Shirokova [1]
Scientific consultant – O.K. Titova[2]

An important role in the attractiveness of a recreational facility for vacationers is played by the infrastructure, which is located next to the place of rest. This is the road network, its quality and length, the quality and occupancy of beaches, recreation centers of various price ranges. It is these aspects that affect the comfort and quality of rest. At present, this issue does not lose its relevance for the following reasons: 1) an increase in domestic tourist flows in Russia; 2) the remaining high demand for quality infrastructure among vacationers.

The purpose of the work is to analyze the correlations between the survey results and the infrastructure on the Gamov Peninsula.

Infrastructure is a set of buildings, structures, systems, services necessary for the functioning of the material production process and ensuring the daily life of the population [1]. The authors assume that there is a close correlation between the results of the survey of vacationers on the Gamov Peninsula and its tourist infrastructure.

The analysis of the results of the survey of 255 respondents was taken from a previous work [3]. The QGIS program was used to identify infrastructure objects. The 7 most popular bays were taken as places of rest: Andreevka, Astafyeva. Vityaz, Vodolaznaya, Idol, Telyakovskogo and Risovaya Pad.

The authors decided to create a buffer zone around the beaches of each of the bays to calculate infrastructure indicators. According to GOST R 55698-2013, walking distance for beaches is 1000 m [2]. In each buffer zone with a radius of 1 km, 15 indicators were identified: the occupancy of the beach by 5 and 15 meters in percent, average building density, average building density coefficient, average deviation of the building density coefficient from Zarubino in the Russian Federation, average deviation from the building density coefficient of the Russian Federation, number and density of tourist bases, their evaluation in the Internet search engines (Google and Yandex), average cost of accommodation per person per day, and the length, quantity and density of the road surface.

The correlation analysis method was used to analyze the results.

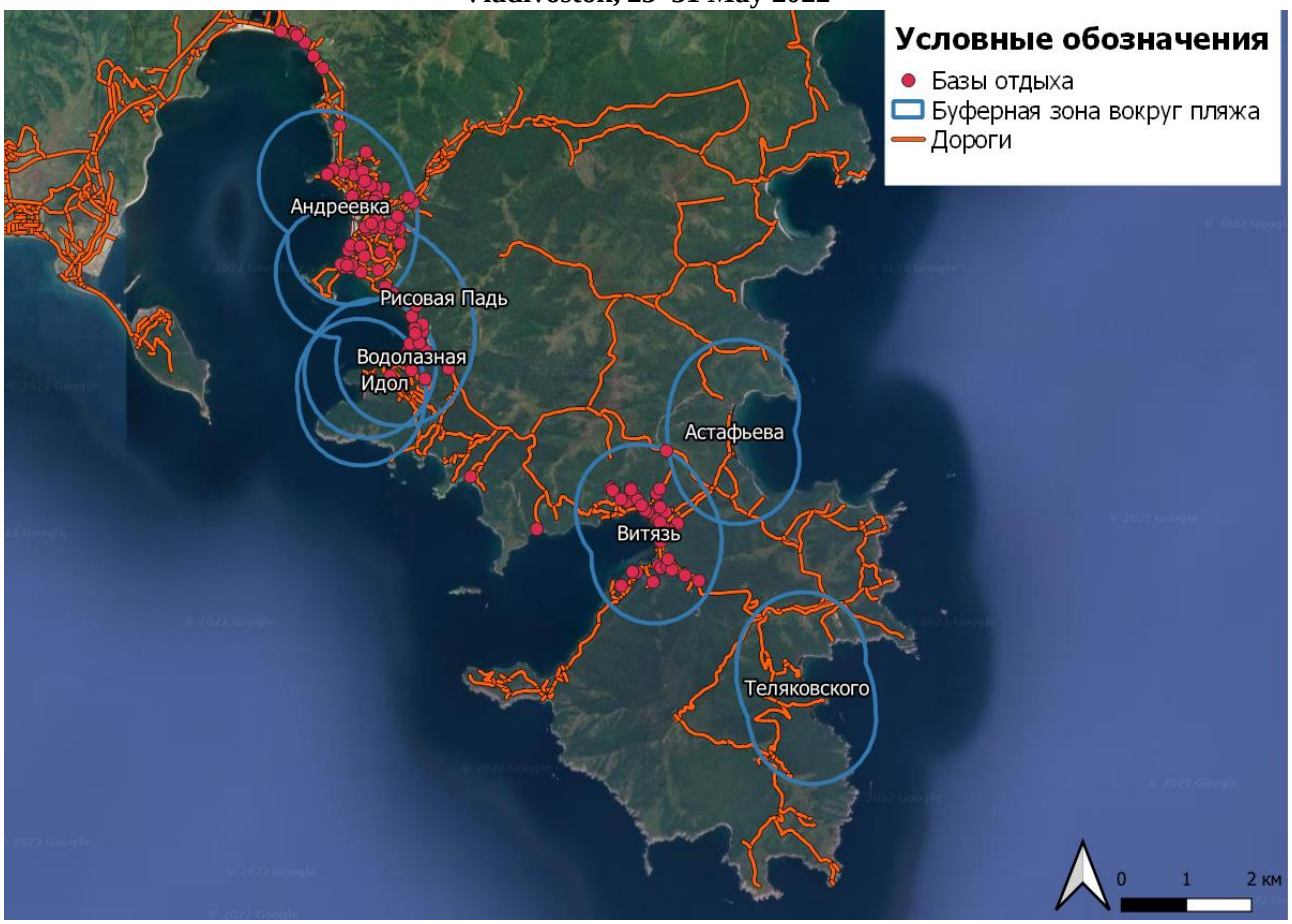

Figure 1 - The study area map. (Made by the authors)

Results. Based on the data obtained, a correlation matrix was compiled (Figure 2). A strong positive relationship (0.80 - 0.98) was found between average building density, building density ratio, road network performance and the number of bases in buffer zones. Therefore, the determining factor in the development of infrastructure is tourism.

For the final analysis, a summary correlation matrix was compiled (Figure 3). The survey results were compared with infrastructure indicators.

	Зап_5	Зап_15	Площа	СР_ПЗ	СР_КП	СР_От	СР_О_1	СР_О_2	К_баз	Оц_Гу	Оц_Ян	Ср_це	Пл_ба	Дл_до	Кол_д	Плот_
Зап_5	1															
Зап_15	1	1														
Площа	-0,33485	-0,33477	1													
СР_ПЗ	0,197462	0,197554	0,361949	1												
СР_КП	0,216517	0,216634	0,459635	0,960807	1											
СР_От	-0,62598	-0,62594	0,438485	-0,50965	-0,32682	1										
СР_О_1	-0,58768	-0,5876	0,679958	-0,10787	0,095303	0,9089	1									
СР_О_2	-0,423	-0,42291	0,621427	-0,11029	0,129203	0,8794	0,977	1								
К_баз	-0,2106	-0,2105	0,602549	0,906046	0,87785	-0,187	0,206	0,1386	1							
Оц_Гу	0,399492	0,399528	-0,00189	0,888811	0,754214	-0,843	-0,55	-0,549	0,68	1						
Оц_Ян	0,441726	0,441758	-0,04563	0,869041	0,733659	-0,867	-0,59	-0,578	0,64	0,998444	1					
Ср_це	0,498302	0,498315	-0,14939	0,737161	0,570299	-0,908	-0,7	-0,709	0,476	0,939095	0,949336	1				
Пл_ба	-0,21038	-0,2103	0,373875	0,902456	0,830055	-0,328	0,036	-0,035	0,962	0,758465	0,723977	0,56088	1			
Дл_до	-0,23154	-0,23142	0,798196	0,800916	0,856071	0,0658	0,458	0,4184	0,934	0,468169	0,425508	0,24488	0,82	1		
Кол_д	-0,11672	-0,11661	0,649432	0,917284	0,93351	-0,14	0,274	0,238	0,983	0,650012	0,612818	0,44282	0,91	0,966	1	
Плот_	-0,1883	-0,1882	0,473768	0,887332	0,896761	-0,163	0,232	0,2028	0,947	0,646695	0,611934	0,40894	0,94	0,9056	0,95	1

Figure 2 - Correlation matrix of infrastructure indicators. (Made by the authors)

	Пол	Возраст	гион / гор	Транспорт	о дней от	человек в	став групп	об размеще	проживани	активно	ды на от	Оценка	ание верну	онравилос	онравило
Зап_5	-0,031641	-0,034841	0,069471	0,04890114	0,022885	0,1931098	0,2054243	0,04781352	-0,005373	-0,046187	0,0909384	-0,079728	-0,009481	-0,1182394	-0,193268
Зап_15	-0,031615	-0,034857	0,069452	0,04889893	0,022929	0,1931382	0,2054544	0,04788172	-0,0053065	-0,046202	0,0909917	-0,079753	-0,009483	-0,1181956	-0,193246
Площа	0,0259525	-0,084842	-0,153306	0,0305991	0,08567	0,0049103	0,087853	0,17059124	0,2802365	-0,000749	0,1011046	-0,273922	-0,115447	0,1417501	-0,015407
СР_ПЗ	0,1476894	-0,075386	-0,025554	-0,0621334	0,33363	0,1554855	0,1344879	0,44110374	0,2689787	-0,047417	0,2328167	-0,206829	-0,086091	0,2085	-0,034889
СР_КП	0,1423205	-0,087882	-0,055362	-0,0382689	0,318431	0,1566345	0,1542455	0,41727092	0,3006924	-0,065186	0,2686117	-0,205489	-0,068406	0,2166199	0,0039471
СР_От	-0,047677	-0,004377	-0,138447	0,0683595	-0,174808	-0,140914	-0,072224	-0,1982429	0,0672388	-0,002081	-0,021013	0,0714871	0,066314	0,0337891	0,2176305
СР_О_1	0,0325319	-0,05338	-0,168658	0,04385845	0,007448	-0,056498	0,0107314	0,04269138	0,2366201	-0,034846	0,1245552	-0,049597	0,022715	0,1570118	0,2143349
СР_О_2	0,0276817	-0,06116	-0,161489	0,05771711	0,015784	-0,029327	0,0427257	0,03692308	0,2321729	-0,052258	0,1565286	-0,049893	0,033392	0,1402439	0,202719
К_баз	0,1464948	-0,074399	-0,062588	-0,0661321	0,318396	0,0913991	0,0851721	0,43913799	0,3010232	-0,028709	0,2069742	-0,209496	-0,091096	0,2444444	0,016851
Оц_Гу	0,1271823	-0,047213	0,048419	-0,0815642	0,316109	0,1646494	0,1151447	0,40519876	0,1533327	-0,026109	0,161545	-0,17547	-0,09401	0,1339058	-0,124302
Оц_Ян	0,1245015	-0,044932	0,055679	-0,0805332	0,311109	0,1705807	0,1183006	0,3957754	0,1409466	-0,027446	0,1590316	-0,16895	-0,091133	0,1237532	-0,13127
Ср_це	0,1007315	-0,014939	0,093983	-0,0829032	0,222312	0,1870675	0,1087478	0,29693768	0,0498973	-0,009979	0,0768913	-0,126502	-0,090147	0,0542448	-0,181399
Пл_ба	0,1577732	-0,057583	-0,030397	-0,086691	0,335433	0,0844748	0,0545747	0,44319229	0,2564653	-0,02748	0,1960614	-0,156118	-0,071597	0,2411814	0,0317184
Дл_до	0,1277894	-0,088688	-0,108873	-0,0312458	0,279139	0,0773662	0,0977758	0,35572414	0,3133897	-0,043576	0,2235539	-0,239854	-0,095907	0,2420683	0,0344445
Кол_д	0,1439193	-0,083499	-0,075313	-0,0500389	0,311054	0,1102981	0,1121116	0,42278454	0,315683	-0,04341	0,2334057	-0,21828	-0,085684	0,2420465	0,0218126
Плот_	0,1583267	-0,069686	-0,064571	-0,0620983	0,329167	0,0841031	0,0656299	0,37893714	0,2619767	-0,055432	0,2391463	-0,16271	-0,062646	0,2535685	0,0689906

Figure 3 - Correlation matrix of infrastructure indicators and survey results (made by the authors).

Findings. A direct average dependence was revealed (0.31–0.44) between the number of days of rest, the method of accommodation and infrastructure indicators. This indicates that the number and quality of bases, as well as the quality of the road network, play an important role in choosing a place to stay and the time that vacationers want to spend there. A weak inverse relation (-0.05–-0.27) was found in the overall assessment of rest. This suggests that vacationers set the final score for their vacation to a greater extent guided by the aesthetic component of the environment.

References

1. Geography / Ch. ed. A. P. Gorkin; ed. Art. V. V. Avdonin [and ot.]. - Moscow: ROSMEN, 2006 (Tver: Tver Polygraph Combine). - 623 p. : ill., col. ill., portrait; [Electronic resource] – Access mode: https://pdf.11klasov.net/2534-geografiya-sovremennaya-illyustrirovannaya-enciklopediya.html

2. GOST R 55698-2013. Tourist services. Beach services. General requirements [Electronic resource] - Access mode: https://internet-law.ru/gosts/gost/55704/

3. Kiyanitsin V.V., Chermashentsev A.Yu. Distribution of Social Groups among Recreants on the Gamov Peninsular by the Degree of Their Possible Environmental Impact // Scientific and practical conference of students, graduate students, and young scientists, 2022.

Section IV
MATHEMATICS AND COMPUTER SCIENCES

Burakov A.A. [1], Kalinichenko P.A. [1]

REVIEW OF SOFTWARE FOR REMOTE PATIENT MONITORING

[1]Far Eastern Federal University, Institute of Mathematics and Computer Technologies, FEFU
[2]Far Eastern Federal University, Oriental Institute School of Regional and International Studies, FEFU
Scientific advisor — S.V. Smagin [1]
Scientific consultant — E.V. Kravchenko [2]

In 2018, according to the Federal State Statistics Service, 80.9% of the Russian population extensively uses the Internet by means of a personal computer or smartphone [1]. The widespread use of computer technology with Internet access allows modern medicine to increasingly use telemonitoring systems to monitor the condition of patients with chronic diseases and illnesses that can suddenly lead to irreversible negative consequences.

Medical telemonitoring systems also allow patients who do not have the opportunity to get a face-to-face doctor's appointment to keep in touch with a specialist and receive medical care remotely, which is especially important for low-mobile people and residents of remote communities. In today's COVID-19 pandemic conditions, remote access to a doctor remains a relevant and convenient method of obtaining medical care.

It should be noted that patients monitored by telemonitoring systems had lower all-cause mortality and a lower rate of heart failure-related hospitalizations [2]. Remote monitoring allows the doctor to intervene during therapy before the patient's condition worsens due to unforeseen complications. There is an opinion that telemonitoring has proven its effectiveness and needs to be expanded in its the scope. This requires a computer-computer channel (smartphone-smartphone) linking doctor and patient. The chain looks like this: patient →wearable device → analysis of the indicators→ server of the medical institution → automated workstation of the doctor → doctor [3].

The patient's state of health can be assessed by analyzing objective indicators obtained with special devices, taking into account the subjective assessment of his condition by the patient. One of the ways to analyze the patient's condition that can be used for remote monitoring is a questionnaire survey. The process can be divided into several main stages:

1. Preparation of questionnaires and evaluation criteria.
2. Data collection using the question-and-answer methodology.
3. Processing the collected data.
4. Analyzing the survey results and making decisions based on them.

Remote questionnaire survey involves the use of electronic means for timely analysis of the survey results and decision-making by the doctor [4].

Survey often provides a comprehensive picture of the patients' attitude towards their disease and, in general, their quality of life. There are general questionnaires, which are designed to identify the state of health status of healthy and sick, and specialized questionnaires, used for specific diseases. One of the goals of the survey is to study the confidence of patients with a disease in various therapy methods and means. A gradation of answers from "yes" to "no" is usually used [3].

Today there are software systems that allow you to create a channel linking the doctor and the patient. Such systems allow the patient to keep in touch with the specialist after the appointment, monitor his or her health state using various measuring devices and a health diary. Let us consider their categories: health self-observation systems (Electronic medical record); patient-to-doctor communication systems (SberHealth); control systems for medical institutions (Remsmed).

Medical institutions can connect to the above systems to facilitate the work of doctors and increase the efficiency of treatment. Let us consider their functionality.

Table

Comparison of software tool categories

Functions	Health self-observation systems	Patient-to-doctor communication systems	Control systems for medical institutions
Add health metrics	+	+/–	+/–
Maintenance of medical record	+	+/–	+
Storage of data about all patients	–	+	+
Analysis of indicators and display of the dynamics of the state of health	+	+/–	+/–
Remote Disease Monitoring	–	+/–	+/–
Create questionnaires	–	–	–
Providing questionnaires to patients	+	+	+
Availability of ready-made templates of medical questionnaires	–	–	–

Analyzing the table, we can conclude that none of the considered software tools can create typed medical questionnaires necessary for questioning patients to achieve mutual understanding of doctor and patient, fast and successful work of the doctor, effective selection of treatment method. To solve the problem of remote questionnaires, an application is required that allows the doctor to compile individual questionnaires for patients, according to state standards [5].

In order to use scales, tests and questionnaires in systems designed for remote patient monitoring, storage and analysis of complaints, it is necessary to study the standards for creating and using questionnaires. As a result, it will be possible to identify common features and rules to be considered in the development of a universal questionnaire designer. The clinical guidelines available on the resource of the Russian Ministry of Health "Rubricator of clinical guidelines" were chosen for the analysis [5]. The result of the analysis is the division of medical scales into four groups.

1. Scales suitable for self-diagnosis, based on a point system, or scales reduced to this type. Such questionnaires define ranges of sum scores in the key that correspond to the degree of illness or risk of illness. They are used for a wide range of diseases. There are a total of 67 scales.
2. Scales designed to assess pain. Such scales establish the gradation of pain and relate it to an illustration or numerical line. They are needed to help assess a patient's pain level and their overall condition, pain threshold. There are 3 scales in total.
3. Narrowly specialized scales designed for specialists and doctors. They help to determine the extent of disease using descriptions of symptoms, clinical examinations. They are necessary for filling in medical records, organizing the work of specialists. There are 13 scales in total.
4. Scales of tests and questionnaires with qualitative assessment. These questionnaires do not use scoring system and cannot be converted to point system. A total of 6 scales.

At present, a team of programmers from the Department of Software Engineering and Artificial Intelligence at FEFU IMCT is developing a software tool that has the following functionality: compiling surveys to monitor the well-being of patients with various diseases; taking the surveys by the patient or observer; viewing the patient's medical history; analyzing patient dynamics based on survey data; providing access to the system through the corporate network for authorized employees of the medical institution.

References

1. Information Society in the Russian Federation. 2019: Statistical Compendium [E-resource] / M.A. Sabelnikova, G.I. Abdrakhmanova et al. Federal Service of State Statistics. – M.: HSE, 2019. – ISBN 978-5-7598-2053-6.

2. Sukhanov M.S., Karakulova Yu.V., Prokhorov K.V., Spasenkov G.N., Koryagina N.A. Experience of remote monitoring of patients with cardiovascular diseases in the Perm Krai. Cardiovascular Therapy and Prevention. 2021; 20(3):2838. (In Russ.) URL: https://doi.org/10.15829/1728-8800-2021-2838

3. Gelman V.Ya., Dokhov M.A. Problems of Development of Health Monitoring at Residential Settings [E-resource] // Journal of Medicine. – 2020. – № 2. URL: https://www.fsmj.ru/015414.html

4. Nosov R.O., Chekalova S.A. Development of an application for processing and visualization data obtained as a result of survey / collection of materials of the 29th All-Russian Scientific and Practical Conference on Graphic Information Technologies and Systems. – 2019. pp. 160–162.

5. Rubricator of clinical recommendations of the Ministry of Health [E-resource] URL: https://cr.minzdrav.gov.ru/

Vasyliev O.I.[1]

QUALITY ASSESSMENT OF SOFTWARE SYSTEMS AS A FACTOR OF SUCCESSFUL INTEGRATION OF SOFTWARE IN THE SPHERE OF INFORMATIZATION OF EDUCATION

[1]Far Eastern Federal University, Institute of Mathematics and Computer Technologies, FEFU
[2]Far Eastern Federal University, Oriental Institute School of Regional and International Studies, FEFU
Scientific adviser – I.L. Artemieva [1]
Scientific consultant - I.F. Veremeeva [2]

Over the decades of the second half of the twentieth - the first half of the twenty-first century, education has been transformed by the introduction of information technology in its various aspects [4, 5]. On the example of higher education, these moments are clearly visible within the framework of the expansion of distance education.

Distance education is based on the use of special software and hardware, which may have the ability to integrate various software systems, which in turn allow you to manage, monitor and, accordingly, improve the effectiveness of distance education.

These software systems include, in principle, any software system involved in the educational process, however, of course, it is necessary to single out e-learning systems that are positioned as a basic software product for distance education, but in practice it can be stated that the process of distance education is possible without them, based on various software capable of providing communication between the teacher and the student.

Of course, it should be noted automated library and information systems, which are basic in the work of libraries, including universities [3]. We should also mention electronic library systems that complement the traditional resources of the library and without the use of which it is difficult to imagine the modern activities of the university library.

All these software systems, as a rule, are interconnected and interact with the developed automated control system of the university. Accordingly, they must meet the potentially necessary software quality criteria set by a specific potential customer carrying out informatization in this case in the field of education, including in terms of librarianship.

In the process of introducing, for example, automated library information systems in practice, there are many nuances from the correct automation of the library process to the correctness and completeness of integration with other software systems, on which the success of informatization of education depends. Accordingly, the factor of assessing the quality of software systems in relation to their capabilities in terms of integration with other software

becomes important without taking into account, which is difficult to build an educational information space.

In turn, the successful integration of library systems within the larger innovative environment of the university allows us to observe the expansion of the educational opportunities of the university we are observing. This, in turn, contributes to an increase in educational, scientific activities not only among students, but also among the teaching staff. Ultimately, it contributes to increasing the reputation and significance of the institution itself among other scientific centers of the country and the world [1, 2, 6].

Summing up, we can say that by developing new approaches, methods, models, metrics for assessing the quality of software systems, it is possible to potentially contribute to increasing the informatization of education at the level of choosing a software product used in educational activities.

References

1. Ataeva, O.M. Development and implementation of a semantic digital library as a basis for building a space of scientific knowledge : dissertation. … Candidate of Engineering Sciences / O.M. Ataeva. – Moscow, 2019. – 155 p.
2. Baryshev, R.A. Proactive library in the information and educational environment of the University : monograph / R.A. Baryshev. – Moscow : INFRA-M ; Krasnoyarsk : Siberian Federal University, 2021. – 261 p.
3. Library Encyclopedia / Rossijskaja gosudarstvennaja biblioteka. – Moscow : Pashkov dom, 2007. – 1300 p.
4. Russian Pedagogical Encyclopedia : V 2 t. / Gl. red. V. G. Panov. – Moscow : The Great Russia Encyclopedia, 1993-1999. V. 1: A – Moscow / Editor-in-Chief V. V. Davydov. – 1993. – 607 p.
5. Explanatory Dictionary of terms of the conceptual apparatus of informatization of education. – Moscow : Binom. Knowledge Lab, 2013. - 69 p.
6. Reference model of a new generation electronic library for university and business / L.V. Lapidus, A.I. Pogodaeva, D.A. Mukanin, E.I. Mukanina // Information Society. – 2017. – №6. – P. 42 – 53.

Dzhumagaliev E.V. [1], Kuzmin V. A. [1]

ONLINE COURSE CATALOG SUPPORT SYSTEM FOR PEOPLE WITH HEARING DISABILITIES

[1]Far Eastern Federal University, Institute of Mathematics and Computer Technologies, FEFU
[2]Far Eastern Federal University, Oriental Institute School of Regional and International Studies, FEFU
Scientific adviser – I.L. Artemeva[1]
Scientific consultant — E.V. Kravchenko [2]

At present, the problem of communication with people with hearing and speech impairments is very important, because the coverage of this problem is very wide, and there are quite a few specialists who speak Russian Sign language (RL), and the cost of their services is very high.

There is also a problem of cultural assimilation for people with hearing and speech disabilities. They cannot adapt to the market economy because they need to be trained before they can offer anything to the market. However, there are peculiarities of sign language: words that exist in sign language cannot be translated into Russian, and since there are fewer words in sign language than in Russian, translation problems arise. For this reason, the deaf-mutes need educational courses created and adapted specifically for their needs.

This project aims to develop a support system for a library of online courses created and adapted specifically to the needs of people with hearing and speech disabilities.

Product development technology

The difficulty in developing this system lies in the fact that due to the peculiarities of thinking of hearing-impaired people [1,2], it is difficult to understand in what form the information presented to this audience will be the most understandable and informative. In this regard, surveys were conducted among the hearing-impaired

population, which showed that the best way for the hearing-impaired to absorb information is in the form of a video. Therefore, it was decided to implement a video course system, for the development of which a sign language interpreter was hired.

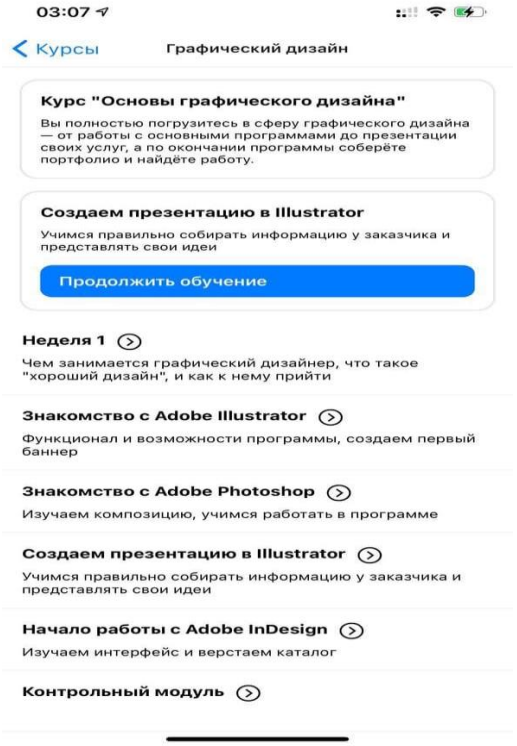

Fig. 1. MVP of Application

The application implements a course catalog (Figure 1), from which you can get to a specific course and start studying a module by watching videos, reading text notes, and performing various tasks. Creating a discussion thread on a task, course, or video is possible.

Each screen of the application has the ability to open a chat with technical support, and technical support automatically receives data about the context of the conversation (open application screen).

References

1. ALMANAC of the Institute of Correctional Pedagogy [Online resource] – URL: https://alldef.ru/ru/articles/almanac-45/hearing-loss-and-deafness-global-problem-of-the-modern-health-care.

2. Bogdanova, T.G. The study of the thinking of people with hearing impairments: problems and prospects. / T.G. Bogdanova // Psychological problems of modern education. – 2009. – P. 167-171.

Dilla Dagim Sileshi [1]

COMPUTER SIMULATION AND ANALYSIS OF ATOMIC STRUCTURE OF AMORPHOUS ALLOYS

[1]Far Eastern Federal University, Institute of Mathematics and Computer Technologies, FEFU
[2]Far Eastern Federal University, Oriental Institute School of Regional and International Studies, FEFU
Scientific adviser – E.V. Pustovalov [1]
Scientific consultant — E.V. Kravchenko [2]

Atomic scale computer simulations are a critical component of modern research in order to discover new materials as well as fully comprehend the physicochemical properties and atomic structure of amorphous alloys. The atomic structure of amorphous alloys is studied using graph theory as well as parametric geometry. This article discusses a little-known perspective on the study of atomic structure and physicochemical properties of amorphous

alloys. It displays highlights of implementation of the event-driven dynamics algorithm in sequential and parallel programming to ponder the macroscale atomic structure and physicochemical properties of amorphous alloys besides the stages and crucial issues of computer simulation of the atomic structure of amorphous alloys, as well as a cluster analysis of computational experiment results to study the atomic structure and physicochemical properties of amorphous alloys.

Amorphous materials have recently sparked renewed interest, owing to their potential technological applications as well as a lack of understanding of their properties, which differ significantly from those of crystalline materials. With the same material, some of their properties can differ from one sample to another. Because of imperfections and disorder, an ideal crystal has translational order in all dimensions [8]. This isn't the case with amorphous materials. Long-range order is a key distinction between an amorphous material and a crystal. Long-range order exists in crystals, however, not in amorphous materials. Individual atoms' bond lengths, bond angles, and coordination numbers vary resulting in a lack of long-range order.

Due to the lack of periodicity, most experimental techniques for determining structure without ambiguity are rendered ineffective. In structural studies, computational methods are extremely useful, but the analysis of the results is still hampered by a lack of atomic symmetry and a scarcity of experimental data for comparison and validation. The inability to accurately describe the structure of most amorphous metallic materials has proven to be a major roadblock to their effective understanding, development, and use. Based on the analysis of electron microscopic images of an amorphous alloys, a method for studying local atomic ordering with any kind of symmetry, including non-crystallographic symmetry, is proposed in this study. It is demonstrated that under thermal action, there is a 30% change in the density of atomic clusters with an ordered structure of 1–2 nm in size, using the structure of amorphous alloys CoP, NiW. It has been demonstrated that heating causes both an increase and a decrease in the degree of order.

Electrochemical deposition was used to create samples of CoP, CoNiP, and NiW amorphous alloys. High-resolution transmission electron microscopy on FEI Titan 80-300 at 300 and 80 kV with aberration correction is used to examine the atomic structure of the samples. The thickness of samples placed on a standard cupper grid ranges from 2 to 10 nm. Because of the thinness of the samples, we can investigate the local atomic structure and demonstrate different levels of ordering. HRTEM images were obtained at temperatures ranging from 20°C to 300°C. HRTEM image processing using GPU software to cross-correlate with double-core:

$$H_{\varphi,r_0}(x,y) = h(x,y) \cdot \sum_{\varphi} h(x - r_0 \cdot sin\varphi, y - r_0 \cdot cos\varphi), \quad (1)$$

Where $h(x,y) = sinc(\rho/\rho_0) - h_0$. We select $r_0 = 0.25$ nm, $\rho_0 = 15\,nm$ Parameter h_0 selected from following condition: $\sum_{x,y} h(x,y) \approx 0$.[7]

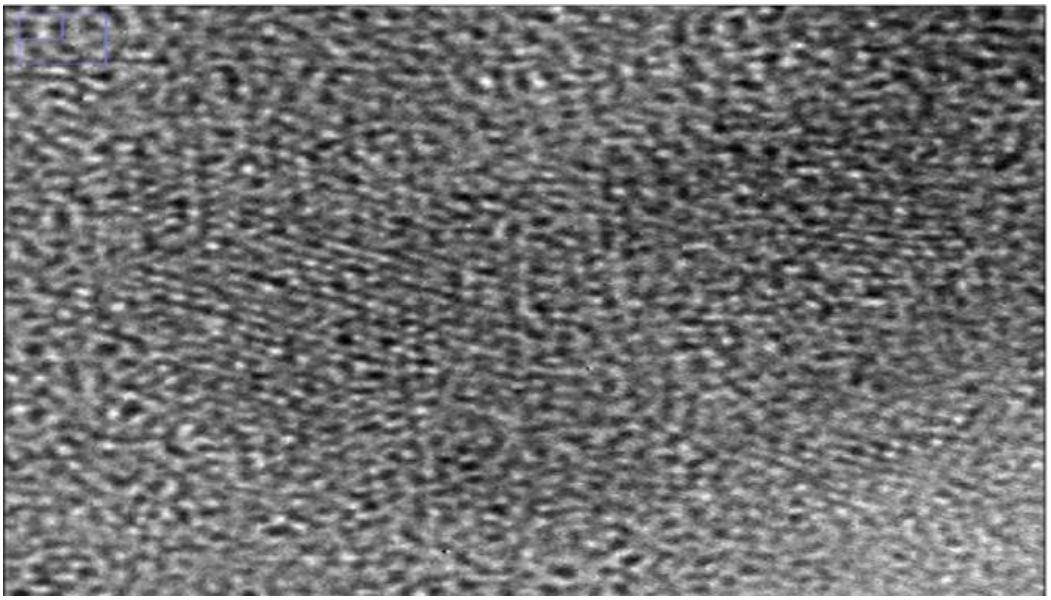

Fig. 1. HRTEM images of Amorphous alloy samples from series4 00001.dm3

In general, atomic clusters were defined as groups of similar atoms that existed at a distance not greater than or less than a given radius. If two atoms come into contact with each other, they belong to the same cluster. The developed app calculates the distance between two points in the Euclidean 2D plane using the electron microscope image pixels as coordinate points. which is nothing more than the Euclidean distance and finds the nearest neighbor for each point in a dataset within a radius of r=2 nm. Using Pythagoras Theorem [2]. Distance, assume point p have Cartesian coordinates $(p_1, p_2)$and let q have coordinate (q_1, q_2)Then the distance between p and q is given by [3].

$$d(p,q) = \sqrt{(q_1 - p_1)^2 + (q_2 - p_2)^2} \quad (2)$$

And then plot a graph for each cluster using NNG algorithm. After plotting undirected graph, it calculates Adjacency matrix, eigenvalues, graph energy and some other graph topology parameters for each graph or clusters.

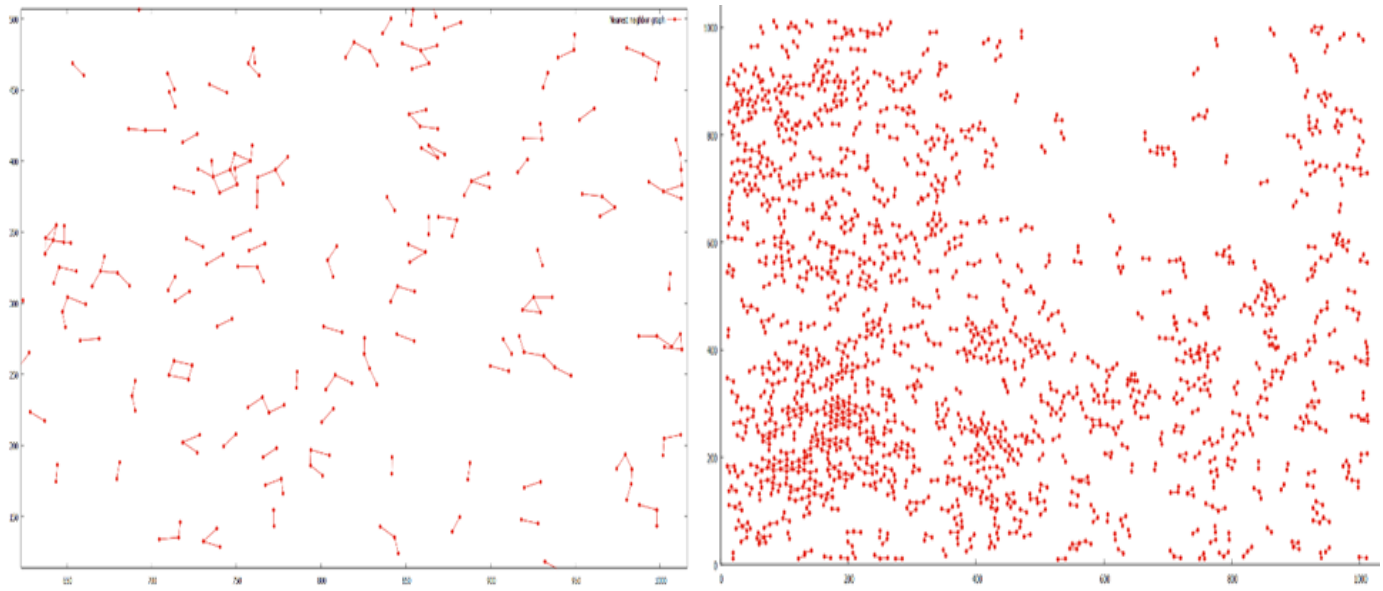

Fig.2 &3. A nearest neighbor graph of 2997 points in the Euclidean plane

Ivan Gutman introduced the concept of graph energy three decades ago. This concept is related to total electron energy in computational chemistry, of a class of organic molecules The overall the energy of π -electrons is calculated using the formula

$$\mathrm{E}_\pi = \sum_{j=1}^{n} |\lambda_j| \quad (2)$$

where: n is the number of the molecular orbital energy levels
λ_j s are eigenvalues of the adjacency matrix of the so called molecular or Huckel graph [3].

If G is a graph, then the energy of G, denoted by E (G), is the sum of the absolute values of G's eigenvalues, i.e., if λ_1,..., λ_n are G's eigenvalues, then $E(G) = \sum_{i=1}^{n} |\lambda_i|$

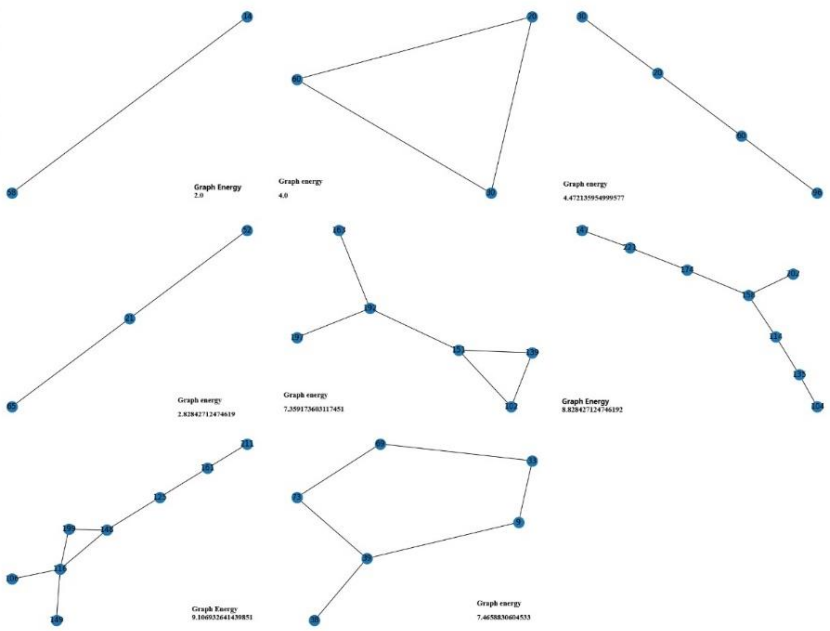

Fig. 2. Graph Energy

In order to simulate electron microscopic image studies, we created a software program that can compute large amounts of information in our datasets. The nearest neighbor graph is a directed graph that defines the Euclidean distance in the plane for a set of points in a metric space. A directed edge from p to q is produced whenever q is a nearest neighbor of p, that is, a point whose distance from p is the shortest among all the supplied points other than p itself [4]. In our applications of these graph, the edge orientations are ignored, and the NNG is instead specified as an undirected graph.

Amorphous alloys were studied in terms of their atomic structure and physicochemical properties. Several algorithms were used to simulate electron microscopy images of amorphous alloys in this study. Using the electron microscope image pixels as coordinate points, our software calculates the distance between two points in the Euclidean 2D plane. Finally, using the NNG algorithm, plot a graph for each cluster. It calculates Adjacency metrics, eigenvalues, graph energy, and other graph topology parameters for each graph or cluster after plotting an undirected graph. This enables us to study the atomic structures and physicochemical properties of amorphous and amorphous crystalline alloys in greater depth. We can provide detailed information with our software in much less time and with fewer resources, but more research is needed to fully comprehend the physicochemical properties of amorphous alloys.

References

1. Andoni, A., Indyk, P. and Razenshteyn, I., 2019. Approximate Nearest Neighbor Search in High Dimensions. Proceedings of the International Congress of Mathematicians (ICM 2018).

2. Dokmanic, I., Parhizkar, R., Ranieri, J. and Vetterli, M., 2015. Euclidean Distance Matrices: Essential theory, algorithms, and applications. IEEE Signal Processing Magazine, 32(6), pp.12-30.

3. Ivan Gutman. The energy of a graph: old and new results. Algebraic Combinatorics and Applications, pages 196–211, 2001

4. Li, W., Zhang, Y., Sun, Y., Wang, W., Li, M., Zhang, W. and Lin, X., 2020. Approximate Nearest Neighbor Search on High Dimensional Data — Experiments, Analyses, and Improvement. IEEE Transactions on Knowledge and Data Engineering, 32(8), pp.1475-1488.

5. Liu, J., 2021. Advances and Applications of Atomic-Resolution Scanning Transmission Electron Microscopy. Microscopy and Microanalysis, 27(5), pp.943-995.

6. Miller, M., Rodriguez, M. and Cox, I., n.d. Audio fingerprinting: nearest neighbor search in high dimensional binary spaces. 2002 IEEE Workshop on Multimedia Signal Processing.,.

7. Pustovalov E.V. et al., 2019, Effect of the Process Conditions for the Preparation of CoNiFeSiB Amorphous Alloys on Their Structure and Properties. Journal of Surface Investigation: X-ray, Synchrotron and Neutron Techniques, Vol. 13, No. 4, pp. 600–608.

8. Svatiuk, O., 2016. Contrast of Electron Microscopy Images of Amorphous Objects. Journal of Nano- and Electronic Physics, 8(1), pp.01005-1-01005-7.

Zhlutkin R.V. [1]

DEVELOPMENT AND IMPLEMENTATION OF A METHOD FOR EXTRACTING SPEECH FEATURES IN VOICE COMMANDS

[1]Far Eastern Federal University, Institute of Mathematics and Computer Technologies, FEFU
[2]Far Eastern Federal University, Oriental Institute School of Regional and International Studies, FEFU
Scientific adviser – I.L. Artemeva[1]
Consultant – M. S. Chusov, "Rhonda Software"
Scientific consultant - I.F. Veremeeva [2]

Automatic speech recognition is a dynamically developing area in the field of artificial intelligence. Significant advances have been made in this area over the last half century with many commercial applications available that make investment in this area worthwhile and profitable.

Automatic speech recognition systems are widely used in medical examinations requiring information input when the operator's hands are busy (e. g. X-ray), or when it is necessary to operate autonomous apparatus for examining internal organs. [1]

Despite the significant progress, the main goal of research which was originally intended, free communication between a person and a "machine", has not yet been achieved. The development of the field has revealed new difficulties that pose a challenge to the researchers at the present stage when the task of speech recognition merges with the problem of understanding the meaning of the message and requires the involvement of scientific psychology. The first two sections of the manual are devoted to the issues of speech production and perception.[2]

Obviously, understanding the structure of the speech signal and the underlying motions of the speech-forming organs can help in solving the problem of automatic speech recognition. To an even greater extent, this applies to understanding issues related to the perception of sounds in general and particularly speech sounds.

An essential question to be answered in this article is the question of the features or parameters of the speech signal which contain information sufficient for speech recognition. Obviously, by their very meaning, these parameters should be the result of consciously controlled movements of the speech organs. It is also clear that the selection of these parameters should be the main task of the auditory system in speech recognition.

The first step in speech recognition, when the recorded signal is analog, is that the analog speech signals need to be converted into digital ones, which the system can easily recognize. Then the digital signals are moved to the speech pre-processing modules to spectrally flatten the signal, which increases the energy of the signals at a higher frequency. This step is called the feature extraction step. In addition, this step is one of the most important parts of speech recognition and helps to distinguish one speech from another since each speech has unique individual characteristics embedded in its utterances. It extracts features by identifying the component of the audio signal and discarding irrelevant information such as noise, emotion, etc., i.e. retaining relevant speech information and discarding irrelevant.[2]

This article is devoted to the development and research of a feature extraction method based on the selection of segments from a speech signal that can be used to recognize human speech. The general approach to the speech signal processing procedure is to use short-term analysis, i.e. the signal is divided into time windows of a fixed size,

on which, as it is assumed, the signal parameters do not change. For a more accurate representation of the signal, an overlap is made between the windows. Then, feature extraction algorithms, such as spectral analysis, linear prediction, or others, are applied to each window. The task of speech recognition differs from many others in the field of speech technologies as there is no need to study the entire content of speech. It is enough to extract elements suitable for recognition.[2]

Most of the existing methods are not resistant to noise, or they work too slowly and inaccurately which, in general, affects the quality of the recognized voice sequence, the accuracy and speed of the program. Therefore, the following problem can be singled out: the lack of methods for extracting features in a speech signal that could encode a sequence of words in a voice command with good accuracy and speed.

Hence, **the purpose of this work** is as follows: taking as a basis one of the existing methods for extracting features in a speech signal, to modify it and formally describe a module capable of encoding a sequence of words in a voice command with the highest accuracy and speed possible.

To successfully achieve the given goal, it is necessary to perform the following **tasks**: to analyze existing methods, compare them, build a model of the subject area, justify the method of feature extraction in a speech signal taken as a basis, and describe possible modifications in the operation of this method.

References

1. Rabiner L.R. Introduction to Digital Speech Processing / L.R. Rabiner, R.W. Schafer. - M.: Radio and communication, 2008. - 469 p.

2. Tampel I.B. Automatic speech recognition. Textbook / I.B. Tampel, A.A. Karpov. - St. Petersburg: ITMO University, 2016 - 138 p.

Kilichov U. Sh. [1]

ANALYSIS OF MODELS FOR DETECTING CRIMINALS IN THE FIELD OF AML / CFT USING SOCIAL NETWORK ANALYSIS

[1]Far Eastern Federal University, Institute of Mathematics and Computer Technologies, FEFU
[2]Far Eastern Federal University, Oriental Institute School of Regional and International Studies, FEFU
Scientific adviser – G.V. Alekseev [1]
Scientific consultant — E.V. Kravchenko [2]

The Internet has become indispensable thanks to advanced technologies. Many people can run their business with an internet connection. While these events have a positive impact on the well-being of human life, they have also led to some negative consequences. In particular, the information disseminated in almost all spheres of life through social networks, which is becoming more and more widespread, represents a huge source of abuse. Organized crime groups find both supporters and followers using information on social media profiles and can easily identify their victims from there. The criminals who use these networks, who collect information from everywhere, commit new crimes with the help of information obtained from these environments. The mass affected by the virtual environment is large and the domain is very wide. This is a threat to one of the fundamental principles of society, such as the security of life, the security of goods, the security of religion, and the certainty of reason and generation, which has arisen through the imposition of opinion. Social networks are becoming a part of the daily life of society. Social networks with users from almost any environment are connecting users around the world and spreading rapidly. These features expand the use of social media as a potential tool for committing crimes, and new areas of crime become available to individuals and groups who can commit crimes.

The use of social networks to identify potential criminals implies network analysis itself. Social network analysis is the mapping and measurement of relationships (and flows) between individuals, groups, organizations,

or other information/knowledge processing entities. Entities are represented as nodes in the network along with links, with or without attribute weight age. SNA attempts to provide both a mathematical analysis and a visual representation of relationships in a network. SNA is an interesting cross-fertilization of sociology, mathematics, computer science, etc.

The idea of using SNA to understand networks is not new [1] in one form or another, network analysis has been used to detect illicit entities and activities. It has been used to map evidence in fraud and conspiracy cases, for example [2]. A suspect's network can be built from relational information, including internet blogs, email, phone logs, travel bookings, credit card transactions, etc. [3] Recently, network methods have become a useful part of intelligence work. As terrorists establish new relationships or break existing relationships with others, their role and power may change accordingly. This node dynamics resulting from relationship changes can be captured using a set of centrality measures from social network analysis functions.

Degree measure. The degree determines how active a particular node is. It is defined as the number of direct links that node "a" has. [4] This calculation is based on formula 1.

$$C_D(a)=\sum_{i=1}^{n} c(i,a) \quad (1)$$

where n is the total number of nodes in the network, $c(i,a)$ is a binary variable indicating whether there is a connection between nodes i and a. A high degree network member may be the leader or "center" in the network.

In a directed graph, degree can be divided into intrinsic and extrinsic to distinguish between links entering and leaving a node, respectively.

Intermediate measure. Betweeness measures the extent to which a particular node is between other nodes in the network. The distance between nodes, say a, is defined as the number of geodesics (shortest paths between two nodes) passing through a. [4] This calculation is based on formula 2.

$$C_B(a) = \sum_{i<n} \sum_{j}^{n} g_{ij}(a) \quad (2)$$

where $g_{ij}(a)$ indicates whether the shortest path between two other nodes i and j passes through node a. A participant with high intermediateness may act as a gatekeeper or "broker" in the network for the smooth interaction (transmission of information) or the flow of goods (such as drugs).

A measure of closeness. Proximity is the sum of the geodesic lengths between a particular node, say a, and all other nodes in the network. It actually measures how far one node is from other nodes and is sometimes referred to as "remoteness". This calculation is based on formula 3.

$$C_C(a) = \sum_{i=1}^{n} l(i,a) \quad (3)$$

where $l(i,a)$ is the length of the shortest path connecting nodes i and a.

Related research in social media analysis and money laundering.

Social networks have been studied in order to study the roles and behavior of nodes. The analysis of criminal networks has also been a concern in the last decade.

In [5], the authors developed a system for solving crimes, in which the analysis of social networks was combined with hierarchical clustering. The clustering methodology divided the network into subgroups, and then the block modeling method made it possible to identify interaction models between these subgroups. However, this approach did not reveal the detailed roles of offenders. Only the key participants in the network are listed in the systems.

In [6], the authors applied social network analysis to destabilize terrorist networks. The purpose of the system was to investigate terrorist networks in order to figure out how to destabilize them and determine who was capable of carrying out terrorist activities. The approaches suggested in this article focus on how to deal with terrorist organizations. Incidentally, the phenomenon of money laundering is taken into account. Therefore, there is no special methodology focused on this type of crime.

An analysis of social networks at the level of subjects was used in [7] to help identify the roles of individuals

who could potentially be involved in criminal activity. Analysis of social networks made it possible to identify key members of criminal gangs. These papers do not propose an algorithm and study of parameters that can be used in the detection of money laundering in order to reveal the detailed roles of criminals.

In a research paper [8], social network analysis was applied to identify neighbors between nodes in order to form networked communities through which individuals can be grouped based on their social ties. They found that groups within the network with similar behaviors and characteristics are critical in detecting money laundering activities. In addition, analyzing the differences in different types of interactions between people through links in their social networks can lead to the detection of suspicious activity. These social ties typically include family members, relatives, co-workers, friends, related friends, and other 2nd and 3rd level connections. However, the document focuses more on social learning content and uses user cookie data, which can be a problem for ethical data use.

Recently [9] social media analysis has been introduced to prevent money laundering. They matched relational data with their proposed model and presented a predictive model based on network metrics to identify risks associated with the economic market. They found that social media features are critical in predicting the risk profile of clients, and their experimental results indicated that social media metrics are important to consider when evaluating risk profiles. The work provides an early analysis of the importance of social media metrics in effectively identifying suspicious customers/transactions using social media features, and the results of the qualitative study demonstrate that the impact of social media and relationships on the socio-political dimension.

Reviewing the literature review and overcoming the aforementioned limitations and issues, the following papers will propose a relational model for identifying relationships and associations with suspicious AML clients using social network analysis that can create a social network of client profiles.

References

1.M.K. Sparrow, "The application of network analysis to criminal intelligence: An assessment of the prospects", Social Networks, vol. 13, pp. 251-274, 1991.

2. P. Klerks, “The Network Paradigm Applied to Criminal Organizations,” Connections, vol. 24, no.3, 2011.

3. W. Krebs, Mapping Terrorist Networks, Vol. 24, No. 3, 2018

4. Q. Jialun, J.J. Xu, H. Daning, M. Sageman, and H. Chen, "Analyzing Terrorist Networks: The Case of a Global Salafi Jihad Network", Proceedings of the IEEE International Conference on Security Intelligence and Informatics, pp. 287-304, 2005

5.J.J. Xu, H. Chen, Crimenet explorer: a framework for detecting criminal networks, ACM Trans. Information. System. 23 (2005) 201–226. URL: https://dl.acm.org/doi/10.1145/1059981.1059984 (accessed 20.04.2022).

6. M. Nasrullah, Detecting Terrorist Patterns with a Data Mining Tool, Int. J. Knowl. Syst. sci. 3 (2005) 43–52. URL: https://www.scopus.com/record/display.uri?eid=2-s2.0-84961350913&origin=inward (accessed 04/20/2021).

7. K. Dowd, R. Alhaj, J. Rockne, A global measure of the degree of organization of terrorist networks, in: N. Memon, R. Alhaj (eds.), International Conference on Advances in Social Network Analysis and the Mining Industry, 2010 (ASONAM), IEEE Computer Society, Los Alamitos, CA, Washington, Tokyo, 2010, pp. 421–427. URL: https://ieeexplore.ieee.org/document/5563065 (accessed 04/22/2022).

8. Shum S.B., Ferguson R. Social Learning Analytics. J Educ Technol Soc. 2012; 15 (3): 3 - URL: https://www.jstor.org/stable/pdf/jeductechsoci.15.3.3.pdf (Accessed: 05/05/2022).

9. Colladon A.F., Remondi E. Using social network analysis to prevent money laundering. Expert SystAppl. 2017; 67:49–58. – URL: https://www.sciencedirect.com/science/article/abs/pii/S09574174163051 39 (accessed 05.05.2022).

Kim P.Kh. [1], Kosenok M.V. [1]

DATA ANALYSIS FOR THE DISABILITY EMPLOYMENT PLATFORM

[1]Far Eastern Federal University, Institute of Mathematics and Computer Technologies, FEFU
[2]Far Eastern Federal University, Oriental Institute School of Regional and International Studies, FEFU
Scientific advisor – T.V. Pak [1]
Scientific consultant — E.V. Kravchenko [2]

Archival and up-to-date information about resumes, vacancies, responses from applicants and invitations to an interview is processed. There is a search and comparison of related professions. The data is processed taking into account the responses of applicants and the skills required for the vacancy.

A platform has been created that adaptively compares the capabilities of people with disabilities and available vacancies (both offline and online) in the Far East, including the ability to form targeted educational programs (individual and group).

Anonymous data characterizing the applicant (location, experience, personal wishes, education, willingness to move and retrain) and existing jobs are added to the Quota-Service program

Enterprises receive a convenient service for designing workplaces for the disabled (for example, an enterprise will be able to assess in real time whether there will be a demand for the vacancy it offers, if so, what will be the costs of "closing the vacancy" on a turnkey basis (equipment of the workplace, creating an accessible environment, etc.) and what part of these costs the state is ready to compensate (relocation, targeted educational programs, including the financing of internships, etc.).

The relevance of the topic lies in the fact that ~ 90% quota jobs for the disabled remain unclaimed, as the quota jobs to a large extent do not correspond to the professional and qualification structure of the disabled. The job recommendation system will be improved.

Problem.

Enterprises are forced to create jobs for people with disabilities in complete uncertainty, having no idea about the scope of job seekers and possible government support measures.

Persons with disabilities do not have the opportunity to choose an interesting and / or highly paid job due to the narrow scope of their specialization or its absence.

The paper analyzes the data to compare related professions. A convenient service has been created to design attractive jobs for people with disabilities at minimal cost with the support of the state, which allows not only to comply with the standards, but also to attract loyal staff.

For the project it is necessary to solve the following tasks:

1. Data processing. The data is published in XML format and may contain unnecessary characters, errors, and other shortcomings, which is the result of both manual entry of information by employers and job seekers, and insufficient procedures for cleaning and preprocessing published open data.
2. Optimize the server side of the platform.
3. Improve user interface in WEB version.
4. Develop a mobile version of the service.

Project structure.

The company → Registers itself on the platform → When creating a workplace, the system, according to this entered table, issues a list of people who have the qualifications of one of the listed positions → completes the creation of a workplace

Disabled person → Registers → fills out the questionnaire receives - current offers Software used:

HTML5, CSS, JS, Django framework, mySQL, Bootstrap[2-5]; Figma (website design); Pandas (test data processing) [6].

References

1. Kim P.Kh., Kosenok M.V. KVOTA-SERVICE platform for enterprises wishing to employ disabled people [electronic resource] - Access mode: https://www.elibrary.ru/item.asp?id=48101569
2. Kozhemyakin A. A. HTML and CSS in examples. Creation of Web pages - M.: Alteks-A, 2014.
3. Django framework documentation [electronic resource] - Access mode: https://django.fun/docs/django/ru/3.0/
4. mySQL documentation [electronic resource] - Access mode: https://dev.mysql.com/doc/
5. Bootstrap official site [electronic resource] - Access mode: https://bootstrap-4.ru/docs/4.0/getting-started/introduction/
6. Pandas documentation [electronic resource] - Access mode: https://pandas.pydata.org/docs/

Larina V. I.[1]

THE PROBLEM OF OPTIMAL DISTRIBUTION OF GOODS (DIGITAL AND HOUSEHOLD APPLIANCES) IN THE TRADING NETWORK OF A FEDERAL COMPANY

[1]Far Eastern Federal University, Institute of Mathematics and Computer Technologies, FEFU
[2]Far Eastern Federal University, Oriental Institute School of Regional and International Studies, FEFU
Scientific adviser – A.L. Abramov[1]
Scientific consultant - I.F. Veremeeva [2]

Annotation. The article deals with the problem of optimal distribution of goods across the distribution network of a federal company specializing in the sale of digital and household appliances.

Keywords: Inventory management, distribution of goods, logistics

One of the criteria for the effective operation of a trading company is the inventory turnover, - the ratio of the cost of inventories sold for a period to the total inventory.

The formation of the turnover rate is influenced by many factors, of which the most important include:

- category and purpose of the goods, its weight and size and quality characteristics
- product price segment;
- demand for the product in terms of consumer demand;
- price and commodity policy of the company;
- inventory management system, which includes the optimal distribution of goods from the company's warehouses to retail outlets (shops) and others.

The size and structure of commodity stocks are determined by the volume and structural composition of the turnover of a trading company. Maintaining the optimal ratio between the value of turnover and the size of inventory, along with a reasonable pricing policy, is one of the most important problems, without which it is impossible to ensure the efficient operation of retail chain stores [4, 6, 7].

Among the listed factors that determine the commercial success of a retail trade enterprise in the market, an important role belongs to the distribution of goods.

The distribution of goods in the retail system covers a set of problems for managing the flow of consumer goods at the supplier-end consumer site, from the moment the goods are purchased to the moment they are sold to the consumer [5].

The problem of developing a method for the optimal distribution of goods from warehouses to retail outlets (shops) is a solution to a multicriteria optimization problem in which it is necessary to distribute goods from warehouses to stores with minimal costs in such a way as to satisfy the needs of stores with high sales of goods and not form inefficient stocks of goods in stores with low sales. The distribution of commodity stocks of the trading network should be focused on increasing the efficiency of commodity stocks. While solving this problem, it is

necessary to take into account the characteristics of the product, as well as the locations where it needs to be distributed among the stores.

Let a large company specializes in the sale of digital and household appliances, have its own automated logistics system and a federal network of stores.

The specifics of digital goods and household appliances is that some goods do not need a display case and can be delivered to the store if they are purchased directly by the buyer through the company's website (system units, computers and accessories), and some are required to be placed (large household appliances: refrigerators , washing machines), which is due to consumer preferences and the purpose of the product.

The problem of optimal goods distribution among the company's stores is to calculate the required level of stock of such a product and distribute it at minimum cost in such a way as to ensure its availability in stores with a high level of sales, without forming an inefficient inventory in stores with its low turnover.

This problem as well as the problem of placing a certain number of service points across a network of consumers [3] belongs to the class of problems of optimal placement of objects, described by many features [2]. The solution of such problems can be obtained using the theory of complex networks that describe objects that have a number of properties characteristic of real arrangements of economic, analytical and social objects in systems of various nature. These systems are often called networks due to the fact that they combine collections of elements connected by many different relationships that have the emergent property [1,2,3].

References:

1. Abramov A.L., Velichko A.S., Drekko E.V., Anoshkina M.V., Molochkova M.A. Graph models of complex networks // The_32th_Congress_Jangjeon_Mathematical_Society (ICJMS-2019), 32nd International Conference of the Jangjeon Mathematical Society, Far Eastern Federal University, July 16-19, 2019.

2. Abramov, A.L. Development and use of hierarchical hypergraph models and algorithms in discrete manufacturing automation systems [Manuscript] : author. dis. for the competition scientific degree cand. tech. sciences: spec. 05.13.07 - Automation of technological processes and production / A. L. Abramov; scientific hands L. T. Ashchepkov, 1991. - 24 s - access mode: http://elib.kstu.kz/lib/ ?e_kls=%D0%BC%D0%BE%D0%B4%D0%B5%D0%BB %D0%B8&e_viewdb=AVTOR

3. Larina V.I. Application of the theory of complex networks for setting the problem of locating logistics centers // Proceedings of the Regional Scientific and Practical Conference of Students, Postgraduates and Young Scientists in Natural Sciences, Vladivostok, April 15-30, 2021 [Electronic resource] / Ed. ed. V.Yu. Ermachenko. – Electron. Dan. - Vladivostok: Dalnevost. federal. un-t, 2021. - Access mode: https://www.dvfu.ru/schools/school_of_natural_sciences/sciences/the-conference/new-page.php. - Zagl. from the screen. ISSN 2500-3518.

4. Lototskii V. A. Models and methods of inventory management / V. A. Lototskii, - M.: Nauka, 1991. - 192 p

5. Maizner, N. A., Pavkin, S. O. Organization of distribution of goods in a retail trade network on a logistic basis / N. A. Maizner, S. O. Pavkin // Economic analysis: theory and practice. - 2011. - No. 32 (239). – P. 51 -56

6. Pankov, V. V., Smirnov, A. I., Golovin A. L. Analysis of inventory at retail enterprises / V. V. Pankov, A. I. Smirnov, A. L. Golovin // Financial Analytics : problems and solutions. - 2008. - No. 11. - P. 74 - 77

7. Ryzhikov Yu. I. Queue theory and Inventory management / Yu. I. Ryzhikov. - M.: Peter, 2001. - 384 p

Mikheev R.Yu. [1], Sinyagina A.D. [1]

DEVELOPMENT OF AN EXPERT RECOMMENDATION SYSTEM USING NEURAL NETWORKS FOR IMAGE PROCESSING

[1] Far Eastern Federal University, Institute of Mathematics and Computer Technologies, FEFU
[2] Far Eastern Federal University, Oriental Institute School of Regional and International Studies, FEFU
Scientific adviser – I.P. Yarovenko [1]
Scientific consultant - I.N. Lazareva [2]

Currently, neural networks [1] for image processing are gaining more and more popularity, since it is a powerful tool with which you can create, edit and analyze images. Most users face difficulties in understanding how to edit images and make them visually pleasing. There are many programs, but they are too complex and not clear enough to use. At the same time, neural networks make it possible to simplify the task, since the user does not have to understand the work of applications, but such a solution is often intended only for one type image or one processing style.

The purpose of this work is to develop an expert recommendation system using neural networks for image processing. This resource interacts with the user in order to process the uploaded image [2], providing the opportunity to choose the appropriate color correction option [3].

Neural networks (artificial neural network, ANN) [4] is a computational nonlinear model based on the neural structure of the brain, capable to learn how to perform classification, prediction, decision-making, visualization, and some other mental activities merely by considering examples.

Any ANN architecture consists of artificial neurons — processing elements having a structure of 3 interconnected layers: input, a structure consisting of one or more hidden layers, and output.

The input layer consists of input neurons that transmit information to hidden words. The hidden layer, in turn, transmits information to the output. Each neuron has inputs with weights — synapses, an activation function that determines the output information for a given input, and one output. By synapses we man regulated parameters that convert a neural network into a parameterized system.

The weighted sum from the inputs — the activation signal — passes through the activation function to output data from the neuron. There are several types of activation function: linear, stepwise, sigmoid, tangential, rectifier (Rectified linear unit, ReLU). Training is the process of optimizing weights, in which the prediction error is minimized, and the network reaches the required level of accuracy. The most used method for determining the error of each neuron is the reverse propagation of the error, with which the gradient is calculated. This is one of the modifications of the gradient descent method.

With the help of additional hidden layers, it is possible to make the system more flexible and powerful. ANN with many hidden layers are called deep neural networks (DNN); they create complex nonlinear connections.

In the course of work, popular neural network architectures were considered [5], which have proven themselves well in NLP tasks and can be recommended for use.

Moreover, existing software solutions were considered. Among them the following products were selected: Zyro AI Image Upscaler [6], Waifu2x [7], Let's Enhance [8], AI Image Enlarger [9], Deep Image [10], Vance AI Image Enlarger [11], Topaz Gigapixel AI [12].

Based on the study of the above software, we can conclude that our future development has some particulars, therefore it is original – in comparison to those considered above. This project is nor targeted to retouch or remove the background of a picture because the main purpose of the neural network is to improve the images as they were provided by the user for the system to work.

References

1. Khaykin S. Neural networks: a complete course, 2nd edition. – Williams Publishing House, 2008.
2. Image Completion with Deep Learning in TensorFlow [Electronic resource] -

https://bamos.github.io/2016/08/09/deep-completion/

3. Deng L., Yu D. Deep learning: methods and applications //Foundations and trends in signal processing. - 2014. – Vol. 7. – no. 3-4. – pp. 197-387.

4. Portnova E. A. The origin of deep learning //Actual problems of science and technology. 2019. – 2019. – pp. 364-364.

5. Nikolenko S., Kadurin A., Arkhangelskaya E. Deep learning. – " Publishing House"" Peter""", 2017.

6. Zyro AI Image Upscaler [Electronic resource] - https://zyro.com/ru/instrumenty/uluchshyt-kachestvo-foto

7. Waifu2x [Electronic resource] - https://github.com/nagadomi/waifu2x

8. Let's Enhance [Electronic resource] - https://letsenhance.io/

9. AI Image Enlarger [Electronic resource] - https://imglarger.com /

10. Deep Image [Electronic resource] - https://deep-image.ai /

11. Vance AI Image Enlarger [Electronic resource] - https://vanceai.com/

12. Topaz Gigapixel [Electronic resource] - https://www.topazlabs.com/gigapixel-ai

---

Moiseeva A.V. [1]

MODEL AND DATA MINING TOOLS FOR THE FORMATION OF INTERPRETABLE KNOWLEDGE BASES IN MEDICINE

[1]Far Eastern Federal University, Institute of Mathematics and Computer Technologies, FEFU
[2]Far Eastern Federal University, Oriental Institute School of Regional and International Studies, FEFU
Scientific advisor — V.V. Gribova [1]
Scientific consultant — E.V. Kravchenko [2]

Systems based on knowledge bases (expert systems, intelligent assistants, decision support systems, computer simulators, etc.) have not lost their relevance. Moreover, they are becoming increasingly important, since for many systems of this class it is required not only to obtain a solution, but also generate a detailed explanation of the results obtained. Systems with knowledge bases formed on the basis of ontologies ensure the fulfillment of this requirement. However, a well-known limitation of systems of this class is the process of forming knowledge bases. There are two main approaches to their implementation. The first one is used when knowledge is known, and their formalization is required. In this case, as a rule, expert formation or automatic formation of knowledge bases based on texts is used. The second method is associated with the formation of knowledge bases based on data (training samples) - the so- called knowledge discovery - the detection of patterns in data in order to build knowledge bases. There are many methods, approaches and technologies (decision trees, artificial neural networks, genetic algorithms, evolutionary programming methods, etc.) that are designed to extract new information from data warehouses by building various models. The disadvantage of these technologies is that knowledge is presented implicitly (in the form of models), which causes distrust among users in the results obtained. There are known works on inductive generalization of data in order to build interpretable knowledge bases based on ontologies (for example, for medicine), but the developed approaches and methods are limited to a single subject area and use simplified ontology models.

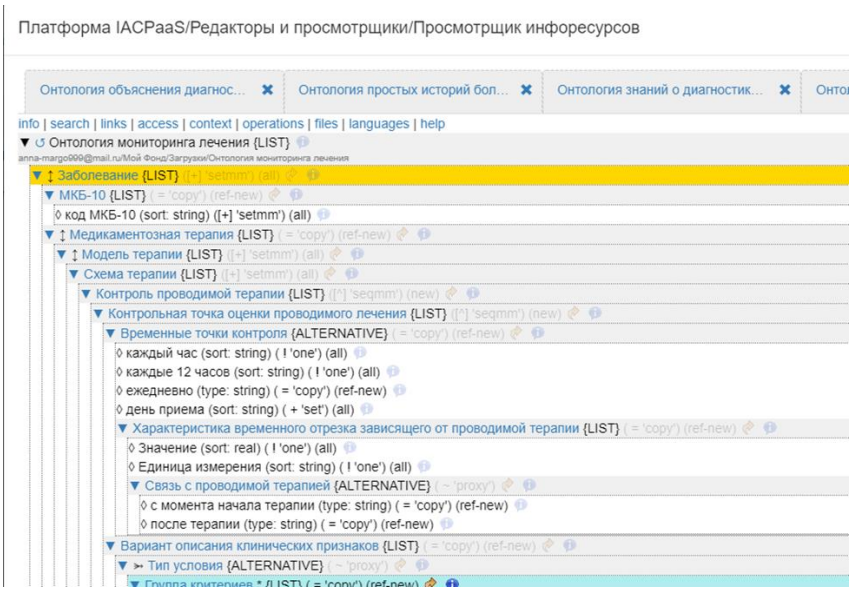

Fig. 1 An example of disease ontology

The aim of the work is to develop models, methods and algorithms of data mining to build interpretable knowledge bases (ontological knowledge bases) on process diagnostics and development of its application technology for various subject areas.

As a basis, we will take the already created prototype of the disease anthology (see Fig. 1), which describes the symptoms of diseases and their indicators.

This ontology is compiled manually, but we would like to supplement our ontology and help doctors make diagnoses, based on cognitive analysis, namely artificial intelligence. This will simplify the formation of the knowledge base and help doctors to diagnose more accurately.

References

1. V. V. Gribova, Dr. Sci. sciences, deputy dir. on scientific work, e-mail: gribova@iacp.dvo.ru, A. S. Kleshchev, Dr. Sci. sciences, ch. scientific co-worker, F. M. Moskalenko, Ph.D. tech. Sciences, art. scientific co-worker, V. A. Timchenko, Ph.D. tech. Sciences, art. scientific co-worker, E. A. Shalfeeva, Ph.D. tech. Sciences, art. scientific collaborator Federal State Budgetary Institution of Science Institute of Automation and Process Control, Far Eastern Branch of the Russian Academy of Sciences, Vladivostok Extensible tools for creating visited systems with knowledge bases

2. Zagoruiko Nikolai Grigorievich. Cognitive data analysis Zagoruiko N.G. ; Ros. acad. Sciences, Sib. Department, Institute of Mathematics im. S.L. Sobolev. - Novosibirsk: Geo, 2013. - 183, [3] p., [1] l. portrait : ill., tab. — Bibliography: p. 178-183. - ISBN 978-5-906284-04-4. Yarushkina N.G., Intellectual analysis of time series: textbook /N.G.Yarushkina, T.V.Afanasyeva, I.G.Perfilieva –Ulyanovsk: UlSTU, 2010.–320s.

Saritskaia Zh.Yu. [1]

OPTIMISATION METHODS FOR PROBLEMS OF MINIMIZATION OF TECHNOLOGICAL ACCIDENTS' CONSEQUENCES

[1]Far Eastern Federal University, Institute of Mathematics and Computer Technologies, FEFU
[2]Far Eastern Federal University, Oriental Institute School of Regional and International Studies, FEFU
Scientific adviser – G.V. Alekseev [1]
Scientific consultant – R.V. Brizitskii [1]
Scientific consultant - I.F. Veremeeva [2]

Studying of boundary value and control problems for heat-and-mass transfer models has been attracting a lot of attention in the last years. One should bear in mind that the applications of the mentioned control problems

are not restricted to the search of effective mechanisms of physical fields' control. In the framework of the optimization approach inverse problems are reduced to control ones. Inverse problems consist in recovering unknown functions and coefficients in the equations and in boundary conditions of the considered models with the help of the additional information about the solution of the boundary value problems. In its turn, the problem of locating of the source of the pollution via emissions of polluting substance, which were measured in some domain, can be reduced to the problems of distributed control. It should be stressed that the source of the pollution can be concealed, for example, it can be a drowned object. So the fastest detection of this source can prevent the damage to ecology (see [1-4]).

In a bounded domain $\Omega \in \mathbb{R}^3$ with boundary Γ the following boundary value problem is considered:

$$-\nu\Delta\mathbf{u} + (\mathbf{u}\cdot\nabla)\mathbf{u} + \nabla p = \mathbf{f} + \beta\mathbf{G}\varphi, \quad \operatorname{div}\mathbf{u} = 0 \text{ in } \Omega,$$
$$-\operatorname{div}(\lambda(\mathbf{x})\nabla\varphi) + \mathbf{u}\cdot\nabla\varphi + k(\varphi,\mathbf{x})\varphi = f \text{ in } \Omega,$$
$$\mathbf{u} = \mathbf{0}, \qquad \varphi = 0 \text{ on } \Gamma.$$

Here $\mathbf{u}$ is a velocity vector, φ denotes a concentration of polluting substance, $p = P/\rho$, where P stands for pressure, $\rho = \text{const}$ is fluid's density and $\nu = \text{const} > 0$ is constant kinematic viscosity. Also, a diffusion coefficient is denoted by $\lambda = \lambda(\mathbf{x}) > 0$, β stands for a coefficient of mass expansion, $\mathbf{G} = (0,0,G)$ is acceleration of gravity, $\mathbf{f}$ and f denote volume densities of external forces and of external sources, respectively, and, finally, function $k = k(\varphi,\mathbf{x})$ has the sense of a reaction coefficient, where $\mathbf{x} \in \Omega$.

One should keep in mind that the model under consideration generalizes the Boussinesq approximation. It is clear that the less restrictions are imposed on the model, which is used in applications, the more opportunities arise for searching effective control mechanisms.

In its turn, the control mechanisms for physical fields include the processes of cooling and heating of liquid due to heat dissipation from the parts of the boundary of the domain or, conversely, due to their heating, to adding reagents, which accelerate the decay of oil slicks during man-made accidents.

This work was supported by the state assignment of Institute of Applied Mathematics FEB RAS (Theme No. AAAA-A20-120120390006-0) and by the Ministry of Science and Higher Education of the Russian Federation (project no. 075-02-2021-1395).

References

1. Brizitskii R.V., Saritskaya Zh.Yu. Optimization analysis of the inverse coefficient problem for the nonlinear convection-diffusion-reaction equation // J. Inverse Ill-Posed Probl. – 2018. – V. 26. – № 6. – P. 821-833.

2. Brizitskii R.V., Saritskaya Z.Y., Kravchuk R.R. Boundary value and extremum problems for generalized Oberbeck-Boussinesq model // Sib. El. Math. Rep. – 2019. – V 16. – P. 1215-1232.

3. Brizitskii R.V., Saritskaia Zh.Yu. Multiplicative control problems for nonlinear reaction-diffusion-convection model // J. Dynamical and Control Systems. – 2021. – V. 27. № 2. – P. 379-402.

Sakharov I. A. [1]

PROJECTIVE UNARS

[1]Far Eastern Federal University, Institute of Mathematics and Computer Technologies, FEFU
[2]Far Eastern Federal University, Oriental Institute School of Regional and International Studies, FEFU
Scientific advisor — A.A. Stepanova [1]
Scientific consultant — E.V. Kravchenko [2]

An object P in a category $\mathcal{C}$ is called *projective* if for any epimorphism α: $B \to A$ and a morphism φ: $P \to A$ there exists a morphism $\bar{\varphi}$: $P \to B$ such that $\alpha\bar{\varphi} = \varphi$ (see [1]). Projective objects in Abelian categories are widely used in homological algebra. In this paper, we study the structure of projective unars, i.e., projective objects in the category of unars.

Let us recall some definitions necessary for the formulation of the main result (see [2]).

An algebra is called *unar* if its signature consists of a single symbol of the unary operation f. Let P be an unar, $p \in P$. Let us introduce the notations: $f^0(p) = p$, $f^{n+1}(p) = f(f^n(p))$. The unar P is called a *semichain* if $P = \{p_i | \, i \in \omega\}$, $p_i \neq p_j$ for $i \neq j$ and $f(p_i) = p_{i+1}$ for any $i, j \in \omega$. *The coproduct of unars* P_i, $i \in I$, is their disjoint union.

The following theorem gives a necessary and sufficient condition for unars to be projective.

Theorem. A unar is projective if and only if it is a coproduct of semichains.

References

1. Maclane, S. Homology / S. Maclane. — M.: Mir, 1966. — 544 p.
2. Skornyakov, L. A. Elements of general algebra / L. A. Skornyakov. — M.: Nauka, 1983. — 272 p.

Ustiugov I. F. [1]

INDOOR POSITIONING SYSTEM BASED ON WI-FI AND BLUETOOTH DATA COMPLEXING

[1]Far Eastern Federal University, Institute of Mathematics and Computer Technologies, FEFU
[2]Far Eastern Federal University, Oriental Institute School of Regional and International Studies, FEFU
Scientific adviser – V.M. Griniak [1]
Scientific consultant – I. F. Veremeeva [2]

To date, there are many solutions to the problem of determining the location of an object in space. The most popular of them are satellite navigation solutions, among which GPS and GLONASS are the most common, as they provide complete coverage and stable work for the entire globe.

However, the task of finding the location of an object inside buildings and closed structures is difficult for such technologies to solve, since the satellite navigation system is practically inaccessible in such places. Moreover, this system can only calculate the height of an object above the earth's surface with little accuracy compared to longitude and latitude, so the problem of floors is not considered at all.

In this regard, to solve such problems Indoor positioning system is used. A key issue that requires careful consideration is the positioning accuracy in real conditions and ways to improve it.

There are a lot of technologies used to implement Indoor positioning systems: camera, infrared radiation, tactile systems, sound, RFID and many others. But the most commonly used in practice are only two - Wi-Fi and Bluetooth [1], [2].

Technically, an Indoor positioning system can be implemented by the following Wi-Fi methods:

1. Methods based on signal propagation model construction. An example of such a model can be the Motley-Keenan model, which will be discussed below.

2. Methods based on the ideas of classification theory: deterministic methods that use the nearest neighbor group methods and probabilistic methods that apply Bayes' theorem.

In practice, the main methods used in solving the problem of local positioning using WiFi networks are:

1. Motley-Keenan model. It is a classic model of Wi-Fi signal propagation:

RSS(d) = RSS(d0) – 10 * a * log(d/d0),

where RSS(d) – Received Signal Strength, determined by the device at a distance d from the access point; RSS(d0) – signal strength measured at a distance d0 from the access point; a - coefficient taking into account the propagation of the Wi-Fi signal in the environment.

2. Modified k-nearest neighbors method. Determines the estimate of the location of the object as a weighted value of the center of mass of the figure - the centroid.

3. Naive Bayes classifier. Based on the application of Bayes' theorem. An estimate of the object's location

is obtained by determining the maximum of posterior probability of the object's location.

Both the simultaneous use of several positioning methods and the simultaneous use of several wireless technologies can serve as an improvement in the technical solution of the problem [3]. More about the latter: the solution to increase the efficiency of the positioning system can be the installation of additional stationary sources using BLE (Bluetooth Low Energy) wireless technology.

One of the problems that can be solved using Indoor navigation methods can be the improvement of the fire safety system indoors.

This system can help determine the number and location of people in the event of a fire in a building. This can be done as long as every person in the building has a Wi-Fi and/or Bluetooth enabled device. The simplest example of such a device is a smartphone that each of us uses in everyday life.

Data from the sensors to which people's devices are connected will be sent to the monitor to the fire safety operator, who will be able to see exactly where the devices are located, taking into account the possible error in the data received from the sensors. In addition, the system will allow you to display the number of devices connected to the sensors at the moment. The operator will be able to transfer all the collected data to the firefighters, who will be able to adjust their actions if necessary.

References

1. Falkov E. V., Romanov A. Y. The use of Beacon beacons and Bluetooth Low Energy technology for creating navigation systems in buildings // New information technologies in automated systems. 2015. №18. P. 62-65.

2. Filaretov G. F., Assur O. S. Development of an complex method for positioning objects based on data from Wi-Fi wireless networks and BLE (Bleutooth Low Energy) devices // News of the Institute of Engineering Physics. 2015. №2(36). P. 2-10.

3. International Conference on Indoor Positioning and Indoor Navigation [website]. URL: https://ipin-conference.org.

Sheshin M.S.

DEVELOPMENT AND IMPLEMENTATION OF A METHOD FOR VOICE COMMANDS RECOGNITION

[1]Far Eastern Federal University, Institute of Mathematics and Computer Technologies, FEFU
[2]Far Eastern Federal University, Oriental Institute School of Regional and International Studies, FEFU
Scientific adviser – I.L. Artemieva [1]
Consultant – M.S. Chusov, “Rhonda Software”
Scientific consultant - I.F. Veremeeva [2]

The most widely used and, really, the most convenient way for a person to exchange information is their voice, therefore, since the advent of human-machine interfaces, people have been dreaming about interacting with a computer using voice commands. However, many problems are associated with the implementation of this solution, such as the interdisciplinary nature of the preparation of the solution, which requires knowledge even from philology and linguistics; high computational complexity of already existing algorithms for processing voice commands, as well as very high standards for their accuracy. The need for convenient and accurate automatic speech recognition systems is felt in scientific, commercial and everyday areas of human activity [1].

Many already existing software solutions that implement voice command recognition algorithms for user interaction, such as Google Now or Yandex SpeechKit, have wide capabilities in terms of working with human speech, and the algorithms they implement are efficient and accurate.

However, they also have a number of disadvantages: first, because of a high computational complexity of

the implemented algorithms, it is not uncommon to encounter a truncated or completely inoperative functionality in the absence of Internet connection. Second, the scope of application of existing software solutions is very limited. Third, many solutions are corporate property, because of which they do not support cross-platform functionality, and are not free.

Three main categories can be distinguished among speech recognition methods: methods based on comparison with a standard; methods that perform the construction of decision functions, as well as methods based on hidden Markov models. Each of these implementation methods have their own strengths and weaknesses: methods of the first category are easy to implement, have good accuracy on noisy and low-quality input signals, but are very demanding on large amounts of data. Machine learning based methods are highly accurate but require a very large training set. Methods based on hidden Markov models work well with non-integral data, but are difficult to cope with large vocabularies of implementable recognizers [2].

Voice command recognition methods that are widely used in practice are based on machine learning [3]. The principle of building recognizers in this way is certainly effective, but gives rise to a number of specific problems, the solution of which seems possible only for large companies. The corporate ownership of currently existing solutions in the field of speech recognition is reflected not only in the secrecy of their implementation, but also, mainly, in the secrecy of the data with which the training set of recognition algorithms is built.

Considering all of the above, we can single out the following **problem**: the lack of a method for recognizing voice commands, which shows particular accuracy when working with small training samples, capable of working with hardware implementation without access to the Internet.

Therefore, the **goals of this work** are as follows: to use existing algorithms for recognizing voice commands to develop a recognition method that can work efficiently and accurately on a hardware basis without access to the Internet with dictionaries of 15-20 words, and to implement the developed algorithm.

References

1. Rabiner L.R. Introduction to Digital Speech Processing / L.R. Rabiner, R.W. Schafer. - M.: Radio and communication, 2008. - 469 p.

2. Sharma, D. Automatic speech recognition systems: Challenges and recent implementation trends // D. Sharma, J. Atkins - International Journal of Signal and Imaging Systems Engineering, 2014. - p. 16.

3. Sun, M. Amazon Alexa wake word - compressed time delay neural network, 2017. – URL: https://www.youtube.com/watch?v=Dk4bw3WaNts

---

Shutov K.S. [1]

CREATION OF A SOFTWARE AND HARDWARE PROTOTYPE OF AN UNMANNED SHIP WITH REMOTE CONTROL

[1]Far Eastern Federal University, Institute of Mathematics and Computer Technologies, FEFU
[2]Far Eastern Federal University, Oriental Institute School of Regional and International Studies, FEFU
Scientific adviser – V.M. Griniak [1]
Scientific consultant - I.F. Veremeeva [2]

Currently, the marine navy in the world is intensively developing in many areas, new modern ships are put into exploitation, several initiatives have already been implemented to equip water vehicles with autonomous navigation systems.

The subject of the research has a great practical significance for the development of shipping. Therefore, the introduction of a remote-control system for unmanned water vehicles is an urgent task today [1].

Presently, architectural solutions of software for controlling unmanned water vehicles have not been worked out, there are no well-established standard solutions. At the same time, remote control algorithms should provide a

reliable solution to the problems of controlling the movement of the ship for various purposes and control quality criteria. Exactly this opens up the perspective for innovation.

The purpose of this work is creation of a software and hardware prototype of an unmanned ship with remote control.

To implement the software and hardware prototype, the following communication systems will be required: GPS (Global Positioning System), which allows to determine the coordinates of the ship with high accuracy, and the global standard of digital mobile cellular communication GSM (Global System for Mobile Communications) [2].

Raspberry Pi 4 Linux-based miniature single-board computer was chosen as the equipment for remote control of the unmanned ship. The WebSocket protocol, designed for real-time messaging, will be used to send control commands, and monitor the status of the unmanned ship. The Redis message broker will also be used, which will solve the problem of synchronicity and sequence of requests sent to the board.

The functioning scheme of the developing remote control software system is shown in Figure 1.

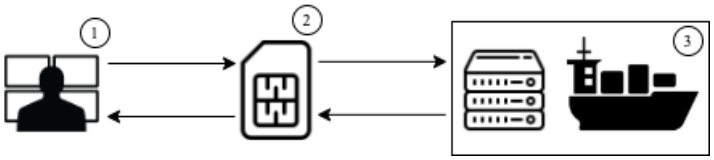

Fig. 3. The functioning scheme of the developing remote control software system

1 – Unmanned ship control center

2 – Communication system (GPS, GSM)

3 – Unmanned ship with remote control equipment

The practical application of the results of this research will allow water transport specialists engaged in the process of developing their own software systems to use a uniform approach at the stage of preparation of working and design documentation [3]. Thanks to this, the construction of ships will reach a new level.

References

1. Karetnikov V. V., Rudykh S. V., Butsanets A. A. On the issue of developing conceptual statements of technical fleet remote control system // Vestnik of Astrakhan State Technical University. Series: Marine engineering and technologies. 2019. – V. 2019. – № 2. – P. 7 – 15. – DOI: 10.24143/2073-1574-2019-2-7-15.

2. Bezrukikh A.G., Chenskiy A.G. Remote control and data collection based on GSM networks. // Vestnik IrGTU №11 (58) 2011. P. 186–189. – National Research Irkutsk State Technical University, Institute of Physics and Technology, Irkutsk.

3. Transport: Problems, goals, prospects (TRANSPORT 2020): Materials of the All-Russian Scientific and Technical Conference (Perm, February 15, 2020) / ed. by Candidate of Pedagogical Sciences, assoc. E.V. Chabanova – Perm: Perm branch of the FSUE PO «VGUVT », 2020. – 332 p.

Section V PHYSICS

V.R. Polishchuk [1], D.A. Saritsky [1], A.M. Ziatdinov [1]

ELECTRON PARAMAGNETIC RESONANCE OF ZINC FERRICYANIDE AND THEIR POLYETHYLENIMINE-BASED NANOCOMPOSITES

[1] Institute of Chemistry, Far Eastern Branch of Russian Academy of Science
[2] Far Eastern Federal University, Oriental Institute School of Regional and International Studies, FEFU
Scientific adviser – A.M. Ziatdinov[1]
Scientific consultant – I.N. Lazareva[2]

Transition metal ferricyanides attract increasing attention due to their potential applications in many areas of high technology, such as gas storage, catalysis, the development of molecular magnets, highly selective sorbents, etc. However, in many cases, they are used in practice only after immobilization in organic or inorganic matrices. For this reason, the study of changes in the physicochemical characteristics of ferricyanides during immobilization is an important and urgent problem [1, 2].

The objective of this work was to study by electron magnetic resonance (EMR) some spin states of zinc ferricyanide, with an emphasis on revealing changes in these states upon immobilization of zinc ferricyanide in polyethylenimine (PEI), as well as upon ultraviolet irradiation of the sample.

Electron magnetic resonance (EMR) spectra were recorded on a JES-X330 spectrometer in the X-range of operating frequencies (Institute of Chemistry, Far East Branch, Russian Academy of Sciences). Temperature-dependent measurements were carried out in a continuous flow of nitrogen gas using a standard variable temperature unit ES-13060 DVT5. The samples were irradiated with ultraviolet light using a standard ES-USH500 ultraviolet irradiation unit.

The experimental spectra were approximated using the «EasySpin» software package for simulation and analysis of EPR spectra written in the MATLAB programming language.

Fig.1 shows the EMR spectra of zinc ferricyanide at different temperatures. At room temperature, the EPR spectrum of $Zn_3[Fe(CN)_6]_2$ is dominated by a broad asymmetric resonance with a less intense resonance in its high-field wing. The effective g-factors of these resonances, determined from the low-field peaks of the first derivative of their absorption lines, are ~5.1 and ~3.2, respectively. As the temperature decreases, the peak intensity of the main resonance increases, the effective value of its g-factor decreases, and the smaller resonance merges with the main one and ceases to be observed. Under ultraviolet irradiation, the spectrum of the sample does not change.

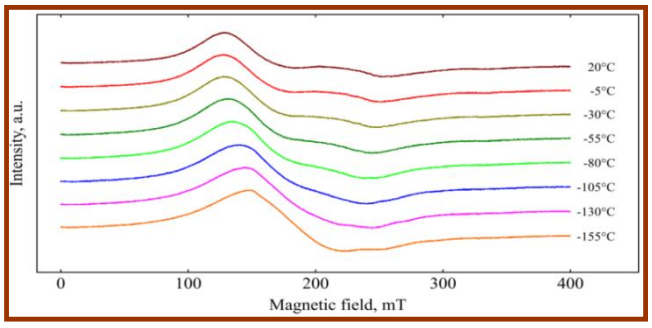

Fig.1. EMR spectra at different temperatures

Table 1

Spin Hamiltonian parameters of simulated EPR spectra

T , ° C	Component 1				Component 2			
	g_x	g_y	g_z	w, %	g_x	g_y	g_z	w, %
150	3.72	3.27	>1	42.8	2.77	2.59	>1	57.2
20	5.23	4.21	>1	52.1	3.7	2.89	>1	47.9
- 1 5 5	4.81	4.04	>1	51.8	3.89	3.6	>1	48.2

We tested two variants of approximation of the EMR spectra of zinc ferricyanide, assuming that they belong to 1) electron paramagnetic resonance (EPR) on ferric ions in the low-spin state and 2) electron ferromagnetic resonance (EFR) of magnetically ordered states of the same ion. Under the assumption that these spectra belong to

the paramagnetic ferric ions in the low-spin state ½, an acceptable approximation of the spectra at different temperatures is possible. The g-factor values for which the considered approximations were obtained are given in the Table 1. As you can see, some of them are noticeably larger than 3.2, which contradicts the data of theoretical calculations.

According to the calculations of J. Tesler et al., the effective value of the g-factors of ferric ions in the low-spin state in octahedral complexes with any distortion cannot exceed 4, and in the octahedral field the field of cyanide ligands cannot even exceed 3.2 [4]. These contradictions between the experimental and theoretical data led us to the idea of a different origin of the considered spectrum.

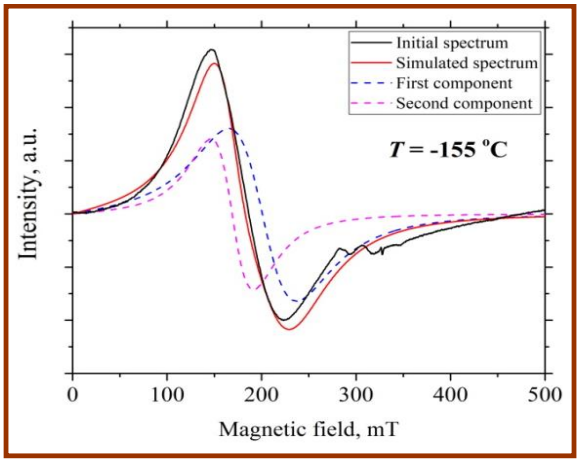

Fig.2. Result of the approximation of the EMR spectrum at -155 °C, assuming that it belongs to the electron ferromagnetic resonance

Fig.2 shows the results of the approximation of the EMR spectra at -155 °C, assuming that they belong to the electron ferromagnetic resonance (EFR). The advantages of this approach to spectrum analysis are not only acceptable quality of spectral approximations, but also the possibility of describing spectra in low magnetic fields in the absence of their significant temperature dependence.

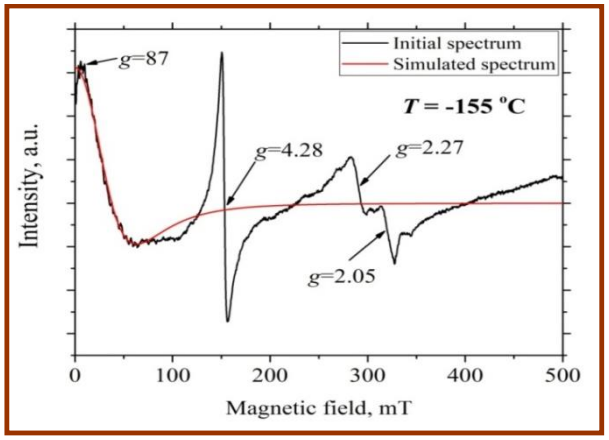

Fig.3. Result of the approximation of the EMR spectrum of a nanocomposite of zinc ferricyanide with PEI at -155 °C

Fig.3 shows the result of the approximation of the EMR spectrum of a nanocomposite at -155 °C. The spectrum of this nanocomposite at all temperatures contains: a wide asymmetric resonance with an effective g-factor of about 85; narrow asymmetric resonance with a g-factor of about 4.36; and an unresolved spectrum, the most intense components of which are characterized by g-factors of 2.26 and 2.05.

The shape and anomalously large value of the g-factor of the low-field absorption peak are characteristic of ferromagnetic materials. Resonances with g-factors of 4.28 and 2.27 belong to single ferric iron ions in the high-spin state, which are exposed to crystal fields with strong rhombic distortion [5]. The resonance with a g factor of 2.05 presumably belongs to single divalent copper ions, which are uncontrollably introduced into the sample during synthesis with one of the precursors.

The presence in the EMR spectrum of the zinc ferricyanide nanocomposite with PEI of resonances on

paramagnetic ferric ions in the high-spin state indicates a change in the electronic structure of the surface layers of zinc ferricyanide due to the interaction with PEI.

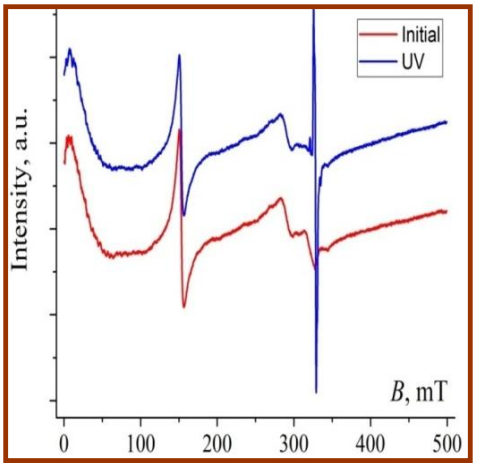

Fig.4. Changes in the EMR spectrum of a nanocomposite of zinc ferricyanide with PEI when it is irradiated with ultraviolet light

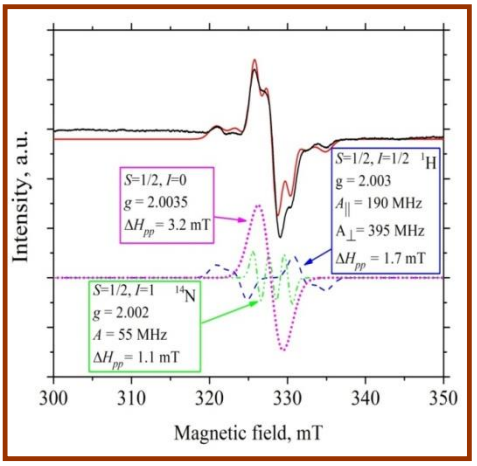

Fig.5. Approximation of the part of the EMR spectrum of a nanocomposite of zinc ferricyanide with PEI, which occurs upon ultraviolet irradiation of the sample

Fig.4 shows the changes in the EMR spectrum of a nanocomposite when it is irradiated with ultraviolet light. Under the influence of ultraviolet irradiation, a group of closely spaced resonances appears in the spectrum of the zinc ferricyanide nanocomposite with PEI, the most intense of which is characterized by a g-factor value of 2.003. The time of relaxation of these resonances after turning off the irradiation depends both on the time of illumination of the sample with ultraviolet light and on the chosen temperature for studying the spectrum reconstruction process.

Fig.5 shows an approximation of the part of the EMR spectrum of a nanocomposite, which occurs upon ultraviolet irradiation of the sample. The spectrum can be decomposed into three groups of lines: 1) a group of two lines whose contours are distorted due to the anisotropy of the hyperfine interaction, 2) a group of three equidistant undistorted lines, and 3) a single line with g-factor 2.0035.

Taking into account the absence of the influence of ultraviolet irradiation on the EMR spectra of zinc ferricyanide and PEI, it can be assumed that the UV-sensitive regions of PEI are formed in the regions adjacent to the surface of zinc ferricyanide, and their appearance there is somehow associated with the transition of a part of the near-surface low-spin ferric ions to the high-spin state.

Changes in the bulk magnetic characteristics of zinc ferricyanide nanoparticles upon their immobilization in PEI were found. A transition from a low-spin to a high-spin state was revealed during the immobilization of zinc ferricyanide of some ferric iron ions in near-surface rhombically distorted cyanide complexes.

The authors are grateful to Corresponding Member of the RAS S.Yu. Bratskaya for providing samples for research, to D.V. Balatskiy and I.A. Malakhova for the synthesis of $Zn_3[Fe(CN)_6]_2$ and PEI/$Zn_3[Fe(CN)_6]_2$, to N.S. Saenko for recording some EMR spectra.

References:

1. Stepanov I. K., Muratov O. E., Ignatov A. A. et al. [Composite Material for Immobilization of Liquid Radioactive Waste, and its Application Method]; publication date: 27.05.2013.
2. D. Gatteschi, R. Sessoli. Angew. Chem., Int. Ed. 42(2003)268.
3. J. Telser. J. Braz. Chem. Soc. 2006. V. 17. P. 1501
4. Kokorin, R. Amal, W.Y. Teoh, A.I. Kulak. App. Magn. Reson. (2017) 447

Rivas Velasquez D.A.[1]

NITROGEN-CONTAINING COMPOUNDS (METHYLAMINES AND ALLYLAMINES)

[1]Far Eastern Federal University, Institute of High Technologies and Advance Materials,
[2] Far Eastern Federal University, Oriental Institute, School of Regional and International Studies, FEFU
Scientific adviser – Dr. V.I. Vovna [1]
Scientific consultant – I.S. Os'mushko[1]
Linguistic consultant -I. N Lazareva [2]

Organic ammonia derivatives have a wide variety of uses in the medical, agricultural and textile dyeing industries. Experimentation and processing of these compounds are difficult, as most of them are classified as highly toxic with a level 3 Health hazard in the NFPA system. The internal electronic structure of these derivatives has interesting characteristics that connect the compound's shape and the electron-electron interactions with other ligands, requiring very complex theoretical models to predict physical characteristics at the micro and macro scale. For our study, we collected data from Nitrogen containing compounds and their derivatives, so that we can compare them with experimental PES (Photo-Emission Spectra in liquid and gas phase).

In this work, the results of quantical-chemical calculations of molecular monomers models [1] were analyzed, in the approximation DFT/B3LYP using the quantum-chemistry package Gamess (US) (2019.R1.P1.mkl) [2], normal coordinates were used in relation to the central Nitrogen atom as a basis.

Six compounds with interesting geometrical and electrical characteristics were selected for this initial phase of study:

Methylamine (NH_2Me), Di-Methylamine ($NHMe_2$), Tri-methylamine (NMe_3), Allylamine ($NH_2-(CH_2-CH=CH_2)$), Di-Allylamine ($NH-(CH_2-CH=CH_2)_2$), Tri-Allylamine ($N(CH_2-CH=CH_2)_3$).

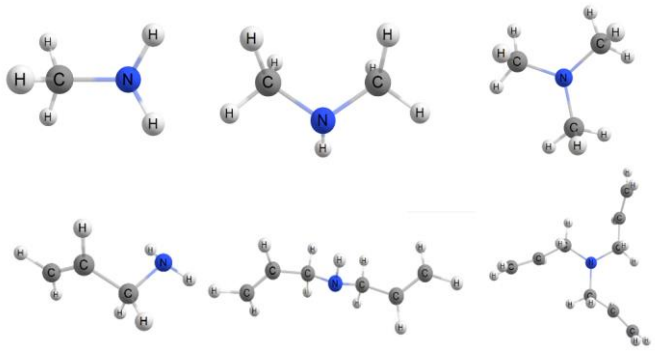

Fig 4. Molecular models of Methylamines and Allylamines after optimization

Molecular orbitals (MO) constructed by several atomic orbitals can be represented by an iso-surface, created from electron density data, calculated in Gamess (US). In virtue of conserving space, we only attached the data for methylamine. The results are as follow:

Methylamine				
	Iв [eV]	MO		I Theo [-eV]
1	9,66	5a'	N(n)	9,58
2	13,11	2a''	CH	13,92
3	14,35	4a'	NC	14,62
4	15,46	3a'	CH	15,94
5	16,89	1a''	NH	17,38
6	21,8	2a'	C 2s	24,17
7	27,6	1a'	N 2s	30,89

Table 1 – Comparation between Experimental and Theoretical data of Principal Energetical states of methylamine. (I_B − vertical ionization potential MO's, Experimental) (I_{Theory} − Ionization energy MO's, Theoretical)

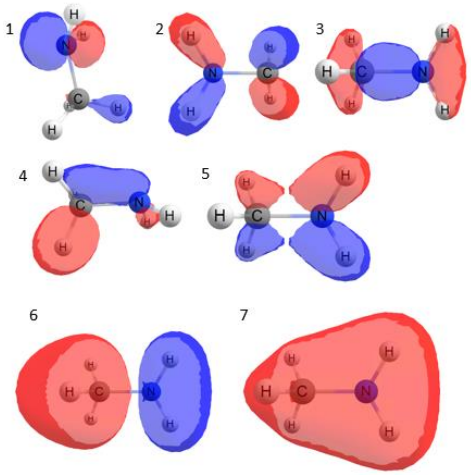

Fig 2 – Theoretical representation of the MO iso-surface corresponding to Table 1
(Red: Bonding MO, Blue: Anti-Bonding MO)

Post-optimization, the ionization energies for each MO are very close to their experimental counterparts, although we can see the value starts to diverge in the external shells of the molecule $(NH,\ \Delta = 0.49 \rightarrow C\ (2s),\ \Delta = 2.37 \rightarrow N\ (2s),\ \Delta = 3.29)$, this is due to the one-molecule approximation used for these calculations, where in the experimental part; millions of molecules occupy a very small space, making their external shells interact with one another, therefore lowering their energy states.

Comparing the data for the methylamines, we can observe that the Ionization energy of the first main MO (N(n)) decreases with the addition of each methyl-ligand $(CH_3)_n$. A similar phenomenon was observed before with formaldehydes and n-amines when adding the methyl-ligand $(CH_2)_n$ in consecutive chains (Fig 3. a) [1].

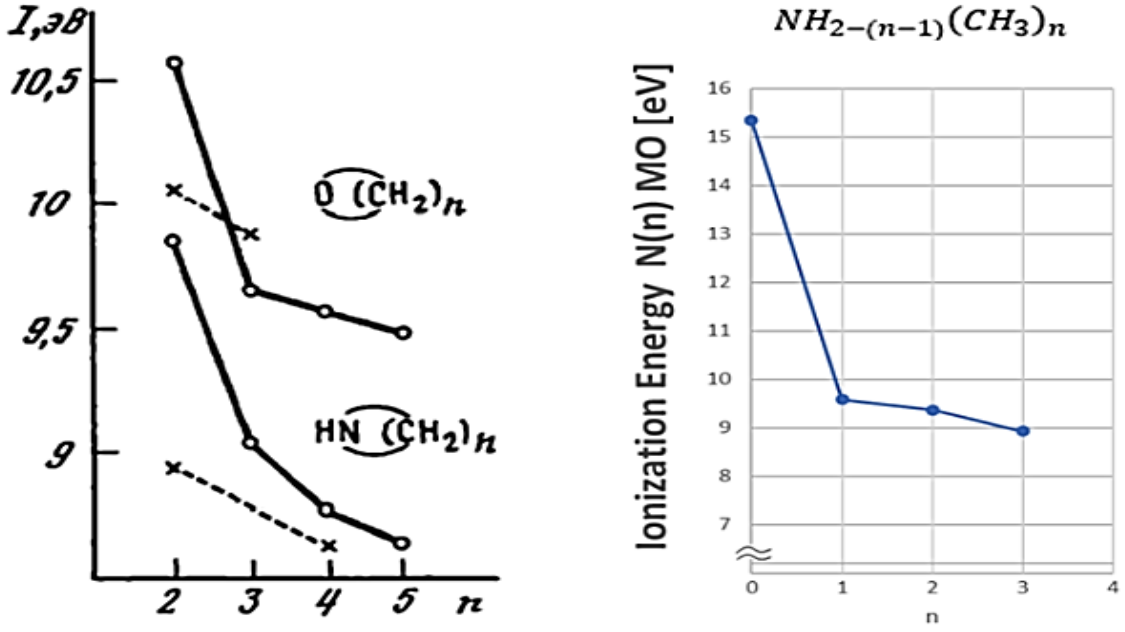

a) b)

Fig 3 – a) Ionization energy of N(n) and O(n) MO in formaldehydes (O=$(CH)_n$) and n-amines (H-N = $(CH_2)_n$) $n \epsilon 2 \div 5$, The dashed lines show the change of I in open-chain compounds [1]
b) Ionization energy of N(n) MO in methylamines $\left(NH_{2-(n-1)}(CH_3)_n\right)$ $n \epsilon 0 \div 3$

Here it is possible to conclude that the binding energy of the central Nitrogen atom with the surrounding methyl's is affected by the addition of said ligands, lowering the energy necessary to ionize in these internal shells of the molecule. Meanwhile there is a necessity of a bigger study of similar molecules to bind these phenomena together.

References

1. Vovna, V.I. Электронная Структура Органических Соединениями по данным фотоэлектронной спектроскопии (Electric Structure of Organical Compounds from Photo-Emission Spectra), Moscow “NAUKA”, 7, 115–114 (1991).

2. Barca, Giuseppe M. J. and Bertoni, Colleen and Carrington, Laura and Datta, Dipayan and De Silva, Nuwan and Deustua, J. Emiliano and Fedorov, Dmitri G. and Gour, Jeffrey R. and Gunina, Anastasia O. and Guidez, Emilie and Harville, Taylor and Irle, Stephan and Ivanic, Joe and Kowalski, Karol and Leang, Sarom S. and Li, Hui and Li, Wei and Lutz, Jesse J. and Magoulas, Ilias and Mato, Joani and Mironov, Vladimir and Nakata, Hiroya and Pham, Buu Q. and Piecuch, Piotr and Poole, David and Pruitt, Spencer R. and Rendell, Alistair P. and Roskop, Luke B. and Ruedenberg, Klaus and Sattasathuchana, Tosaporn and Schmidt, Michael W. and Shen, Jun and Slipchenko, Lyudmila and Sosonkina, Masha and Sundriyal, Vaibhav and Tiwari, Ananta and Galvez Vallejo, Jorge L. and Westheimer, Bryce and Wloch, Marta and Xu, Peng and Zahariev, Federico and Gordon, Mark S. GAMESS & Recent developments in the general atomic and molecular electronic structure system // The Journal of Chemical Physics (2020) p. 154102 DOI:10.1063/5.0005188 https://www.msg.chem.iastate.edu/gamess, https://aip.scitation.org/doi/10.1063/5.0005188.

Podlesnykh A.A.[1]

UNDEGROUND MINE TESTS OF MACH-ZENDER INTERFEROMETRIC STRAINMETER

[1]Far Eastern federal university, Institute of Hight Technologies and Advanced Materials
[2]Institute of Automation and Control Processes, Vladivostok
[3] Far Eastern Federal University, Oriental Institute, School of Regional and International Studies, FEFU
Scientific adviser – O. T. Kamenev[2]
Scientific consultant - Yu. S. Petrov[2]
Linguistic consultant -I. N Lazareva [3]

Fiber-optic interferometric sensors are compact, have high sensitivity, and are capable of stable operation for a long time under adverse conditions. They are used in hydroacoustics, geophysics, for short-term and long-term observation of large-scale structures such as high buildings, bridges, dams, tunnels, mines [1].

To register seismic vibrations by the strainmeter, a scheme of a fiber-optic Mach-Zehnder interferometer with a 3x3 splitter was used. The advantages of this circuit are compactness, immunity to electromagnetic interference, high sensitivity and a large dynamic range of the received signal [2]

Multi-turn optical-mechanical converter (MOC) is used as a sensitive element of the strainmeter. MOC is integrated into the measuring arm of the Mach-Zehnder interferometer (optical fiber wound on cylinders 6 and 9). (Fig. 1). The data obtained from the fiber optic strainmeter were processed using the algorithm described in [3].

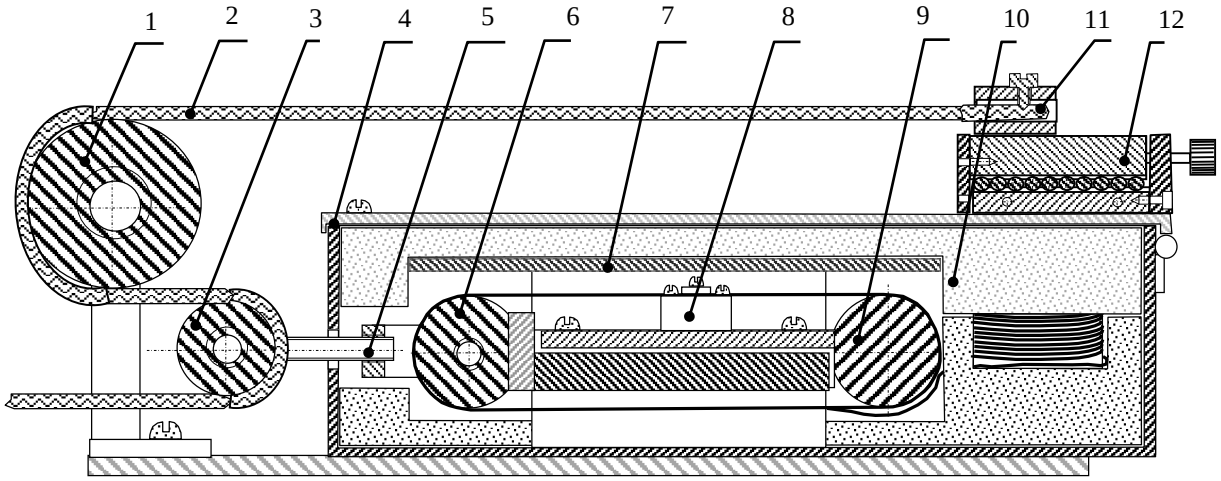

Fig.1 - Drawing of an optoelectronic strainmeter

1 - pulley 1; 2 - cable; 3 - pulley 2; 4 - casing; 5 - p-shaped bracket and rod; 6 - movable cylinder of the fiber optic coil; 7 - protective plate; 8 - fiber clamp; 9 - cylinder connected to the body; 10 - foam filling; 11 - cable fastening; 12 – optical translator.

Performing an initial calibration is necessary to determine the MOC conversion factor (from radians to meters), which cannot be predetermined. With a measuring length of the strainmeter of 10 m, the parameters of the cable-MOC system begin to depend on the tension force, which is set when the strainmeter is deployed at the installation site. Also, the data processing algorithm needs to determine the direction of change in the phase difference corresponding to the strain increment. Figure 2 shows the calibration strain Δl = 500 μm, the corresponding phase increment is $\Delta\varphi$ = 820 rad. Thus, the MOC conversion factor is $\Delta l/\Delta\varphi$ = 0.61 μm/rad. All subsequent data were recorded taking into account this coefficient in micrometers.

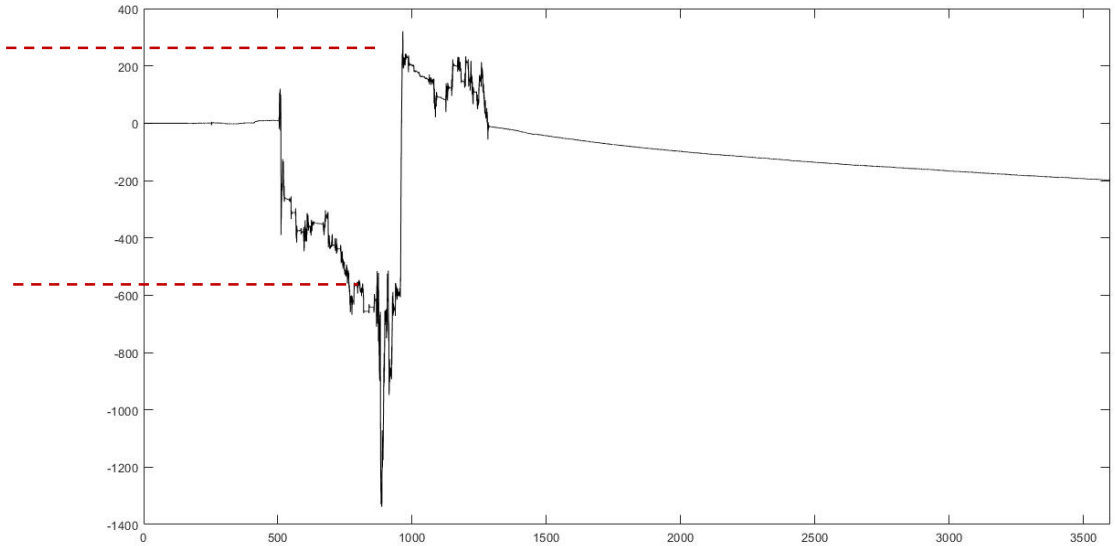

Fig.2 Calibration

Red lines indicate corresponding to 500 μm strain phase difference

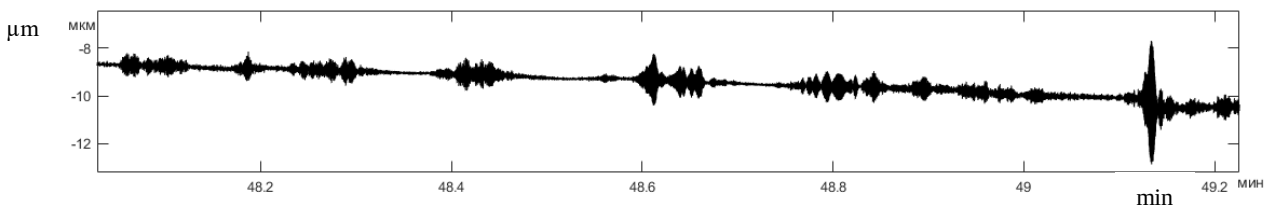

Fig.3 The signal recorded by the strainmeter at the mine when deformation processes occur in the rock

The analysis of the obtained experimental results made it possible to estimate the threshold sensitivity of the strainmeter, which corresponded to the noise level in the range of 500 ... 1000 Hz 0.3 nm, the calculated threshold sensitivity of 1 nm was confirmed.

References

1. Inaudi, D., Elamarib A., Pflug L. // Sensors and Actuators A. – 1994. - V. 44. - P. 125-130.
2. Kulchin Yu. N. , Kamenev O.T., et al. // Vestnik of Far Eastern Branch of Russian Academy of Sciences. - 2016. - № 4. - C 56-59
3. Her, S.-C.,. Yang C.-M., // Sensors. 2012. V. 12(3). P 3314-3326.

Esenkin I. S. [1].

EXPERIMENTAL ENERGY SOURCE. EARTH BATTERY

[1]Far Eastern Federal University, School of Natural Sciences, FEFU
[2]Far Eastern Federal University, Oriental Institute, School of Regional and International Studies, FEFU
Scientific adviser - P.L.Titov [1]
Scientific consultant - I.N. Lazareva[2]

An earth galvanic cell consisting of various metals works due to the difference in their electrical properties in the ground. As the materials used for the "plus" electrode, coal, copper can be used, while the "minus" electrode uses zinc, aluminum, iron, and zinc. When choosing materials for the battery, you can use a number of redox potentials(Table 1)

Depending on the alkaline-acid balance and the depth of the electrodes in the green environment, the resulting voltage, current strength and power at the electrodes also depend. To make the chemical reaction better, water is used.

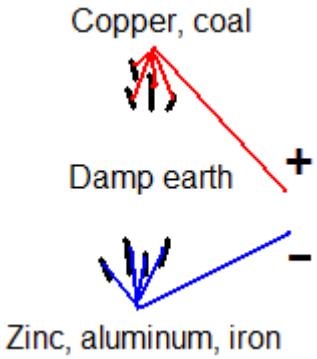

Fig 1. Construction of an "earthen" electric batteryand

The service life of this batteryи is about 2-3 years. The negative electrode is gradually destroyed by corrosion (if it is metal) or dissolved (in the case of using soluble materials, such as coal). The greatest power from one element can be obtained at a current consumption of 1-5 mA, while the voltage is tenths of a volt

Table 1

Metal stress series (electrochemical series of standard redox potentials)

Mettal (chem.designation)	Voltage (V)
Al (Aluminum)	-1.66
Fe (Iron, steel)	-0.4
Cu (Copper)	+0.34
S (Graphite, coal, wood ash)	+0.4
Au (Gold)	+1.50

Both electrodes are placed in moist soil, which plays the role of the electrolyte of the galvanic cell, to a depth of 1-2 m (below the depth of freezing of the soil in winter for this area). Depth is important if you plan to use the battery all year round.

The most suitable electroplating pairs: copper, coal are used as the positive electrode, and zinc, aluminum, and iron (including galvanized) are used as the negative electrode. The terminal of the negative electrode is isolated from the ground.

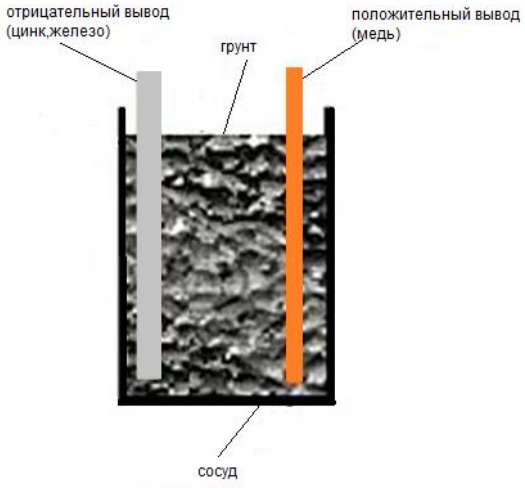

Fig 2.. Scheme of the "earthen" batteryand

To obtain a voltage of the order of several volts, batteries are assembled from series-connected elements (Fig. 3). To increase the current, increase the area of the electrodes, use a parallel connection of elements, and also water the elements with water.

The positive electrode (copper/carbon, must be deeper than the southern one) is located at the northern point (if the line is oriented along the magnetic meridian), the negative one is located to the south

Usually, in practice, a combined, series-parallel connection of elements is used, which is sufficient to power, for example, a radio receiver

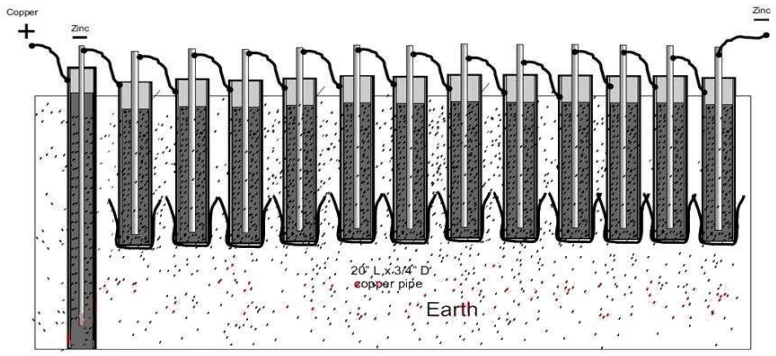

Fig. 3. Connecting serial batteries to produce 12 volts

When the distance between the electrodes changes, the voltage changes at the source poles are not recorded.

Table 2. Investigation of the dependence of the voltage at the source poles and the current strength in the circuit on the size of the electrodes

Table 3

Investigation of the dependence of the current in the circuit and the voltage at the source poles on the type of electrodes

Distance between electrodes, d(mm)	Pole voltage, U(B)	Current I(mA)
80mm	0.7 V	2mA
45mm	0.7 V	3.5 mA
20mm	0.7 V	5.5 mA
10mm	0.7 V	7.5 mA

Electrodes	Pole voltage, U(B)	Current I(mA)
Zinc-copper	0.7 V	3mA
Copper-Aluminum	0.4 V	1.5 mA
Zinc-Aluminum	0.3 V	0.5 mA
Copper-Lead	0.3 V	1mA
Zinc-Lead	0.5 V	3mA

The voltage at the source poles and the current strength in the circuit depend on the substance from which the electrodes are made.

References

1. Nathan's Earth BatteryStablefield [Electronic resource].2020. URL: http://electrik.info/main/fakty/942-zemlyanaya-batareya-stablfilda.html (Accessed on 20.03.2022).

2. Free electrical energy. Earth battery [Electronic resource]. 2020. URL: https://www.kakras.ru/mobile/electropotential-earth-batteries.html (Accessed on 19.03.2022).

Lisovitckii A.S.[1], Moskovchenko L. G.[1]

FRACTAL ANALYSIS OF THE EARTH CRUST MICROSTRAIN DATA OBTAINED WITH CLASSICAL LASER STRAINMETERS

[1]Far Eastern Federal University, Institute of High Technologies and Advanced Materials, FEFU
[2]Far Eastern Federal University, Oriental Institute, School of Regional and International Studies, FEFU
Scientific adviser - L.G. Moskovchenko[1]
Scientific consultant - I.N. Lazareva[2]

Our aim is to study the fractal dimension of microstrain data of the Earth's crust, recorded by laser strainmeters in a seismically quiet period and in active period, and calculate the fractal dimension of this system with the Higuchi methods of fractal analysis. After evaluating the fractal dimension of the time series, it is possible to analyze the evolution of this characteristic in a calm and active period and draw conclusions.

The time series of microstains of the earth's crust were studied, since they reflect a characteristic feature of the earth's crust - fractality, when parts of an object are similar to the whole. The study of fractal characteristics based on the fact that the earth's crust has evolved to the state of self-organized criticality, that is a stable state characterized by fractality.

The data were taken from three strainmeters operated by the Pacific Oceanological Institute of V.I. Ilyichev located at the Cape Schulz test site during the quiet period 01/01/2021-01/31/2021 and the active period 01/01/2022-03/14/2022 (the fractal dimension was calculated for each day of both periods). An earthquake with a magnitude of more than 7.0 was registered in March [2]. The schemes of strainmeters are based on the Michelson interferometer, which measures the path difference between the reference and measurement arms. The location of the strainmeters is as follows: the first of them is oriented in the North-South direction, the second in the West-East direction, the third is similar to the first. The obtained data were processed by the decimation procedure, and then they underwent a special filtering to remove device resets.

The fractal length method belongs to the group of fractal analysis methods based on measuring the length of a fractal curve. In the implementation method proposed by T. Higuchi, for each δ, the calculation of L(δ) is performed δ times, that is, from a finite set of observations X(1),X(2),X(3),…,X(N) conducted with a specific interval, first form a new time series Xmk, defined as follows: X(m),X(m+k), X(m+2k),…, X(m+k[{N-m}/k]), m=1,2,…,k. For each Xmk, the length of the curve was determined by the formula:

$$L_m(k) = \left\{ \left(\sum_{i=1}^{\left[\frac{N-m}{k}\right]} |X(m+ik) - X(m+(i-1)\cdot k)| \right) \frac{N-1}{\left[\frac{N-m}{k}\right]\cdot k} \right\} \Big/ k$$

N is the number of points, m is the initial offset, k is the scale (time interval). Finally, the length of the curve for the time interval k is defined as the arithmetic mean.

$$\langle L(k) \rangle = \frac{\sum_{m=1}^{k} L_m(k)}{k}$$

The length of the curve is defined as the arithmetic mean over k points, each of which is equal to Lm(k). We average <L(δ)> over all m and plot log<L(δ)> as a function of log(m). Then we approximate this plot with a straight line using the least squares method. The slope angle tangent gives us the value of the fractal dimension according to the Higuchi method (Fig. 1.).

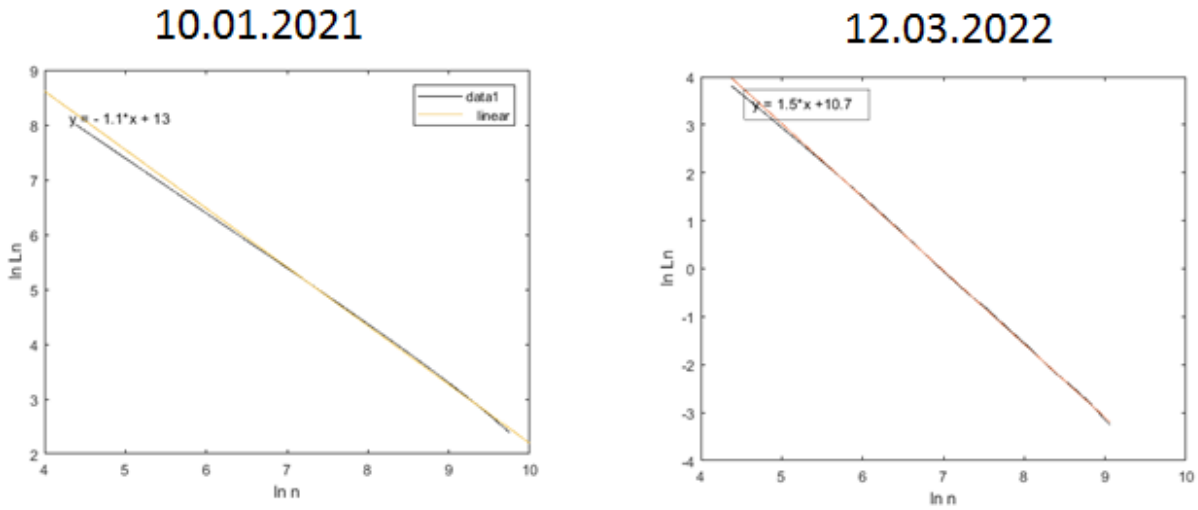

Fig. 1. Comparison of the fractal characteristics of time series in a quiet period and an active period for the second strainmeter

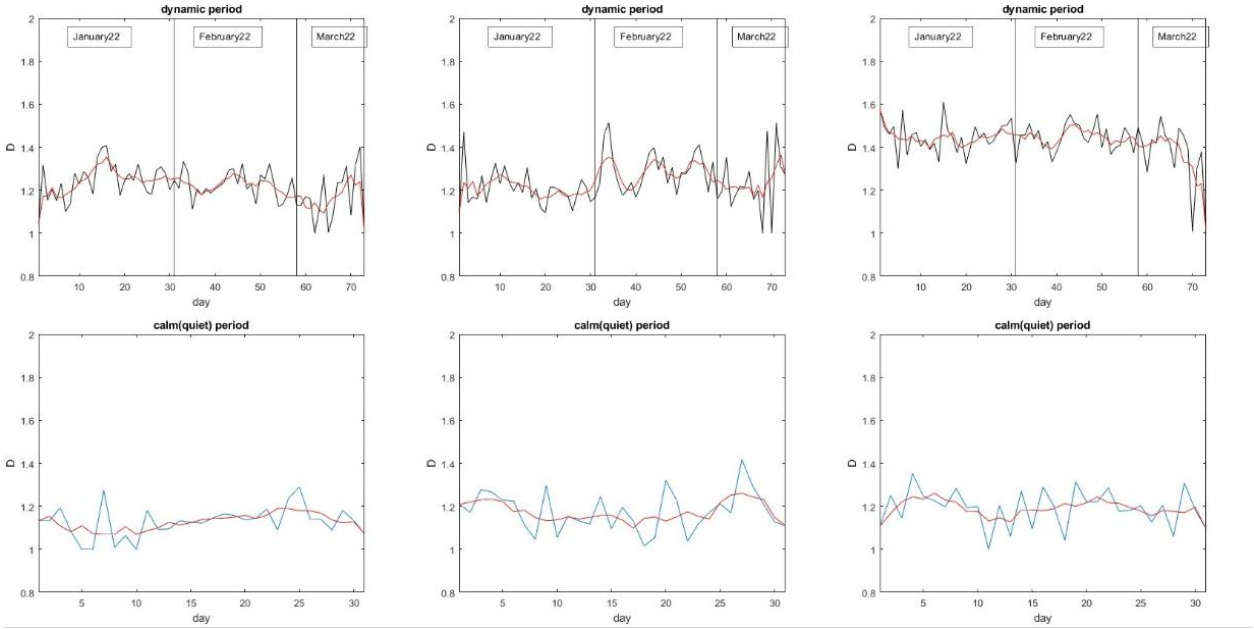

Fig. 2. Fractal characteristics of time series for all devices in a quiet and active period (1st column - the first strainmeter, 2nd column - the second strainmeter, 3rd column - the second strainmeter)

Thus, it can be seen that (Fig. 2.) in the active period, the evolution of the fractal dimension has greater variability and sharp jumps than in the quiet period.

References

1. Krylov S.S., Bobrov N. Yu. Fractals in geophysics /Krylov S.S., Bobrov N.Yu. - SPb .: Publishing house of St. Petersburg University, 2004. 132 p
2. Dolgikh, G.I., Privalov, V.E. Laser Physics. Basic and Applied research. – Vladivostok: Reya, 2016. 352p

---

Saritsky D.A.[1], Ziatdinov A.M.[1], Opra D.P.[1], Sokolov A.A.[1], Sinebryukhov S.L.[1], Gnedenkov S.V.[1]

ELECTRONIC PARAMAGNETIC RESONANCE ON MANGANESE IONS IN NANOCRYSTALLINE TITANIUM DIOXIDE SYNTHESIZED UNDER HYDROTHERMAL CONDITIONS

[1]Institute of Chemistry, Far Eastern Branch of the Russian Academy of Sciences
[2] Far Eastern Federal University, Oriental Institute School of Regional and International Studies, FEFU
Scientific adviser – A.M. Ziatdinov[1]
Scientific consultant – I.N. Lazareva[2]

Titanium dioxide (TiO_2) possesses many desirable properties (chemical stability, high photocatalytic activity, ferromagnetism, etc.) and for this reason, it is one of the most attractive objects for today's research. Highly dispersed and nanosized materials based on TiO_2 are of particular interest due to the unique properties that distinguish them favorably from micro and macro-sized analogs. The physicochemical properties of titanium dioxide can be changed by alloying them with various impurities. In this way, it is possible to obtain a semiconductor material that has both photocatalytic and ferromagnetic properties at the same time (so-called magnetic photocatalyst) [1, 2].

This paper presents the results of electron paramagnetic resonance (EPR) studies of some aspects of nanosized TiO_2 powders structure and spin states in the form of anatase doped with manganese ions (hereinafter TiO_2:Mn). The samples were prepared by a one-step method under hydrothermal conditions. [3].

The EPR spectra of TiO2(B):Mn powders were recorded on a JES-X330 instrument (JEOL, Japan) in the X-band of work frequencies. The power of the microwave field during the recording of the spectra was 2.00 mW. The applied magnetic field (B) was deployed in the ranges of 0–500 mT and modulated at a frequency of 100 kHz. Temperature-dependent measurements were carried out in a continuous flow of nitrogen gas using a standard variable temperature unit ES-13060 DVT5 (JEOL, Japan). The integral intensities and g-factors of the EPR lines were calibrated, respectively, by the integral intensity and the value g=2.002293±0.000003 of the spin resonance signal at the conduction electrons of Li nanoparticles in the reference LiF:Li sample, which does not change in the range from 2 to 400 K [4].

The experimental spectra were approximated using the EasySpin – software package for simulation and analysis of EPR spectra written in the MATLAB language.

Figure 1 shows the EPR spectra of the TiO_2:Mn powder in the X-band at different temperatures. It can be seen that the spectrum is dominated by an intense broad line with the value of the spectroscopic splitting factor $g \sim 2.00$. A low-intensity sextet structure emerges on its weak-field wing. The center of this sextet is shifted relative to the center of the main component of the spectrum towards lower magnetic field values by ΔB = 22.1 mT. The average peak-to-peak interval of the sextet is 7.2 mT.

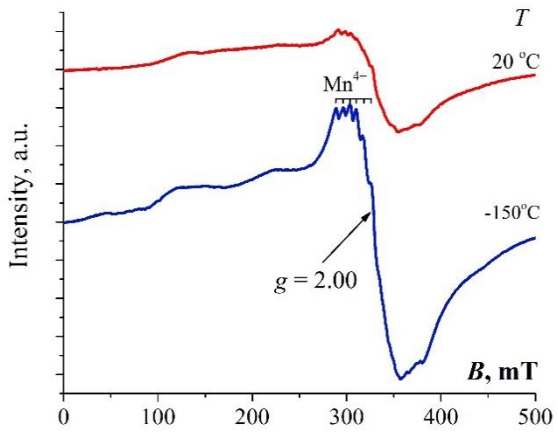

Fig. 1. EPR powder spectra of TiO_2:Mn at various temperatures. The X-band

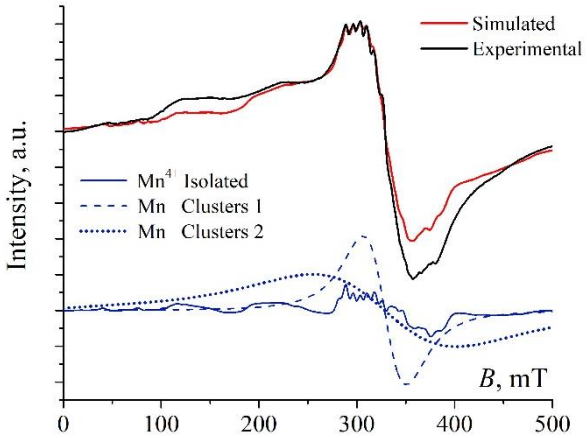

Fig. 2. Experimental and simulated EPR powder spectra of TiO_2:Mn at -150 °C

Naturally occurring manganese is an almost practically isotopically-pure element and consists of the only stable isotope Mn with nuclear spin I=5/2. Therefore, the sextet structure observed in the low-field wing of the main component of the EPR spectra of the TiO_2:Mn powder should be considered a hyperfine structure of paramagnetic resonance on the ions of this element. In principle, impurity manganese ions in TiO_2(B) can exist in three paramagnetic oxidation states: Mn^{2+} ($3d^5$, S = 5/2, I = 5/2), Mn^{3+} ($3d^4$, S = 2, I = 5/2) and Mn^{4+} ($3d^3$, S = 3/2, I = 5/2). However, only the first and last of them in solids at room temperature have sufficiently long spin-lattice relaxation times to allow them to observe paramagnetic resonance. [5]. Consequently, the sextet structure observed in the low-field wing of the main component of the spectra of these samples belongs to one of these ions. The peak-to-peak interval of the sextet structure, 7.2 mT, under consideration is close to the value of the hyperfine structure constants of the EPR spectrum of Mn^{4+} in TiO_2 [6] and the oxygen octahedra of other compounds. [7, 8]. The discrepancy between the centers of the sextet structure under discussion and the main component of the EPR spectra of TiO_2:Mn powders indicates the splitting of the electronic spin energy levels of Mn^{4+} in a zero magnetic field (i.e., for the presence of a fine structure).

To estimate the fine structure parameters of the EPR spectra of TiO_2:Mn powders, we calculated the EPR spectrum of the Mn^{4+} ion in an octahedral crystal field and averaged it over all possible orientations of powder particles. The spin Hamiltonian in the calculations had the following form:

$$\hat{H}=g\beta(\vec{B},\vec{S})+D\left(\hat{S}_z^2-\frac{S(S+1)}{3}\right)+E\left(\hat{S}_x^2-\hat{S}_y^2\right)+A(\vec{I},\vec{S}) \quad (1)$$

where: β is the Bohr magneton,
$\vec{B}$ is the applied magnetic field,
g is the spectroscopic splitting factor,
$\vec{S}$ is the vector of the spin angular momentum of the system,
$\hat{S}_x$, $\hat{S}_y$ and $\hat{S}_z$ – spin angular momentum operators along the x, y, and z axes, respectively, S is the spin value,
D and E – axial and rhombic components of the crystal field,
$\vec{I}$ – nuclear spin angular momentum vector,
A – is the constant of hyperfine structure (HFS).

The parameters were varied manually. The calculation results are shown in Figure 2. When approximating the spectra, two broad components with the Voigt line shape were also considered. As a result of the approximation, we obtained the following parameters of the spin Hamiltonian (1): g=1.996, A=7.49 mT, D=98.8 mT, and E=9.67 mT.

A comparison of the experimental and calculated spectra allows us to conclude that the EPR spectra in the studied TiO_2: Mn powders belong to Mn^{4+} ions located in crystal fields with weak rhombic distortion. The presence of broad components in the EPR spectrum indicates the presence of manganese ion clusters of various sizes, which

can be located both on the surface of TiO_2 nanoparticles and in their bulk.

References

1. K.C. Nguyen. Magnetic Ni-doped TiO_2 Photocatalysts for Disinfection of Escherichia coli Bacteria / K.C. Nguyen, N.M. Nguyen, Duong, K.V. Nguyen, H.M. Nguyen, Dao, Q. Nguyen, D.A. Nguyen, Vu, Dang, Phan. // J. Electron. Mater. – 2021. – Vol. 50, № 4. – P. 1942-1948.

2. Z. He. A magnetic TiO_2 photocatalyst doped with iodine for organic pollutant degradation / Z. He, T. Hong, J. Chen, S. Song. – // Sep. Purif. Technol.. – 2012. – Vol. 96, № 21. – P. 50-57

3. В.В. Железнов. Магнитные фотокатализаторы на основе нанодисперсного диоксида титана легированного in situ марганцем в гидротермальных условиях / В.В. Железнов, Д.П. Опра, И.А. Ткаченко, М.С. Васильева, А.М. Зиатдинов, Д.А. Сарицкий, В.Г. Курявый, С.В. Гнеденков – ЖНХ. – 2022. In print.

4. F.G. Cherkasov. Electron paramagnetic resonance measurement of static magnetic susceptibility / F.G. Cherkasov, I.V. Ovchinnikov, A.N. Turanov, S.G. L'vov, V.A. Goncharov, A.Ya Vitols. – DOI 10.1063/1.593350 // Low Temp. Phys. – 1997. – Vol. 23, № 2. – P. 174-176.

5. Weil J. Electron Paramagnetic Resonance: Elementary Theory and Practical Applications. Second edition / Weil J., Bolton J.R. – New Jersey: Wiley_Inter., – 2007. – 688 pp.

6. Miyamoto N.S. Evaluation of coexistent metal ions with TiO_2: an EPR approach. / Miyamoto N.S., Miyamoto R., Giamello E., Kurisaki T., Wakita H. / Res. Chem. Intermed. – 2018. – Vol. 44, № 7. – P. 4563–4575.

7. Muller K.A. Electron paramagnetic resonance of manganese IV in $SrTiO_3$ / Muller K.A. – DOI 10.1103/physrevlett.2.341 // Phys. Rev. Lett. – 1959. – Vol. 2, № 8. – P. 341-343.

8. Serway R.A. Electron paramagnetic resonance of three manganese centers in reduced $SrTiO_3$ / Serway R.A., Berlinger W., Muller K.A., Collins R.W. // Phys. Rev. B. – 1977. – Vol. 16, № 11. – P. 4761-4768.

Pochinok A.S.[1]

PHASE TRANSITION ON A FERROMAGNETIC SPHERICAL FIBONACCI LATTICE

[1]Far Eastern Federal University, Institute of High Technologies and Advanced Materials, FEFU
[2]Far Eastern Federal University, Institute of Life Sciences and Biomedicine, FEFU
[3] Far Eastern Federal University, Oriental Institute School of Regional and International Studies, FEFU
Scientific adviser – A.V. Molochkov [2]
Scientific consultant – I.N. Lazareva[3]

The study of phase transitions on lattices with spherical symmetry and natural curvature is an urgent task for astrophysics, physics of nanomaterials, etc. The main problem of spherical lattices is the uniformity of the distribution of sites.

As a solution to this problem, the work uses the Fibonacci lattice [1]. The Fibonacci lattice has a fairly uniform and isotropic distribution of sites on the surface of the sphere. Another property is the preservation of equality of areas between three neighboring points. This leads to a continuous limit with infinite filling of the lattice. This property makes the model a potential candidate for further solving phase transition problems in quantum field theory.

The purpose of research is to simulate the phase transition of the spin Ising model on the Fibonacci sphere.

The spherical Fibonacci lattice was defined by the formulas (1). Delaunay triangulation was performed to determine the nearest neighbors of sites (figure 1) [2]. The analysis of the triangulation result showed that the number of neighbors varies from 5 to 7, and 6 neighbors are most common. Fluctuations in the number of neighbors are associated with a milder uniform distribution of sites at the poles of the spherical lattice.

$$\begin{cases} x = r\ \sin\theta\ \cos\varphi\,; \\ y = r\ \sin\theta\ \sin\varphi\,; \\ z = r\ \cos\theta\,, \end{cases} \qquad \varphi = \frac{2\,\pi\,i}{g}\,;\ \theta = arcos\left(\frac{1-2\,(i+0.5)}{L}\right) \qquad (1)$$

In formulas (1) i – is the site number running through all L sites of the lattice, $g = (1+\sqrt{5})/2 \approx 1.618$ golden ratio.

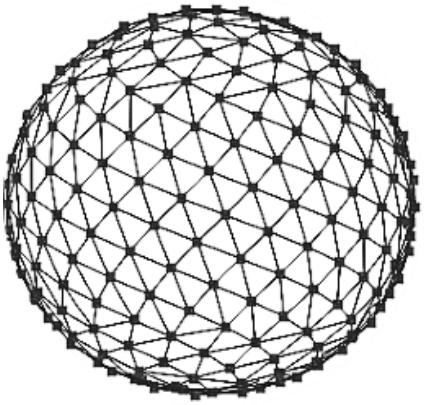

Fig. 1. Spherical Fibonacci lattice with Delaunay triangulation

Each site of the lattice was randomly assigned to the value of the spin variable $S_i = \pm 1$. The implementation of a large number of random configurations and the averaging of system characteristics was carried out by the Monte Carlo method. The configuration was generated by the Metropolis algorithm corresponding to a single Monte Carlo step.

The phase transition in the absence of an external magnetic field was modeled on a triangulated spherical Fibonacci lattice with a temperature step of 0.04. The result was averaged over 10^6 Monte Carlo steps.

One of the best ways to estimate the phase transition temperature is to calculate the 4th order Binder cumulant $U(L,T)$ (3):

$$U\,(L,T) = 1 - \frac{\langle M^4(T,L)\rangle}{3\langle M^2(T,L)\rangle^2}\,, \qquad (3)$$

where $M = \sum_i S_i$ magnetization.

The temperature of the phase transition corresponds to the intersection of the cumulative curves for different fillings of the lattice. The critical point determined for lattices of 1000, 2000, 3000 sites turned out to be equal to $T_c \approx 3.32$ (figure 2). The obtained value is close to the phase transition temperature on a flat triangular lattice $T_c \approx 3.64$ [3]. The difference is probably due to fluctuations in the number of neighbors for the sites on the sphere.

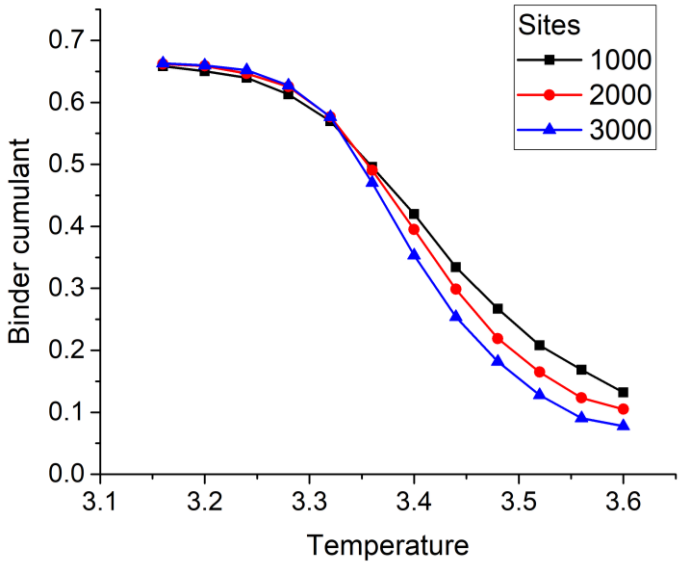

Fig. 2. Temperature dependence of the Binder cumulant for lattices of 1000, 2000, 3000 sites

References

1. Richard Swinbank and R. James Purser. Fibonacci grids: A novel approach to global modelling. Quarterly Journal of the Royal Meteorological Society, 132(619):1769–1793,jul 2006.
2. Skvortsov A.V. Delaunay triangulation and its applications. Tomsk: Publishing House of Tomsk State University, page 128, 2002.
3. Luo Zhi-Huan, Loan Mushtaq, Liu Yan, and Lin Jian-Rong. Critical behaviour of the ferromagnetic Ising model on a triangular lattice. Chinese Physics B, 18(7):2696–2702,jul 2009.

Tanashkin A.S.[1]

THE INFLUENCE OF CASIMIR EFFECT ON THE VACUUM STRUCTURE OF COMPACT ELECTRODYNAMICS

[1]Far Eastern Federal University, Institute of high technologies and advanced materials,
[2]Far Eastern Federal University, Oriental Institute, School of Regional and International Studies, FEFU
Scientific adviser — A.V. Molochkov[1]
Scientific consultant - I.N. Lazareva[2]

Casimir effect is the one of the quantum field theory effects which captures the influence of physical objects on the quantum vacuum fluctuations. In the simplest case the putting two neutral perfectly-conducting and closely-spaced plates into vacuum leads to emerging an attractive force which is known as Casimir force [1]. This effect is observed in a number of theories but the best understood in quantum electrodynamics (QED) [2]. QED describes physical processes in the weak coupling regime but nevertheless the case of strong coupling, while not to be physically real, is of profound interest for the reason of present of deconfinement phase for the high values of coupling constant [3]. QED is the simplest theory for studing this phenomenon and confinement-deconfinement phase transition. The classic pertubative methods tranditionally implemented for investigation of QED with weak coupling are inapplicable here and lead to divergencies. The lattice regularization of QED is one of the possible solutions to deal with this problem. It is divided on compact and noncompact versions [4,5]. In compact theory fields are represented by the elements of unitary U(1) group geometrically belonging to unit circle while in noncompact theory fields are unbounded. Despite the fact that both theories are equivalent in continuous limit, there are topological monopoles in compact theory – the important objects which starting from some concentration lead to confinement phase [6].

In this work we study how the change of distance between plates influences the concentration of monopoles (Fig. 1) and the confinement-deconfinement phase transition point inside the plates. We make comparison with ordinary vacuum without plates. We show that monopole density reduces with decreasing distance between plates (Fig. 2) which leads to shift of phase transition point towards higher values of coupling constant [7].

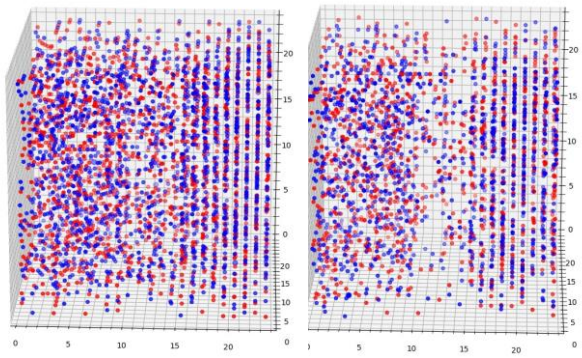

Fig. 1. The examples of monopoles distribution in confinement (left) and deconfinement (right) phases for the plates placed vertically at the center of the lattice at the distance of three lattice units.

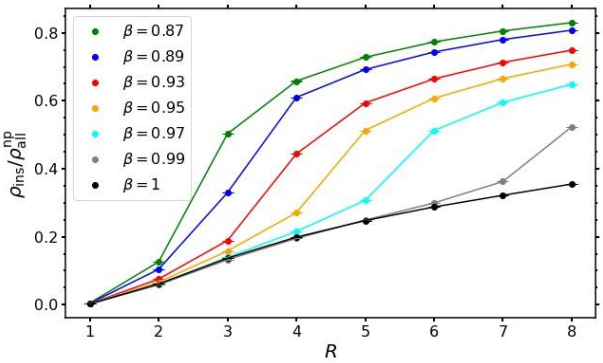

Fig. 2. The dependence of ratio monopole density inside Casimir plates to monopole density in the absence of the plates from the inter-plate separation R for fixed values of lattice coupling β.

References

1. H.B.G. Casimir and D. Polder, Phys. Rev. 73, 360 (1948).
2. M. Bordag, G.L. Klimchatskaya, U. Mohiden and V.M. Mostepanenko, Advances in the Casimir Effect, Vol. 145 (OUP Oxford, 2009).
3. C. Gattringer and C.B. Lang, Quantum Chromodynamics in the lattice, Vol. 788 (Springer, Berlin, 2010).
4. O. Pavlovsky and M. Ulybyshev, Casimir energy in the compact QED on the lattice, arXiv:0901.1960 (2009).
5. O. Pavlovsky and M. Ulybyshev, Casimir energy calculations within the formalism of the noncompact lattice QED, Int. J. Mod. Phys. A 25, 2457 (2010).
6. L.C. Loveridge, O. Oliveira, P.J. Silva, The lattice Landau gauge photon propagator for 4D compact QED, Phys. Rev. D 103, 094519 (2021).
7. M.N. Chernodub, V.A. Goy, A.V. Molochkov and A.S. Tanashkin, Casimir boundaries, monopoles, and deconfinement transition in 3+1 dimensional compact electrodynamics, arXiv:2203.14922 (2022).

Chernousov N.N.[1]

MAGNETIC PROPERTIES OF Co/Cu/Co STRUCTURES WITH IN-PLANE AND PERPENDICULAR MAGNETIC ANISOTROPY

[1]Far Eastern Federal University, Department of General and Experimental Physics, FEFU
[2]Far Eastern Federal University, Oriental Institute, School of Regional and International Studies, FEFU
Scientific adviser - A.V. Davydenko [1]
Scientific consultant - I.N. Lazareva[2]

The paper is focused on magnetic properties of Co/Cu/Co films with in-plane and out-of-plane perpendicular magnetic anisotropy (IMA and PMA) in Co layers. The main goal of study was to form the so-called T-structure in which magnetization in both Co layers in residual state is oriented in one layer in its plane, and in the other layer - perpendicular to its plane. The interest to T-structures is related to possible switching of magnetization in PMA layer due to spin current of electrons caused by the spin-dependent scattering of electrons IMA layer [1]. These studies may be useful for developing a non-volatile memory with a high information recording density.

The structure of the first sample was as follows: Si (111)/Cu (10 ML)/Co (4 nm)/Cu (5 nm)/Co (0.7 nm). Fig. 1 shows magnetic hysteresis loops for the first sample. These hysteresis loops demonstrate two-phase behavior:

in low fields, magnetization in one layer switches and then in high fields, magnetization in the second Co layer smoothly saturates. The ratio of magnetic moments of the layers, determined from hysteresis loops approximately corresponds to Co layers thicknesses ratio.

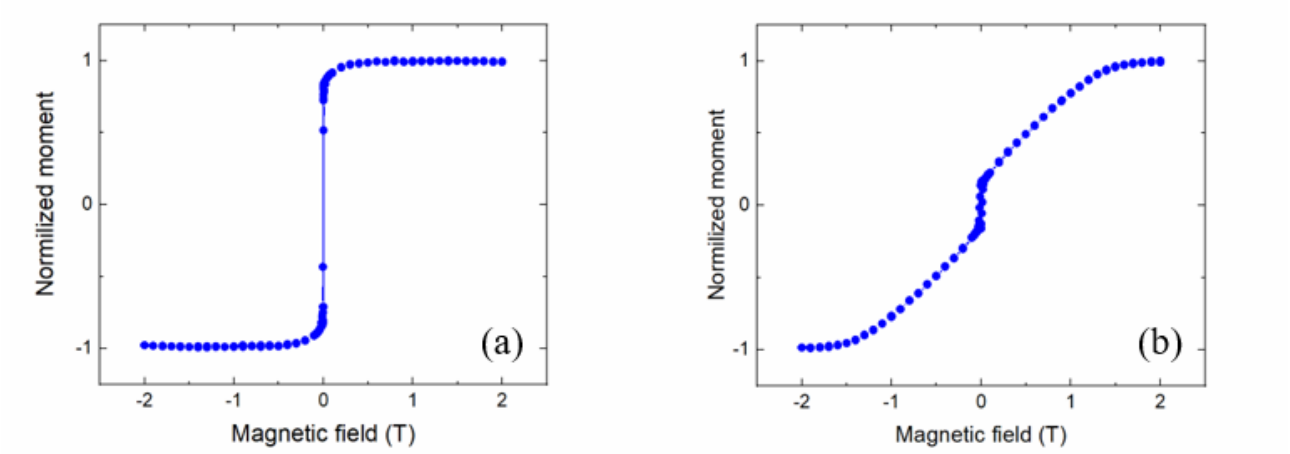

Fig. 1. Normalized magnetic hysteresis loops for Si(111)/Cu(10 ML)/Co(4 nm)/Cu(5 nm)/Co(0.7 nm) sample, measured when magnetic field is applied (a) in-plane and (b) perpendicular of sample's surface.

The size of domains in the first sample, observed by magnetic force microscopy in PMA layer, was 600 nm less. Such small domains cannot be observe by magneto optical Kerr effect microscopy (MOKE), which complicates the further study of such samples. Such a small size of domains is caused by high roughness of top Co layer and strong magnetostatic interaction between Co layers.

To check the effect of interlayer interaction on domain structure a sample was deposited with the structure: Si (111)/Cu (11 nm)/Co (0.7 nm)/ Pd (3 nm). The roughness of Co layer in such sample is comparable to the roughness of the first sample, but the second sample does not reveal interlayer interaction. The density of this sample nucleation centers is equal to 0.146 μm^{-2}. The domains are distinguishable under MOKE.

To decrease the impact of roughness on magnetic structure, the second multilayer sample was deposited in which Co layer with PMA is in the bottom. The structure of the second multilayer sample is Si (111)/Cu (2 nm)/Pd (3 nm)/Co (0.6 nm)/Cu (5 nm)/Pd (3 nm). In the second sample, PMA energy at the Co layer bottom increased as it was expected. This was possibly because an additional magnetoelastic contribution. The roughness of the bottom Co layer compared to the first sample decreased significantly. Nevertheless, PMA Co layer was remagnetized by a number of nucleation domains. The density of nucleation centers in this sample is equal to 0.102 μm^{-2}, which is 1.4 times less than in the sample with the thin Co layer on the top, though with high roughness.

In the samples with single magnetic Co layer and sufficiently strong PMA, the magnetization reversal occurs by nucleation of 10-20 domains over the entire sample area of 25 mm^2. Both magnetic layer roughness increase and strong interlayer interaction greatly reduce the size of domains in T-structure. Meanwhile, roughness effect on the domain size is more apparent. Thus, based on the results obtained, it can be concluded that, it is better to form Co layer with PMA at the bottom of T-structures in order to reduce its roughness. The thickness of Cu layer must be increased in order to reduce an interlayer magnetostatic interaction.

References

1. Tianyi. Ma. Efficient Spin-Orbit-Torque Switching Assisted by an Effective Perpendicular Field in a Magnetic Trilayer / Tianyi Ma, Caihua Wan, Jing Dong et al // Physical Review Applied – 2021. – Vol. 16. – P. 014016.